Eph-ephrin signalling in cell sorting and directional migration

Lauren Georgina Louise Gregory

May 2011

Division of Developmental Neurobiology
MRC National Institute for Medical Research
The Ridgeway
Mill Hill, London
NW7 1AA

Department of Cell and Developmental Biology
University College London

This thesis is submitted to University College London for the degree of Doctor of Philosophy

DECLARATION

This PhD project has been completed in the laboratory of Dr. David Wilkinson in the Division of Developmental Neurobiology at the National Institute for Medical Research, London.

I, Lauren Gregory, hereby declare that the work presented in this thesis is my own. Where information has been derived from other sources, I confirm that this has been indicated in the thesis. I acknowledge that establishing the *in vitro* assays used in this work, with the exception of the boundary sharpening assay, was done in collaboration with Rosalind Morley in the Wilkinson laboratory.

ACKNOWLEDGEMENTS

I would first like to thank my supervisor, David Wilkinson, for giving me the opportunity to do my PhD in his laboratory, and for his encouragement, support and guidance. In addition I would like to particularly thank Rosalind Morley for her tireless back-up, endless discussions and constant friendship.

Thanks in particular goes to Chen Qian and Robert Gilchrist for designing custom made programs for enabling automated analysis of our results, and the members of the Confocal Imaging and Analysis Laboratory, NIMR, who have assisted with the problems that come with long hours of imaging.

I would like to thank all members of the Wilkinson laboratory for their advice and help, in particular Alexei Poliakov for teaching me cell culture techniques, and Tomomi Watanabe and Sebastian Gerety for teaching me zebrafish and cloning techniques.

Last but not least, I would like to thank my parents, sister and Paul for their constant support and encouragement throughout all these years of studying.

ABSTRACT

An important problem in developmental biology is to understand how precise patterns of cell types are maintained during development. Eph receptor tyrosine kinases and ephrins have key roles in stabilising these patterns of cell organisation and segregation during development and can restrict the movement of cells by promoting cell repulsion. Previous work by Alexei Poliakov in the Wilkinson lab has shown that Eph-ephrin signalling leads to directional persistence of migration, and modelling suggests that this can contribute to cell segregation.

In order to test experimentally the contribution of directional persistence in cell segregation, I have used and developed *in vitro* assays to dissect the roles of EphB2-ephrinB1 signalling in cell segregation, boundary sharpening and directional persistence. In these assays, stable HEK293 cell lines expressing EphB2 or ephrinB1 are mixed in cell culture and this leads to segregation of the two cell populations. Plating these cells either side of a removable barrier and allowing migration of cells towards each other leads to the formation of a sharp boundary on interaction. Analysis of cell behaviour shows EphB2 cells to move more persistently after interaction with ephrinB1 cells.

To analyse how EphB2-ephrinB1 interactions lead to directional persistence of migration, my studies have focussed on the role of components potentially involved in directional persistence that act downstream of EphB2-ephrinB1 signalling, including the planar cell polarity (PCP) pathway (Dishevelled and Daam1) and core polarity components such as the PAR proteins (PAR-3 and PAR-6B). The PCP and PAR components were all found to have roles in cell segregation, as siRNA-mediated knockdown of each of these components disrupted EphB2-ephrinB1 mediated cell segregation and boundary sharpening. However, cell behaviour studies showed that only Dishevelled and PAR-6B have roles in EphB2-ephrinB1 mediated directional persistence, whilst Daam1 knockdown has no effect on the migratory response of cells. PAR-3 knockdown affects the basal ability of cells to migrate, potentially due to its role in establishing front-rear polarity.

Taken together, these findings can be explained by a model in which Dishevelled and PAR-6B have a role in EphB2-ephrinB1 mediated directional persistence required for cell segregation and boundary sharpening. I propose that Daam1 may function in the contact inhibition of locomotion between cells also required for segregation.

TABLE OF CONTENTS

TABLE OF FIGURES

ABBREVIATIONS

r	:	Rhombomere
Eph	:	Erythropoietin-producing hepatocellular receptor
A-P	:	Anterior-Posterior
D-V	:	Dorsal-Ventral
RTKs	:	Receptor tyrosine kinases
GEF	:	Guanine nucleotide exchange factor
GAP	:	GTPase activating protein
PCP	:	Planar cell polarity
PAR	:	Partitioning defective protein
LE	:	Leading edge
TE	:	Trailing edge
CIL	:	Contact Inhibition of Locomotion
CE	:	Convergent Extension
MO	:	Morpholino oligonucleotide
DN	:	Dominant-negative
NN	:	Nearest neighbour
PRI	:	Perimeter Regularity Index
HCI	:	Heywood Circularity Index
MSD	:	Mean Squared Displacement
Dsh	:	*Xenopus* Dishevelled
Dvl	:	Mammalian Dishevelled
MSC	:	Multiple Cloning Site
ss	:	Somite stage
hfp	:	Hours-post-fertilisation
WT	:	Wild-type
HS	:	Heat-shock
DLG	:	Discs Large
LGL	:	Lethal giant larvae
MTOC	:	Microtubule organising centre
ADAM	:	A-Disintegrin-And-Metalloprotease
Daam	:	Dishevelled-associated activator of morphogenesis
ECM	:	Extracellular matrix

1 INTRODUCTION

1.1 Introduction to mechanisms of cell segregation and boundary formation

An important problem in developmental biology is to understand how precise patterns of cell types are maintained during development, despite potential for rearrangement due to processes such as cell division and intercalation. This applies particularly to a phase during the development of some tissues in which distinct domains are formed by subdivision, each with a specific regional identity that specifies a particular set of cell types. The restriction of intermingling between specific cell populations is crucial for maintaining these organised patterns during development (Irvine & Rauskolb, 2001; Pasini & Wilkinson, 2002).

1.1.1 Compartments

Segmentation occurs during both invertebrate and vertebrate development in order to segregate groups of cells that have distinct functions. Developmental compartments and the maintenance of compartment boundaries was first recognised in developing *Drosophila* embryos in the abdomen and wing imaginal discs. Lineage restriction boundaries form to subdivide regions into compartments with borders that cells do not cross (Garcia-Bellido *et al.*, 1973; Lawrence, 1973), and correspond to gene expression domains, an example of which is *engrailed* (Garcia-Bellido & Santamaria, 1972). These boundaries also act as signalling centres to regulate both patterning and growth in the developing embryo (Irvine & Rauskolb, 2001; Kiecker & Lumsden, 2005; Vincent, 1998). Compartments can also form in a sequential manner, such as the periodic formation of somites controlled by cyclic gene expression (reviewed by (Pourquie, 2001)), which are subdivided by non-lineage boundaries.

One of the best examples of cell segregation during vertebrate development is found in the hindbrain (rhombencephalon) (Fraser *et al.*, 1990), where sharp boundaries form at the interface of segments called rhombomeres (Lumsden & Krumlauf, 1996; Pasini & Wilkinson, 2002). This pattern of subdivision shares similarities with the segmentation of the *Drosophila* embryo, discussed later.

1.1.2 Hindbrain segmentation

Hindbrain development is characterised by a metameric segmentation pattern, where the neural epithelium is morphologically subdivided into a series of seven or eight lineage-restricted compartments (rhombomeres) that are arranged along the anterior-posterior axis (Fig. 1 A). Neurogenesis and axonal projections are also arranged in a segmental pattern (Clarke & Lumsden, 1993; Lumsden & Keynes,

1989), and mutations that disrupt the morphological segmentation also disrupt the segmental patterning of hindbrain neurons (Cooke *et al.*, 2005; Moens *et al.*, 1996). This relationship between hindbrain segmentation and neuronal organisation highlights the importance of rhombomeres as discrete structures. Rhombomeres follow a two-segment periodicity with even- versus odd-numbered rhombomeres displaying distinct characteristics; motor neurons in chick differentiate in even-numbered before odd-numbered rhombomeres (Lumsden & Keynes, 1989): even- and odd-numbered rhombomeres exhibit different affinity properties (Guthrie *et al.*, 1993); and rhombomeres exhibit an alternating segmental pattern of gene expression, for example rhombomeres 3 and 5 (r3/r5) express the zinc-finger gene *krox20* (Wilkinson *et al.*, 1989a).

1.1.2.1 Selector genes confer rhombomere identity and positional information for boundary formation

"Selector gene" expression is required to confer segmental identity by defining the fate of a tissue domain; the boundary of the selector gene expression domain corresponds to the compartment boundary. Loss of selector genes causes loss of identity in the domain, and ectopic expression confers this identity in the ectopic territory. Studies of compartments in *Drosophila* have shown the positional identity of each body segment of the main axis of the fly embryo to be defined by the combinatorial control of expression of *Hox* selector genes (chromosomally clustered homeotic selector genes) (Lewis, 1978). Hindbrain architecture shows a resemblance to the developing *Drosophila* embryo, as *Hox* gene expression precedes morphological rhombomere formation and subsequently the borders of expression coincide with rhombomere boundaries (Wilkinson *et al.*, 1989b). *Hox* genes are expressed in a nested fashion with a two-rhombomere periodicity (Wilkinson *et al.*, 1989b), and in general genes 3' in the genomic cluster are expressed more anteriorly than those at the 5' of clusters.

A combinatorial expression of *Hox* genes defines each rhombomere as different *Hox* genes are expressed in each segment at different levels (Fig. 1 B) (Graham *et al.*, 1989; Wilkinson *et al.*, 1989b). The role of *Hox* genes in regulating rhombomere identity has been uncovered in gain- and loss-of-function studies in several species, most particularly of *Hoxb1*, a gene that is uniquely expressed in r4. Knockdown of this gene confers r2 identity on certain r4 neurons, while overexpression of *Hoxb1* in the r2 domain leads to neurons adopting r4-like characteristics, such as the innervation of these neurons into the second branchial arch (Bell *et al.*, 1999; Studer *et al.*, 1996). Other *Hox* genes have also been shown to act in a selector-like gene fashion and confer positional identity. However, many *Hox* mutations produce subtle phenotypes and this is thought to be due to partial redundancy between *Hox* paralogue genes (Gavalas *et al.*, 1998; Gavalas *et al.*, 2003; Greer *et al.*, 2000). Interestingly, embryos in which most *Hox* function has been removed exhibit anterior homeotic transformation of r2-r6 to r1 identity (Waskiewicz *et al.*, 2002), which is consistent with the observations that *Hox* genes are not expressed in r1 (Moens & Prince, 2002) and that *Hox* genes confer positional segmental identity.

Figure 1: Hox gene expression and rhombomere identity

(A): Schematic diagram showing the lateral view of embryonic avian brain (Hamburger–Hamilton stage 13, anterior to the left, dorsal to the top). Cell lineage restriction is found between compartments (dark blue) and arrows represent bidirectional signalling from the midbrain–hindbrain boundary (adapted from (Kiecker & Lumsden, 2005)).

(B): Schematic diagram showing the expression of *Hox* genes and key molecules during hindbrain segmentation in zebrafish. Anterior is to the left and posterior to the right. Paralogue groups are colour coded. *Fgf3* and *8* control the expression of segmentation genes like *krox20*. Eph receptors and their interacting ephrin ligands are expressed in odd- and even-numbered segments, respectively, and are important for restricting the intermingling of cells between adjacent rhombomeres (adapted from (Pasini & Wilkinson, 2002)).

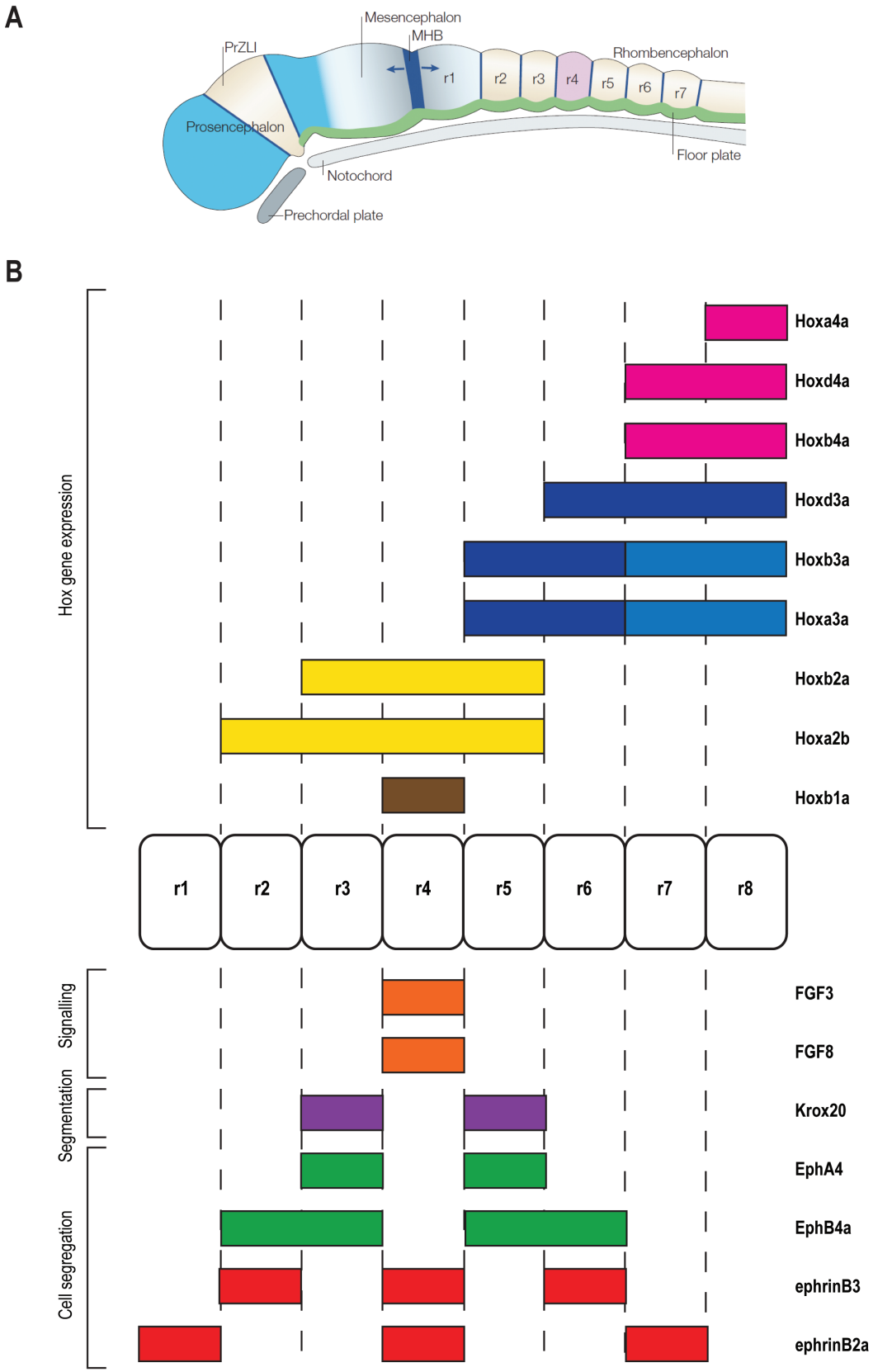
A
Mesencephalon
MHB
PrZLI
Rhombencephalon
r1
r2
r3
r4
r5
r6
r7
Prosencephalon
Floor plate
Notochord
Prechordal plate
B
Hox gene expression
Hoxa4a
Hoxd4a
Hoxb4a
Hoxd3a
Hoxb3a
Hoxa3a
Hoxb2a
Hoxa2b
Hoxb1a
r1
r2
r3
r4
r5
r6
r7
r8
Signalling
FGF3
FGF8
Segmentation
Krox20
EphA4
Cell segregation
EphB4a
ephrinB3
ephrinB2a

Regulation of *Hox* gene expression is complex and it is unclear how *Hox* genes are activated at appropriate timings and levels, although it is known that retinoic acid and segmentation genes, such as *krox20 and kreisler*, play a role (reviewed in (Alexander *et al.*)). *Krox20* is a zinc finger transcription factor known to be involved in segmentation and is expressed in r3 and r5 (Wilkinson *et al.*, 1989a). *Krox20* exerts a role in segment identity, as in the absence of *krox20*, r3 and r5 are lost at later stages (Schneider-Maunoury *et al.*, 1997). *Krox20* also directly activates the transcription of *Hoxa2, Hoxb2* and *EphA4* in r3 and r5 (Maconochie *et al.*, 1996; Nonchev *et al.*, 1996), so coupling *Hox* gene expression to segmentation.

1.1.2.2 Compartments and restriction of cell mixing in the hindbrain

Rhombomeres of the developing hindbrain are lineage-restricted compartments. This was shown by cell lineage tracing experiments in chick that have demonstrated rhombomeres to be polyclonal groups of neuroepithelial cells (Fraser *et al.*, 1990). Clonally marked neuroepithelial cells disperse within a rhombomere but do not spread into neighbouring rhombomeres, and this restriction of cell mixing begins when boundaries are formed (Birgbauer & Fraser, 1994). This suggests that rhombomeres are compartments and that boundaries restrict the clonal expansion of cells into adjacent rhombomeres.

Rhombomere boundaries correspond to the borders of segmental, periodic domains of gene expression of members of the *Hox* gene family, as discussed previously, and also the Eph and ephrin gene families, which underlie boundary formation (Fig. 1 B). A role for Eph receptor tyrosine kinases and their ligands, the ephrins, in the hindbrain was suggested by their complementary rhombomere-restricted patterns of gene expression in many species; Eph receptors are expressed in odd-numbered rhombomeres and ephrins in even-numbered rhombomeres (Flenniken *et al.*, 1996; Nieto *et al.*, 1992). Mixing between cells of different rhombomeres displays two-segment periodicity i.e. cells from r2, r4 or r6 can freely mix with each other, as can r3 and r5, but cells from odd-numbered segments do not mix with cells from even-numbered segments (Guthrie *et al.*, 1993). Functional experiments revealed that Eph-ephrin signalling at rhombomere boundaries restricts intermingling between domains (Mellitzer *et al.*, 1999; Xu *et al.*, 1999). This suggests that segmental gene expression underlies segmental cellular identity and these differing characteristics between odd- and even-numbered segments could be the primary mechanism for lineage restriction and boundary formation at the interface of segments. The importance of Eph-ephrin interactions in mediating cell segregation and differences in cell-cell affinity will be discussed later.

1.1.3 Hindbrain boundaries

The apposition of even- and odd-numbered rhombomeres has been shown to induce boundary cells at their interface in chick. Boundaries fail to form when any two odd- or even-numbered segments are juxtaposed (with the exception of r5 and r7) (Guthrie & Lumsden, 1991). This suggests that interactions

between neighbouring rhombomeres induce the formation of boundaries. As these interactions involve properties specific to either even- or odd-numbered rhombomeres, similar to the affinity differences previously described, Eph-ephrin signalling is a candidate pathway for rhombomere boundary cell induction. It is known that boundary markers are lost on disruption of Eph-ephrin signalling (Cooke *et al.*, 2005; Xu *et al.*, 1995), but the short range signalling events that lead to boundary cell induction are unknown.

Boundary cells are defined as a separate population by their distinct cellular properties and specific gene expression pattern, which is distinct from rhombomere centres. A number of transcription factors are expressed at higher levels at rhombomere boundaries, such as the homeobox gene *pax6* (Heyman *et al.*, 1995; Xu *et al.*, 1995) and the forkhead box-containing *foxb1.2* (Moens *et al.*, 1996). In addition, the Notch modulator *rfng* is expressed in boundaries in the zebrafish hindbrain (Cheng *et al.*, 2004). Since several signalling molecules are expressed in boundary cells, such as *fgf3* (Mahmood *et al.*, 1995) in the mouse and chick hindbrain but not zebrafish, and several Wnt family members (Riley *et al.*, 2004), this raises the possibility that hindbrain boundaries act as signalling centres.

Boundaries are thought to coordinate both patterning and growth in specific tissues, by preventing the intermingling of lineage-restricted cells and by regulating the growth and patterning of adjacent cell populations (Irvine & Rauskolb, 2001; Vincent, 1998). Analysis of rhombomeric gene expression domains has shown that interfaces at first appear fuzzy, but are sharpened over a short period of time (Cooke *et al.*, 2005; Irving *et al.*, 1996) with the formation of morphological boundaries and expression of boundary specific markers. It has been proposed that the sharpening of boundaries occurs by the segregation of cells to the correct side of the forming boundary and the switching of cell identity to that of their neighbours (Fig. 3 A) (Cooke *et al.*, 2005; Pasini & Wilkinson, 2002). Further evidence for cell identity switching shows that *krox20* can induce its own expression non-autonomously (Giudicelli *et al.*, 2001), which suggests it might regulate switching of identity of even-numbered rhombomere cells found in odd-numbered segments.

Boundaries can act as barriers to the spread of signals that regulate regional identity. Increased extracellular space is present between boundary cells (Heyman *et al.*, 1993) and this is thought to be due to repulsive interactions occurring at interfaces mediated by Eph-ephrin signalling (Xu *et al.*, 1999). This correlates with the findings that rhombomere gap junctional communication is reduced across boundaries (Martinez *et al.*, 1992) and gap junction formation is inhibited by Eph-ephrin signalling at interfaces (Mellitzer *et al.*, 1999). Eph-ephrin signalling could therefore stabilise the properties of hindbrain segments by restricting both cell intermingling and the communication of cells across interfaces (Mellitzer *et al.*, 1999).

Cell divisions can lead to cell rearrangements that challenge compartment boundaries. Rhombomere boundary cells show a reduced rate of proliferation to that in the centre of segments (Guthrie & Lumsden, 1991), which may contribute to the maintenance of boundaries. In addition, rhombomeres are sites for extracellular matrix accumulation (Heyman *et al.*, 1995; Lumsden & Keynes, 1989), which has been shown to be important for the maintenance of the somite boundaries in zebrafish (Koshida *et al.*, 2005). This mechanism could provide a physical barrier to intermingling; however, the mechanical ablation of rhombomere boundaries does not lead to an increase in cell mixing between adjacent rhombomeres (Guthrie & Lumsden, 1991), and suppression of boundary cell formation using retinoic acid beads does not affect the sharpness of the border (Nittenberg *et al.*, 1997). This data suggests that the formation of boundary cells is not the primary cause of cell lineage restriction between rhombomeres, and that the restriction of intermingling is due to cell affinity differences.

1.1.4 Mechanisms of boundary maintenance

The precision of regional patterning can be mediated by the inhibition of cell mixing between domains using three different mechanisms to allow the formation of sharp boundaries (Dahmann *et al.*, 2011; Pasini & Wilkinson, 2002). Firstly, cells can be confined within a domain due to preferential adhesion, for example by homophilic adhesion via cadherins (reviewed in (Foty & Steinberg, 2004)). A second mechanism involves the mutual inhibition of cell invasion via bidirectional activation of Eph receptors and ephrins at the interface of domains (Mellitzer *et al.*, 1999; Xu *et al.*, 1999). In addition, an Eph receptor has been found to also regulate cell segregation within tissue subdivisions (Cooke *et al.*, 2005), and so may sharpen boundaries by modulating cell adhesion both at interfaces and within regional domains, suggesting there might be cooperation between these mechanisms. Thirdly, recent studies have revealed a role of mechanical tension in border sharpening (Dahmann *et al.*, 2011). These mechanisms are discussed below.

1.1.4.1 Differential cell adhesion

The concept that cells along compartment boundaries separate due to differences in the adhesion or affinity between cells in neighbouring compartments (Garcia-Bellido, 1975) is based on the differential cell adhesion hypothesis of Malcom Steinberg. Steinberg proposed that different adhesive properties underlie the clustering of dissociated embryonic cells representative of their layer of origin (Steinberg, 1963), and that this sorting is driven by thermodynamic principles similar to those that induce the separation of two immiscible liquids (Duguay *et al.*, 2003).

Work on cadherins in tissue culture has shown that artificially intermingled populations expressing cadherins will segregate from each other (Nose *et al.*, 1988). This sorting is driven either by the

preferential adhesion of cells expressing the same adhesion molecules i.e. in mixtures of cells expressing different cadherin molecules, or by differences in the expression level of an adhesion molecule between populations (Fig. 2 A) (reviewed (Foty & Steinberg, 2004)). Aggregate surface tension was shown to be a linear expression of cell-cell adhesiveness (based on cadherin expression), and the relative tissue surface tension between two groups dictates that the less cohesive group surrounds the other (Fig. 2 A) (Foty & Steinberg, 2005). However, the strength of interaction between cadherins is not sufficient to fully account for cell sorting (Niessen & Gumbiner, 2002).

Although sorting of completely intermingled populations is likely to be of limited relevance *in vivo*, adhesion molecules are likely to play a role in preventing intermingling of previously segregated populations at interfaces. Cadherins have spatially restricted expression patterns in the vertebrate central nervous system (Redies & Takeichi, 1996) and could play a role in maintaining the segregation of adjacent populations during development. There is good evidence for a role for cadherins in maintaining compartment boundaries; for example, cadherin-4 and cadherin-6 are differentially expressed in mice on either side of the corticostriatal compartment boundary, and misexpression of either protein leads to cell segregation across the boundary (Inoue *et al.*, 2001).

Recently, an Eph receptor has been found to also regulate cell segregation within rhombomeres of the developing zebrafish hindbrain (Cooke *et al.*, 2005), thus contributing to boundary formation. Mosaic experiments in which EphA4-knockdown cells were transplanted into a wild-type host led to sorting of EphA4-knockdown cells to the boundaries, and wild-type cells transplanted into an EphA4-knockdown host clustered to the centre of r3 and r5 (Cooke *et al.*, 2005). These findings suggest that EphA4 function is required within segments to regulate cell affinity and that EphA4 may sharpen boundaries by modulating cell adhesion both at interfaces and within regional domains. In addition, the regulation of cell affinity by EphA4 and ephrinB2a in the zebrafish hindbrain has been shown to prevent cells from one rhombomere territory from dividing into adjacent rhombomeres (Kemp *et al.*, 2009), so maintaining rhombomere boundaries.

1.1.4.2 Restriction by repulsion

Eph receptor tyrosine kinases and ephrins mediate contact-dependent cell interactions that are implicated in repulsion mechanisms important for the guidance of migrating cells and neuronal growth cones and in restricting the intermingling of cells across hindbrain boundaries (Poliakov *et al.*, 2004; Xu *et al.*, 1995; Xu *et al.*, 1999). In the hindbrain, expression of specific ephrinB proteins and interacting EphB and EphA4 proteins occurs in even-numbered (r2, r4, r6) and odd-numbered rhombomeres (r3, r5) respectively. Disruption of localised Eph receptor activation in the *Xenopus* or zebrafish hindbrain, by expression of dominant-negative EphA4 or ephrinB2, leads to the presence of cells with an r3/r5 identity in even-numbered territory (Xu *et al.*, 1999). Further evidence has come from experiments where cells expressing

Figure 2: Differential adhesion and Eph-ephrin signalling can drive cell segregation

(A): Differential adhesion can drive cell segregation. Two N-cadherin-transfected L cell clones expressing N-cadherin at their surfaces in the ratio of 2.4 (green):1 (red), were mixed in equal proportions and cultured as hanging drops. The aggregate after 4 h of incubation shows the initial cell mixture. The aggregate after 24 h of incubation shows the cell population expressing the lower level of N-cadherin (red) envelops the cell population expressing higher amounts of N-cadherin (green) (adapted from (Foty & Steinberg, 2005)).

(B-C): Eph-ephrin signalling leads to sharp boundaries between populations and cell segregation in zebrafish animal cap explants (B) and the zebrafish hindbrain (C). Perturbation of Eph-ephrin signalling causes disruption to cell segregation and the sharp interface between populations, and formation of a fuzzy boundary (B', C') (adapted from (Cooke *et al.*, 2005; Mellitzer *et al.*, 1999)).

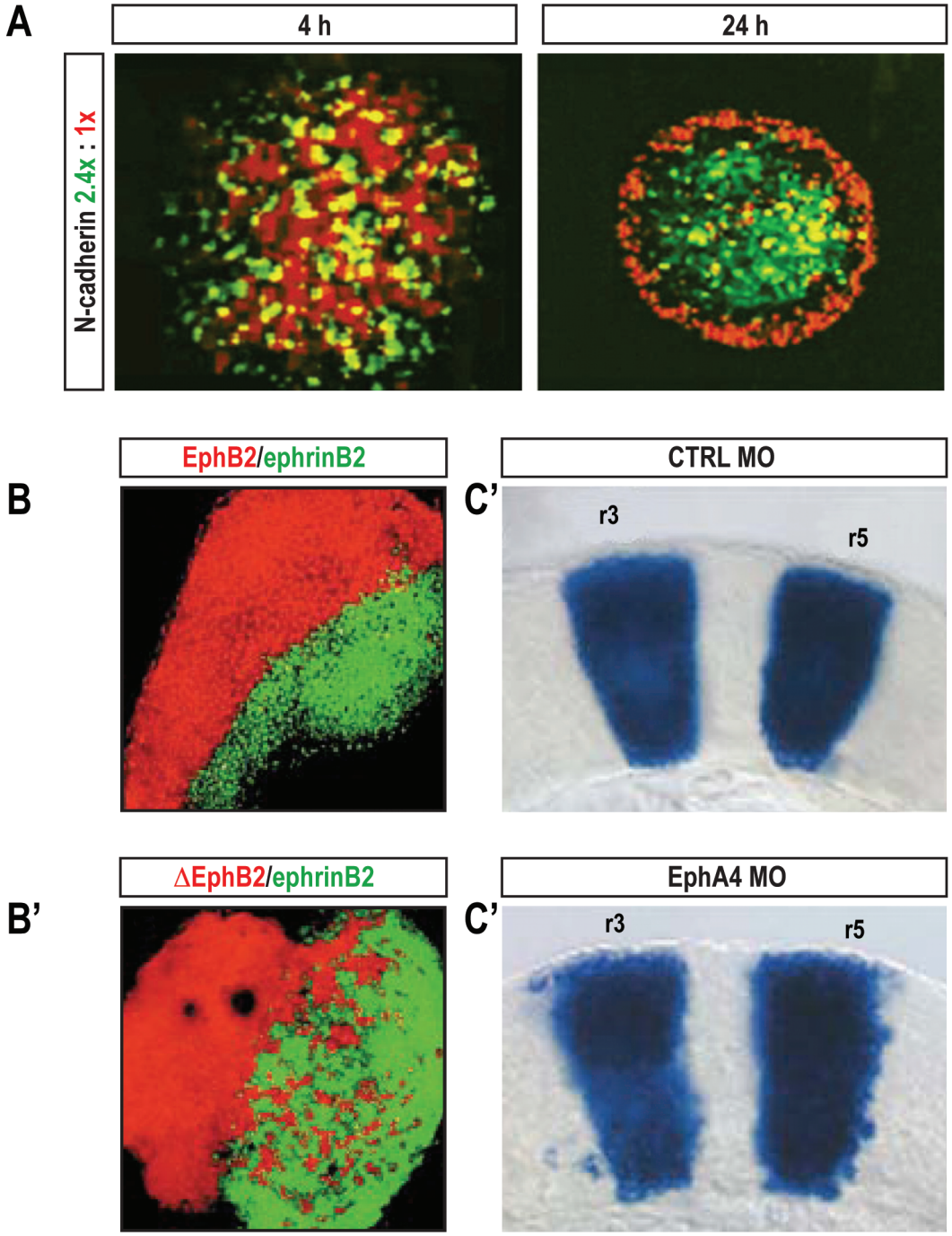
A
4 h
24 h
N-cadherin 2.4x : 1x
B
EphB2/ephrinB2
C'
CTRL MO
r3
r5
B'
ΔEphB2/ephrinB2
C'
EphA4 MO
r3
r5

truncated EphA4 or ephrinB2 (which interact with ephrinB or EphA4/EphB2 respectively) were found to sort to boundaries of even- or odd-numbered rhombomeres respectively (Xu *et al.*, 1999). The cells expressing exogenous ligand do not cross into the adjacent rhombomere presumably as they continue to express endogenous Eph receptors or ephrins appropriate for their location (Pasini & Wilkinson, 2002). In addition, knockdown of EphA4, using injection of antisense morpholino oligonucleotides, lead to fuzzy interfaces between r3 and r5 and adjacent segments (Fig. 2 C, C') (Cooke *et al.*, 2005).

Embryo explant experiments show that complementary populations of cells expressing an Eph receptor and its cognate ephrinB are sufficient to maintain segregation of the populations with the formation of smooth boundaries (Mellitzer *et al.*, 1999). Bi-directional Eph-ephrin signalling at the interface of *in vitro* cell aggregates was found to restrict cell invasion (Fig. 2 B, B'), whereas unidirectional signalling in either direction was not sufficient (Mellitzer *et al.*, 1999).

Together these findings suggest that the localised activation of Eph receptors and ephrinB ligands at the interface of complementary expression domains underlies a mutual repulsion that prevents intermingling across hindbrain boundaries. However, EphA4 function is also required within segments to regulate cell segregation (Cooke *et al.*, 2005) and Eph-ephrin interactions therefore could contribute to the sharpening of segments by regulating both repulsion at interfaces and adhesion of cells.

1.1.4.3 Differential mechanical tension

Mechanical tension can be generated by cell cortex contractile elements such as actomyosin filaments (reviewed in (Lecuit & Lenne, 2007)), and has been shown to play a role in the maintenance of sharp boundaries in *Drosophila* epithelia. Filamentous (F)-actin (Major & Irvine, 2005) and non-muscle Myosin II (Major & Irvine, 2006) are enriched at compartment boundaries in *Drosophila* including the parasegment boundaries of the embryonic epidermis (Monier *et al.*, 2010) and the anterior-posterior (A-P) and dorsal-ventral (D-V) boundaries of the wing imaginal disc (Landsberg *et al.*, 2009; Major & Irvine, 2005; Major & Irvine, 2006), and provide a physical barrier through which cells cannot cross. Cell divisions along the parasegment boundary normally have no effect on the boundary, but when Myosin II activity was locally reduced by chromophore-assisted laser inactivation (CALI), cell division causes the boundary to become irregular (Monier *et al.*, 2010).

Mechanical tension has also been shown to be present in the A-P boundary of wing imaginal discs by laser-ablating cell borders and analysing the displacement of cell corners (vertices) (Landsberg *et al.*, 2009). The initial velocity of vertex displacement after ablation is a relative measure of mechanical tension on cell borders (Rauzi *et al.*, 2008), and when the borders of either two anterior or two posterior cells were ablated, the velocity of displacement was similar. In contrast, when cell borders of the A-P boundary were

Figure 3: Boundary concepts: challenges and mechanisms

(A): Two basic mechanisms maintain sharp boundaries. Cell identity switching occurs at non-lineage boundaries, where cells move across gene expression boundaries and switch their identity to adapt to the identity of their local neighbours (left). At lineage boundaries, cell identity is inherited, and displaced cells are sorted back into the territory of cells with the same identity (arrows, right) (adapted from (Dahmann *et al.*, 2011)).

(B): Simulations of tissue growth based on a vertex model can be used to predict boundary straightness. Cell proliferation results in irregular and unstable boundaries when the mechanical tension on cell borders is uniform. A local increase in mechanical tension on cell borders along the interface results in a sharper boundary during tissue growth (adapted from (Dahmann *et al.*, 2011)).

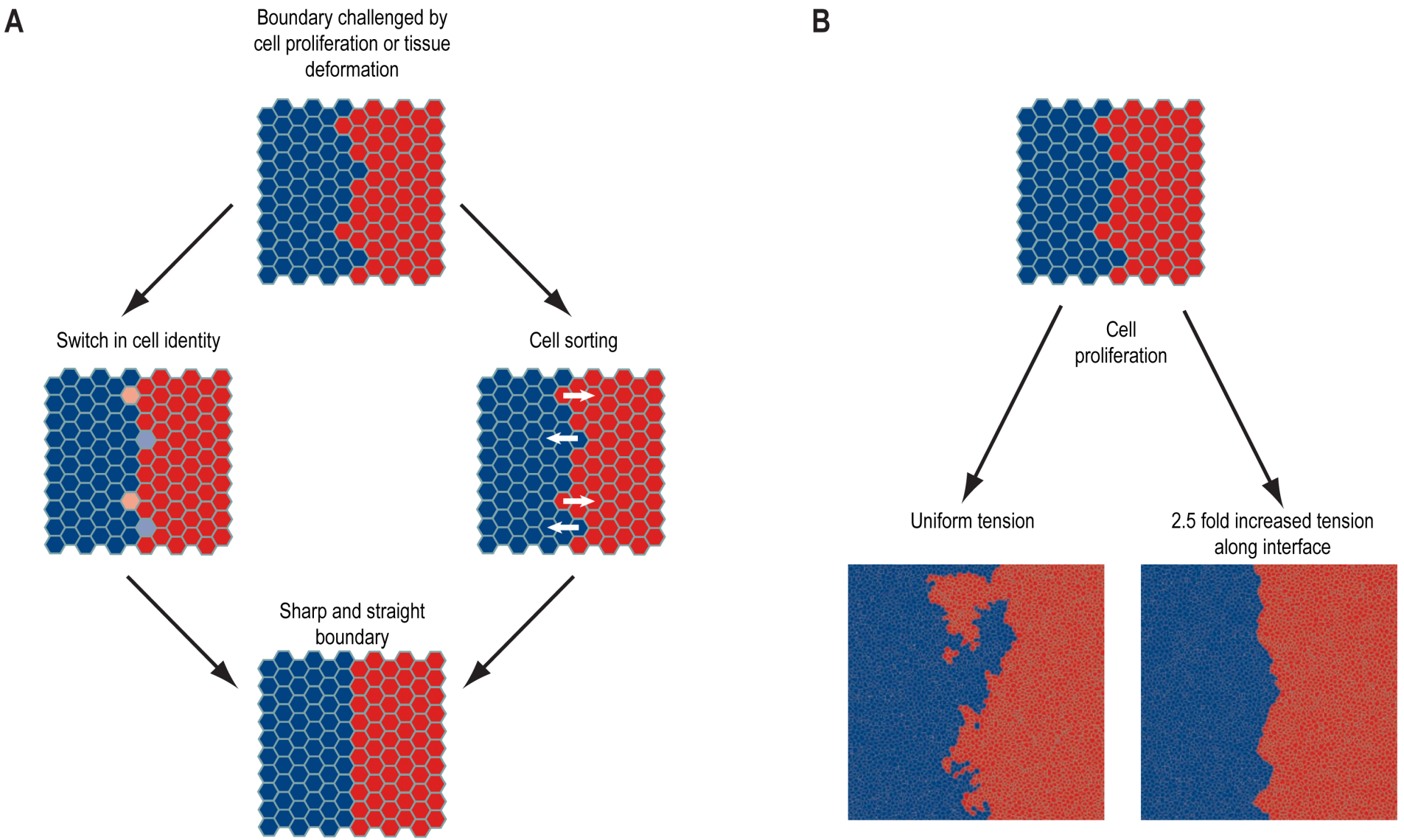
A
Boundary challenged by cell proliferation or tissue deformation
Switch in cell identity
Cell sorting
Sharp and straight boundary
B
Cell proliferation
Uniform tension
2.5 fold increased tension along interface

ablated, velocity increased by 2.5 fold (Landsberg *et al.*, 2009). The actomyosin-dependent mechanical tension along the A-P boundary is disrupted in the presence of Rho-kinase (Myosin II activator) inhibitor (Dahmann *et al.*, 2011), suggesting a role for Myosin II in tension at the A-P boundary.

Modelling has addressed whether an increase in mechanical tension is sufficient to maintain compartment boundaries. Simulation of cell proliferation causes initially straight interfaces between two populations to become fuzzy, whereas increasing mechanical tension along the interface caused the interface to become straighter (Fig. 3 B) (Landsberg *et al.*, 2009). This modelling suggests an increase in mechanical tension is sufficient to maintain straight interfaces between compartments in *Drosophila* (Fig. 3 B) (Dahmann *et al.*, 2011). Cortical tension has also been shown to regulate cell segregation between germ layers in zebrafish (Krieg *et al.*, 2008), suggesting that mechanical tension generated by cell cortex contractile elements such as actomyosin filaments, plays a role in the regulation of sharp boundaries and cell segregation.

1.1.4.3.1 Differential mechanical tension and cell affinity

Intercellular tension of individual cells depends on cortical contractile elements as well as cell-cell adhesive contacts. Increasing contractility increases intercellular tension, whereas increasing adhesive contacts reduces tension (reviewed in (Lecuit & Lenne, 2007). Interfacial tension at a boundary between two populations depends on the balance between cortical contractile elements and cell-cell adhesive contacts both at the boundary and within a population. De-adhesion between cells at a boundary could cause increased intercellular tension in cells at the boundary with increased interfacial tension, and increased adhesion between cells of the same population (not at a boundary) would cause decreased intercellular tension between these cells but increased overall interfacial tension. It is easy to speculate that as Eph-ephrin interactions mediate repulsion between rhombomeres (Mellitzer *et al.*, 1999; Xu *et al.*, 1999), Eph-ephrin signalling may play a role in modulating tension at these boundaries. In addition to the tension caused by differential adhesion, the differential expression of cell adhesion molecules has been shown to cause the local enrichment of F-actin and Myosin II, for example the differential expression of *Echinoid* in *Drosophila* (Wei *et al.*, 2005), suggesting a link between actomyosin contraction and cell affinity.

In some tissues the generation of interfacial tension at an interface between two populations has been shown to be independent of differential adhesion, and instead due to actomyosin-dependent cell cortex tension regulated by different signalling pathways. Differential actomyosin-dependent cell cortex tension, regulated by Nodal signalling, is a critical factor that regulates germ cell progenitor sorting, whereas differential intercellular adhesion alone is not sufficient (Krieg *et al.*, 2008). In addition, Notch activation at the D-V boundary of the *Drosophila* wing disc and subsequent F-actin accumulation, is sufficient for the segregation of cell populations either side of the boundary (Major & Irvine, 2005).

1.1.5 Eph receptors and ephrins; structure and binding

Eph receptor tyrosine kinases are transmembrane proteins that are the largest subfamily of receptor tyrosine kinases (RTKs). In mammals, Eph receptors and their ligands, the ephrins, are divided into two classes based on sequence similarity and binding specificity (Flanagan & Vanderhaeghen, 1998; Gale *et al.*, 1996). There are nine EphA receptors (EphA1-8 and EphA10) and five EphB receptors (EphB1-4 and EphB6). The extracellular Eph domain contains a globular ephrin binding domain, a cysteine-rich region, and two fibronectin type III repeats. The intracellular cytoplasmic region contains the tyrosine kinase domain and two protein-protein interaction domains: a SAM domain and C-terminal PDZ-binding motif (Fig. 4 A).

Ephrins are also divided into sub groups: class A ephrins (A1-5) are tethered to the plasma membrane by a glycosyl phosphatidylinositol (GPI) linkage and preferentially bind EphA receptors, and class B ephrins (B1-3) have integral transmembrane and intracellular domains and preferentially bind EphB receptors (EphNomenclatureCommittee, 1997; Kullander & Klein, 2002; Pasquale, 2005). Binding is promiscuous within a class, but different combinations of receptor and ligand interact with different affinities (Fig. 4 B) (Flanagan & Vanderhaeghen, 1998). Two exceptions have been found: EphA4, which binds to ephrinB2 and B3 in addition to ephrinA ligands, and EphB2, which interacts with ephrinA5 in addition to ephrinB ligands (Gale *et al.*, 1996; Poliakov *et al.*, 2004).

1.1.5.1 Clustering

Clustering and activation of Eph receptors occurs on binding to membrane-bound ephrin ligands in *trans* (Davis *et al.*, 1994), and this mediates contact-dependent cell-cell communication, a feature that distinguishes Eph-ephrin signalling from other RTKS. Eph-ephrin interactions can lead to bidirectional signalling into both the Eph cell (forward signalling) and the ephrin cell (reverse signalling), and these signalling events can occur simultaneously by phosphorylation of tyrosine residues and kinase activation (Fig. 4 A) (Flanagan & Vanderhaeghen, 1998; Poliakov *et al.*, 2004). *Cis* interactions between Eph receptors or Eph receptors and ephrins expressed in the same cell are also possible and have different functions.

Cis interactions between co-expressed Eph receptors, i.e. Eph-Eph interactions, might have a role in expanding the receptor signalling clusters (in an ephrin-independent manner) beyond the region of cell contact (Wimmer-Kleikamp *et al.*, 2004), and be used as a signal amplification mechanism. However, *cis* interactions between EphA and ephrinA molecules co-expressed in the same cell lead to the reduction in tyrosine phosphorylation levels of EphA and decreased sensitivity to ephrinA expressed in an interacting cell i.e. in *trans*. These interactions can therefore be used to limit the forward signalling response and help explain why partially overlapping expression of EphA and ephrinA molecules can generate gradients of

Figure 4: Eph-ephrin structure, binding specificities and function

(A): Schematic diagram showing an ephrinA- and ephrinB-expressing cell (top) in contact with an Eph-expressing cell (bottom). Structural features of ephrin and Eph molecules are indicated.
Abbreviations: RBD, receptor-binding domain; LBD, ligand-binding domain; SAM, sterile a-motif (adapted from (Egea & Klein, 2007)).
(B): Summary of the structural classes of vertebrate Eph receptors and ephrins and their binding specificities. Although binding is promiscuous within each class, the differences in affinity might be functionally important (adapted from (Wilkinson, 2001)).
(C): Model of contact repulsion regulated by ephrinB trans-endocytosis. Activation of Eph receptors at the site of contact between an Eph-expressing and an ephrinB-expressing cell triggers local Rac-dependent membrane protrusions. These protrusions engulf the surface of the ephrin-expressing cell, causing full-length ephrinB molecules to be trans-endocytosed into Eph-expressing cells. These events destabilise contacts between Eph-expressing and ephrin-expressing cells and are necessary for cell repulsion responses (adapted from (Marston *et al.*, 2003)).

A

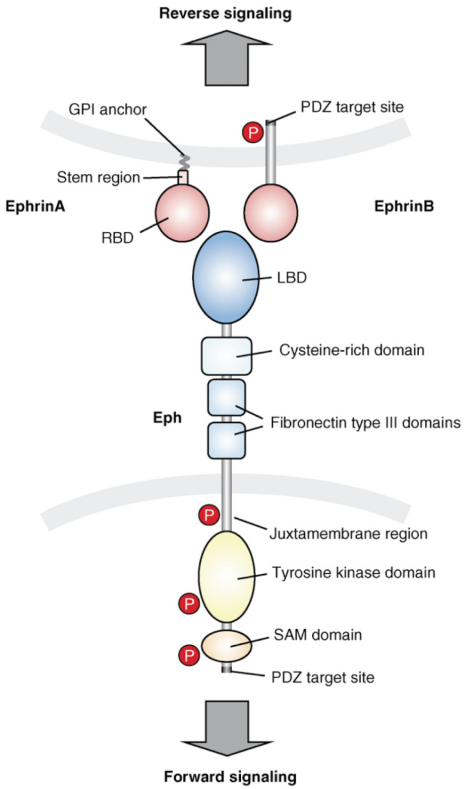
Reverse signaling
GPI anchor
PDZ target site
Stem region
EphrinA
EphrinB
RBD
LBD
Cysteine-rich domain
Eph
Fibronectin type III domains
Juxtamembrane region
Tyrosine kinase domain
SAM domain
PDZ target site
Forward signaling

B

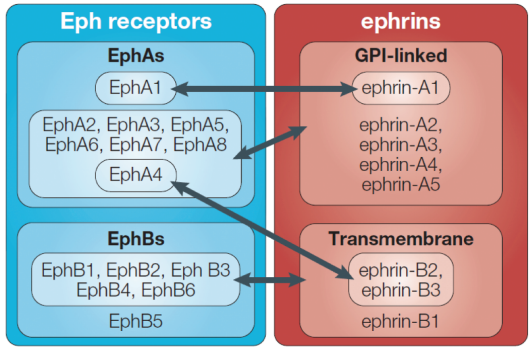
Eph receptors
ephrins
EphAs
GPI-linked
EphA1
ephrin-A1
EphA2, EphA3, EphA5, EphA6, EphA7, EphA8
ephrin-A2, ephrin-A3, ephrin-A4, ephrin-A5
EphA4
EphBs
Transmembrane
EphB1, EphB2, Eph B3 EphB4, EphB6
ephrin-B2, ephrin-B3
EphB5
ephrin-B1

C

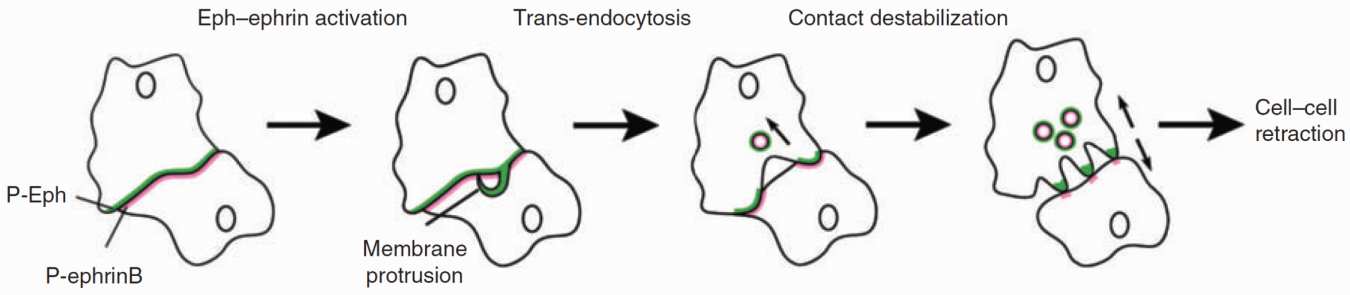
Eph–ephrin activation
Trans-endocytosis
Contact destabilization
P-Eph
P-ephrinB
Membrane protrusion
Cell–cell retraction

response (Carvalho *et al.*, 2006). However, it has also been reported that coexpressed EphA and ephrinA molecules segregate into distinct membrane domains with opposing functional roles in cell adhesion and repulsion: EphA receptors direct growth cone collapse and repulsion, and ephrinA ligands direct growth and attraction (Marquardt *et al.*, 2005). This allows co-expressed EphA receptors and ephrinA ligands on the same cell surface to avoid reciprocal silencing by localising to distinct membrane microdomains (Marquardt *et al.*, 2005).

The degree of clustering is important for the nature of the response (Huynh-Do *et al.*, 1999; Stein *et al.*, 1998). Low levels of forward Eph signalling can mediate attractive effects that change to repulsion when signalling increases (Hansen *et al.*, 2004), so the degree of clustering might change the balance of opposing signalling pathways. Furthermore, reverse signals through the ephrins, particularly the ephrinA ligands, favour attractive effects more than Eph signals do (Pasquale, 2005).

1.1.5.2 Contacts cause repulsion

Eph-ephrin signalling mediates contact-dependent cell interactions that are implicated in repulsion mechanisms important for the guidance of migrating cells and neuronal growth cones and in restricting the intermingling of cells between adjacent tissue domains (Poliakov *et al.*, 2004). However, the regulation of repulsion by a membrane-bound receptor-ligand system presents a paradox: how does the extensive clustering and high-affinity binding of Eph receptors and ephrins result in a contact-mediated repulsion response? Possible solutions to this paradox are ectodomain cleavage and endocytosis.

Cell-cell detachment can occur by proteolytic cleavage of the extracellular domain of the ephrin by ADAM-10 (A-Disintegrin-And-Metalloprotease). Interaction of ephrinA2 with EphA3 activates ADAM-10, which cleaves the extracellular domain of the ephrin (Hattori *et al.*, 2000). ADAM-10 constitutively binds to ephrinA2 in *cis* and cleavage is only initiated on binding of EphA. It has also been shown that ADAM-10 can stably bind EphA3 such that ephrinA2 is cleaved in *trans* only after binding to EphA3 (Janes *et al.*, 2005). Cytoskeletal collapse is initiated in parallel with the cleavage of the ephrin, leading to disengagement of the cells (Poliakov *et al.*, 2004). In addition, ADAM-13 is known to have a similar role in the cleavage and attenuation of ephrinB1 and ephrinB2 signalling (Wei *et al.*, 2010).

A second mechanism to enable the detachment of cells involves the endocytosis of the Eph-ephrin signalling complex from the cell membrane into either the Eph- or ephrin-expressing cell (Marston *et al.*, 2003; Zimmer *et al.*, 2003). The endocytosed complex contains full-length proteins and possible associated proteins, so either the Eph or ephrin is *trans*-endocytosed into the opposing cell. Eph receptor endocytosis might regulate cell retraction by simply enabling cells to disengage or it might be directly responsible for switching the response to ephrin interaction from attractive to repulsive (Fig. 4 C).

The direction of endocytosis is determined by Eph-ephrin mediated signal transduction: signalling-deficient EphB2 (lacking the cytoplasmic region) directs endocytosis of the Eph-ephrin complex into the adjacent ephrinB1 expressing cell, and *vice versa*. Truncation of both EphB2 and ephrinB1 prevents internalisation and strongly prolongs cell-cell contact (Zimmer *et al.*, 2003). Both endocytosis and cell retraction require actin polymerisation and the activity of the small GTPase Rac1 (Marston *et al.*, 2003). Signalling from the internalised Eph-ephrin complex persists after *trans*-endocytosis, and active signal transduction might be shifted into the Eph-expressing cell (Marston *et al.*, 2003). In addition, the Rac exchange factor Vav has been implicated in EphB-mediated endocytosis (Cowan *et al.*, 2005), and reverse endocytosis of ephrinB ligands depends on the clathrin-mediated pathway (Parker *et al.*, 2004).

1.1.6 Multiple roles of Eph-ephrin signalling

Eph receptors and ephrins are highly versatile regulators of processes as diverse as modulation of synaptic plasticity, cell sorting and migration in the intestinal crypt, and the morphogenesis of the vascular system. However they are best understood as patterning and axon guidance molecules in the nervous system (Flanagan & Vanderhaeghen, 1998; Kullander & Klein, 2002).

Growth cones at the distal ends of growing axons respond to repulsive or attractive guidance cues in their environment to ensure correct directional migration of axons. Eph receptor activation in growing neurons typically leads to a growth cone collapse response from an ephrin-expressing substrate (Pasquale, 2005; Poliakov *et al.*, 2004), but adhesive and attractive responses can also occur; for example, ephrinB1 can repel or attract different populations of EphB-expressing neural crest cells (Santiago & Erickson, 2002). Eph receptors and ephrins can sometimes be expressed in a gradient to allow neurons to respond differentially to repellent cues (Klein, 2004). On reaching their targets, the growth cone is converted into a presynaptic terminal. Synapse maturation requires Eph-ephrin molecules and is strongly linked to internalisation processes (Klein, 2009).

Eph receptors regulate cell morphology and behaviour by rearranging the cytoskeleton and Eph-ephrin bidirectional signalling is frequently coupled to the Rho family of GTPases: Cdc42, Rac1 and RhoA (Groeger & Nobes, 2007; Noren & Pasquale, 2004b). Rac1 activation is required for Eph-ephrin induced membrane ruffling, lamellipodia formation, *trans*-endocytosis and cell repulsion (Marston *et al.*, 2003). Cdc42 promotes the formation of filopodia and dendritic spines and RhoA regulates actin dynamics, cell contractility and is involved in Eph-induced growth cone collapse (Pitulescu & Adams, 2010).

Rho GTPases function as molecular switches that switch between a GDP-bound inactive state and a GTP-bound active state in which they bind and activate downstream effectors. Guanine nucleotide exchange factors (GEFs) catalyse the exchange of bound GDP for GTP, and GTPase-activating proteins

(GAPs) activate the intrinsic GTPase activity of the Rho GTPases. One of the mechanisms by which Eph receptors mediate their functions in neurons is the direct recruitment of GEFs.

Growth cone collapse is mediated by binding of ephexin with EphA receptor. Ephexin1 (Eph-interacting exchange protein-1) is a Rho GEF that constitutively binds to EphA receptors, enabling the activation of Rho (Sahin *et al.*, 2005; Shamah *et al.*, 2001). Other GEFs, such as the Vav proteins (Vav1-3) have no binding preferences to type A or B Eph receptors and bind to activated, tyrosine phosphorylated Eph receptors through the Src homology 2 domain (Cowan *et al.*, 2005). These GEFs differ in their functions downstream of Eph receptors.

In the absence of ephrins, Eph-bound ephexin activates Rac1, RhoA and Cdc42 in the growth cone so stimulating outgrowth. Ephrin stimulation of Eph induces tyrosine phosphorylation of ephexin (probably by Src), which enhances exchange specificity towards RhoA so promoting growth cone collapse (Knoll & Drescher, 2004). In synapse formation, another family member ephexin5, constitutively binds EphBs causing RhoA activation and inhibition of synapse development. Binding of ephrinB to EphB, triggers the phosphorylation and degradation of ephexin5, so allowing EphB signalling to activate Rac for synapse development (Margolis *et al.*, 2010).

Vav2 can bind the intracellular region of EphA4 and EphB2 and is tyrosine phosphorylated in response to ephrin binding. Phosphorylation of Vav2 promotes local Rac1-dependent endocytosis of the ephrin-Eph complex (Cowan *et al.*, 2005), so converting the initial adhesive interaction to repulsion and mediating growth cone collapse. In contrast to EphA receptors, internalisation of activated EphB receptors correlates with the recovery of retracted cells rather than the retraction phase itself, and is required for the recovery of cells to a fully spread morphology (Groeger & Nobes, 2007). Rho and Cdc42 function, in a complementary way, to mediate ephrinB2-induced cell retraction, but recovery to a fully spread morphology requires functioning Rac and the internalisation of ephrin–Eph complexes (Groeger & Nobes, 2007). This highlights differences between the EphB and A signalling pathways (Cowan *et al.*, 2005).

Eph-ephrin signalling also plays a role in cell migration, as well as axon guidance, and the removal of activated Eph receptors from the membrane may be important in enabling cells to continue migrating after a temporary Eph-mediated contact-inhibition response. In addition, the binding of Eph receptors to adaptor proteins including Nck, Crk (Poliakov *et al.*, 2004) and Dishevelled (Tanaka *et al.*, 2003), leads to modulation of Rho family GTPase signalling in other contexts. Tiam1, a Rac1 GEF, is also known to play a role in Eph/ephrin endocytosis and neurite outgrowth (Pitulescu & Adams, 2010).

Transmembrane ephrinB reverse signalling is important for several processes such as axon guidance, cell migration, midline fusion, plasticity and synaptogenesis (Egea & Klein, 2007). EphrinB proteins are activated by clustering, which causes the recruitment and activation of Src family kinases that can

phosphorylate specific tyrosine residues of the ephrinB cytoplasmic domain. Phosphorylated ephrinB acts as a docking site for SH2-containing adaptor proteins, such as Grb4, which can activate signalling pathways that can lead to changes in the actin cytockeleton and focal adhesion (Cowan & Henkemeyer, 2001). Interestingly, recent evidence has identified that ephrins have an intrinsic signalling potential independent of phosphorylation by Eph receptors. Dishevelled, for example, has been shown to bind directly to the cytoplasmic tail of ephrinB1, or indirectly via Grb4 (Fig. 6 A) (Tanaka *et al.*, 2003). In X*enopus*, Dishevelled association with ephrinB1 mediates reverse signalling through the planar cell polarity (PCP) pathway (Boutros & Mlodzik, 1999) in migrating retinal progenitor cells during eye field formation (Lee *et al.*, 2006), independently of phosphorylation by EphB2.

Taken together, the complementary and combinatorial expression pattern of Eph receptors and ephrins in their *in vivo* contexts combined with both biochemical mechanisms of regulation, such as cleavage, endocytosis and clustering, and the ability of both Eph receptors and ephrins to interact with multiple downstream signalling pathways, allows versatile and diverse cellular responses in different developmental situations. This complexity allows multiple roles as regulators of repulsion, adhesion and migration.

1.1.6.1 Motility

Cell migration is critical for many processes such as wound healing and embryonic morphogenesis. Abnormal cell migration contributes to disease processes such as tumour invasion and metastasis. Eph receptors and ephrins have recently emerged as important regulators of cell motility, and a deregulation of Eph receptor and ephrin expression and/or Eph-ephrin signalling has been shown to play a role in cancer progression and metastasis (Pasquale, 2010).

In the small intestine, EphB receptors and ephrinB ligands are expressed in opposite gradients and their compartmentalised expression contributes to the migration and positioning of epithelial cells along the crypt-villus axis (Batlle *et al.*, 2002). Studies in cell culture have shown a complex regulation of motility by combinations of Eph receptors and ephrins. *In vitro* migration assays show that endothelial cells expressing ephrinB2 are attracted toward the EphB4-expressing tumour cells, and that signalling downstream of ephrinB2 may play a role in endothelial cell migration (Noren *et al.*, 2004a). Recent evidence has suggested a role of endocytosis and activation of VEGF receptors downstream of ephrinB2 in this process (Sawamiphak *et al.*, 2010; Wang *et al.*, 2010). In addition, EphB3-ephrinB1 interaction has been shown to suppress epithelial cell migration, mediated by an inhibition of Rac1 and Cdc42 and a relocalisation from the leading edge, allowing enhanced RhoA activity that inhibits migration (Miao *et al.*, 2005).

Ephrins have also been shown to have cell autonomous functions and be required for directional migration; for example, loss of ephrinB2 causes random migration, unstable lamellipodial protrusions and cell detachment at the rear of the migrating cell is compromised (Foo *et al.*, 2006). Analysis of ephrinB2- and ephrinB1-expressing freely migrating cells have shown an increase in migration speed and a decrease in the persistence of directional migration (Bochenek *et al.*, 2010), although this response is cell type specific.

In addition, the role of Eph-ephrin signalling as a potential regulator of contact inhibition of locomotion (CIL) has been analysed (Astin *et al.*, 2010). CIL is the "the stopping of the continual locomotion of a cell in the same direction after collision with another cell" (Abercrombie, 1970), and the fact that Eph-ephrins are activated by cell-cell contacts and control cell movements by regulating the cytoskeleton makes them possible mediators. Rac1 and Cdc42 can regulate an attractive EphB-ephrinB response by locally stimulating actin polymerisation and maintaining the direction of polarised migration; for example EphB3 and EphB4 receptors are required for Cdc42-directed migration towards ephrinB2 ligand (Astin *et al.*, 2010). In addition, EphB receptors can have an opposing function in mediating repulsion; EphB2 mediates repulsion triggered by ephrinB1 in prostate cancer cells (Astin *et al.*, 2010) and EphB4-ephrinB2 signalling has been shown to mediate cell repulsion in fibroblasts and endothelial cells (Marston *et al.*, 2003). Forward EphA signalling via activation of RhoA at the site of cell contact is necessary for homotypic CIL in prostate cancer cells. RhoA activation may cause a loss in forward migration due to membrane withdrawal at the front, the concurrent inhibition of Rac and loss of leading lamella (Astin *et al.*, 2010), or by local Rho-ROCK disruption of cell polarity (Nakayama *et al.*, 2008). Taken together, these results suggest an integrated response to repulsive EphA versus attractive EphB3/EphB4 or repulsive EphB4/EphB2 pathways in different cellular contexts, allowing a broad range of behaviours.

1.1.7 What underlies Eph-ephrin mediated cell sorting?

As previously described, embryo explant experiments show complementary populations of cells transiently overexpressing an Eph and its cognate ephrin are sufficient to drive and maintain segregation of the populations (Fig. 2 B, B') (Mellitzer *et al.*, 1999; Tanaka *et al.*, 2003). These previous approaches have the disadvantage that overexpression itself and the presence of endogenous ligands lead to high baseline activation of receptor. EphB receptors have been shown to become autoactivated and autophosphorylated by overexpression (Tanaka *et al.*, 2003) and ephrinB2 and ephrinB1 have been shown to signal in a cell autonomous mode in the absence of receptor binding (Bochenek *et al.*, 2010; Lee *et al.*, 2006). Overexpression of ephrinB2 can lead to increased motility and trigger repeated cycles of cell contraction and respreading, but activation by EphB4 leads to a sustained response that is terminated by ligand internalisation (Bochenek *et al.*, 2010). This suggests different signalling responses can be initiated depending on the presence or absence of cognate receptors and on the expression levels. Recent segregation assays in cell culture with stable HEK293 cell lines overexpressing either EphB2 or ephrinB1,

Figure 5: EphB2-ephrinB1 signalling can drive cell segregation and a collapse response

(A): EphB2-ephrinB1 signalling leads to EphB2 cell segregation from ephrinB1 cells in a cell culture segregation assay (A). Perturbation of Eph-ephrin signalling causes disruption to cell segregation (A') (adapted from (Poliakov *et al.*, 2008)).

(B): EphB2-expressing cells undergo a collapse response after interaction with an ephrinB1-expressing cell. An EphB2+GFP cell (green) is not repelled and remains in contact with an EphB2 cell (grey) after interaction (B), whereas an EphB2+GFP cell (green) rapidly retracts and rounds up after touching an ephrinB1 cell (grey) (B') (adapted from (Poliakov *et al.*, 2008)).

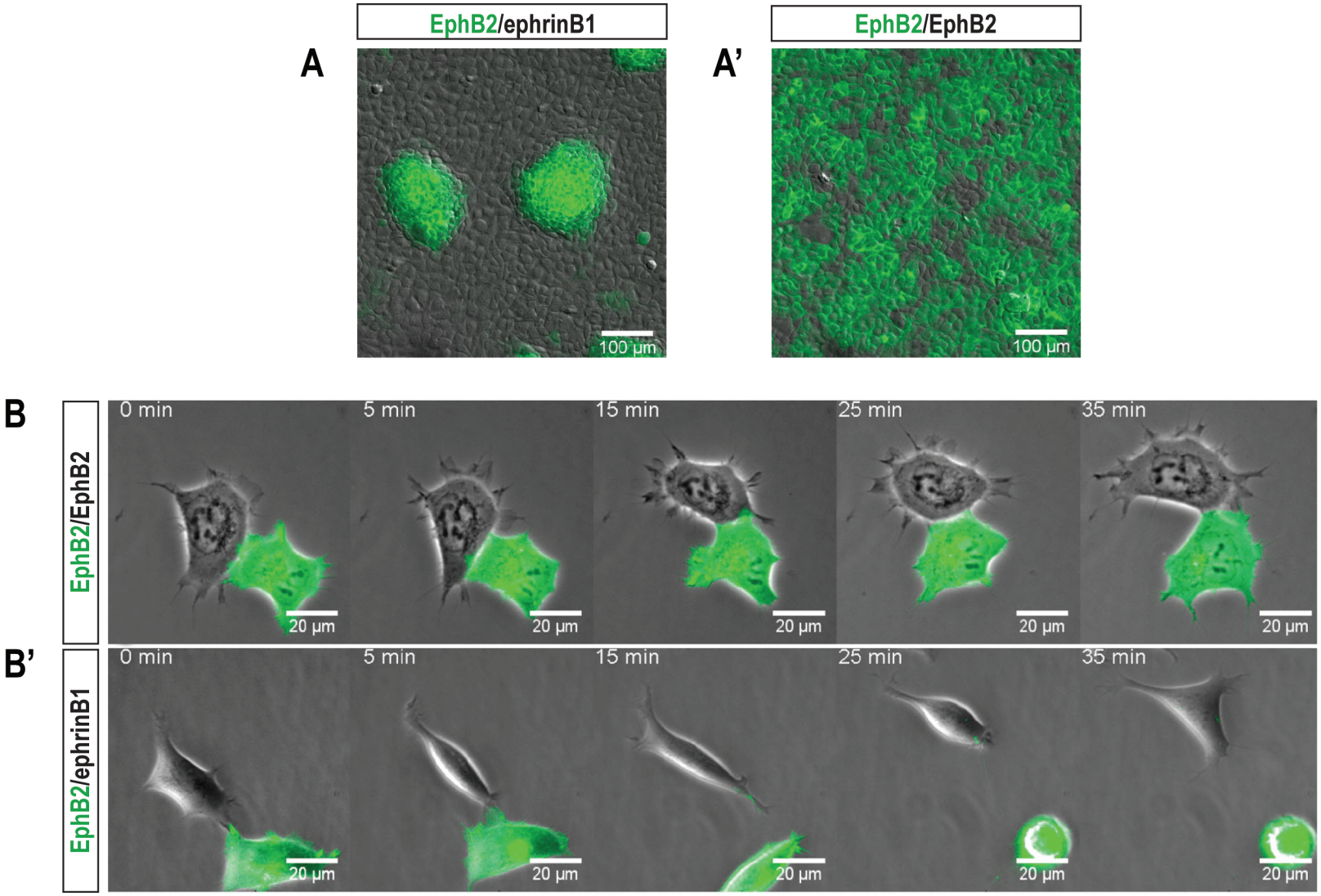
A
EphB2/ephrinB1
100 µm
A'
EphB2/EphB2
100 µm
B
EphB2/EphB2
0 min
5 min
15 min
25 min
35 min
20 µm
B'
EphB2/ephrinB1
0 min
5 min
15 min
25 min
35 min
20 µm

but with low levels of endogenous EphB or ephrinB proteins, showed little receptor autoactivation and lead to segregation of EphB2 cells from ephrinB1 cells (Fig. 5 A, A') (Poliakov *et al.*, 2008). In addition, EphB2 cells showed a rapid collapse of cell processes after interaction with ephrinB1 cells, but not EphB2 cells (Fig. 5 B, B') (Poliakov *et al.*, 2008). Taken together, these assays show that Eph-ephrin signalling leads to segregation of EphB2 cells from ephrinB1, and repulsion and collapse responses of EphB2 cells to ephrinB1 cells.

Recent evidence has shown a role for EphB-ephrinB signalling in controlling *Xenopus* embryonic germ layer separation by cycles of transient adhesion and contact-induced cell detachment (Rohani *et al.*, 2011). Adhesion brings ephrins and Ephs into contact, inducing a Rac- and RhoA-based repulsion, which decays after segregation, so allowing re-adhesion. Two antiparallel forward signals are sufficient for complete repulsion at the boundary, and local activation of RhoA and Rac suggests Eph-ephrin signalling is activated only at the boundary, despite the widespread co-expression of receptors and ligands. Regulation of tissue cohesion by Eph-ephrin signalling is independent of the control of tissue segregation. This mechanism prevents invasion of mesoderm cells into the blastocoel roof, whilst providing substrate contacts for migration (Rohani *et al.*, 2011), and demonstrates a role of Eph-ephrin signalling in regulating dynamic adhesion and repulsion.

Separating the roles of adhesion and repulsion is difficult, and different mechanisms may have distinct roles in different contexts. In epithelial cells E-cadherin is required for EphA2 receptor localisation at cell-cell contacts, and is either directly or indirectly required for the membrane localisation of Eph receptors and ephrins (Orsulic & Kemler, 2000). EphB signalling has also been shown to couple cell contraction with cell-to-cell adhesion by promoting the recruitment of E-cadherin to the membrane of epithelial tumour cells, and segregation of cell lines expressing EphB3 and ephrinB1 was severely impaired when E-cadherin was knocked down, suggesting that adhesion plays a role in Eph-ephrin mediated cell sorting (Cortina *et al.*, 2007). In addition, EphB2 signalling in Schwann cells induces cell sorting, at least in part by the redistribution of N-cadherin to cell-cell contacts (Parrinello *et al.*, 2010).

The downstream mechanisms and signalling pathways that control Eph-ephrin mediated cell sorting and boundary formation are not well understood, but recent evidence has identified many downstream signalling components that are phosphorylated on Eph-ephrin signalling, some of which may play a role in cell sorting (Jorgensen *et al.*, 2009; Zhang *et al.*, 2008a). The large-scale screen of Jorgensen *et al.* used proteomic approaches to identify cell-specific phosphorylation events upon interaction of EphB2 and ephrinB1 cells, and used the *in vitro* segregation assay developed in the Wilkinson lab (Fig. 5 A) (Poliakov *et al.*, 2008). Functional associations between specific phosphotyrosine signalling events and cell sorting were established with a small interfering RNA (siRNA) screen in the same assay. This identified many components downstream of EphB2-ephrinB1 signalling that are involved in a wide variety of cellular

functions: adhesion, polarity (PAR-3, PAR-6), lipid signalling, actin and myosin turnover, endocytosis and recycling and adaptor proteins (Jorgensen *et al.*, 2009). Their individual roles have yet to be determined.

A key issue is to identify the downstream pathways by which Eph-ephrin signalling inhibits cell mixing across boundaries, in order to understand the processes that lead to boundary sharpening. In addition to specific components identified in the Jorgensen *et al.* screen, a further candidate pathway is the planar cell polarity pathway (Lee *et al.*, 2006; Tanaka *et al.*, 2003).

1.2 Planar cell polarity (PCP)

Planar cell polarity (PCP) was first described as a global, tissue-level phenomenon that coordinates cell behaviour in the plane of an epithelium. A global directional cue converts tissue gradients to subcellular asymmetry, and cellular factors interpret this cue to align cells with each other and the axis of polarity (Zallen, 2007). Spatial information that organises PCP is transmitted locally from one cell to the next and can influence both the behaviour and orientation of groups of cells. Original evidence for epithelial planar polarity came from studies of the pupal wing and compound eye in *Drosophila.* The fly wing has a hexagonally packed epithelial layer in which a single bristle points distally from the distal side of each cell, and the fly eye is a lattice of repeating ommatidia, each containing eight photoreceptor cells, the asymmetric arrangement of which imparts chirality. In vertebrate epithelia, PCP is known to regulate the orientation of the inner ear sensory hair cells, skin follicles and motile cilia in multiciliated epithelia (reviewed in (Vladar *et al.*)).

A set of evolutionary conserved core PCP genes are involved in establishing and communicating asymmetric subcellular polarity both within and between cells. The core PCP pathway consists of the cell-surface proteins Frizzled, Van Gogh (or Strabismus) and Flamingo (or Starry night), and the cytoplasmic proteins Dishevelled, Prickle, and Diego (Zallen, 2007). The core PCP proteins are first recruited to the apical cell surface and subsequently segregate into complementary apical subdomains before the onset of hair formation; Flamingo localises to proximal and distal surfaces whereas Van Gogh and Prickle become proximally enriched at cell junctions and Frizzled, Dishevelled and Diogo become distally enriched (reviewed in (Zallen, 2007)). Mutual inhibition between Frizzled/Dishevelled and Van Gogh/Prickle complexes is proposed to cause and maintain an asymmetric distribution, and this intracellular feedback at the interface of neighbouring cells may involve regulated vesicle trafficking. Evidence for communication of polarity between cells is shown by dominant nonautonomy, a phenomenon in which wildtype epithelial cells adjacent to a clone of PCP mutant cells exhibit a misorientation in polarity (Wang & Nathans, 2007), and this is mediated by PCP-dependent cytoskeletal rearrangements (Eaton *et al.*, 1996).

A second group functions downstream of these genes, for example E-cadherin, RhoA, Daam1 (Dishevelled-associated activator of morphogenesis 1), Inturned and Fuzzy, which couple signalling from

core proteins to a cell-type-specific response (Zallen, 2007). The signal that directs the asymmetry with respect to the tissue axis, i.e. the global polarity cue, remains unclear but evidence suggests a link with the Wnt family of secreted glycoproteins. The PCP (non-canonical Wnt) pathway is just one of several pathways downstream of Wnt intracellular signalling, that include the ß-catenin (canonical Wnt) pathway, which activates target genes in the nucleus, and the Wnt/Ca^{2+} pathway (Huelsken & Birchmeier, 2001). PCP is complicated in vertebrates by the existence of multigene families of PCP proteins, of which some function redundantly. There is one Dishevelled gene in Xenopus (Dsh) but three homologues in mammals (Dvl1, Dvl2, Dvl3). However, both the PCP proteins and patterns of asymmetric localisation are conserved (Vladar *et al.*, 2009).

Dishevelled is a component of Wnt-Frizzled signalling that regulates two pathways through distinct protein domains. The DIX (Dishevelled-Axin) domain of Dishevelled is required to activate the canonical β-catenin-TCF-Wnt signalling pathway that regulates target gene transcription. The DEP (Dishevelled-EGL-10-Plexkstrin) domain and the PDZ domain are essential for Dishevelled's function in the PCP pathway, and the DEP domain is essential for the recruitment of Dishevelled to the cell membrane by binding to specific Frizzled receptors (Fig. 6 A) (Boutros & Mlodzik, 1999; Poliakov *et al.*, 2004). Membrane localisation of Dishevelled is thought to be one of the key processes in the establishment of PCP (Axelrod *et al.*, 1998), presumably leading to the formation of a functional complex (Tada *et al.*, 2002).

The PCP pathway branches at the level of Dishevelled and involves a Daam1-RhoA- or JNK-Rac-dependent pathway (Boutros *et al.*, 1998; Gao & Chen, 2010). The formin homology protein Daam1 can bind the DEP domain of Dishevelled and interact with WGEF (RhoA GEF), leading to activation of RhoA and ROCK and remodelling of the cytoskeleton (Fig. 6 A). Daam1 function is required for RhoA activation and gastrulation movements in *Xenopus* embryos (Habas *et al.*, 2001). PCP signalling through Daam1 has also been shown to coordinate cell growth and migration in endothelial cells, predominantly through microtubule assembly and stabilisation (Ju *et al.*, 2010). In addition, Dishevelled can activate Rac1, which stimulates its downstream effector JNK to regulate cell polarity and movements during *Xenopus* gastrulation in a Rho/Daam-independent manner (Habas *et al.*, 2003). Rac1 directs lamellipodia formation and focal complex formation via JNK at the leading edge of cells (Ridley *et al.*, 2003), and so suggests a role for PCP in the migration of cells.

Recent evidence has suggested a signal-dependent degradation mechanism for the control of the asymmetric distribution of PCP components. PAR-6 is engaged in a trimeric complex with Prickle and Dishevelled that recruits Smurf ubiquitin ligase (in a phosphorylation dependent manner) to Dishevelled in response to Frizzled signalling. This leads to Prickle ubiquitination and degradation, and so PCP controls the asymmetric distribution of Prickle (Narimatsu *et al.*, 2009). Although Wnt stimulation induces Dishevelled phosphorylation, the role of phosphorylation remains incompletely understood (Gao & Chen, 2010).

Figure 6: Planar cell polarity and core PAR polarisation

(A): Relationships between the canonical Wnt pathway, planar cell polarity (PCP) pathway and ephrinB1 are linked at the level of Dishevelled. Interacting components are linked with blue lines. Different domains of Dishevelled are required for activation of the canonical Wnt pathway and the PCP pathway. Localisation of Dishevelled at the cell membrane is required for activation of the PCP pathway and this can be achieved by interaction of the DEP domain of Dishevelled with Frizzled or ephrinB1 (adapted from (Poliakov & Wilkinson, 2006)).

(B): Front-rear polarisation of migrating epithelial cells, such as astrocytes and fibroblasts. Polarity proteins of the partitioning defective (PAR), Scribble and Crumbs−3 complexes, the small GTPases Cdc42, Rac1 and some of their regulator proteins are localised and activated at the leading edge. Active RhoA and its effector proteins localise mainly to the trailing edge (adapted from (Iden & Collard, 2008)).

(C): Crosstalk between small GTPases and polarity proteins controls front–rear polarisation of epithelial cells, astrocytes and fibroblasts. Relationships are shown between different signalling components at the leading edge of migrating cells (adapted from (Iden & Collard, 2008)).

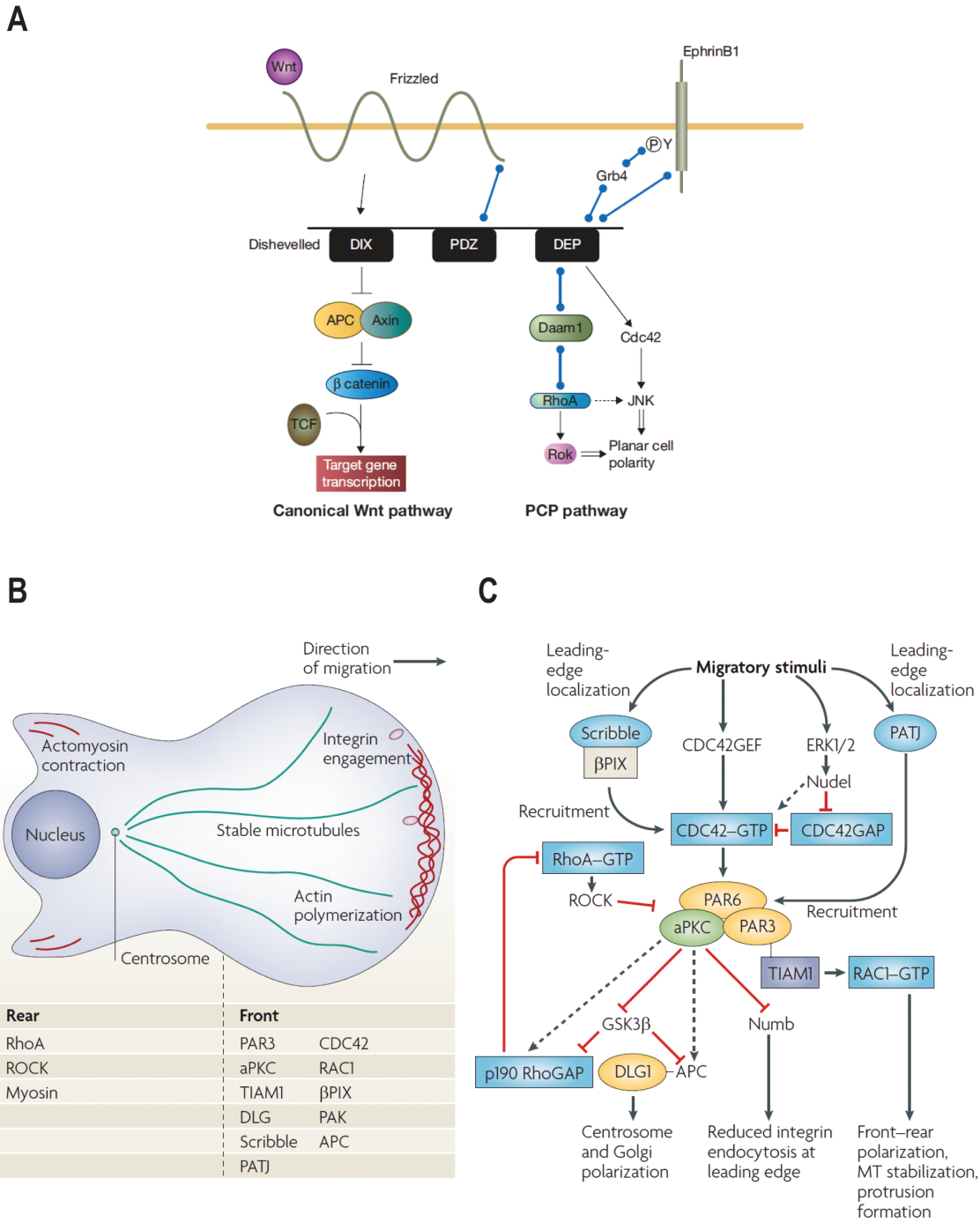
A
Wnt
Frizzled
EphrinB1
Ⓟ Y
Grb4
Dishevelled
DIX
PDZ
DEP
APC
Axin
β catenin
TCF
Target gene transcription
Daam1
Cdc42
RhoA
JNK
Rok
Planar cell polarity
Canonical Wnt pathway
PCP pathway
B
Direction of migration
Actomyosin contraction
Integrin engagement
Nucleus
Stable microtubules
Actin polymerization
Centrosome
Rear
RhoA
ROCK
Myosin
Front
PAR3
aPKC
TIAM1
DLG
Scribble
PATJ
CDC42
RAC1
βPIX
PAK
APC
C
Migratory stimuli
Leading-edge localization
Leading-edge localization
Scribble
βPIX
CDC42GEF
ERK1/2
Nudel
PATJ
Recruitment
CDC42–GTP
CDC42GAP
RhoA–GTP
ROCK
PAR6
aPKC
PAR3
Recruitment
TIAM1
RAC1–GTP
GSK3β
Numb
p190 RhoGAP
DLG1
APC
Centrosome and Golgi polarization
Reduced integrin endocytosis at leading edge
Front–rear polarization, MT stabilization, protrusion formation

1.2.1 Asymmetric cell division/orientation

PCP is also involved in oriented cell division, asymmetric cell morphology and axon guidance (reviewed in (Vladar *et al.*, 2009)). Interestingly, the role of PCP in these processes involves interactions with core polarity components, such as the PAR proteins, that are involved in establishing cellular polarity. The generation of sensory bristles in the *Drosophila* epidermis requires the asymmetric division of sensory organ precursor cells along the A-P axis. Van Gogh/Prickle and Frizzled/Dishevelled complexes localise to opposite membrane domains along the A-P axis, and on entry into mitosis, Frizzled/Dishevelled recruits PAR-3/PAR-6/aPKC complex posteriorly to regulate spindle orientation (Vladar *et al.*, 2009). In addition, PCP signalling has been shown to control the orientation of cell divisions during gastrulation (Gong *et al.*, 2004).

1.2.2 Convergent Extension

PCP genes have been shown to play a role in the morphogenetic process of convergent extension, which is the process of medio-lateral narrowing (convergence) and anterior-posterior elongation (extension) of vertebrate embryos during gastrulation (Wallingford *et al.*, 2002a). Mutation of core PCP proteins, such as Dishevelled, disrupts embryonic axis formation without affecting cell fate in zebrafish and *Xenopus* embryos (Tada & Smith, 2000; Wallingford *et al.*, 2000). PCP controls convergent extension of mesoderm during gastrulation by causing a directional activity of the lamellipodia that favours movement in one direction (Carreira-Barbosa *et al.*, 2003; Wallingford *et al.*, 2000).

Studies in *Xenopus* have shown non-canonical Wnt5a and Wnt11 signalling to be important in convergent extension through two different signalling cascades. Wnt5a signalling is mediated via Dishevelled by the JNK signalling pathway involving PI3K, Cdc42 and JNK. Wnt11 interacts with Frizzled7 and induces accumulation of Dishevelled at the membrane (Witzel *et al.*, 2006), activating Daam1 (Habas *et al.*, 2001), WGEF (weak-similarity guanine nucleotide-exchange factor) and RhoA, leading to formation of focal adhesion complexes and stress fibres (Tanegashima *et al.*, 2008; Zhu *et al.*, 2006). Wnt11 has also been shown to affect cell adhesion through control of E-cadherin subcellular localisation (Ulrich *et al.*, 2005; Witzel *et al.*, 2006). Wnt11 has also been shown to act as a directional cue to organise the orientation and elongation of early muscle fibres (Gros *et al.*, 2009).

1.2.3 PCP and directional migration

Other cell migration processes require directed motility over large distances in comparison to convergent extension. PCP has been implicated in the directional migration of some neurons (Bingham *et al.*, 2002; Wada & Okamoto, 2009) and neural crest cells (Carreira-Barbosa *et al.*, 2003; De Calisto *et al.*, 2005;

Matthews *et al.*, 2008), and is involved in regulation of cytoskeletal changes, cell adhesion, protrusive membrane activity and directional migration.

The role of PCP in neural crest migration is particularly interesting as Wnt11, Dishevelled, Prickle and Van Gogh are required for the CIL of neural crest cells, in which a cell becomes polarised and sustains directional migration away from contact with another neural crest cell (Fig. 7 A) (Carmona-Fontaine *et al.*, 2008). Wnt11, Frizzled7 and Dishevelled accumulate at the site of cell-cell contact and RhoA is activated causing lamellipodia inhibition and repolarisation of the cell. PCP may therefore function in initiating migration away from points of cell-cell contact, and activation of RhoA by PCP signalling is required for the delamination and/or migration of neural crest cells, whereas canonical Wnt signalling is required for induction (Carmona-Fontaine *et al.*, 2008; De Calisto *et al.*, 2005).

Both Daam1 and Dishevelled have been shown to play a role in intracellular polarity by regulating centrosome orientation in monolayer scratch assays (Ang *et al.*, 2010; Schlessinger *et al.*, 2007), which is important for directionality of migration. The involvement of Daam1 at the centrosome (Ang *et al.*, 2010) potentially links the PCP machinery to core polarity components: PAR-6, Cdc42 and aPKC (Etienne-Manneville & Hall, 2003; Schlessinger *et al.*, 2007). Daam1 knockdown cells show multiple protrusions, with a less organised microtubule network, and randomised Golgi orientation at the wound edge (Ang *et al.*, 2010) and in parietal endoderm migration (LaMonica *et al.*, 2009). This results in a Rac1-independent loss of directionality during cell migration (Ang *et al.*, 2010; LaMonica *et al.*, 2009), and an increase in speed for parietal endoderm migration (LaMonica *et al.*, 2009). ROCK inhibition also leads to an increase in migration in a non-persistent and random manner (LaMonica *et al.*, 2009). These cells show disruption to microtubule orientation and increased filopodial protrusions with few focal adhesions (LaMonica *et al.*, 2009). This could account for the increase in migration speed due to a loss in cell-extracellular matrix interactions. Taken together, this evidence suggests that cell orientation and migration can be directed by the PCP pathway acting via RhoA.

1.2.4 Eph-ephrin signalling and PCP

Connections between Eph-ephrin signalling and PCP have been described in multiple tissues and have been shown to have a role in different morphogenetic processes, such as cell segregation and migration (Kida *et al.*, 2007; Lee *et al.*, 2006; Tanaka *et al.*, 2003). The effect of inhibiting Dishevelled or Daam1, using truncated forms of Dishevelled (specifically disrupting the PCP pathway) and Daam1 morpholinos, has suggested that the PCP pathway is required for *in vitro* cell segregation (Tanaka *et al.*, 2003) and for the migration of cells into the *Xenopus* eye field (Lee *et al.*, 2006), described below.

Dishevelled mediates the forward and reverse signalling of EphB2 and ephrinB1 leading to the activation of RhoA during the segregation of EphB2-expressing cells from ephrinB1-expressing cells in an *in vitro*

aggregation assay (Tanaka *et al.*, 2003). Dishevelled interacts with the C-terminal region of tyrosine-phosphorylated EphB1/2 (auto-activated) or ephrinB1 (EphB2-stimulated) via association with the adaptor protein Grb4, causing phosphorylation of the tyrosine residues of Dishevelled (Fig. 6 A) (Tanaka *et al.*, 2003). Dishevelled can also be constitutively recruited directly to unphosphorylated ephrinB1, but this interaction does not activate RhoA. Dishevelled has also been shown to play a role in the patterning of the *Xenopus* hindbrain, as expressing dominant-negative Dishevelled (specifically disrupting the PCP pathway) causes irregular shaped and distorted rhombomeres 3 and 5. This disruption to hindbrain segmentation is thought to be independent of convergent extension (Tanaka *et al.*, 2003).

Both JNK and RhoA are required downstream of ephrinB1 for cell migration to the *Xenopus* eye field, whereas the Eph forward signalling and the canonical Wnt pathway are not required (Lee *et al.*, 2006). By testing whether different deletion mutants of Dishevelled can rescue the effects of Dishevelled knockdown, it was demonstrated that the DEP domain is essential for normal Dishevelled function in this process. Furthermore, the DEP domain interacts with the C-terminal region of ephrinB1 leading to localisation of Dishevelled at the cell membrane, a hallmark of PCP signalling (Fig. 6 A) (Lee *et al.*, 2006). Activation by Eph receptor or FGF receptor can block the interaction between ephrinB1 and Dishevelled through tyrosine phosphorylation of ephrinB1, and inhibit the migration of cells (Lee *et al.*, 2009). Wnt11, a PCP pathway activator, and ephrinB1 act in parallel and normal levels of expression of both are required for correct migration (Lee *et al.*, 2006). Interestingly, convergent extension movements that require activation of the PCP pathway by Wnt11 (Wallingford *et al.*, 2002a) are also disrupted on knockdown of ephrinB1 (Lee *et al.*, 2006).

In addition, Daam1 forms a complex with phosphorylated EphB receptor and Dishevelled2, the dynamin-dependent internalisation of which is required for convergent extension of the zebrafish notochord and axis formation (Kida *et al.*, 2007). The role of Daam1 as a dynamic coordinator of endocytosis and cytoskeletal remodelling is shown as the Daam1-dependent endocytosis of this complex induces cell repulsion, and at later stages the association of Daam1 with the actin cytoskeleton suggests a role in cell elongation required during convergent extension (Kida *et al.*, 2007).

These data suggest a number of mechanisms that link Eph-ephrin signalling and PCP. Eph-ephrin signalling could activate the PCP pathway and recruit Dishevelled to the site of cell contact. This could promote directional migration of ephrin cells away from Eph-expressing territory. A second possibility is that constitutive activation of the PCP pathway by ephrinB1 is blocked by interaction with Eph receptor, which could occur in two ways. Firstly, after binding of Eph with ephrin the complex is endocytosed, so removing ephrin-bound Dishevelled from the membrane, and down-regulating the PCP pathway and enabling repulsion. Secondly, Eph-ephrin interaction could prevent/remove Dishevelled from binding by phosphorylation of the tyrosine residues of ephrinB1. PCP inactivation at the site of Eph-ephrin interaction

could antagonise migration promoted by non-activated ephrinB1, and contribute to the restriction of intermingling (Poliakov & Wilkinson, 2006).

It is important to note that ephrinB1 signalling has recently been linked to the Wnt canonical signalling pathway in *Xenopus*, as ADAM13 cleavage of ephrinB1/2 is required for the activation of canonical signalling. Extracellular cleavage of ephrin by ADAM13 inhibits the PCP activation of receptor-independent ephrinB1 signalling. As the canonical and non-canonical pathways are known to inhibit each other, this could cause the de-repression of canonical signalling (Wei *et al.*, 2010).

These data have raised the interesting possibility of a connection between polarised migration and cell segregation driven by Eph-ephrin signalling. However, cell polarisation can be established by other mechanisms apart from PCP, an example of which is PAR protein polarity.

1.3 Polarity proteins in cell polarisation

Cell polarity is essential for many biological processes and is regulated by conserved protein complexes. Polarity contributes to axon guidance and dendritic spine formation in neuronal cells, apical-basal polarity in the formation of epithelial tissues (Mertens *et al.*, 2006), and directional movement in migrating cells (Jaffe & Hall, 2005; Pegtel *et al.*, 2007). Cell morphology changes require cell asymmetry/polarity that is achieved by the combined actions of polarity proteins and dynamic regulation of the cytoskeleton (Jaffe & Hall, 2005; Mertens *et al.*, 2006). These molecules respond to extrinsic or intrinsic polarity cues and assemble multiprotein complexes, such as the highly conserved PAR, Crumbs and Scribble complexes, to trigger downstream signalling and the establishment of cellular asymmetry (Goldstein & Macara, 2007).

Rho GTPases (RhoA, Rac1 and Cdc42) are key regulators of actin and microtubule dynamics and have been implicated in cell polarisation (Jaffe & Hall, 2005). Rho GTPases function as molecular switches that switch between an inactive GDP-bound state and an active GTP-bound state, and large numbers of regulators and effector proteins have been described that act as kinases or scaffolding proteins that couple the activation of Rho GTPases to downstream signalling pathways. Rho GTPases can regulate each other's activity through crosstalk; Cdc42 can activate Rac1 (Nobes & Hall, 1995) and Rac1 can downregulate RhoA (Iden & Collard, 2008; Nakayama *et al.*, 2008). The contracile forces that are induced by RhoA antagonise the adhesive forces that are induced by Rac1, and the temporal and spatial balance of these activities is crucial for many different processes in many different cell types. Studies of polarisation mechanisms have revealed crosstalk between small GTPases and polarity complex proteins in the regulation of cell polarisation (Fig. 6 B, C).

1.3.1 Introducing the PAR proteins

The PAR (partitioning-defective) genes were first identified in *C. elegans* in a screen for regulators of cytoplasmic partitioning, and encode six different proteins required for asymmetric cell division. Some PAR proteins localise asymmetrically and form complexes with each other (Goldstein & Macara, 2007). Two of these genes encode the PDZ-domain proteins PAR-3 and PAR-6, which together with the atypical protein kinase C (aPKC), make up the PAR complex (Mertens *et al.*, 2006) and act as a signalling scaffold. The kinase activity of aPKC is required for a functional complex and aPKC-mediated phosphorylation of target proteins is a key event in downstream polarity signalling (Iden & Collard, 2008). Mammalian PAR-3, PAR-6 and aPKC can exist in a complex with Cdc42 (Joberty *et al.*, 2000; Lin *et al.*, 2000), with PAR-6 binding aPKC through its N-terminal domain (Lin *et al.*, 2000). The localisation of the PAR complex is important for the recruitment of signalling proteins to precise locations on the plasma membrane.

PAR proteins have several basic properties that are relevant to polarity mechanisms. PAR proteins signal to multiple effectors, allowing them to target a range of cellular processes, including regulators of the actin and microtubule cytoskeleton, organisers of the cell membrane and components of cell-cell junctions. PAR proteins have dynamic turnover, which allows polarised structures to adapt quickly to changes within cells and to changes in the extracellular environment. In addition, PAR proteins operate within networks, the organisation of which into positive and negative feedback loops amplifies molecular asymmetries and causes rapid and dynamic changes to cell polarity (Nance & Zallen, 2011). The asymmetric localisation of the PAR proteins plays a crucial role in many cellular processes such as epithelial apical-basal polarity, asymmetric cell division (e.g. one cell stage C. elegans, *Drosophila* neuroblast), neuronal outgrowth, specification and maturation, T-cell polarity and polarised migration. There are many core polarity components and Rho GTPase effector proteins that have roles in establishing polarity in these processes, but this literature review has predominantly focussed on the central role of PAR-3 and PAR-6 in directional migration.

1.3.1.1 Asymmetric localisation and role in neuronal polarity

Asymmetric localisation of members of the PAR complex together with Rac and/or Cdc42 GTPases, controls different aspects of neuronal polarity, including the establishment of apical-basal and front-rear polarisation (Mertens *et al.*, 2006; Pegtel *et al.*, 2007). Cdc42 and Rac1 promote the formation of lamellipodia and filopodia at the neurite growth cone, and RhoA mediates growth cone collapse and neurite retraction (Iden & Collard, 2008). At the tip of a developing axon or at the leading edge (LE) of migrating cells, PAR-3 binds the Rac activator Tiam1/2 and associates with the active aPKC/PAR-6/Cdc42-GTP complex. This triggers localised Cdc42-dependent Rac1 activation and actin reorganisation (Mertens *et al.*, 2006; Pegtel *et al.*, 2007). In dendritic spine maturation, PAR-3 can also recruit Tiam1 to locally activate Rac, but this function is independent of association with aPKC/PAR-6 (Mertens *et al.*,

2005; Zhang & Macara, 2006). Cdc42 plays a crucial role in asymmetrically localising PAR-6/aPKC at the cell cortex and the localisation of PAR-3 is largely dynein dependent, which suggests that even though the PAR-3/PAR-6/aPKC complex can be isolated from mammalian cells, PAR-3 and PAR-6 can act independently and be both functionally and spatially separate (Goldstein & Macara, 2007). Rac1 and Cdc42 can therefore function as mediators and/or regulators of the PAR complex.

1.3.1.2 Epithelial apical-basal polarity

The establishment of epithelial cell-cell contacts and apical-basal polarisation requires E-cadherin mediated cell-cell adhesion and recruitment of structural proteins involved in the formation of both adherens (cell-cell adhesion) and tight junctions (diffusion barrier for soluble molecules) (Iden & Collard, 2008). E-cadherin clustering and dimerisation activates Rac1 and Cdc42, which bind to PAR-6 and cause the activation of aPKC. Rac1 activation is also coupled to aPKC activation by Tiam1/PAR-3, which plays a role in tight junction formation (Iden & Collard, 2008; Mertens *et al.*, 2005). The TGFβ-receptor complex (present at tight junctions) associates with and phosphorylates PAR-6, which binds Smurf1 and results in proteasomal degradation of RhoA. This is linked to morphological changes, including the loss of tight junctions during epithelial-mesenchymal transition (Goldstein & Macara, 2007; Iden & Collard, 2008). RhoA activity and actin contractility are required for early cell-cell adhesion, but RhoA activity decreases with maturation of cell–cell contacts. Rac1 suppresses RhoA activity at adherens junctions by stimulating the association of p190RhoGAP with cadherin-bound p120catenin during cell–cell contact formation, and downregulating RhoA (Iden & Collard, 2008). The balanced activity of each of RhoA, Rac1 and Cdc42 therefore contributes to overall tissue stability.

Dishevelled, a central scaffold component of the Wnt signalling pathways, has been shown to interact with PAR proteins, so linking separate polarity pathways. Dishevelled associates with PAR1 to upregulate canonical Wnt signalling (Sun *et al.*, 2001), and is also required for epithelial polarisation by regulating Lethal giant larvae (Lgl), a target of aPKC (Goldstein & Macara, 2007). More recent evidence has suggested a link between the PCP pathway and downstream effectors of the PAR complex, or with the complex itself via Dishevelled-mediated aPKC activation. Dishevelled was found to accumulate at the tip of growing hippocampal axons and bind to phosphorylated aPKC via the DEP domain, resulting in stabilisation of activated aPKC. Dishevelled, aPKC, PAR-3 and PAR-6 can indeed form a complex, with aPKC serving as a connecter. This interaction is required for axon differentiation and guidance in isolated hippocampal neurons (Zhang *et al.*, 2007). In addition, a constitutive interaction was detected between PAR-6 and Dishevelled. Non-canonical signalling-induced phosphorylation of Dishevelled, bound to PAR-6, causes the recruitment of Smurfs and degradation of Prickle, so causing the asymmetric localisation of PCP components (Narimatsu *et al.*, 2009).

1.3.2 Polarised migration

The migration of individual or groups of adherent cells is crucial in many processes during development and morphogenesis, for example wound healing. Cell migration is the overall effect of Cdc42- and Rac1-mediated expansion of cellular protrusions (lamellipodia and filopodia) and cytoskeleton polarisation in the direction of migration, membrane adhesive interactions with the substratum, and RhoA-driven retraction of membrane and cell–matrix adhesions at the trailing edge (TE) (Nobes & Hall, 1999; Pegtel *et al.*, 2007; Ridley *et al.*, 2003). Migration can be directed or random, but in each case the cells must become polarised to generate a LE and TE. This front-rear polarity is mediated by an asymmetric distribution of cytoskeleton components, adhesion proteins and PAR proteins, leading to localised activation of Rho GTPases (Fig. 6 B). Given the multiple ways that crosstalk between Rho GTPases and PAR proteins impact cytoskeleton dynamics, it is not surprising that they play a key role in the motility of some cells such as fibroblasts and astrocytes.

Increased actin nucleation at the LE, stabilisation of microtubules and repositioning of the Golgi apparatus and centrosome, are hallmarks of directional migration, for example of migration of cells into a wound (Etienne-Manneville & Hall, 2001). The direction of migration can be determined by signals such as growth factors and chemoattractants or environmental cues such as the extracellular matrix (ECM), but cultured cells can migrate with a high directionality in the absence of chemoattractants. Golgi and centrosome reorientation occurs during wound-induced cell motility due to the cytoskeletal rearrangements downstream of conserved signal transduction pathways (Nobes & Hall, 1999), and there is a tight link between the position of the Golgi and centrosome in front of the nucleus in most cells (Dupin *et al.*, 2009; Palazzo *et al.*, 2001). The positioning of the Golgi apparatus reflects the centrosome position and promotes microtubule formation and directional vesicular transport to the LE to facilitate dynamic membrane protrusion formation/disassembly and cell movement (Ang *et al.*, 2010; Miller *et al.*).

A central centrosome position is maintained by a dynein and microtubule-dependent process, while the nucleus moves rearward and becomes off-centered during centrosome orientation in wound-edge fibroblasts (Gomes *et al.*, 2005). Anisotropic cell-cell adhesion can also induce nucleus positioning by displacing the nucleus towards cell-cell contacts during collective cell migration, and away from the contact-free edge (Desai *et al.*, 2009; Dupin *et al.*, 2009). This gives the illusion of ‘‘centrosomal reorientation’’, although this process does not affect cell migration (Desai *et al.*, 2009; Dupin *et al.*, 2009). This process requires contractile Myosin II and Cdc42 but is independent of RhoA and Rac1 activity (Desai *et al.*, 2009). N-cadherin and E-cadherin at cell-cell contacts control intracellular organisation, nucleus and centrosome positioning, and cell orientation in various cell types.

1.3.2.1 At the leading edge

In scratch-wound assays of cell monolayers, wound-edge cells orient their centrosomes towards the wound, and this process is driven by the recruitment of the PAR-3/PAR-6/aPKC complex to the LE via a Cdc42- or Rac1-dependent pathway (Joberty *et al.*, 2000) to promote the outgrowth of protrusions. However, PAR-3 and PAR-6 can act independently at the LE; PAR-3/Tiam1/aPKC mediates stable front–rear polarisation of keratinocytes through activation of Rac1 and stabilisation of microtubules (Pegtel *et al.*, 2007), and Cdc42 localises and activates PAR-6/aPKC at the wound-induced LE of migrating astrocytes (Etienne-Manneville & Hall, 2001; Etienne-Manneville & Hall, 2003). PAR-6/aPKC localisation at the LE mediates the directionality of migration by orientating the centrosome (dynein-dependent) and direction of protrusions with respect to the nucleus and axis of movement, but not the formation of protrusions (Etienne-Manneville & Hall, 2001; Etienne-Manneville & Hall, 2003). This is due to the aPKC-dependent inactivation of glycogen synthase kinase−3β (GSK3β), which causes the adenomatous polyposis coli (APC)/Discs large−1 (DLG1)-dependent repositioning of the centrosome/Golgi and nucleus axis due to microtubule capture at the LE (Etienne-Manneville & Hall, 2003). Rac1 can also be activated at the LE due to down-regulation of RhoA activity via the PAR-6/aPKC dependent-activation of the negative regulator of RhoA, p190ARhoGAP (Fig. 6 C) (Iden & Collard, 2008). This process also has roles in stimulating dendritic spine formation (Zhang & Macara, 2008b). GSK3β also inhibits p190ARhoGAP, and therefore aPKC−mediated inactivation of GSK3β could suppress RhoA activity at the front of the cell. In addition, recent evidence has suggested that Cdc42/Rac-dependent activation of PAR-6/aPKC recruits the ubiquitin ligase Smurf1 to the front of migrating cells, where it binds RhoA and promotes RhoA ubiquitination and degradation (Wang *et al.*, 2003).

In wound-induced migrating astrocytes or fibroblasts, PAR-3 is not localised at the LE, but instead to the cell-cell contacts of migrating cells (Etienne-Manneville & Hall, 2001; Schmoranzer *et al.*, 2009). However, knockdown of PAR-3 did not affect the localisation of junctional markers, such as N-cadherin and ß-catenin (Schmoranzer *et al.*, 2009). Interestingly, the Cdc42/PAR-6/aPKC pathway is also required for centrosome and Golgi localisation in scratch-induced migrating fibroblasts, but the spatial localisation of protrusive activity is instead controlled by Pak-induced Rac1 activation (Cau & Hall, 2005). Work in the *Drosophila* pupal notum has suggested that PAR-3 can act in opposition (but independently of cell-cell contacts) with Cdc42/PAR-6/aPKC and Tiam1 in the activation of Rac1 and generation and positioning of basal protrusions (Georgiou & Baum, 2010). PAR-3 might sequester Tiam1 to prevent its association with Rac1. This is another example of how PAR-3 and PAR-6 can have distinct molecular targets and suggests a mechanism for how different structures could be formed at distinct regions of a polarised cell: high levels of Rac1 form filopodia and lower levels form lamellipodia (Georgiou & Baum, 2010).

1.3.2.2 At the trailing edge and antagonising polarised migration

A recent study suggests that polarity proteins function in the antagonistic regulation of Rho GTPase activities. The Rho effector ROCK can phosphorylate PAR-3 (in its aPKC-binding region), which disrupts the association of PAR-3 with the aPKC/PAR-6 complex. This prevents the assembly of a functional PAR complex and (Cdc42-dependent) Rac1 activation at the TE (Nakayama *et al.*, 2008), and leads to reduced cell migration (Nakayama *et al.*, 2008). RhoA activity and PAR-3 phosphorylation is higher in the central and rear portions than in the front area in the migrating cells (Nakayama *et al.*, 2008; Ridley *et al.*, 2003), suggesting PAR-3 phosphorylation by Rho-kinase may prevent Cdc42-induced and Tiam1-mediated activation of Rac1 and lamellipodia formation at the TE to control front-rear polarity and directional migration (Nakayama *et al.*, 2008). RhoA activation at the TE of migrating cells is essential for disassembly of adhesive structures. Retraction of the TE requires ROCK and is myosin-dependent, allowing the forward movement of the cell (Ridley *et al.*, 2003).

PAR-3 is also phosphorylated at the LE of migrating cells, as is active RhoA. This pathway may serve as a local negative feedback signal to control the levels of Rac1 activation at the LE to allow dynamic assembly/disassembly of membrane protrusions necessary for cell migration (Iden & Collard, 2008; Jaffe & Hall, 2005; Kardash *et al.*, 2009; Nakayama *et al.*, 2008).

The PAR complex therefore plays a central role in the cross talk between RhoA and Rac1 GTPases necessary for proper front-rear polarisation and directional movement of migrating cells. However, the precise mechanisms by which Rac1, RhoA, and the PAR complex integrate signalling from extracellular cues to regulate the cytoskeleton and front-rear polarity of migrating cells remain undefined, and they have different roles in different polarisation events (Fig. 6 B, C).

1.3.3 Random versus directionally persistent cell migration

Directionally persistent migration of neural crest cells and epithelial cells is important for early embryo development and wound healing. Aberrant persistent migration can lead to developmental disorders and contribute to metastasis of cancers (Pegtel *et al.*, 2007). Cells achieve directionally persistent migration by forming and stabilising actin-rich protrusions or lamellipodia that maintain the orientation of the LE, which is an important component of cell motility (Harms *et al.*, 2005). Chemotactic or other extrinsic factors such as topography of the ECM, cell polarity and cell adhesion, are coupled to the intracellular polarity that guides migration by regulating LE formation through the activity of Rho GTPases (Petrie *et al.*, 2009).

The intracellular signalling pathways at the LE that regulate actin cytoskeleton remodelling or adhesion formation to create or stabilise local protrusions are therefore likely to contribute to directional migration. As previously described, the PAR complex couples Rho GTPase activity to arrange the nucleus,

centrosome and LE along the front-rear axis (Etienne-Manneville & Hall, 2001), the stability of which correlates with the extent of directional cell movement (Iden & Collard, 2008). Additional pathways can cooperate with Cdc42 and the PAR complex to promote directional migration. In scratch wound assays of fibroblasts, disruption of cell-cell contacts at the wound edge leads to the activation of non-canonical Wnt signalling that causes the binding of Dishevelled to aPKC (independent of its activation). This couples Dishevelled and Cdc42/PAR-6/aPKC pathways to trigger Golgi and centrosome orientation through APC, and stabilise microtubules towards the LE (Schlessinger *et al.*, 2007).

PAR-mediated crosstalk between Rho GTPases regulates migration, the perturbation of which affects the persistence of directional migration. The PAR-3-aPKC complex and Tiam1 function together in controlling the persistence of migrating epidermal keratinocytes by stabilising transient front-rear cell polarisation via the microtubule system. Depletion of Tiam1 or PAR-3, normally localised at the LE of migrating cells with aPKC, decreases the activity of Rac1 and decreases the persistence of cell migration (of freely migrating cells) independently of speed (Pegtel *et al.*, 2007). Interestingly, there was no correlation between orientation of the centrosome or Golgi and the nucleus in persistently versus randomly migrating cells (Pegtel *et al.*, 2007; Uetrecht & Bear, 2009). Tiam1 control of migratory persistence is context dependent, as knockdown stimulates migration in an adhesive environment due to loss of cell-cell adhesions and apical-basal polarity (Pegtel *et al.*, 2007).

The level and localisation of Rac1 has been shown to control the direction of migration and act as a switch in the intrinsic polarity that underlies directionally persistent and random migration (Pankov *et al.*, 2005). Rac1 promotes the formation of peripheral lamella during random migration, while lower levels of Rac1 suppress peripheral lamella and favour the formation of lamella only at the LE, so contributing to the polarisation of migrating cells in a Cdc42- and RhoA-independent manner (Pankov *et al.*, 2005). Persistence of migration usually depends on the orientation of cell protrusion, and once Rac1 is active numerous feedback loops help to maintain directional protrusions (Ridley *et al.*, 2003). Consequently, local restriction of active Rac1 to the LE by the combined actions of PAR-3 and Tiam1 might be a key factor for the promotion of directionally persistent motility.

Other work has linked ECM receptors, trafficking and motility to persistent migration. The PAR complex can contribute to polarised integrin trafficking and adhesion formation at the LE by regulating Numb-mediated endocytosis of integrins, and plays a role in persistent migration (Petrie *et al.*, 2009). However, work in the *Drosophila* pupal notum argues against a role of integrins and the ECM in protrusion positioning (Georgiou & Baum, 2010). Focal complex formation leads to adherence to the ECM in a Rac1- and Cdc42-dependent manner, and provides traction sites over which the cell moves. This can stabilise lamellipodia formation and mediate efficient migration, but formation of large integrin clusters causes cells to become non-migratory. Migration speed is a function of the strength of cell attachment, which is derived

from the interaction of Myosin II with actin filaments, and is positively regulated by RhoA (Ridley *et al.*, 2003).

1.3.3.1 Persistence mediated by contact inhibition of locomotion

The transmembrane proteoglycan Syndecan-4 restricts Rac1 activation to a dominant lamella, to promote directionally persistent migration in response to linear fibrils in the ECM (Bass *et al.*, 2007). Other work has shown a role of Syndecan-4 with non-canonical Wnt signalling to control directional migration of neural crest cells (Matthews *et al.*, 2008). Syndecan-4 restricts Rac1 activation to the LE of migrating cells, and cells that lack Syndecan-4 undergo increased random migration resulting from larger numbers of random membrane protrusions (Matthews *et al.*, 2008). PCP signalling through Dishevelled is essential for the delamination and/or migration of neural crest cells (De Calisto *et al.*, 2005), and Dishevelled recruitment to the site of contact triggers the RhoA-dependent collapse of protrusions, independently of Cdc42. This mediates CIL, which is partially responsible for the directional migration of neural crest cells, and is dependent on homotypic contacts conferring directionality (Fig. 7 A) (Carmona-Fontaine *et al.*, 2008). Activation of RhoA by PCP signalling may also result in Rac1 inhibition via the inhibitory activity of ROCK on Rac1 (Matthews *et al.*, 2008). Neural crest cells expressing a dominant-negative dishevelled construct, specific to the PCP pathway, showed fewer lamellipodia and more filopodia (De Calisto *et al.*, 2005), and lamellipodia of PCP-inhibited cells failed to collapse on contact (Carmona-Fontaine *et al.*, 2008).

N-cadherin-dependent cell contacts are required for collective cell migration and CIL between neural crest cells, and can polarise the cells by inhibiting Rac1 at the cell contact and increasing Rac1 activity at the free edge; this polarised distribution of Rac1 activity is essential for the cells to respond to a chemoattractant and for directional and collective cell migration (Fig. 7 B) (Theveneau *et al.*, 2010). Therefore mutually exclusive areas of Rac1 and RhoA activity are controlled by Syndecan-4 or CIL driven by PCP or N-cadherin. Local inhibition of Rac1 or activation of RhoA at the site of cell contact causes the collapse of protrusions and the generation of a new protrusion away from the site of contact or at the free edge. This contact inhibition-mediated repolarisation underlies directional and persistent migration away from the site of contact (Carmona-Fontaine *et al.*, 2008; Matthews *et al.*, 2008; Mayor & Carmona-Fontaine, 2010).

Taken together this evidence suggests that the polarity proteins serve as spatial-temporal cues, locally activating Rho GTPases that subsequently act on the cytoskeleton to stimulate cell polarisation and migration (Ridley *et al.*, 2003). The regulation of this can be contact- and cell type-specific. How cells interpret extracellular directionality cues is still largely unknown.

Figure 7: Contact inhibition of locomotion and collective cell migration

Diagram representing contact inhibition of locomotion (CIL) in isolated cells (A) or in a group of cells (B), represented by yellow inhibitory arrows.

(A) Contact between single migrating cells leads to collapse of cell protrusions, generation of a new protrusion away from the site of cell contact and migration in the direction of the new protrusion (green arrows).

(B): CIL between the inner cells of a group of migrating cells leads to inhibition of protrusions, whereas CIL between the leader cells, at the free edge, can lead to cell polarisation of the leaders (green arrows) and directional migration (adapted from (Mayor & Carmona-Fontaine, 2010)).

A

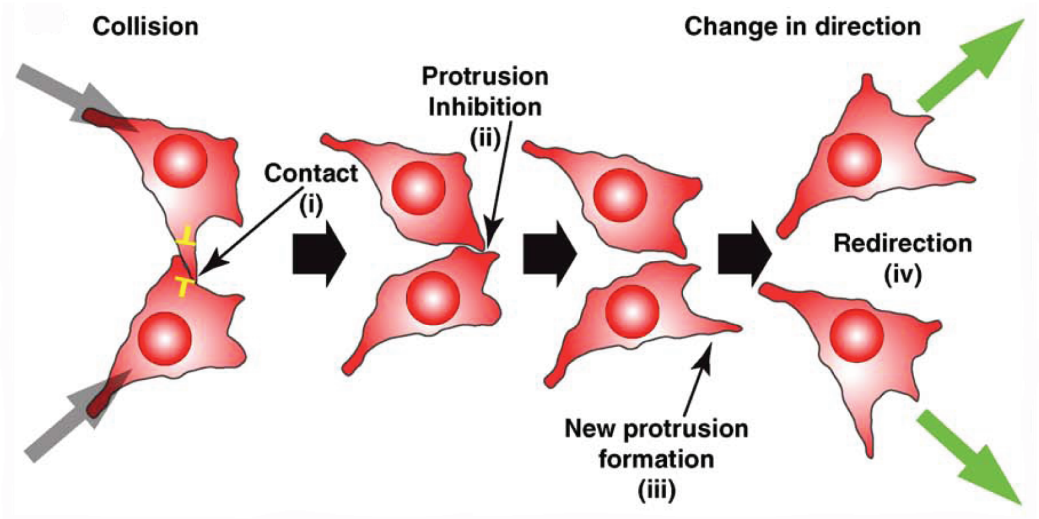
Collision
Change in direction
Protrusion
Inhibition
(ii)
Contact
(i)
Redirection
(iv)
New protrusion
formation
(iii)

B

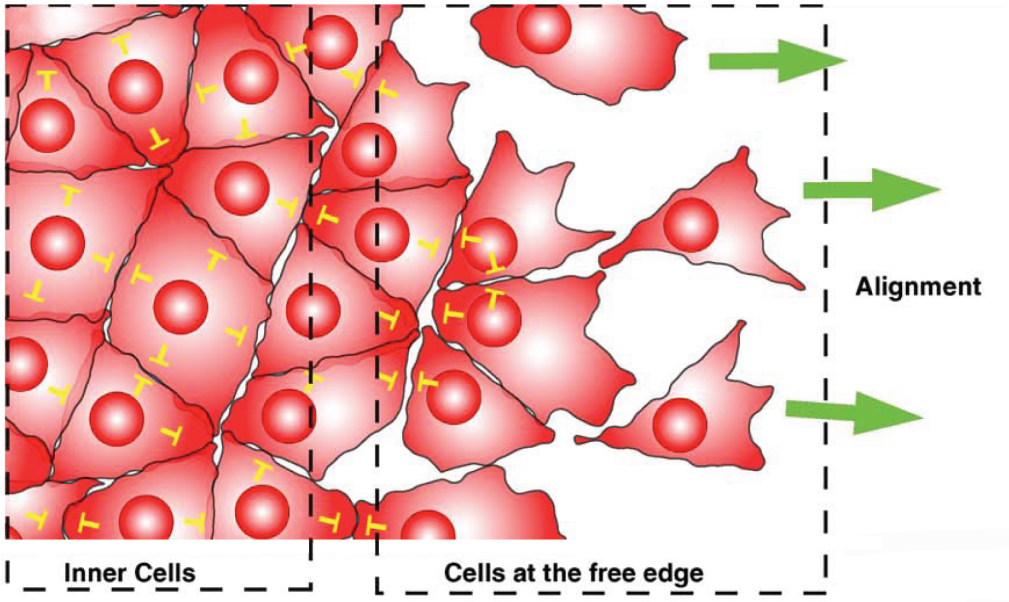
Alignment
Inner Cells
Cells at the free edge

1.3.4 Eph-ephrin signalling and polarity

Eph-ephrin signalling has been linked to core cellular polarity in a number of ways. EphB-ephrinB signalling has a role in tight junction integrity and localisation, and ephrinB1 can regulate tight junctions via the PAR complex (Lee *et al.*, 2008). The localisation of the PAR-6/aPKC/Cdc42-GTP complex to apical cell junctions regulates tight junction formation, which associates with the actin cytoskeleton for the reorganisation, formation and maintenance of cell–cell contacts. EphrinB1 can bind PAR-6 via its C-terminus, and compete with Cdc42 for association with PAR-6 (Lee *et al.*, 2008). This competition causes inactivation of the PAR complex, resulting in the loss of tight junctions. The ephrinB1-PAR-6 interaction is disrupted by tyrosine phosphorylation of the intracellular domain of ephrinB1, for example by binding of the cognate EphB receptor or FGF receptor, which results in the proper establishment of tight junctions (Lee *et al.*, 2008). In addition, recent evidence has identified many downstream signalling components that are phosphorylated on Eph-ephrin signalling and play a role in cell segregation. These include the PAR proteins, PAR-6 and PAR-3 (Jorgensen *et al.*, 2009; Zhang *et al.*, 2008a).

CIL involves contact between cells mediated by cell surface receptor/ligand pairs leading to retraction of protrusions from the site of contact and cell repolarisation (Mayor & Carmona-Fontaine, 2010). It is likely that Eph receptors and ephrins function in a CIL-like response, as activation of RhoA has been identified at the site of interaction (Astin *et al.*, 2010) and activation of RhoA causes a collapse response (Poliakov *et al.*, 2008). However, the molecular mechanisms by which this occurs have not been identified, although EphB/ephrinB signalling has been shown to activate RhoA via Dishevelled/PCP signalling (Lee *et al.*, 2006; Tanaka *et al.*, 2003).

1.3.5 Aims of this study

I set out to analyse how EphB2-ephrinB1 signalling mediates cell segregation and boundary formation. Previous work from the lab has shown that EphB2-ephrinB1 signalling leads to directional persistence of migration (Poliakov, unpublished), and modelling suggests that this can contribute to cell segregation. My studies aim to test experimentally the contribution of directional persistence and directional migration in cell segregation.

To analyse how EphB2-ephrinB1 interactions lead to directional persistence of migration, my studies focus on the role of components potentially involved in directional persistence and that act downstream of EphB2-ephrinB1 signalling, including the PCP pathway (Dishevelled and Daam1) (Kida *et al.*, 2007; Lee *et al.*, 2006; Tanaka *et al.*, 2003) and core polarity components (PAR-3 and PAR-6) (Jorgensen *et al.*, 2009). I tested the role of these components in cell segregation assays and with cell behaviour studies to assess their role in directional migration.

The roles of the PCP pathway in rhombomere boundary formation in the zebrafish hindbrain have also been analysed. The approaches used had various technical limitations, which made analysis difficult. This is further discussed in the Appendix.

2 MATERIALS AND METHODS

2.1 Zebrafish embryo work

2.1.1 Fish lines and maintenance

Adult zebrafish were kept in 10 h night/ 14 h day cycles. Embryos were obtained from wild-type (LON/AB) and Tg(*krox20*-Gal4::UAS-RFP) (Distel *et al.*, 2009) zebrafish lines. Embryos were raised at 28.5°C and stage-matched according to hours post-fertilisation (hpf) and morphological criteria (number of somites) (Kimmel *et al.*, 1995).

2.1.2 Morpholino oligonucleotide, DNA and RNA preparation and injections

2.1.2.1 Injection protocol

Morpholino oligonucleotides (MOs), DNA or RNA were injected using a gas microinjector (Picospritzer II, General Valve Corporation) in a volume of 1.8nl into the yolk of 1-4 cell-blastomere stage (in the case of MOs), or into 1-2 cell-blastomere stage (in the case of DNA/RNA) embryos. The needles used for injection were made from 1.0mm glass capillaries with internal filament (Harvard Apparatus, Kent) using a needle puller (David Kopf instruments).

2.1.2.2 Morpholino oligonucleotides

Morpholino oligonucleotides were purchased from Gene Tools (Oregon, USA). MOs were reconstituted at 1mM in sterile water and either kept as stock solutions at -20°C, or further diluted for injection.
The following MOs were used:
EphA4 splice blocking MO: as described (Cooke *et al.*, 2005)
p53 MO: as described (Langheinrich *et al.*, 2002)
Standard control MO: Gene Tools

1-4 cell-blastomere stage embryos were microinjected with 4ng EphA4 splice blocking MO (Cooke *et al.*, 2005) or the standard control MO (Gene Tools). 5ng p53 MO (Langheinrich *et al.*, 2002) was co-injected in all experiments to block non-specific MO toxicity.

2.1.2.3 Dishevelled deletion mutants

Constructs of truncated forms of *Xenopus* Dishevelled, in a pCS2-myc plasmid backbone (gift from Masa Tada (Tada & Smith, 2000)), were as follows: Dsh-WT (amino acids 1-736), Dsh-ΔPDZ (amino acids 1-301 and 381-736, identical to Xdd1 (Sokol, 1996)) and Dsh-DEP+ (amino acids 337-736). Amino acid positions are according to (Sokol *et al.*, 1995).

2.1.2.4 Generation of plasmid DNA constructs

A DNA plasmid pminiTol2-UAS-H2B-Citrine::UAS-MCS was obtained (gift from Sebastian Gerety). For cloning Myc-tagged Dishevelled deletion mutants into the multiple cloning site (MCS) of the pminiTol2-UAS-H2B-Citrine::UAS-MCS plasmid, pCS2-MT-Dsh-WT, pCS2-MT-Dsh-ΔPDZ and pCS2-MT-Dsh-DEP+ were each digested with BsrGI (followed by blunting with Klenow DNA polymerase) and ClaI restriction enzymes, and the inserts each ligated into linear pminiTol2-UAS-H2B-Citrine::UAS-MCS plasmid digested with PmeI and BstBI. The resulting plasmids were then transformed and plasmid DNA prepared using Qiagen miniprep kits.

A DNA plasmid pminiTol2-HSP-MCS-Myc plasmid was obtained (gift from Tomomi Watanabe). For cloning Myc-tagged Dishevelled deletion mutants into the MCS of the pminiTol2-HSP-MCS-Myc plasmid, pminiTol2-UAS-H2B-Citrine::UAS-Myc-Dsh-WT, pminiTol2-UAS-H2B-Citrine::UAS-Myc-Dsh-ΔPDZ and pminiTol2-UAS-H2B-Citrine::UAS-Myc-Dsh-DEP+ were each digested with EcoRV and NotI restriction enzymes, and the inserts each ligated into linear pminiTol2-HSP-MCS-Myc plasmid digested with EcoRV and NotI. The resulting plasmids were then transformed and plasmid DNA prepared using Qiagen miniprep kits.

Plasmids generated:
pminiTol2-UAS-H2B-Citrine::UAS-Myc-Dsh-WT
pminiTol2-UAS-H2B-Citrine::UAS-Myc-Dsh-ΔPDZ
pminiTol2-UAS-H2B-Citrine::UAS-Myc-Dsh-DEP+
pminiTol2-HSP-Myc-Dsh-WT
pminiTol2-HSP-Myc-Dsh-ΔPDZ
pminiTol2-HSP-Myc-Dsh-DEP+

For injection into zebrafish embryos, 25-45pg circular plasmid DNA was injected into the cell at 1-cell stage together with 25pg of *Tol2* RNA to obtain a high level of transposon-mediated DNA integration.

2.1.2.5 Generation of RNA

pCS2+MT plasmids containing inserts encoding Dsh-WT, Dsh-DEP+ and Dsh-ΔPDZ were linearised with NotI. Capped mRNA encoding *Tol2* (Kawakami *et al.*, 2000), Dsh-Myc, Dsh-DEP+ or Dsh-ΔPDZ was prepared using mMessage mMachine transcription kit (Ambion), according to the manufacturer's instructions. The RNA was purified by phenol:chloroform extraction and isopropanol precipitation, diluted in sterile water, and quantified by spectrophotometry before being stored at -80°C. For injection into zebrafish embryos, 25-400pg of capped RNA was injected into the cell at 1-cell stage.

2.1.3 Heat-shock

For injection into zebrafish embryos, 25-30pg circular plasmid DNA was injected into the cell at the 1-cell stage together with 25pg of *Tol2* RNA, to obtain a high level of transposon-mediated DNA integration. At the required stage, injected embryos were heat-shocked at 38.5°C for 1 h in pre-warmed water before recovery at 28°C. Embryos were fixed in 4% PFA (paraformaldehyde/PBS) for 2 h at room temperature or 4°C overnight, before being stored in 100% methanol at -20°C.

2.1.4 Whole mount *in situ* hybridisation and immunohistochemistry

2.1.4.1 Probe synthesis

Digoxigenin-UTP labelled RNA probes were synthesised using linearised cDNA as templates. The following reagents were mixed in order at room temperature. Per reaction: sterile water up to 40µl (Sigma), 8µl 5x transcription buffer (Promega), 4µl 0.1M dithiothreitol (Promega), 2µl nucleotide mix (10mM GTP, 10mM ATP, 10mM CTP, 6.5mM UTP, 3mM dioxygenin-UTP, Roche), 1µg linearised plasmid, 1µl ribonuclease inhibitor (Promega), and 4µl RNA polymerase (T3, T7, Promega; SP6, Roche). When SP6 RNA polymerase was used for transcription, 10x SP6 transcription buffer (Roche) was used instead of 5x transcription buffer and 0.1M dithiothreitol. The mix was incubated at 37°C for 2 h, and the probe precipitated by adding 60µl sterile water, 25µl 4M ammonium acetate, 130µl isopropanol and incubating for 30 min at -20°C. The probe was centrifuged at 4°C, in a microfuge at 13000rpm for 10 min, and washed in 70% ethanol. The pellet was then air-dried and dissolved in 40µl RNase-free water, before adding 160µl hybridisation buffer and storing at -20°C.

2.1.4.2 Fluorescent in situ hybridisation with immunostaining

This protocol is based on that previously described (Xu *et al.*, 1994). Embryos were fixed as described previously for heat-shock method. Rehydration was carried out through washes in 75%, 50%, 25% methanol in PBTw (PBS/0.1% Tween-20), and three washes in PBTw, each for 5 min at room temperature. All further steps were carried out at room temperature unless stated otherwise. Embryos were manually dechorionated and pre-hybridised for at least 1 h at 65°C in hybridisation buffer (50% formamide, 5x SSC pH 4.5, 500µg/ml tRNA, 0.2% Tween-20, 5mM EDTA and DEPC-treated water). Hybridisation was carried out overnight at 65°C by replacing the buffer with 300µl hybridisation buffer containing 50-200ng of labelled probe at the same temperature. The following post-hybridisation washes were carried out: 3x 1 min at 65°C in formamide wash (FW) (containing 25% formamide, 2x SSC, 0.1% Tween20, sterile water), 3x 30 min at 65°C in FW, 3x 15 min at 65°C in SSC wash (2x SSC, 0.1% Tween20, sterile water) and 4x 25 min in PBTw.

After pretreatment in blocking solution (5% sheep serum in PBTW) for 1-2 h, embryos were incubated with alkaline-phosphatase-conjugated anti-dioxigenin antibody (Roche) (1:1200) and the primary antibody of interest e.g. anti-Myc (1:500, Santa-Cruz) in blocking solution. The embryos were incubated overnight at 4°C, and then washed in PBTw all day and overnight (at 4°C). Embryos were rinsed 3 times in Fast Red (FR) buffer (100mM Tris ph8.0 and sterile water), and washed over 30-60 min. The colour reaction was carried out by incubation in FR buffer containing FR tablets (Roche) (1 tablet per 2ml FR buffer and syringe filtered before use) for 1 h in the dark. The reaction was stopped by rinsing the embryos three times in PBTw and washing over 30 min. Embryos were incubated with the secondary antibody of interest i.e. goat anti-rabbit, goat anti-mouse or donkey anti-sheep conjugated to Alexa Fluor 488, 594 or 647 (1:500, Molecular Probes) in 2% sheep serum in PBTw for 3 h or overnight at 4°C. Embryos were washed 8x 15 min in PBTw before being stored and flat-mounted in 70% glycerol/30% PBS. For in situ hybridisations, the *krox20* probe was used as previously described (Oxtoby & Jowett, 1993).

2.1.4.3 Immunohistochemistry

For immunohistochemistry we used the following primary antibodies: rabbit anti-EphA4 (1:500, (Irving *et al.*, 1996), rabbit anti-RFP (1:500, Chemicon International), sheep anti-GFP (1:500, AbD Serotec), mouse anti-Myc (1:500, Santa-Cruz). Embryos fixed in 4% PFA were blocked in blocking solution (5% goat serum in PBS/0.1% Triton X-100 (PBTr)) for at least 1 h at room temperature, and then incubated overnight at 4°C with the antibody diluted in blocking solution. Embryos were washed 8x 15 min in PBTr and incubated (overnight at 4°C or 3 h at room temperature) with secondary antibodies diluted in 2% goat serum in PBS/0.1% Triton X-100. Detection of primary antibodies was carried out using Alexa Fluor 488, 594 or 647 goat anti-rabbit, goat anti-mouse or donkey anti-sheep conjugate (1:500, Molecular Probes). Embryos

were washed 8x 15 min in PBTr and stored and flat-mounted in 70% glycerol/ 30% PBS. Fluorescence images were collected using a Leica TCS SP2 laser scanning confocal microscope.

2.2 Cell culture

2.2.1 Cell culture maintenance

HEK293 cells were cultured at 37°C with 5% CO_2 in media: DMEM (high glucose media 4.5g/l without glutamine) supplemented with 1% L-Glutamine (200mM), 1% Sodium Pyruvate (100mM) and 10% Fetal Bovine Serum Mycoplex (all PAA). Stable HEK293 cell lines expressing membrane-targeted GFP, EphB2, EphB2 plus membrane-targeted GFP (EphB2-GFP) and ephrinB1 were generated using selection with G418 and/or hygromycin, as previously described (Poliakov *et al.*, 2008). Cell populations were counted using a Cellometer T4 Cell Counter (Nexcelom Bioscience).

2.2.2 siRNA knockdowns and quantitative Western blot assays

2.2.2.1 siRNA knockdown

Knockdown of human PCP and PAR genes in EphB2-GFP, EphB2 and ephrinB1 stable HEK293 cell lines was performed using Silencer Select (Pre-designed or Validated) siRNA oligonucleotides from Applied Biosystems. In each experiment, Silencer Select Negative Control siRNA (non-targeting siRNA) was used as control. Cells were plated in 6 well plates at density of 400000 cells/ml, 1ml/well and incubated for up to 24 h. After incubation, cells were transfected with siRNA using Lipofectamine RNAiMAX Reagent (Invitrogen), according to the manufacturer's recommendations for 6 well plate transfection (60pmol siRNA transfected per well and Opti-MEM I Reduced Serum Medium-with GlutaMAX (Invitrogen) was used). 2 or 3 siRNAs to the same gene were pooled, to reduce non-specific/off-target effects, and a total of 60pmol siRNA was transfected per well. The cells were incubated for 6 h before adding 1.5ml media to each well and incubating further until required.

Silencer Select Pre-designed (PD) and Validated (V) siRNAs used:
Negative Control #1
Dvl2: s4396 (PD), s4397 (PD), s4398 (PD)
Dvl3: s675 (V), s223453 (PD)
Daam1: s22811 (PD), s22812 (PD), s22813 (PD)
PAR-3: s32126 (PD), s32127 (PD), s32128 (PD)

PAR-6B: s39171 (PD), 39172(PD), s39173 (PD)
N-cadherin: s2771 (PD), s2773 (PD)

2.2.2.2 Quantitative Western blot assays

The extent of siRNA knockdown 72 h post-transfection was analysed by Western blot. Cells were chilled on ice for 10 min, rinsed in ice-cold PBS, collected in PBS and pelleted by centrifugation. They were lysed in 30µl cell lysis buffer (1% NP-40, 20mM Hepes, pH7.4, 100mM NaCl, 10mM $Na_4P_2O_7$, 1mM $CaCl_2$, 1mM $MgCl_2$, Halt protease inhibitor cocktail (Thermo Fisher Scientific, 1:100) for 10 min at 4°C. Cell lysate was obtained by centrifugation at 13000rpm for 10 min at 4°C, and the supernatent collected. Protein concentration in cell lysates was measured using bicinchoninic acid protein assay (Pierce BCA Protein Assay Kit, Thermo Fisher Scientific), according to the manufacturers instructions, and Thermo Spectronic Genesys 10UV Spectrophotometer. Sample buffer solution (NuPAGE LDS sample buffer (4x) and Reducing Agent (10x) (both Invitrogen), mixed 2.5: 1 respectively) was added to each lysate condition in a ratio 3.5:6.5 respectively, before denaturing for 10 min at 65°C. Lysate/sample buffer solution mixes were loaded (50µg protein per well) onto NuPAGE 10% Bis-Tris Gels (Invitrogen) with 5µl Novex Sharp Pre-stained protein standard, and run in Novex Mini-Cell tanks (Invitrogen) in NuPAGE MOPS SDS Running Buffer (Invitrogen) for 45 min at 200V. Transfer of proteins from gels to rehydrated Immobilon-FL membranes (Millipore) was performed using XCell II Blot modules (Invitrogen) in transfer buffer (NuPAGE Transfer Buffer (Invitrogen), 10% methanol, 0.1% NuPAGE Antioxidant (Invitrogen) and distilled water) for 80 min at 30V.

Membranes were blocked in blocking solution (50% Odyssey Blocking Buffer (LI-COR Biosciences) and 50% PBS) for 1 h at room temperature or 4°C overnight, and incubated with primary antibodies in blocking solution/0.1%Tween. The membranes were incubated for 1 h at room temperature or overnight at 4°C, and washed 4x 5 min in PBTw before incubation with primary antibodies in blocking solution/0.1%Tween/0.01%SDS solution (Bio-Rad laboratories) for 1 h at room temperature or overnight at 4°C. The secondary antibodies used were conjugated to infrared fluorescent dyes IR700 and IR800, and used 1:5000: donkey anti-rabbit, anti-mouse- or anti-goat (Rockland). After staining, the membranes were washed 4x 5 min in PBTw and scanned using 700- and 800-nm channels on an imager (Odyssey; LI-COR Biosciences), and the intensity of staining was determined using the median background method.

Primary antibodies were used at the indicated dilutions: Rabbit anti- γ Tubulin (Sigma 1:1000), mouse anti-α-Tubulin (Sigma 1:5000), rabbit anti- β catenin (Sigma 1:500), rabbit anti-PAR-6B (Sigma 1:1000), goat anti-Dvl2 (N-19 Santa Cruz Biotechnology, Inc. 1:400), mouse anti-Dvl3 (4D3 Santa Cruz Biotechnology, Inc. 1:400), mouse anti-Daam1 (Abnova 1:100), rabbit anti-PAR-3 (Millipore 1:250), rabbit anti-phospho-Eph (gift from Catherine Nobes 1:500), goat anti-EphB2 (R&D Systems 1:1000), goat anti-ephrinB1 (R&D

Systems 1:1000), mouse anti-N-cadherin (BD biosciences 1:1000), mouse anti-pan-cadherin, (Sigma 1:1000).

2.2.2.3 Analysis of EphB2 receptor activation

EphB2-GFP cells were stimulated with recombinant ephrinB1-Fc mouse chimera (R&D systems 1ug/ml). 1ml media was removed from each well and 10µl chimera (or sterile PBS as a control) added per well before incubating at 37°C for 30 min. When analysing the extent of EphB2 receptor activation after knockdown with siRNA, cells were stimulated 72 h after siRNA transfection. Cells were harvested and Western blot analysis carried out, as described in 2.2.2.2 Quantitative Western blot assays, with phosphatase inhibitor cocktail set II (EMD)) added to the lysis buffer. Membranes were blocked, and incubated in primary and then secondary antibodies for 1 h each at room temperature.

2.2.3 Immunocytochemistry

Cells were fixed in fixative (4% Formaldehyde Ultrapure (Thermo Scientific), MEM (GIBCO), sterile water and sodium hydroxide to pH 7.5 (filtered and pre-warmed at 37°C)) for 15 min, washed 3x PBS, 1x PBTw, 1x PBS each for 5 min. After washing, blocking was carried out for 1 h at room temperature or overnight at 4°C in blocking buffer (2% bovine serum albumin, 4% donkey serum (both Jackson Immuno Research) in PBS. The cells were incubated with primary antibodies in blocking buffer for 1 h, washed 3x PBS for 5 min and then incubated with secondary antibodies in blocking buffer (cy5-conjugated donkey anti-mouse, 1:250, Jackson Immuno Research) for 1 h, all at room temperature. After washing, samples were mounted using the ProLong Gold with DAPI antifade kit (Molecular Probes, Invitrogen) and stored at -20°C.

Primary antibodies were used at the indicated dilutions: mouse anti-N-cadherin (BD biosciences 1:250), mouse anti-Pan-cadherin, (Sigma 1:500), mouse anti-GM130 (BD Transduction Laboratories 1:200).

2.2.4 Cell behaviour assays

2.2.4.1 Cell tracking assay

For cell tracking studies, siRNA-transfected cells were fluorescently labelled 48 h after transfection. Media was removed from the cells and replaced with 2ml labelling solution (5µM CellTracker Orange CMRA or Green CMFDA dyes (Molecular Probes, Invitrogen) in pre-warmed DPBS containing 1000mg/l D-glucose and 36mg/l sodium pyruvate, calcium and magnesium (GIBCO, Invitrogen)) for 30 min at 37°C. Labelling

solution was then replaced with fresh media before incubating again at 37°C for 1 h. Dissociated cell suspensions were made using Accutase (PAA Laboratories), re-suspending in media with 2% HEPES (PAA) and filtering through 40µm filters to obtain a single cell dissociation suspension.

An 8 well chambered coverglass system (1.0 borosilicate; Lab-Tek, Nunc), was coated with 50µg/ml fibronectin (from bovine plasma; Sigma) for 30 min at room temperature, washed 3x PBS and left in PBS. Two cell lines were mixed in equal proportion and plated into each well of the coverglass system at a concentration of 30000 total cells/cm^2 (200µl/well). Cells were incubated at 37°C for 1 h before visualisation using an RT live-imaging workstation (Deltavision; Applied Precision, LLC) on a microscope (IX-70; Olympus) with a charge-coupled device camera (MicroMax 1300 YHS; Roper Scientific) and a heated environmental chamber (37°C; 5% CO_2). Images were acquired with a 4x /0.13 NA objective (Olympus) every minute for 2 h using SOFTWORX acquisition software (Applied Precision, LLC).

2.2.4.2 Boundary assay

For the boundary assay, siRNA-transfected cells were fluorescently labelled 48 h after transfection and dissociated, as described in 2.2.4.1 Cell tracking assay. A 4 well chambered slide system (1.0 borosilicate; Lab-Tek II, Nunc), was pre-coated with fibronectin, as described in 2.2.4.1 Cell tracking assay, and a barrier insert (Culture insert, Ibidi) was placed in each culture slide well (after removing the PBS) using sterilised forceps. Two cell lines were plated in equal proportion either side of a barrier, at a concentration of 1.26 million total cells/ml (70µl each side of the barrier). It was important that the chamber slides were not allowed to dry out. Cells were incubated at 37°C for 6 h before removing the barrier (with sterilised forceps) and replacing the media with 1ml fresh media containing 2% HEPES. Cells were incubated at 37°C for 48 h before being fixed and mounted in ProLong Gold, as described in 2.2.3 Immunocytochemistry. Cells were visualised using a Deltavision microscope, as described in 2.2.4.1 Cell tracking assay, and images were acquired with 4x /0.13 NA and 10x /0.4 NA objectives (Olympus). For time-lapse imaging of boundary cell behaviour, a 2 well coverglass system (chambered 1.0 borosilicate; Lab-Tek, Nunc) was used and cells were visualised using a Deltavision microscope, as described in 2.2.4.1 Cell tracking assay, in a heated environmental chamber (37°C; 5% CO_2), and images were acquired with a 10x /0.4 NA objective (Olympus) every 3 min for 48 h. Videos of cell behavior were created using ImageJ software (National Institutes of Health).

2.2.4.3 Cell segregation assay

For cell segregation assays, 48 h after transfection siRNA-transfected cells were dissociated and a 2 well chambered slide system (1.0 borosilicate; Lab-Tek II, Nunc) was pre-coated with fibronectin, as described in 2.2.4.1 Cell tracking assay. Two cell lines were mixed in equal proportion and plated into each well of

the chamber slide system at a concentration of 200000 total cells/cm^2 (2ml/well). Cells were incubated at 37^{o}C for 48 h until confluent before being fixed and mounted in ProLong Gold, as described in 2.2.3 Immunocytochemistry. Cells were visualised using a Deltavision microscope, as described in 2.2.4.1 Cell tracking assay, and images of segregated cells were acquired with a 4x /0.13 NA objective (Olympus). Live imaging of cell segregation used a concentration of 400000 total cells/cm^2 plated in a 2 well chambered coverglass system (1.0 borosilicate; Lab-Tek, Nunc). Camera and microscope set up as described for time-lapse imaging of boundary assay.

2.2.4.4 Hanging drop assay

For the hanging drop assay, siRNA-transfected cells were dissociated, as described in 2.2.4.1 Cell tracking assay. Two cell lines were mixed in equal proportion and dropped in 10µl drops onto a cover glass (22x50mm, Menzel-Glaser) at a concentration of 100000 total cells/ml (1000 cells/drop). Cover glasses were turned over 180^o (so the drops are hanging off the cover glass) and placed over a well of a 6 well plate containing 1ml media. Cells were incubated at 37^{o}C for 48 h before visualisation using a Deltavision microscope, as described in 2.2.4.1 Cell tracking assay. Cover glasses were turned over 180^o so drops were no longer hanging and images of co-aggregates were acquired using a Deltavision microscope with a 10x /0.4 NA objective (Olympus).

2.2.5 Methods of analysis

2.2.5.1 Cell tracking studies

2.2.5.1.1 Mean Squared Displacement (MSD)

Cell tracks from the EphB2-GFP population only were analysed. These were combined from two data points for each condition for each experiment. Measurement of XY coordinates of cells centroids and subsequent analysis of cell movement were performed using the single particle tracking algorithm in GMimPro software (Mashanov & Molloy, 2007), http://www.nimr.mrc.ac.uk/gmimpro/. Mean-squared displacement (MSD) of cells was calculated using overlapping intervals (DiMilla *et al.*, 1993; Martens *et al.*, 2006), and MSD was plotted over change in time.

For each experiment, the average “endpoint” MSD (calculated from the MSD of each track at 57 min intervals) was taken for each condition. The ratio increase in MSD with Eph-ephrin signalling was calculated for control siRNA conditions and experimental siRNA conditions, and averaged over three

experimental repeats. Statistical analysis was carried out to determine the significance of the difference in MSD ratios using the Student's T-Test ($p<0.05$).

2.2.5.1.2 Automated analysis of cell behavior

TrackParser (a custom-made Python program) was written by Robert Gilchrist for the automated analysis of cell behaviour. The XY coordinates of tracks were extracted from GMimPro and inputted into TrackParser. All tracks are aligned and only the full-length tracks analysed (2 h long) for analysing the endpoints, track orientation and turning angles. For track orientation analysis, the XY coordinates of cell positions are plotted relative to a central site of interaction. 100 tracks are plotted, which are randomly selected. For endpoint analysis, the endpoint positions of tracks are plotted as individual points around a central origin with the root mean square displacement of these as a solid line around the origin. For turning angle analysis, tracks are analysed in overlapping 5 min intervals. The likelihood of a cell moving more directionally is determined by analysing the probability distribution function (PDF) for the deviation of a cell from straight-line movement based on its previous directionality.

2.2.5.2 Cell segregation assay

2.2.5.2.1 Perimeter Regularity Index

The perimeter regularity index (PRI) (Hueck *et al.*, 2000) of clusters was calculated to quantify cell segregation. Raw images of the EphB2 cell population were inputted (three per condition) into an automated program (Chen Qian, Confocal Imaging and Analysis Laboratory, NIMR), which identifies cell clusters based on a threshold pixel intensity, and calculates the mean PRI value across all clusters within each image. The significance between conditions compared to control siRNA condition with Eph-ephrin signalling was calculated using the Student's T-Test ($p<0.05$) within each experiment. Experiments where the PRI value for the control siRNA condition with Eph-ephrin signalling was not significantly different to the control siRNA condition without Eph-ephrin signalling were discarded from further analysis. The overall PRI value for each condition was calculated by averaging the PRI values of the condition for each experiment (minimum of three repeats). The significance of the overall PRI value for each condition compared to the control siRNA condition with Eph-ephrin signalling was calculated using the Student's T-Test ($p<0.001$) on the average values for each experiment.

2.2.5.2.2 Nearest Neighbour

Quantification of segregation was also performed using Nearest Neighbour (NN) analysis (Mochizuki *et al.*, 1998). Black and white images of the EphB2-GFP population were binarised and resized so that each pixel represented the area of one cell and the clusters appeared black. These images were then analysed using custom-written software, which assessed the proportion of cells surrounded by like cells. The result of this analysis is represented as a single number, the Nearest Neighbour value, for each image. A value of 0.5 represents a salt and pepper unsegregated pattern, and a value of 1 represents a totally segregated population. At least 3 images were analysed per condition and experiments were repeated at least once.

2.2.5.3 Boundary assay

The length of the boundary (pixels) was calculated to quantify boundary sharpness. Raw images (4x) of the EphB2 cell population were inputted (three per condition) into an automated program (Chen Qian, Confocal Image Analysis Laboratory, NIMR), which calculated the boundary length for each image based on a pixel intensity threshold. Experiments were excluded from further analysis according to the same criteria described for 2.2.5.2.1 Perimeter Regularity Index. The boundary length shown represents the mean boundary length of the condition for each experiment (minimum of three repeats). The significance of the overall boundary length value for each condition compared to the control siRNA condition with Eph-ephrin signalling was calculated using the Student's T-Test ($p<0.01$) on the average values for each experiment.

All error bars on all bar charts represent standard error of the mean (SEM).

2.2.6 Golgi orientation

Angles of Golgi-nucleus position relative to a boundary were calculated as a read-out of cell polarity. Boundary assay conditions were stained (as described in 2.2.3 Immunocytochemistry) with an antibody to GM130, which is localised to the Golgi. Images were taken using a Deltavision microscope, as described in 2.2.4.1 Cell tracking assay, using a 63x objective (Olympus). Four images were taken for each condition for a minimum of three experiments. Angles of Golgi-nucleus position relative to a boundary were calculated for each cell type (either side of the boundary) using ImageJ software (National Institutes of Health). For each cell type, cells were counted as a boundary population if they contacted an unlike cell type, and as a non-boundary population if they were in the 35% of the cell type population furthest from the boundary. Angles were measured relative to the boundary of an EphB2-ephrinB1 interaction on a cell-by-cell level, but relative to the population level boundary for non-boundary cells. Angles for each population of a condition (over all experiments) were grouped into 15^{o} intervals, and the frequency plotted

on a radar graph as a proportion of the total number of angles counted. The statistical significance of angle distributions between populations or conditions was calculated using the F Test ($p<0.01$) on ungrouped angle data.

2.2.7 Quantitative Real Time PCR

2.2.7.1 RNA extraction

RNA was extracted from approximately 200000 cells using PicoPure RNA Isolation kit (MDS Analytical Technologies), according to the manufacturer's instructions, and RNA stored at -80°C.

2.2.7.2 cDNA preparation

Approximately 1µg RNA was used for cDNA preparation using a Superscript kit (Superscipt™ First Strand, Invitrogen), according to the manufacturer's instructions, and cDNA stored at -20°C.

2.2.7.3 Quantitative Real Time PCR (RT-PCR)

RT-PCR was performed with an ABI 7500 Real-Time PCR System (Applied Biosystems) using SYBR Green (Platinum SYBR Green qPCR Supermix-UDG, Invitrogen) in a 20µl reaction volume, according to the manufacturer's instructions (based on (Fijnvandraat *et al.*, 2003; Lekanne Deprez *et al.*, 2002)). Relative levels of gene expression were calculated compared to β-actin controls. Complementary DNA PCR primers were designed using Primer Express software (version 2.0, Applied Biosystems).

3 EPH-EPHRIN MEDIATED CELL SEGREGATION AND BOUNDARY SHARPENING CAN BE ANALYSED EFFECTIVELY IN VITRO

3.1 Introduction to assays

Eph-ephrin signalling plays a key role in the restriction of cell intermingling across hindbrain boundaries (Xu *et al.*, 1999) and the formation of sharp boundaries between rhombomeres (Fig. 2 C, C') (Cooke *et al.*, 2005). Eph-ephrin interactions contribute to the sharpening of segments by regulating both repulsion at interfaces and cell affinity within rhombomeres (Cooke *et al.*, 2005; Pasini & Wilkinson, 2002). Zebrafish embryo explant experiments show that complementary populations of cells transiently overexpressing an EphB receptor and its cognate ephrinB are sufficient to drive segregation of the populations with the formation of smooth boundaries (Fig. 2 B, B') (Mellitzer *et al.*, 1999; Tanaka *et al.*, 2003). These approaches have the disadvantage that overexpression of Eph receptor and the presence of endogenous ligands lead to high baseline activation of the Eph receptor. EphB receptors have been shown to become auto-activated and auto-phosphorylated by overexpression (Tanaka *et al.*, 2003) and ephrinB2 and ephrinB1 have been shown to signal in a cell autonomous mode in the absence of receptor binding (Bochenek *et al.*, 2010; Lee *et al.*, 2006).

Segregation assays in cell culture have been developed in the Wilkinson laboratory with HEK293 cells overexpressing either EphB2 or ephrinB1. These have the advantage of only low levels of receptor auto-activation and show the segregation of EphB2 cells from ephrinB1 cells (Fig. 2 A, A') (Poliakov *et al.*, 2008). In addition, EphB2 cells show a rapid collapse of cell processes after interaction with ephrinB1 cells, but not EphB2 cells (Fig. 2 D, D') (Poliakov *et al.*, 2008). Taken together, these assays show EphB2-ephrinB1 signalling leads to segregation of EphB2 cells from ephrinB1 cells, and EphB2 cells show repulsion and collapse responses on interaction with ephrinB1 cells.

3.2 RESULTS

In order to study the role of Eph-ephrin signalling in cell segregation and boundary sharpening, and to explore the downstream mechanisms that drive these processes, a system was required that is reproducible and quantifiable. It was decided to focus initial experiments on an *in vitro* approach using the cell segregation assay (Jorgensen *et al.*, 2009; Poliakov *et al.*, 2008) developed in the Wilkinson laboratory. This assay uses stable HEK293 cell lines generated to express membrane-targeted GFP (WT-GFP), EphB2, EphB2 plus membrane-targeted GFP (EphB2-GFP), ephrinB1 or untransfected lines, which

are referred to as wild-type (WT) (Poliakov *et al.*, 2008). In order to determine the endogenous and exogenous expression levels of EphB2 and ephrinB1 in each of these cell lines, Western blot analysis was carried out using antibodies against EphB2 and ephrinB1. Both EphB2 and ephrinB1 are expressed endogenously at low levels, and overexpressing either EphB2 or ephrinB1 does not increase endogenous levels of ephrinB1 or EphB2 respectively (Fig. 8).

3.2.1 EphB2 cells segregate from ephrinB1 cells in an *in vitro* cell segregation assay

3.2.1.1 EphB2 cells segregate from ephrinB1 cells but not from other EphB2 cells

To analyse the ability of EphB2 cells to segregate from ephrinB1 cells, stable cell lines expressing EphB2-GFP were mixed in equal proportion with either ephrinB1 cells or EphB2 cells. Cells were plated at low density in a well of a 2-chambered slide system and incubated at 37^{o}C for 48 hours, allowing migration and proliferation until confluence. EphB2-GFP/EphB2 cell mixtures form a salt and pepper pattern (Fig. 9 B), which is indistinguishable from WT-GFP/WT cell mixtures at the same time point (Fig. 9 F). EphB2-GFP cells segregate from ephrinB1 cells into distinct clusters (Fig. 9 A), but not from EphB2 cells (Fig. 9 B).

3.2.1.2 Optimisation of cell segregation assay

It was important first to establish plating conditions that reproducibly produced a cell segregation pattern that was quantifiable. Initially, experiments were carried out to assess how changing the overall density of cells plated or the ratio of EphB2-GFP:ephrinB1 cells at a given plating density, would affect cluster formation and morphology. This was important as it highlighted how changes in cell proliferation or the length of time cells were left to segregate could affect the pattern of segregation seen, which would be independent of the segregation response due to EphB2-ephrinB1 signalling. In addition, it was important to establish plating conditions that reproducibly produced a cell segregation pattern that was quantifiable.

The size and shape of segregated EphB2 cell clusters varied dramatically. When the number of total cells plated was high but the ratio of EphB2-GFP:ephrinB1 cells was kept the same (Fig. 10 A), the number of clusters of EphB2-GFP cells was high and the cluster size was reproducible across the dish. However, the proportion of the slide covered by EphB2-GFP cells seemed to increase as the density of cells increased, and the proportion of the slide covered by ephrinB1 cells seemed to decrease, even though the initial ratio between the two populations is unchanged. When the ratio of EphB2-GFP:ephrinB1 cells was increased,

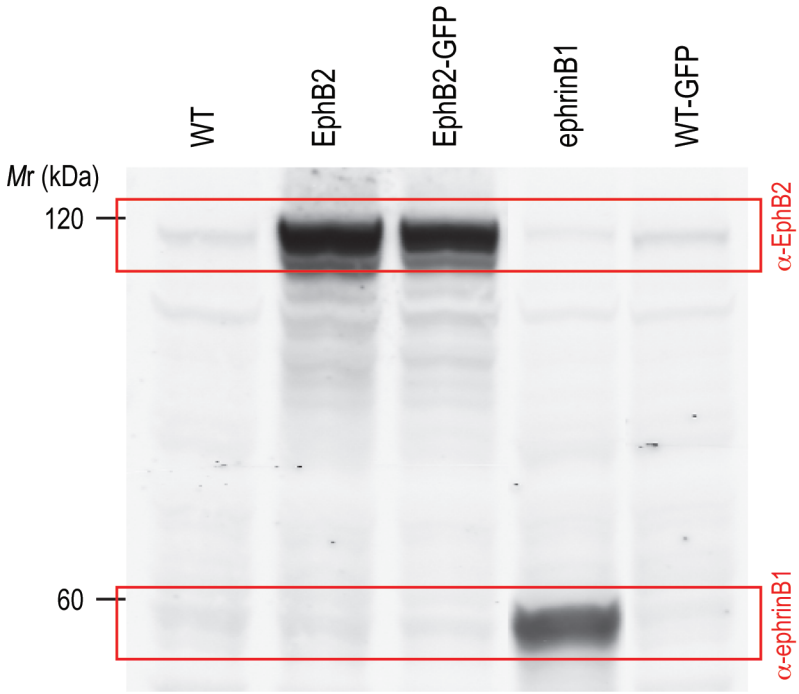

Figure 8: Western blot analysis of endogenous and exogenous expression of EphB2 and ephrinB1 in HEK293 cells and stable cell lines

Western blot analysis of HEK293 cell lines for endogenous and exogenous expression of EphB2 and ephrinB1, using antibodies against EphB2 and ephrinB1. Stable cell lines: WT (HEK293 cell line), EphB2 (HEK293 cell line overexpressing EphB2), EphB2-GFP (HEK293 cell line overexpressing EphB2 and membrane-bound GFP), ephrinB1 (HEK293 cell line overexpressing ephrinB1), WT-GFP (HEK293 cell line overexpressing membrane-bound GFP). Both EphB2 and ephrinB1 are expressed endogenously at low levels, and overexpressing either EphB2 or ephrinB1 does not increase endogenous levels of ephrinB1 or EphB2 respectively.

Figure 9: Sorting of EphB2 cells from ephrinB1 and the quantification of segregation

Analysis of the cell segregation assay with single-section brightfield and GFP images. Mixtures of stable EphB2-GFP and ephrinB1 (A), EphB2-GFP and EphB2 (B) and WT-GFP and WT cells (F) were fixed 48 h after mixing. EphB2-GFP cells sort from ephrinB1 cells (A) but not EphB2 cells (B). No cell sorting is seen when WT-GFP and WT cells are mixed (F).

Images of the GFP channel (A', B', F') are used for automated analysis of segregation parameters; area of clusters (C), Heywood Circularity Index (D) and Perimeter Regularity Index (PRI) (E, G). A significant difference is observed between EphB2-GFP/ephrinB1 and EphB2-GFP/EphB2 mixtures for all three parameters (C-E, $p<0.001$). There is no significant difference in the PRI value between EphB2-GFP/EphB2 and WT-GFP/WT cell mixtures (G).

(H): Nearest Neighbour (NN) analysis of degree of clustering. Represents the number of EphB2-GFP cells surrounding an EphB2-GFP cell out of a maximum possible of four (NN=1). EphB2-GFP/ephrinB1 mixtures (NN=0.79) are more sorted than EphB2-GFP/EphB2 mixtures (NN=0.69), and this difference is significant ($p=0.01$).

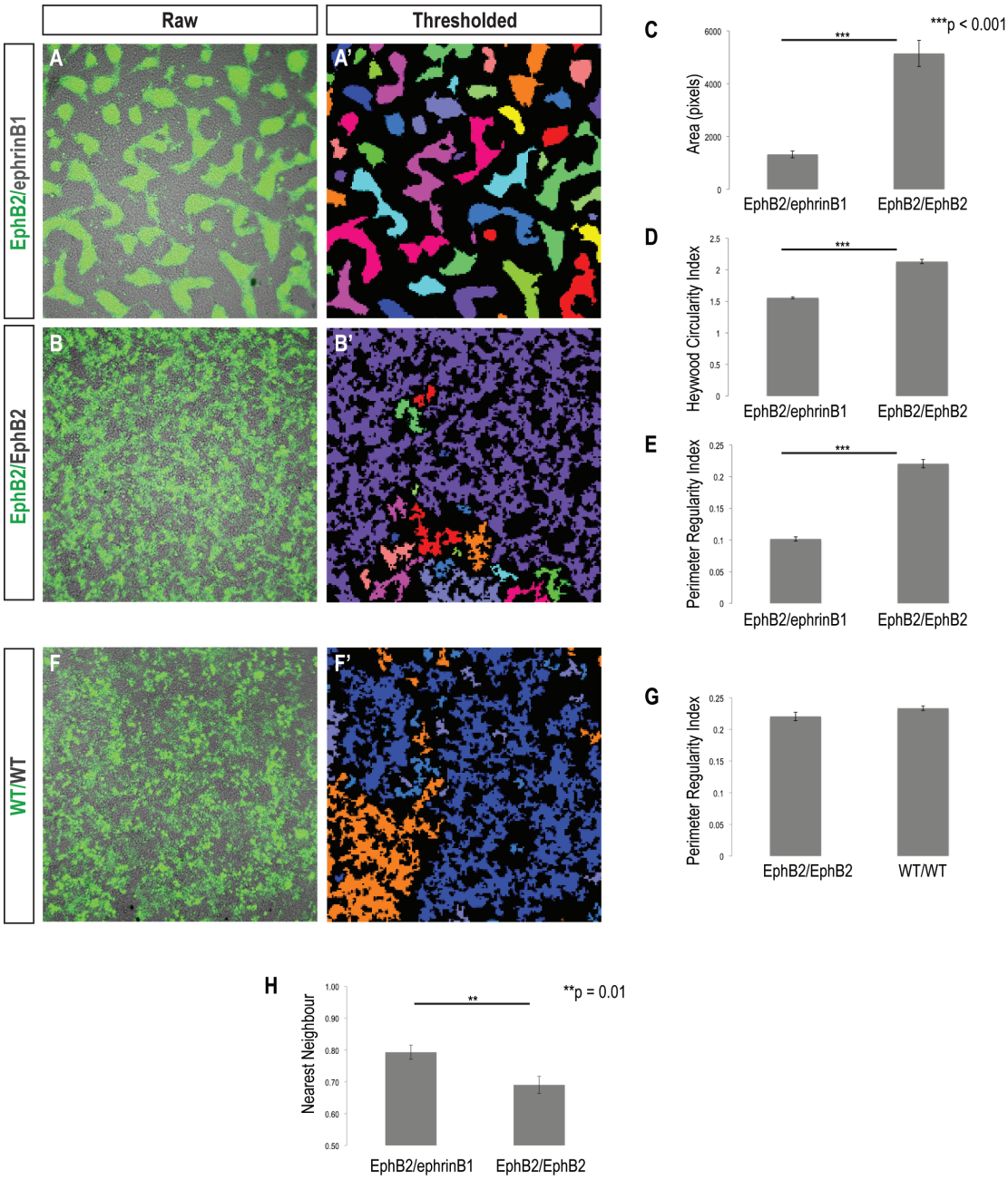
Raw
Thresholded
EphB2/ephrinB1
EphB2/EphB2
WT/WT
A
A'
B
B'
F
F'
C
***p < 0.001
***
Area (pixels)
6000
4000
2000
0
EphB2/ephrinB1
EphB2/EphB2
D
Heywood Circularity Index
2.5
2
1.5
1
0.5
0
E
Perimeter Regularity Index
0.25
0.2
0.15
0.1
0.05
G
WT/WT
H
**p = 0.01
**
Nearest Neighbour
1.00
0.90
0.80
0.70
0.60
0.50

Figure 10: Changes in the ratio and density of cells in the cell segregation assay

Analysis of the effects of varying the ratio and density of EphB2-GFP and ephrinB1 cell populations in the cell segregation assay.

(A): Varying the seeding density of total cells, whilst maintaining a 1:1 ratio of cell populations, reduces connections between clusters. 1x-seeding density is 50000 cells/cm^2, 3x is 150000 cells/cm^2, 4x is 200000 cells/cm^2 and 8x is 400000 cells/cm^2. The phenotype at 200000 cells/cm^2 was the most reproducible across many experimental repeats.

(B): Varying the ratio of EphB2-GFP cells to ephrinB1 cells, each plated at a density of 150000 total cells/cm^2. When ephrinB1:EphB2-GFP ratio is high, EphB2-GFP clusters are smaller and more separated. When EphB2-GFP:ephrinB1 ratio is high, EphB2-GFP clusters are larger and inter-connected. A 1:1 ratio of EphB2-GFP to ephrinB1 cells gave the optimum segregation.

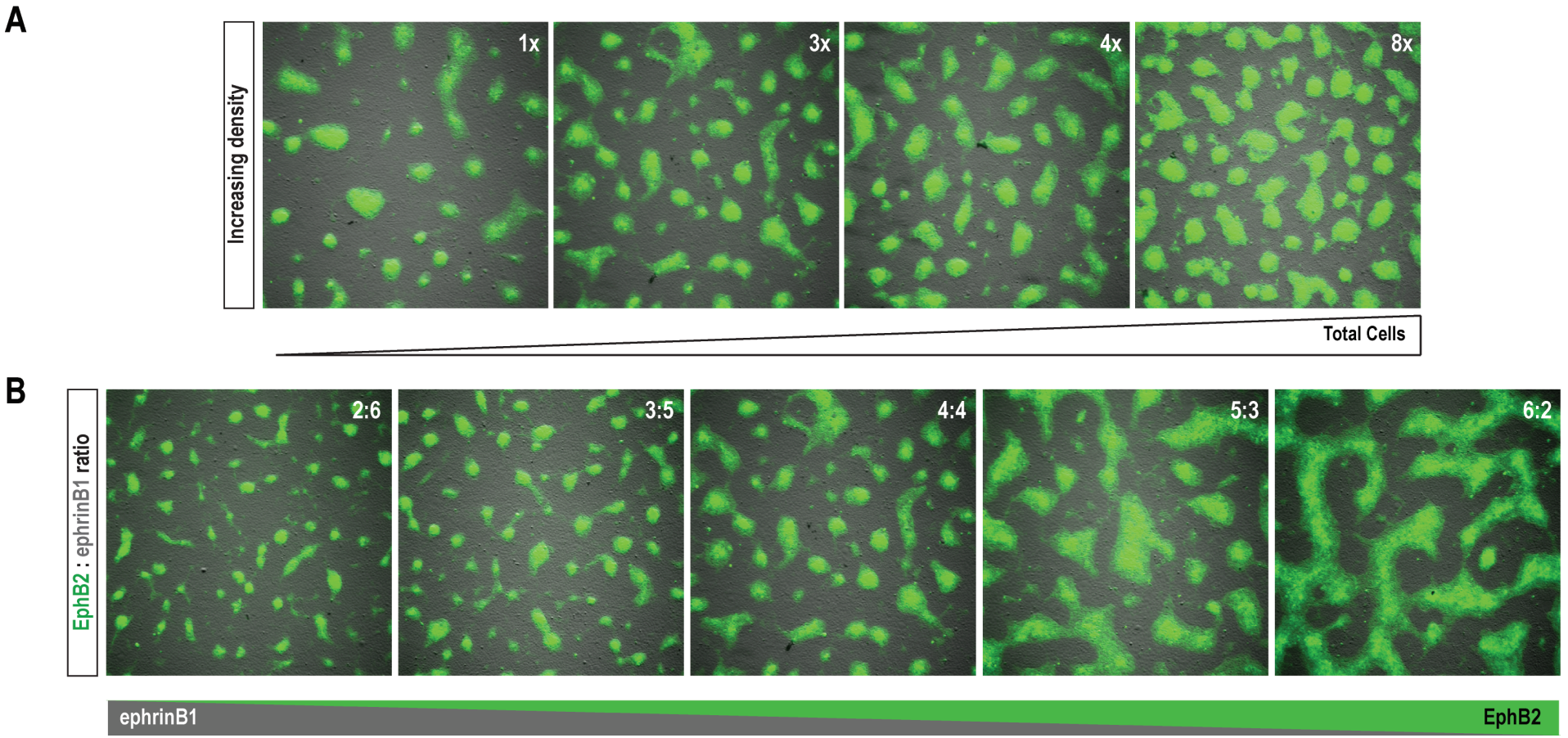
A
Increasing density
1x
3x
4x
8x
Total Cells
B
EphB2 : ephrinB1 ratio
2:6
3:5
4:4
5:3
6:2
ephrinB1
EphB2

the EphB2-GFP cell clusters became larger and more inter-connected (Fig. 10 B). Clusters are brighter too at high density, which is indicative of more cells being part of the cluster. Based on these results, a plating density of 200000 cells/cm^2 with a 1:1 ratio of EphB2-GFP cells to ephrinB1 cells were chosen as the optimum conditions to use in subsequent experiments. Confluence was achieved 24 hours after plating, so allowing migration and interaction between cells before boundary sharpening, with refinement occurring at later stages when confluent.

3.2.1.3 EphB2 cells compact on interaction with ephrinB1 cells

High magnification cluster analysis was carried out in order to analyse differences in cell morphology between EphB2-GFP cells and ephrinB1 cells, which might affect the size of segregated cell clusters. EphB2-GFP/ephrinB1 cell mixtures were analysed both at the endpoint of the segregation assay (when confluence is achieved) (Fig. 11 A) and before confluence is achieved (Fig. 11 B), and stained for pan-cadherin, which labels the membranes of all cells and allows cell morphology to be analysed. EphB2-GFP cells (green) in a cluster are smaller than ephrinB1 cells (unlabelled), whereas EphB2-GFP cells not in a cluster (Fig. 11 A) or in a cluster before confluence has been reached (Fig. 11 B), show no difference in cell size to ephrinB1 cells (not quantified). In addition, Z-sections through clusters show that EphB2-GFP cells in clusters pile up on top of each other, compared to ephrinB1 cells that remain in a monolayer adhered to the substrate (Fig. 11 B). These images were taken by Rosalind Morley in the Wilkinson laboratory. This suggests segregation of EphB2-GFP cells from ephrinB1 cells causes EphB2-GFP cell compaction and the rounding up of clusters from the dish, and will be discussed later.

3.2.1.4 Quantification of cell segregation

In order to assess the degree of segregation observed when EphB2-GFP cells are mixed with ephrinB1 cells compared to EphB2 cells, an approach was taken to quantify the number of cells in contact with “like” vs. “unlike” cells. This Nearest Neighbour (NN) analysis of degree of clustering (Mochizuki *et al.*, 1998) gives an estimate of the degree of segregation by approximating one cell as one pixel. The number of EphB2-GFP pixels surrounding each EphB2-GFP pixel are measured out of a maximum possible of four options; above, below, right and left of each cell, and the degree of segregation is estimated using custom made software. When cells are completely segregated so surrounded by four “like” cells, NN=1, and when cells are totally mixed so surrounded by two “like” and two “unlike” cells, NN=0.5. EphB2-GFP/ephrinB1 cell mixtures (NN=0.79) are more segregated than EphB2-GFP/EphB2 mixtures (NN=0.69), and this difference is significant ($p=0.01$) (Fig. 9 H). Nearest Neighbour for EphB2-GFP/EphB2 mixtures is not 0.5 due to the clonal growth that occurs when there is less mixing at confluence. Even though the difference between segregation in EphB2-GFP/ephrinB1 and EphB2-GFP/EphB2 cell mixtures is reproducible between experiments by eye, the difference between these conditions using NN analysis was surprisingly

Figure 11: Compaction of EphB2 cells in the cell segregation assay

Analysis of cell morphology at the endpoint of the segregation assay, using immunocytochemistry. EphB2-GFP/ephrinB1 cell mixtures are stained using a pan-cadherin antibody (red), as a general membrane marker, and DAPI to mark nuclei (blue). GFP is a marker of EphB2-GFP cells (green) and ephrinB1 cells are unlabelled.

(A): EphB2 cells, which have segregated into clusters, show a more compact cell morphology covering a smaller area than ephrinB1 cells.

(B): Z-sections through clusters show that EphB2 cells in clusters pile up on top of each other, compared to ephrinB1 cells that stay adhered to the dish. Images acquired with a 63x objective (Olympus), Leica SP2 confocal microscope. Images taken by Rosalind Morley, Wilkinson laboratory.

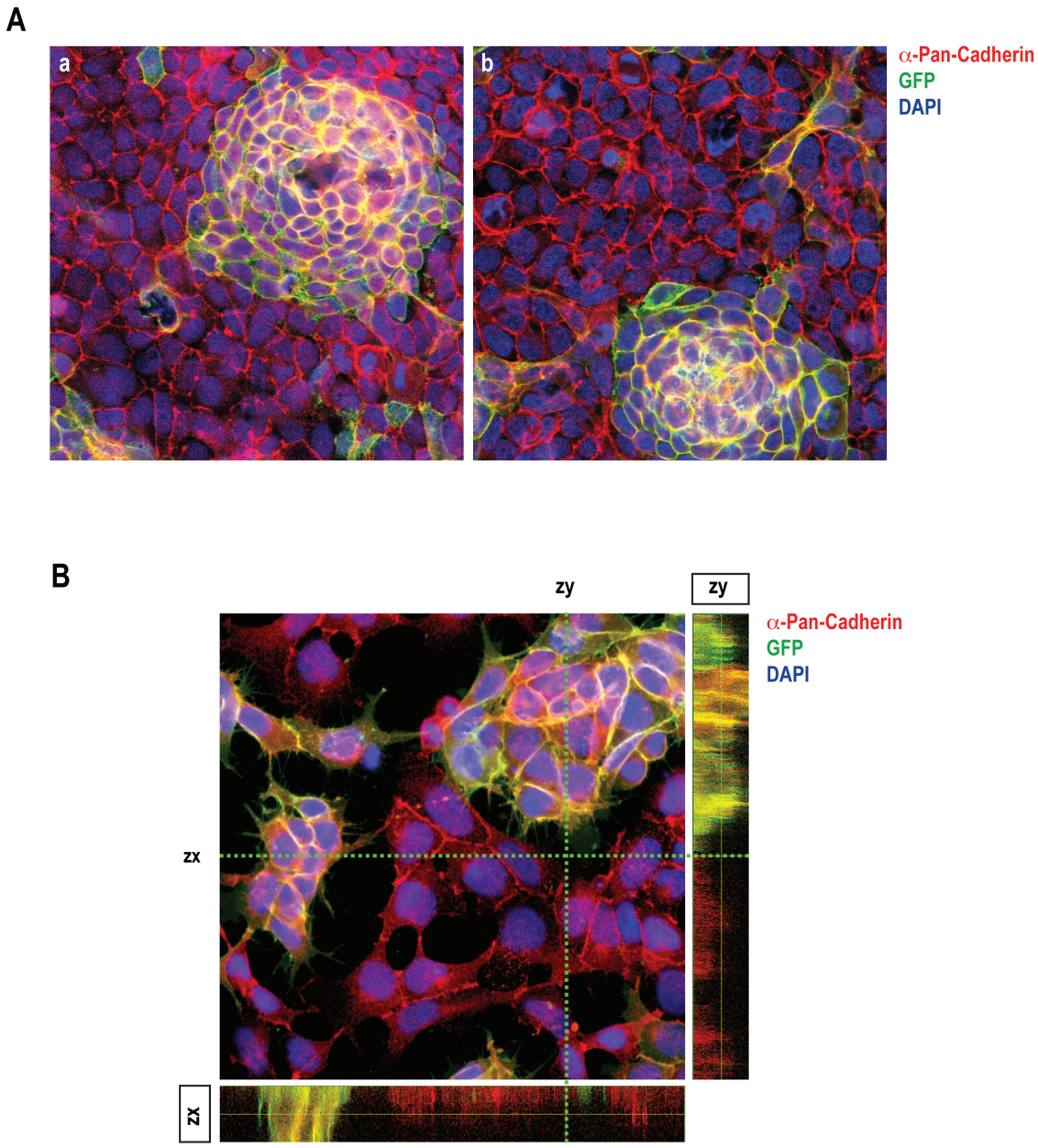
A
a
b
α-Pan-Cadherin
GFP
DAPI
B
zy
zy
zx
zx
α-Pan-Cadherin
GFP
DAPI

small. Further methods of analysis were therefore investigated.

In collaboration with Chen Qian (Confocal Imaging and Analysis Laboratory, NIMR), an automated program was designed to detect clusters of EphB2-GFP cells mixed with either ephrinB1 (Fig. 9 A') or EphB2 cells (Fig. 9 B') for quantification by three different methods. The threshold parameters approximate one cell as one pixel, and so a cluster is defined as a group of pixels of the same population of cells that are connected, and are presented in a colour coded manner, with one colour per cluster (Fig. 9 A'-B'). For all methods of analysis, quantification was calculated as an average based on three images per experiment and a minimum of three experimental repeats. The significance of any difference in quantification seen for each condition was calculated using the Student's T-Test ($p<0.001$) on the average values for each experiment.

An alternative measure of segregation to Nearest Neighbour was to calculate the average size of the cluster i.e. average area (pixels) per cluster per image. For EphB2-GFP cells mixed with ephrinB1 cells, the EphB2-GFP cells sorted into clusters with an average area of 1300 pixels (1 pixel=3.12μm length), whereas for EphB2-GFP cells mixed with EphB2 cells, the EphB2-GFP cells sorted into clusters with an average area of 5400 pixels (Fig. 9 C). This seems counterintuitive, as you would expect the cluster size to be much smaller in the salt and pepper unsorted distribution of EphB2-GFP cells mixed with EphB2 cells. However, because these scattered cells often contact other scattered cells, the method of automated thresholding creates the artefact of large clusters in the image. Many different ranges of threshold values gave similar results. Measuring the area of clusters is therefore not a reliable method of quantification.

A distinctive feature of the sorted clusters is that their boundaries are smooth. Two approaches were tested to analyse this: the Heywood Circularity Index (Christensen *et al.*, 2010) and Perimeter Regularity Index (Hueck *et al.*, 2000). The Heywood Circularity Index (HCI) is a roundness index that compares the perimeter of a cluster divided by the perimeter of a circle with the same area as the cluster. The smoother and more circular the boundary, the closer to 1 the HCI value will be. If the perimeter length is increased and the area is maintained, i.e. the clusters are less segregated and so the boundaries are more irregular, then the HCI increases. For EphB2-GFP cells mixed with ephrinB1 cells, the EphB2-GFP cells segregated into clusters with a HCI value of 1.6, whereas for EphB2-GFP cells mixed with EphB2 cells, the EphB2-GFP cells segregated into clusters with a HCI value of 2.3 (Fig. 9 D). Less complete sorting or irregularities in boundary sharpness, seen in EphB2-GFP/EphB2 cell mixtures, creates a disproportion in the ratio of area vs. perimeter and so the HCI increases. EphB2-GFP/ephrinB1 cell mixtures therefore have smoother boundaries around segregated clusters than in EphB2-GFP/EphB2 cell mixtures; however the shape of the cluster i.e. elongated or circular will also affect HCI, and this creates a large variability in the HCI values obtained.

The Perimeter Regularity Index (PRI) is a measure of the difference of the true membrane perimeter and a convex hull approximation of the same cluster i.e. the length of a smooth line drawn around the same cluster: PRI = (true membrane length - straight line length)/ straight line length (Hueck *et al.*, 2000). The PRI is 0 if the boundary of the cluster is perfectly smooth, and increases the more irregular the boundary is. For EphB2-GFP cells mixed with ephrinB1 cells, the EphB2-GFP cells sorted into clusters with a PRI value of 0.11, whereas for EphB2-GFP cells mixed with EphB2 cells, the EphB2-GFP cells sorted into clusters with a PRI value of 0.23 (Fig. 9 E). EphB2-GFP/ephrinB1 cell mixtures therefore have smoother boundaries around segregated clusters than in EphB2-GFP/EphB2 cell mixtures. Each of these methods of quantification of boundary sharpness showed clusters of EphB2-GFP cells within the EphB2-GFP/ephrinB1 cell mixtures to be significantly different to the EphB2-GFP/EphB2 cell mixtures ($p<0.001$).

3.2.1.5 Live imaging of cell segregation assay

In order to better understand the cellular movements and migratory processes required for EphB2-ephrinB1 mediated cell segregation, live imaging of the segregation assay was carried out. Cells were labelled with CellTracker dyes, then mixed and left to adhere to the dish before being imaged for 28 hours. EphB2-GFP (green) cells were mixed with ephrinB1 (red) cells, and these had begun to segregate from ephrinB1 cells and cluster after 5 hours, even though the cells had not yet reached confluence (Fig. 12 A). Cell movements were dynamic at high density suggesting segregation can occur when cell confluence is high.

Live imaging analysis of the cell segregation assay showed situations where ephrinB1 cells were trapped in a cluster and surrounded by EphB2-GFP cells. These groups of ephrinB1 cells became excluded from the cluster and moved into the ephrinB1-expressing cell domain (Fig. 12 B), but the mechanism for this is not known.

3.2.2 EphB2 cells sort from ephrinB1 cells in an *in vitro* boundary assay

It proved difficult to quantify the degree of segregation between experiments with the cell segregation assay (Fig. 9 C, H), due to sensitivity of the assay to cell density (Fig. 10 A) and its potential to be affected by proliferation rates (Fig. 10 A). As a result, analysis focussed on the sharpness of the cluster boundaries, of which there is a significant difference between EphB2-GFP/ephrinB1 and EphB2-GFP/EphB2 cell mixtures (Fig. 9 D, E). Eph-ephrin interactions are known to maintain sharp boundaries between rhombomeres of the developing hindbrain (Fig. 33 Appendix and (Cooke *et al.*, 2005)). Given this, I designed an *in vitro* boundary assay to better mimic the *in vivo* situation in the hindbrain, where Eph- and ephrin-expressing cells would not be mixed in a salt and pepper like fashion, and to simplify the method of measuring EphB2-ephrinB1 mediated boundary sharpness.

Figure 12: Live imaging of the cell segregation assay

Analysis of cell behaviour at high density (plated at 400000 cells/cm^2) in the segregation assay. EphB2-GFP cells (green) are mixed with ephrinB1 (red) cells.

(A): Cell sorting is evident at 5 h after plating. Sorting is refined over the 28 h and cells retain dynamic movement, even at later time points when they have reached confluence.

(B): Enlarged individual cluster analysis of segregation assay. Arrows depict ephrinB1 cells initially surrounded by EphB2-GFP cells to be excluded over time.

A

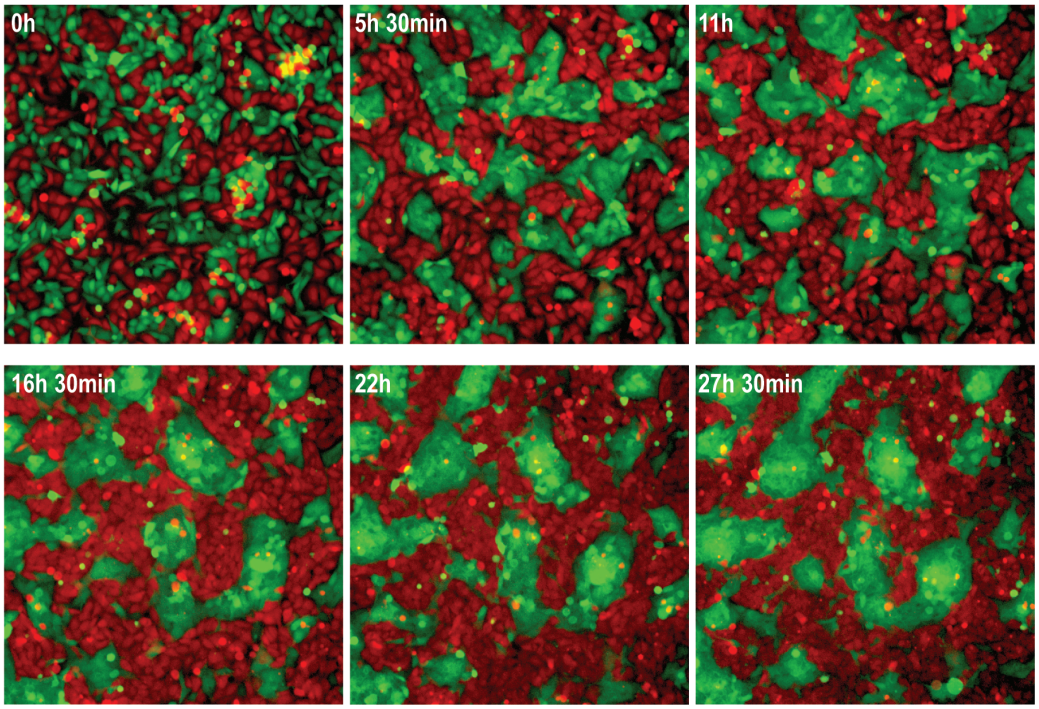
0h
5h 30min
11h
16h 30min
22h
27h 30min

B

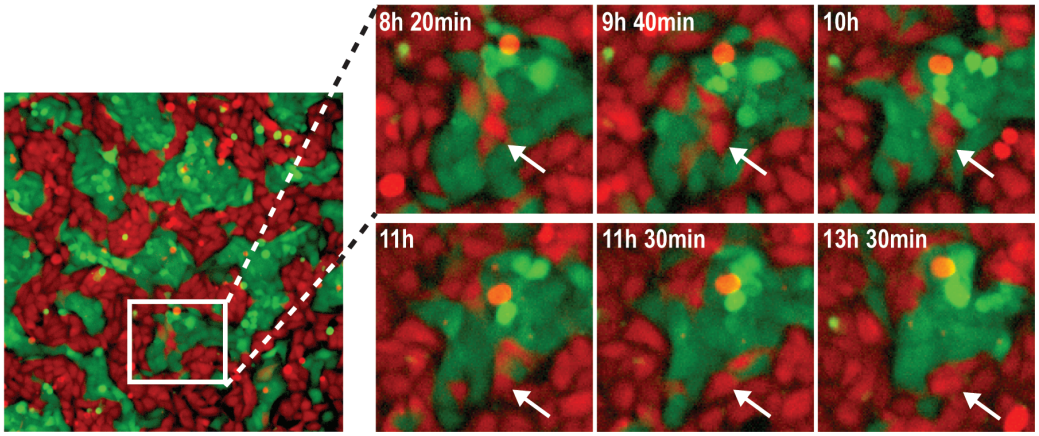
8h 20min
9h 40min
10h
11h
11h 30min
13h 30min

3.2.2.1 EphB2 cells form a sharp boundary with ephrinB1 cells but not with other EphB2 cells

To analyse the ability of EphB2 cells to form a sharp boundary with ephrinB1 cells, cells were labelled with CellTracker dyes before being plated either side of a barrier, preventing them from mixing. EphB2-GFP cells were plated in equal proportions opposite either ephrinB1 or EphB2 cells. Cells were allowed to adhere to the dish before the barrier was removed 6 hours after plating. Boundary sharpness was analysed after 48 hours, by which time opposing cells populations had migrated and interacted in the centre of the dish. A sharp boundary is formed at the interface between EphB2-GFP and ephrinB1 cells (Fig. 13 A), but the cells intermingle at the interface of the EphB2-GFP/EphB2 cell boundary and the boundary remains fuzzy (Fig. 13 B).

3.2.2.2 Optimisation of boundary assay

It was important to establish plating conditions that reproducibly produced a sharp boundary that was quantifiable. Initially barriers were designed and manufactured for experimental use in collaboration with the Engineering department, NIMR. This proved difficult as the manufactured plastic barriers needed to be sterilised before use, to avoid contamination of the cells, and be made to fit the wells of slides used for cell culture. As the wells in each slide varied in size by approximately 0.1mm, leakage and mixing of the two cell populations either side of the barrier was a problem.

An alternative approach was used in the form of small sterile silicone barriers that stick to the base of the well. A concern was that the fibronectin that coats the wells would be removed when the barriers were removed, thus preventing the migration of cells over extracellular matrix. This was tested by comparing the silicone barriers that stick to the dish with the manufactured plastic barriers that do not. This was found not to be the case (data not shown) since cell migration in each of these situations, with or without prior treatment with fibronectin, was indistinguishable. The small size of the silicone barriers meant that the sample area for analysis was small, but as these barriers dramatically reduced leakage and contamination problems, they were used in all subsequent experiments. Timings and cell densities of the boundary assay were kept the same as the cell segregation assay, so these assays can be directly compared to each other i.e. the same relative number of cells were plated per cm^2.

3.2.2.3 Quantification of boundary sharpness

In collaboration with Chen Qian (Confocal Imaging and Analysis Laboratory, NIMR), a custom-made automated program was designed to analyse the boundary at the edge of the migrating EphB2-GFP cell

Figure 13: Boundary formation between EphB2 and ephrinB1 cells and quantification of boundary sharpness

Analysis of the boundary assay. Stable EphB2-GFP and ephrinB1 cell populations (A) or EphB2-GFP and EphB2 cell populations (B) are plated either side of a boundary and fixed 48 h after the boundary is removed. A sharp boundary forms between EphB2-GFP and ephrinB1 cells (A, A') but not EphB2 cells (B, B'). Images taken using 10x lens on Deltavison microscope. Images of the EphB2-GFP channel (4x magnification images, data not shown) are used for automated analysis of boundary sharpness and boundary length measured in pixels (A'', B''). A significant difference between EphB2-GFP/ephrinB1 and EphB2-GFP/EphB2 boundaries is observed for boundary length (C, $p<0.001$).

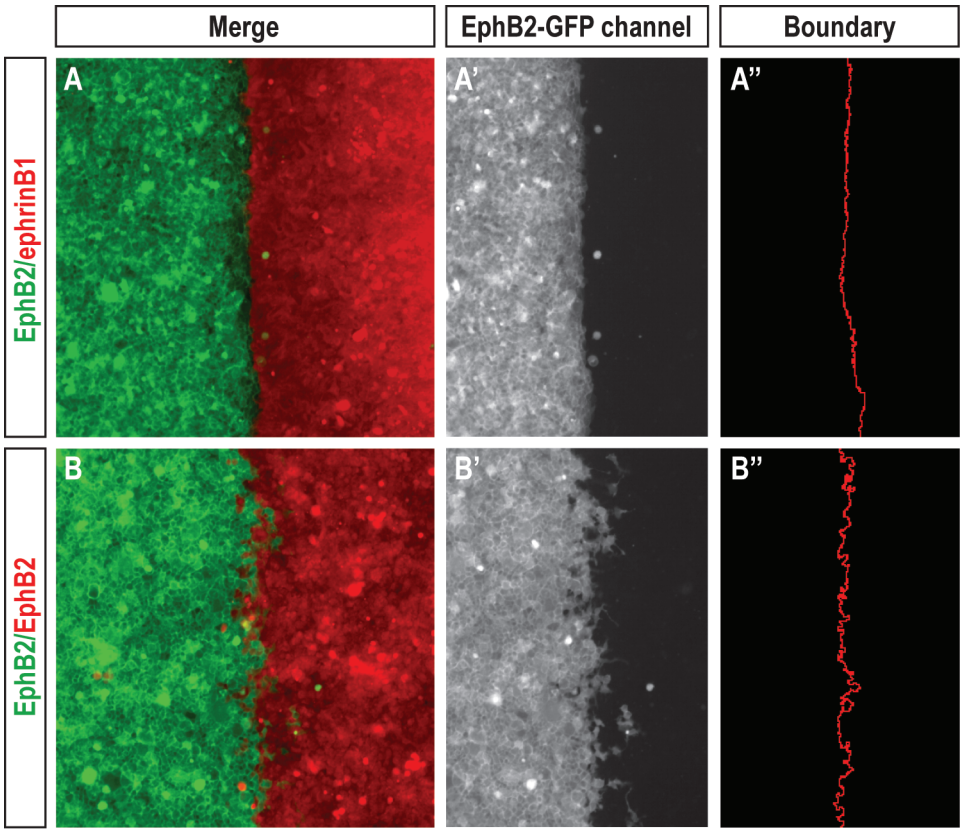
Merge
EphB2-GFP channel
Boundary
EphB2/ephrinB1
EphB2/EphB2
A
A'
A"
B
B'
B"

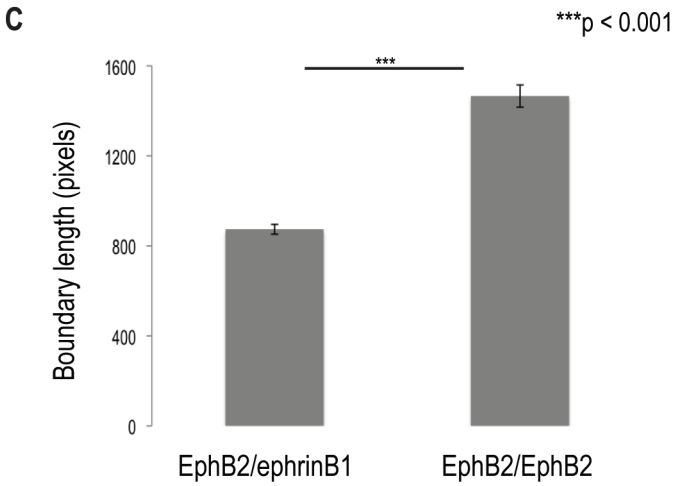
C
***p < 0.001
***
Boundary length (pixels)
1600
1200
800
400
0
EphB2/ephrinB1
EphB2/EphB2

population. The boundaries of the EphB2-GFP cells were analysed since the membrane-GFP expressed in these cells defines the cell edges and allows more accurate measurement of the boundary (Fig. 13 A', B'). From these images the length of the boundary was calculated and quantified as an average based on two images per experiment and a minimum of three experimental repeats. The significance of any difference in quantification seen between EphB2-GFP/ephrinB1 or EphB2-GFP/EphB2 cell boundaries was calculated using the Student's T-Test ($p<0.001$) on the average boundary lengths for each experiment. A sharp boundary has a short length and boundary length increases with boundary irregularity.

For EphB2-GFP cells mixed with ephrinB1 cells, the length of the EphB2-GFP cell boundary is 900 pixels (1 pixel=3.12µm), whereas for EphB2-GFP cells mixed with EphB2 cells, the EphB2-GFP cell boundary length is 1500 pixels (Fig. 13 A'', B'', C). This method of quantification shows the boundaries between EphB2-GFP/ephrinB1 populations to be significantly shorter and therefore sharper compared to the boundaries between EphB2-GFP/EphB2 cell populations ($p<0.001$), and suggests this assay is an effective way to measure boundary sharpness *in vitro.*

3.2.2.4 Live imaging of boundary sharpening assay

Live imaging of the boundary assay was carried out, as with the cell segregation assay, to analyse the cellular movements that underlie the process of EphB2-ephrinB1 mediated boundary sharpening. Cells were imaged for 28 hours after removing the barrier. The two cell populations made contact after approximately 11 hours, and boundary sharpening occurred quickly; within 4 hours of EphB2-GFP cells contacting ephrinB1 cells (Fig. 14 A, C). Sharpness was maintained throughout the imaging period (Fig. 14 C) for EphB2-GFP/ephrinB1 cell boundaries, whereas the length of EphB2-GFP/EphB2 cell boundaries fluctuated and never sharpened (Fig. 14 C). Boundary length of EphB2-GFP cells before interaction with either ephrinB1- or EphB2-expressing cells remained similar to the length of EphB2-GFP/EphB2 cell boundaries across the entire imaging period (Fig. 14 C).

Cell movements continued to occur even when there was minimal space for migration after the two populations had met. This suggests that the processes required for boundary sharpening are dynamic with cell movements causing new interactions to occur between cells even at high density. It is clear from these results that the EphB2-GFP/EphB2 boundary position remains central. Interestingly, the EphB2-GFP/ephrinB1 boundary shifts towards the EphB2-GFP cell population. In addition, high magnification analysis of the boundary assay showed ephrinB1 cells trapped in the EphB2-GFP cell population to be excluded from the EphB2-GFP cell domain (Fig. 14 B).

Figure 14: Live imaging of the boundary assay

Analysis of cell behaviour in the boundary assay when EphB2-GFP cells (green) are mixed with ephrinB1 or EphB2 cells (red).

(A): The boundary is removed at 0 h: interactions between opposing populations occur by 11 h. Boundary sharpening occurs in EphB2-GFP/ephrinB1, but not EphB2-GFP/EphB2 cell mixtures, almost immediately after interaction and is refined in the 17 hours following interaction. Boundary position remains central in the EphB2-GFP/EphB2 mixtures, but moves clearly towards the EphB2 population in EphB2-GFP/ephrinB1 mixtures.

(B): Enlarged images of the boundary in the EphB2-GFP/ephrinB1 boundary formation assay. Arrows depict ephrinB1 cells trapped in EphB2 cluster to be excluded over time.

(C): Analysis of the process of boundary sharpening over time. Boundary length of the EphB2-GFP population was measured (from 10x magnification images) in EphB2-GFP/ephrinB1 (red line) and EphB2-GFP/EphB2 (blue line) mixtures. Measurements begin from the point of interaction between the two populations and occur in 6 min intervals.

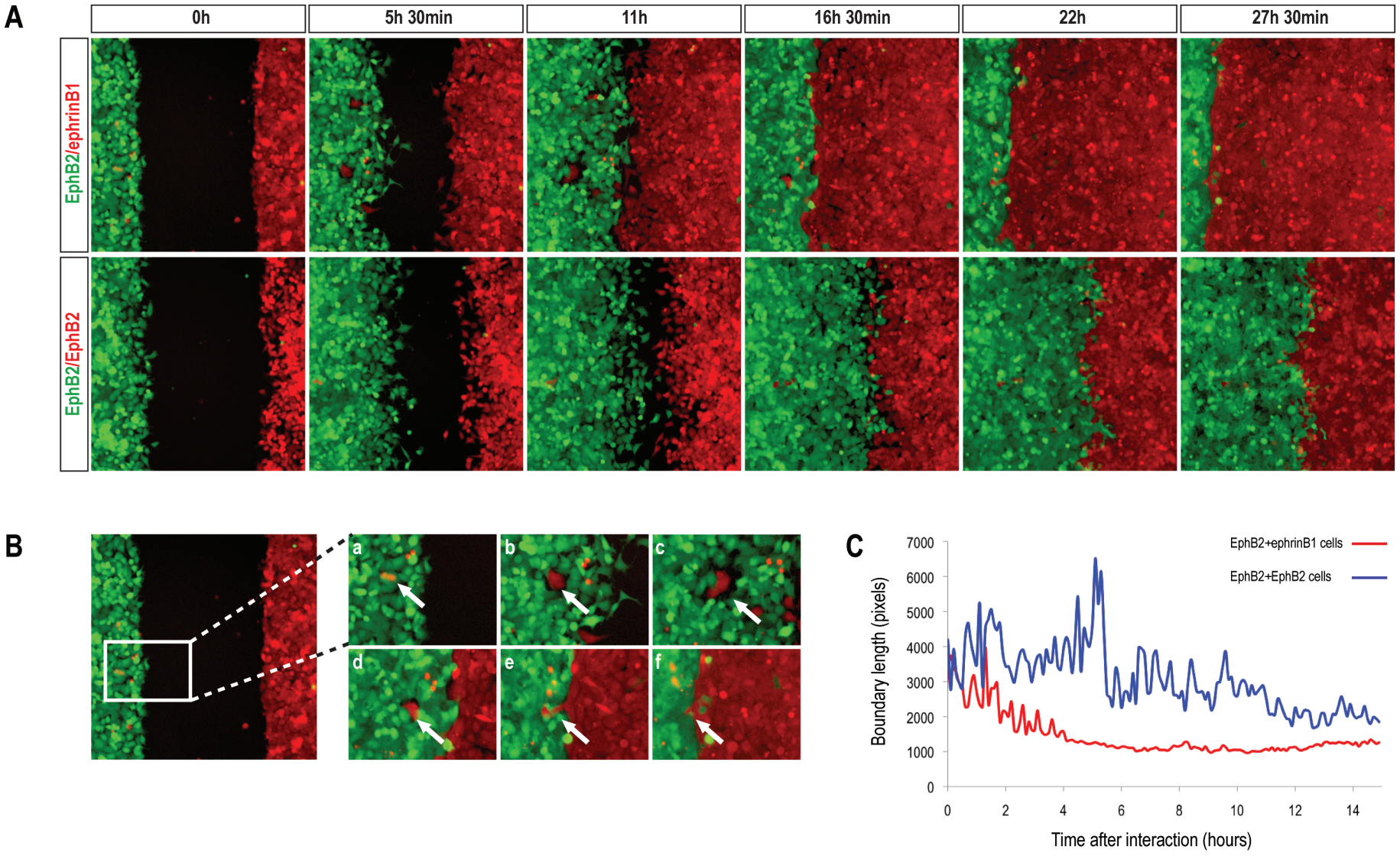
A
0h
5h 30min
11h
16h 30min
22h
27h 30min
EphB2/ephrinB1
EphB2/EphB2
B
a
b
c
d
e
f
C
EphB2+ephrinB1 cells
EphB2+EphB2 cells
Boundary length (pixels)
7000
6000
5000
4000
3000
2000
1000
0
0
2
4
6
8
10
12
14
Time after interaction (hours)

3.2.3 EphB2 cells sort from ephrinB1 cells in an *in vitro* hanging drop assay

Both the cell segregation and boundary assays described are two-dimensional (2D) assays. A three-dimensional (3D) assay would better mimic *in vivo* situations in which cells move relative to each other and respond to signalling from many directions. Previous work has shown that differential adhesion drives cell sorting in hanging drop cell aggregates (Steinberg, 1962; Steinberg, 1963; Steinberg, 1970). In order to determine whether Eph-ephrin signalling can also drive cell segregation in cell aggregates, a similar hanging drop assay was developed to study EphB2-ephrinB1 interactions in a 3D environment, and this assay was optimised by Rosalind Morley in the Wilkinson laboratory.

EphB2-GFP cells were mixed in equal proportions with ephrinB1 cells or EphB2 cells and dropped onto a coverslip. Coverslips were incubated upside down so the drops were hanging (Fig. 15 B), which allowed cells to aggregate together independently of a physical surface. Cells were either unlabelled (Fig. 15 A a-d) or labelled (Fig. 15 A a'-d') before mixing and cell sorting was analysed after 48 hours. As expected, EphB2-GFP cells sort into distinct clusters from ephrinB1 cells (Fig. 15 A a-b, a'-b'), but not from EphB2 cells (Fig. 15 A c-d, c'-d'). The degree of segregation of EphB2-GFP cells from ephrinB1 cells is highly variable under these conditions due to inconsistency in the size and shape of clusters analysed.

3.3 DISCUSSION

Eph-ephrin signalling plays a key role in the restriction of intermingling between hindbrain segments (Xu *et al.*, 1999) and the formation of sharp boundaries between rhombomeres (Fig. 2 C, C') (Cooke *et al.*, 2005). In order to analyse the how Eph-ephrin interactions contribute to the process of boundary sharpening, I took advantage of an *in vitro* Eph-ephrin mediated cell segregation assay previously established in the Wilkinson laboratory (Poliakov *et al.*, 2008), and established an *in vitro* boundary formation assay and hanging drop assay. HEK293 cell lines stably overexpressing EphB2 or ephrinB1 were used that had low levels of endogenous EphB or ephrinB proteins (Fig. 8), and thus low levels of activation by endogenous ligands and little receptor auto-activation (Poliakov *et al.*, 2008). This is an improvement to previous studies that have used transient Eph receptor and ephrin overexpression assays in embryo cells, which have a high baseline activation of receptor due to the presence of endogenous ligands (Mellitzer et al., 1999; Tanaka et al., 2003).

3.3.1 Cell density and ratio affects cluster morphology

In this work, I have further optimised conditions for the cell segregation assay so that the cluster morphology is reproducible between experiments to allow quantification. The plating density was important

Figure 15: Sorting of EphB2 cells from ephrinB1 in the hanging drop assay

(A): Analysis of the hanging drop assay with mixtures of EphB2-GFP/ephrinB1 (a, a', b, b') or EphB2-GFP/EphB2 cells (c, c', d, d'). Cells are labelled before mixing and cell sorting analysed after 48 h. Drops are shown with EphB2-GFP fluorescence (green) and either ephrinB1 or EphB2 with brightfield (a-d, grey) or fluorescence (a'-d', red) images. EphB2-GFP cells segregate from ephrinB1 cells (a, a', b, b') but not EphB2 cells (c, c', d, d').

(B): Diagram showing the experimental set-up of the hanging drop assay. EphB2-GFP cells are mixed in equal proportions with ephrinB1 cells or EphB2 cells and dropped onto a coverslip. Coverslips are incubated upside down so the drops are hanging over 1ml of cell culture media in a well of a 6 well plate. This allows cells to aggregate together independently of a physical surface.

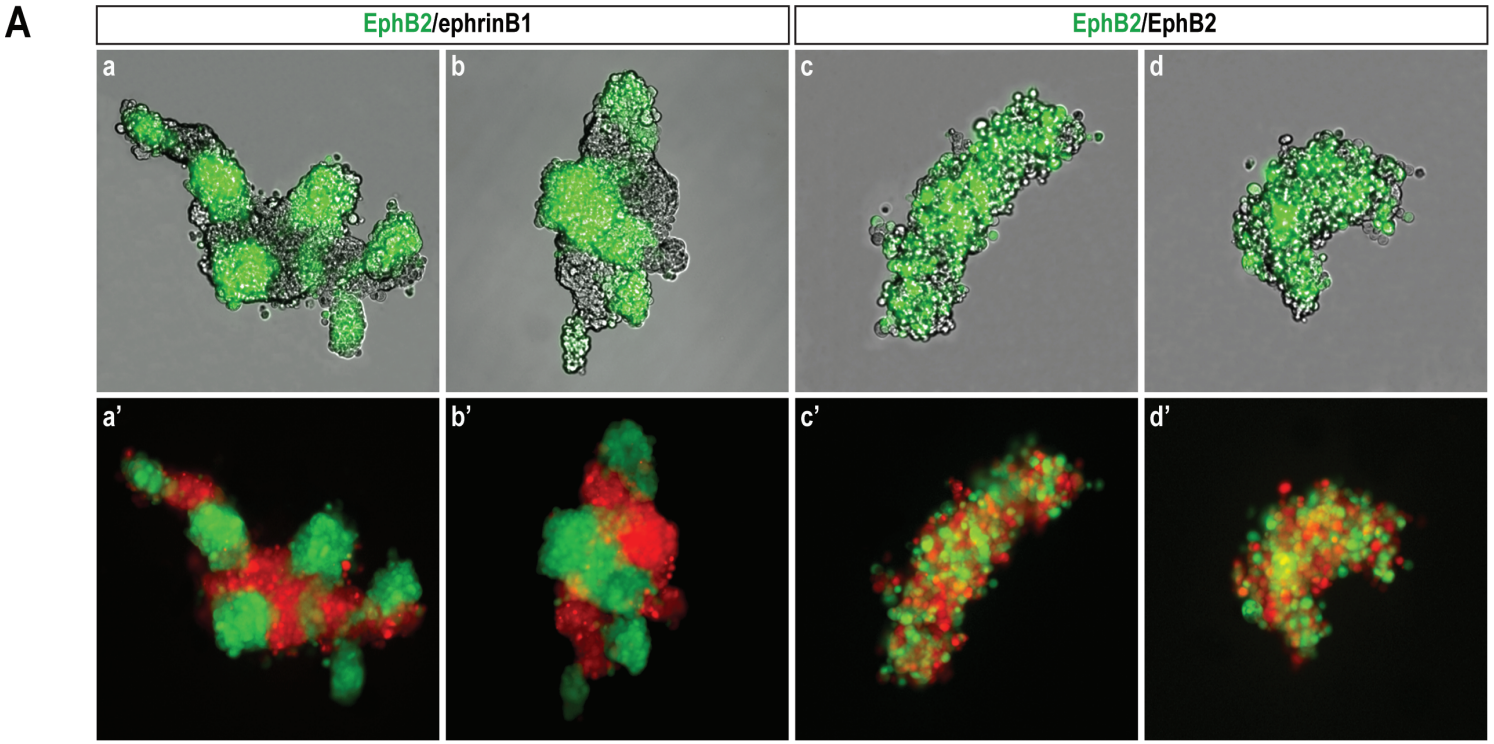
A
EphB2/ephrinB1
EphB2/EphB2
a
b
c
d
a'
b'
c'
d'
B

so that cells could to move as freely as possible before confluence was reached, to allow different cell populations to interact and migrate. The starting density of the cultures and the ratio of the populations plated affected the number of clusters, as well as their size and shape (Fig. 10). This suggests that changes in cell proliferation or the length of time cells were left to segregate could have a secondary effect on the pattern of segregation seen, compared to the segregation response due to Eph-ephrin signalling. It was also important to maintain a 1:1 ratio of EphB2 cells to ephrinB1 cells to aim to have similar numbers of interactions between "like" and "unlike" cells. This causes a distribution of clusters that are large but not connected, so that automated analysis of clusters is reproducible (Fig. 10). A plating density was chosen with a 1:1 ratio of EphB2 cells to ephrinB1 cells, which allowed migration and interaction between cells before boundary sharpening and further refinement at later stages when confluent (after 24 hours).

3.3.2 Eph-ephrin signalling causes Eph cell compaction

When the number of total cells plated was increased but the ratio of EphB2-GFP:ephrinB1 cells was kept the same (Fig. 10 A), the number of clusters of EphB2-GFP cells increased, as would be expected, but the cluster size did not vary hugely. In contrast, the density of ephrinB1 cells seemed to decrease as the total number of cells plated was increased (even though the ratio between the two populations is unchanged), which was seen by an apparent change in the area of ephrinB1 cells. This could be due to a number of reasons: a difference in the relative rates of proliferation between EphB2 and ephrinB1 cell populations causing there to be fewer ephrinB1 cells at higher cell density, apoptosis of the ephrinB1 population, or differences in the morphology of the different cell populations.

Proliferation is known to be regulated by the ephrinB/EphB pathway in the intestine and is mediated by kinase-dependent signalling in EphB-expressing cells (Holmberg *et al.*, 2006). In this case, the relative proliferation rate is increased in EphB-expressing cells compared to ephrinB-expressing cells (Holmberg *et al.*, 2006). If in our assay Eph-ephrin signalling causes the stimulation of proliferation of ephrinB1 cells at the expense of EphB2 cells, at low plating density the proportion of ephrinB1 cells compared to EphB2 cells would be higher (Fig. 10 A): initial plating at low density allows more opportunity for proliferation to occur before contact inhibition of proliferation at cell confluence (Holley & Kiernan, 1968). Therefore differential proliferation between populations would be more easily observed at lower plating density than at higher plating density, where confluence is achieved quicker, and would explain the apparent decrease in the area of ephrinB1 cells as total cell density increases (Fig. 10). In addition, previous work has shown that ephrinA5/EphA7 signalling can cause apoptosis of EphA7-expressing neural progenitors (Depaepe *et al.*, 2005). Therefore it is possible that apoptosis is causing a difference in the area of ephrinB1 cells observed.

However, analysis of cell morphology suggested segregation of EphB2-GFP cells from ephrinB1 cells causes EphB2-GFP cell compaction and the rounding up of clusters from the dish (Fig. 11 A, B), and that

this does not occur before confluence has been reached (Fig. 11 B). This is in line with previous evidence for the role of adhesion in promoting Eph-ephrin mediated Eph cell stable compaction (Cortina *et al.*, 2007; Miura *et al.*, 2009), or the adhesion-independent transient retraction of EphB4 cells on stimulation with ephrinB2 (Groeger & Nobes, 2007; Marston *et al.*, 2003). It is more likely that the EphB2 compaction seen is due to complete cytoskeletal collapse and detachment from ECM on interaction with ephrinB1 cells, as EphB2 cells have previously been shown to undergo a rapid collapse of cell processes after interaction with ephrinB1 cells (Poliakov *et al.*, 2008). However, other work has suggested that the ephrinB population can undergo cycles of cell contraction and respreading when overexpressed, or a single cycle on stimulation with EphB receptor (Bochenek *et al.*, 2010).

We suggest that EphB2-GFP cell compaction would occur in all conditions of increasing the total cell density after confluence has been achieved, presumably to a similar extent (Fig. 10 A). The ratio of EphB2-GFP:ephrinB1 cells (1:1) is kept the same in all conditions and so a similar degree of EphB2-GFP compaction would be expected. However, at higher total cell densities EphB2-GFP cells cluster and round off the dish, so occupying a smaller relative area (Fig. 11 B), as there are more cells are in the clusters in the higher density mixtures, as seen by the increased fluorescent intensity. This could explain why the EphB2-GFP cluster size does not seem to vary hugely as the number of total cells plated was increased. In low cell density mixtures EphB2-GFP cell compaction is similar to high cell density mixtures, so ephrinB1 cells can occupy a greater area and assume a more spread morphology in comparison to higher densities where confluence dictates cell size and ephrinB1 cells become compacted. Therefore plating at higher cell density would cause the area occupied by each cell population to appear equal (Fig. 10 A). It is therefore likely that ephrinB1-stimulated EphB2 cell compaction underlies the size of clusters observed, but the density-dependent ephrinB1 cell compaction is the largest variable and may be responsible for the apparent change in ephrinB1 density on increasing the total density of the cells that are plated. In order to distinguish between changes in cell morphology or rates of proliferation between cell types, the number of cells could be assessed at the endpoint of the segregation assay by counting or FACS analysis, or the amount of cell proliferation could be determined by incorporation of BrdU.

3.3.3 Segregation and boundary sharpening is a dynamic process

Live imaging of cell interactions during both the cell segregation and boundary sharpening assay showed segregation to occur in EphB2-GFP/ephrinB1 mixtures almost immediately after plating (Fig. 12 A), and boundary sharpening to occur quickly after interaction between EphB2-GFP and ephrinB1 cell populations (Fig. 14 A, C). Cell movements occur even at high density. This suggests that only few cell-cell interactions are able to induce the sorting of EphB2-GFP cells from ephrinB1 cells, and that segregation is a dynamic process that is maintained even when processes such as cell proliferation and migration potentially cause a disruption to boundary sharpness.

EphrinB1 cells surrounded by EphB2-GFP cells, in either the cell segregation or boundary assay, are excluded from the EphB2-GFP population back into the ephrinB1-expressing cell domain (not quantified) (Fig. 12 B, 14 B). It is unclear from this analysis whether these ephrinB1 cells are removed from the EphB2-GFP population by repulsion from the EphB2-GFP cells or adhesion to ephrinB1 cells. Cellular protrusions can extend over many cell diameters so either explanation could be valid. This argues that both the segregation assay and boundary assay accurately reflect Eph-ephrin cell interactions, and mimic the results of *in vivo* transplant experiments (Cooke *et al.*, 2005; Xu *et al.*, 1999).

The EphB2-GFP/EphB2 boundary position remains central during the imaging period whereas the EphB2-GFP/ephrinB1 boundary shifts towards the EphB2-GFP population. This is likely to reflect a repulsive response of EphB2-GFP to ephrinB1 cells. The roles of EphB2-ephrinB1 mediated adhesion and repulsion in cell segregation and boundary sharpening need to be further analysed.

3.3.4 Quantification of cell segregation and boundary sharpness

Two different approaches were used in order to quantify the degree of segregation of EphB2-GFP cells in the cell segregation assay; Nearest Neighbour (NN) and area of clusters. NN analysis of the degree of segregation estimated the number of pixels of the same cell type surrounding any given pixel out of a possible four neighbours (Mochizuki *et al.*, 1998). Even though the difference between segregation in EphB2-GFP/ephrinB1 and EphB2-GFP/EphB2 cell mixtures is reproducible by eye between experiments, the difference between NN values for these conditions is surprisingly small (Fig. 9 H). Cells are not square objects and do not interact with only four neighbours, as this method of analysis assumes. Therefore NN represents too crude a method for analysing segregation in our system.

Average area of the clusters is an alternative measure of the degree of segregation; however cluster size was larger in EphB2-GFP/EphB2 mixtures than EphB2-GFP/ephrinB1 mixtures due to single scattered cells or clusters in close proximity causing thresholding artefacts (Fig. 9 C). Variation in cluster size and shape therefore caused variation in the average area.

Limitations of the cell segregation assay include sensitivity to cell density (Fig. 10 A), potential to be affected by relative proliferation rates of EphB2 vs. ephrinB1 cells (Fig. 10 A), and difficulty in quantifying the degree of segregation between experiments (Fig. 9 C, H). However, an additional feature of EphB2-ephrinB1 mediated cell segregation is the smoothness of the boundary of the EphB2 clusters with ephrinB1-expressing population. Even though boundary smoothness is not a direct measure of segregation from intermingled populations, there is a good correlation between segregation and boundary sharpness. It was decided to continue further analysis with boundary sharpness instead of area.

Perimeter Regularity Index (PRI) is a more accurate measure of boundary smoothness than Heywood Circularity Index (HCI), as HCI calculations are dependent on area and an artificial comparison to a circle. As the clusters observed in EphB2-GFP/ephrinB1 cell mixtures are not circular, and this measurement is independent of area, PRI was used for future quantification of boundary smoothness in the cell segregation assay. PRI quantification of boundary smoothness showed EphB2-GFP/ephrinB1 cluster boundaries to be smoother and statistically different to EphB2-GFP/EphB2 cluster boundaries (Fig. 9 E).

Boundary sharpening is a measure of segregation that is relevant *in vivo*. The boundary sharpening assay was designed in order to simplify the approach of measuring boundary sharpness, as straight lines are easier to quantify than boundaries of clusters of variable shape, and to establish an assay that was not so sensitive to the variables that affect the cell segregation assay. Boundary length represents the straightness of the boundary, so a shorter boundary length measurement corresponds to a straighter and smoother boundary. Analysis of boundary length showed EphB2-GFP/ephrinB1 boundaries to be straighter and statistically different to EphB2-GFP/EphB2 boundaries, which are longer in length and fuzzy (Fig. 13 C). This *in vitro* boundary assay better mimics the *in vivo* situation in the hindbrain, where Eph- and ephrin-expressing cells would not originally be mixed in a salt and pepper like fashion. In addition, when EphA4 is knocked down in zebrafish by morpholino injection, the boundaries between rhombomeres 3 and 5 are fuzzy and fail to sharpen (Fig. 33 Appendix) (Cooke *et al.*, 2005). Taken together this suggests the boundary assay provides an easier and more accurate method of measuring boundary sharpness, compared to the cell segregation assay, and better represents boundary sharpening seen *in vivo*.

To demonstrate the 3D movement of cells and more closely represent an *in vivo* situation, a hanging drop assay was established. This assay is also more analogous to work identifying the role of adhesion in segregation in cell aggregates (Steinberg, 1962; Steinberg, 1963; Steinberg, 1970), which suggests that differential adhesion causes surface tension between populations with different affinities, and dictates that the less cohesive group surrounds the other (Fig. 2 A) (Foty & Steinberg, 2005). Interestingly, the segregation induced by EphB2-ephrinB1 signalling is different to the differential adhesion driven segregation observed by Malcolm Steinberg (Fig. 2 A). EphB2 cells sort into distinct clusters from ephrinB1 cells (Fig. 15 A a-b, a'-b'), but not from EphB2 cells (Fig. 15 A c-d, c'-d') in hanging drop cell aggregates. EphB2 cells segregate out into groups from ephrinB1 cells without one population surrounding the other, unlike for differential adhesion. This observation can be explained by signalling only occurring at the boundaries between two populations rather than generating a global adhesive difference between EphB2 and ephrinB1 cells. The size and shape of clusters was highly variable, in part due to the variability in the size and shape of cell aggregates formed, which would prove problematic to quantify. Due to this, and the fact that quantification of sorting in 3D would be difficult to analyse, it was decided that the cell segregation and boundary assay would be used to further investigate the role of EphB2-ephrinB1 signalling in boundary sharpening. Furthermore, these 2D assays may better model cell movements that occur in an epithelium.

In order to analyse how EphB2-ephrinB1 signalling mediates cell segregation and boundary sharpening, subsequent studies focussed on the roles of components known to be downstream of EphB2-ephrinB1 signalling in cell segregation assays.

4 PCP AND PAR GENES ARE REQUIRED FOR EPH-EPHRIN MEDIATED CELL SEGREGATION AND BOUNDARY SHARPENING

4.1 Introduction

Studies by Alexei Poliakov in the Wilkinson laboratory (unpublished) have shown that interaction with ephrinB1 cells leads to increased directional persistence of EphB2 cells. Furthermore, computer simulations have suggested that directional persistence can in principle contribute to cell segregation. However, the molecular pathways downstream of EphB2 activation that underlie directional persistence are not yet known. Identification of these would allow us to test whether directional persistence contributes to EphB2-ephrinB1 cell segregation.

One candidate pathway that could effect EphB2-activation induced directional persistence is the planar cell polarity (PCP) pathway. Dishevelled is a component of Wnt-Frizzled signalling that regulates two pathways through distinct protein domains; the canonical β-catenin-TCF-Wnt signalling pathway through the DIX domain, and the PCP pathway through the DEP domain (Poliakov & Wilkinson, 2006; Tada *et al.*, 2002). The DEP domain is essential for the recruitment of Dishevelled to Frizzled at the cell membrane, a hallmark of PCP signalling (Axelrod *et al.*, 1998; Boutros & Mlodzik, 1999; Poliakov *et al.*, 2004). A role for Dishevelled downstream of EphB2 has been suggested by work using dominant-negative truncated forms of the Dishevelled protein. This has shown that the PCP pathway, and not the canonical Wnt pathway, is required for ephrinB1-expressing cells and EphB2 receptor-expressing cells to segregate *in vitro* (Tanaka *et al.*, 2003). It has also been shown that an interaction between the DEP domain of Dishevelled and ephrinB1 is required for Eph-independent migration of cells to the *Xenopus* eye field (Lee *et al.*, 2006). These results raised the possibility that EphB2 and ephrinB1 act through the PCP pathway to control cell migration during development. The PCP pathway is also required for directional persistence of neural crest migration *in vivo* (Carmona-Fontaine *et al.*, 2008; De Calisto *et al.*, 2005). This evidence has shown a connection between Eph-ephrin signalling and the PCP pathway with cell sorting *in vitro*, and between the PCP pathway and cell migration *in vivo.* The PCP pathway is thus a strong candidate to underlie directional persistence of migration downstream of EphB2, but its role in boundary sharpening is not known.

A second potential candidate mechanism underlying directional persistence and boundary sharpening downstream of EphB2 signalling involves the PAR proteins. These, together with Rac1, RhoA and Cdc42 GTPases, control the front-rear polarisation of migratory cells by localising and activating Rac at the leading edge (LE) (Mertens *et al.*, 2006; Pegtel *et al.*, 2007). The PAR proteins are normally localised to

the LE of migrating cells, and couple Rho GTPase activity to arrange the nucleus, centrosome, Golgi and LE along the front-rear axis (Etienne-Manneville & Hall, 2001). The stability of the complex correlates with the extent of directional cell movement by stabilising lamellipodia formation at the LE of a migrating cell (Iden & Collard, 2008; Ridley *et al.*, 2003). PAR-6B and PAR-3 were recently identified in a proteomic screen of proteins phosphorylated downstream of EphB2-ephrinB1 signalling, and in an siRNA screen of a kinase library in which cell segregation was analysed (Jorgensen *et al.*, 2009); these screens were carried out using the same EphB2 and ephrinB1 cells from the Wilkinson laboratory that are used in my studies. The PAR proteins are therefore potential candidates to underlie EphB2-ephrinB1 mediated directional persistence of migration.

As a first step in analysing the potential role of PCP and PAR components downstream of EphB2-ephrinB1 signalling, I tested the effect of knockdown on cell segregation and boundary formation in our EphB2-ephrinB1 cell assays. In the following chapter, I assess the roles of key PCP components, Dishevelled (Dvl) and Daam1, and core polarity components, PAR-6B and PAR-3, in directional persistence of migration.

4.2 RESULTS

4.2.1 Expression of PCP and PAR polarity components in HEK293 cells

Before addressing the role of PCP and PAR polarity components in our *in vitro* cell segregation and boundary formation assays, I first determined their expression in HEK293 cells using RT-PCR and Western blot analysis. There are three Dvl genes (1, 2, 3) and two Daam genes (1, 2) in humans, and RT-PCR analysis was used to determine their relative expression levels in HEK293 cell lines. All three Dvl genes are expressed in HEK293 cells, with Dvl2 (which shares the highest sequence similarity with the single *Xenopus* gene) expressed at the highest level, and Dvl1 at the lowest level (Fig. 16 A). Both Daam genes are also expressed, but Daam2 is expressed at such a low level that its role is not considered in future analysis (Fig. 16 A). Both PAR-6B and PAR-3 have been previously studied in these cells (Jorgensen *et al.*, 2009) so their expression was not quantified by RT-PCR.

We determined the levels of PAR-6B, PAR-3, Dvl1, 2, 3 and Daam1 expression and the effect of siRNA-mediated knockdown on protein levels by quantitative Western blot. Endogenous expression of Dvl1 proved difficult to determine (with multiple commercial antibodies) as it was expressed at very low levels in our cells, and as RT-PCR analysis showed Dvl1 to be expressed at the lowest level of the three Dvl genes (Fig. 16 A), it was not included in further analysis.

Figure 16: Quantitative RT-PCR and Western blot analysis of endogenous expression of PCP and PAR proteins, and relative knockdown by siRNA in HEK293 cells

(A): Quantitative RT-PCR analysis of the expression of endogenous PCP components in HEK293 cells; Dvl1, Dvl2, Dvl3, Daam1 and Daam2. Expressed as a percentage relative to β-actin expression.

(B): Western blot analysis of PCP and PAR proteins showing endogenous expression and the relative knockdown by siRNA in stable HEK293 lines expressing EphB2-GFP. Each knockdown depicted uses a combination of two or three siRNAs to the same gene. Dvl23 is a combination of the siRNAs to both Dvl2 and Dvl3. A total of 60pmol siRNA was transfected per condition. Knockdown is expressed as the percentage of endogenous protein remaining compared to a transfection with a nonsense siRNA (siCTRL), and is determined using antibodies to endogenous human genes.

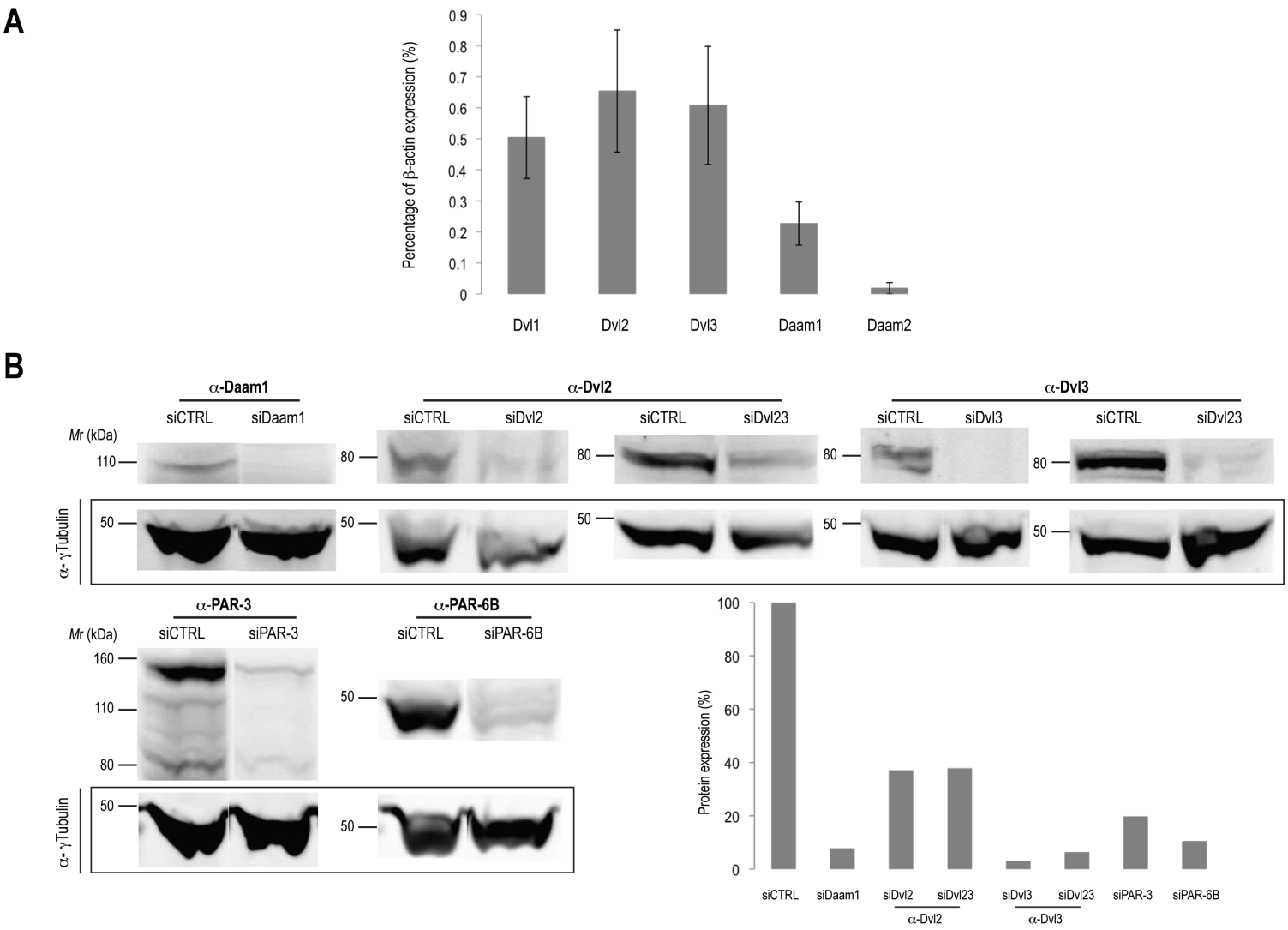
A
Percentage of β-actin expression (%)
0.9
0.8
0.7
0.6
0.5
0.4
0.3
0.2
0.1
0
Dvl1
Dvl2
Dvl3
Daam1
Daam2
B
α-Daam1
siCTRL
siDaam1
α-Dvl2
siCTRL
siDvl2
siCTRL
siDvl23
α-Dvl3
siCTRL
siDvl3
siCTRL
siDvl23
Mr (kDa)
110
80
50
α-γTubulin
α-PAR-3
siCTRL
siPAR-3
α-PAR-6B
siCTRL
siPAR-6B
Mr (kDa)
160
110
80
50
α-γTubulin
Protein expression (%)
100
80
60
40
20
0
siCTRL
siDaam1
siDvl2
siDvl23
siDvl3
siDvl23
siPAR-3
siPAR-6B
α-Dvl2
α-Dvl3

4.2.2 Verification and optimisation of siRNA-mediated knockdown in the cell segregation assay

To test the role of components of the PCP pathway and core polarity components in our *in vitro* assays, we decided to reduce their expression using the technique of siRNA-mediated knockdown. Careful optimisation of siRNA-mediated knockdown in the cell segregation assay was carried out in order to ensure that it would be reproducible and quantifiable across experimental repeats. Three different transfection reagents (Lipofectamine 2000, Lipofectamine RNAiMAX and XtremeGene) were titrated with different amounts of siRNA and levels of protein expression were analysed in a timecourse. Lipofectamine RNAiMAX in combination with 60pmoles siRNA gave the strongest and most reproducible knockdown (data not shown).

Most of the siRNAs used had not been validated previously. It was therefore possible that they have non-specific or off-target effects. In order to minimise these effects, three independent, un-validated siRNAs against the same gene were pooled and used in combination to target one specific gene, as this would dilute any non-specific effects. Knockdown was analysed 72 hours after transfection. If a validated siRNA was available, this was used in combination with one other siRNA. It was also a possibility that, since two Dvl genes are expressed at significant levels in these cells, there might be some functional redundancy between them. To address this issue, knockdowns were carried out for individual Dvl2 and Dvl3 genes, as well as a double knockdown (Dvl23). An siRNA with a scrambled non-coding sequence was used as a control (siCTRL).

Cells transfected with control siRNA reached confluence more quickly than cells transfected with other siRNAs, which suggests an siRNA-mediated effect on cell proliferation. Caspase-3 staining did not differ between siRNA treatments suggesting that siRNA-induced cell death was not the cause of this difference (data not shown). An additional possibility is that transfection of siRNA could change the relative proliferation rate of cells. This could cause the extent of cell segregation to appear to change by changing the ratio of one population to the other (Fig. 10). To circumvent this potential problem, when analysing the role of PCP components and core polarity components in our *in vitro* assays, all cells that were mixed were transfected with the same siRNA, such that there would be an equal or similar effect on both populations.

Treatment of cells with siRNAs to Daam1, Dvl3, Dvl3 with siDvl23, PAR-6B and PAR-3 all reduced protein expression by at least 80%, seen by Western blot. A 65% knockdown of protein was seen after treatment with siRNAs to Dvl2 and Dvl2 with siDvl23 (Fig. 16 B). This was reproducible in three independent experiments, and these conditions were used to test the role of PCP components and PAR polarity components in our *in vitro* cell segregation and boundary formation assays.

The EphB2- and ephrinB1-overexpressing HEK293 cell lines have low levels of endogenous EphB2 or ephrinB1 proteins (Fig. 8), and low levels of receptor autoactivation, seen by staining for phosphorylated EphB2 (Fig. 17). It is possible that knockdown of PCP or PAR genes could affect EphB2-ephrinB1 mediated cell segregation and boundary formation responses by one or both of two mechanisms: by inhibiting EphB2 activation or by interfering with downstream pathways required for cell repulsion. To check the effect of PCP or PAR gene knockdown on EphB2 activation, we analysed the level of EphB2 phosphorylation before and after the addition of an activating ligand, ephrinB1-Fc chimaera. For all siRNA conditions, levels of EphB2 phosphorylation were similar to siCTRL conditions both before and after ephrinB1-Fc addition (Fig. 17). This suggests siRNA knockdown of PAR and PCP genes does not affect the activation of the EphB2 receptor by ephrinB1, and that any disruption to cell segregation or boundary sharpening is due to interference with signalling pathways downstream of EphB2.

4.2.3 Knockdown of PCP and PAR gene expression causes disruption to Eph-ephrin mediated cell segregation

EphB2-GFP, ephrinB1 and EphB2 cells were transfected with siRNA 48 hours before being mixed for the cell segregation assay, and cell segregation was analysed 48 hours after mixing (as previously described). The degree of segregation and boundary sharpness was determined by the PRI value.

Analysis of PCP pathway genes in the cell segregation assay showed that siRNA knockdown of Daam1 strongly disrupts segregation, compared to controls transfected with siCTRL (Fig. 18 B, F $p<0.001$). Single or double knockdown of Dvl genes revealed that Dvl2 knockdown shows the most significant disruption to segregation compared to controls (Fig. 18 C, F $p<0.001$), as disruption of segregation with Dvl3 knockdown was less strong (Fig. 18 D, F $p<0.05$). Interestingly, double knockdown of Dvl2 and Dvl3 together did not disrupt segregation (Fig. 18 E, F). This argues against a role of redundancy of Dvl genes in this system and suggests that both Dvl2 and Daam1 play roles in EphB2-ephrinB1 mediated cell segregation.

Analysis of PAR gene function showed knockdown of PAR-6B and PAR-3 to each disrupt segregation (Fig. 19 B, C). These differences were highly significantly different to the control (Fig. 19 D $p<0.001$), which suggests that knockdown of PAR polarity genes causes disruption to EphB2-ephrinB1 mediated cell segregation. It is important to note that even though each of these conditions has a similar PRI value (boundary smoothness), the level of disruption to segregation and cluster morphology is different.

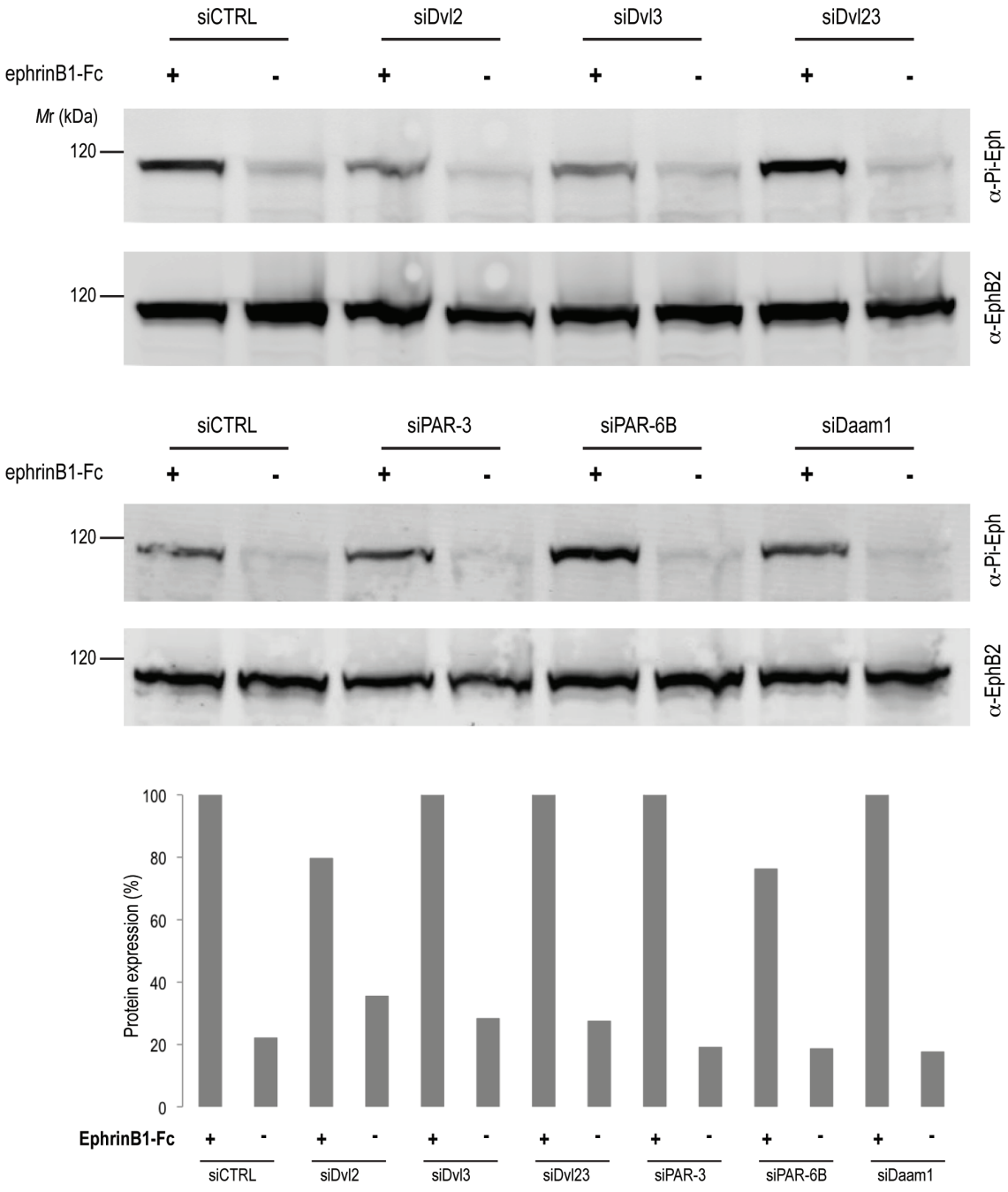

Figure 17: Western blot analysis of EphB2 activation on stimulation with ephrinB1-Fc, and affect of PCP and PAR gene knockdown by siRNA

Western blot analysis of EphB2 activation (by phospho-Eph staining) in EphB2-GFP cells on stimulation with ephrinB1-Fc. EphB2 activation was analysed in cells transfected with siRNA to each PCP and PAR gene, and mock-stimulated or stimulated with ephrinB1-Fc. Phospho-Eph staining increased on stimulation with ephrinB1-Fc compared to a mock stimulation, and this increase was similar to siCTRL for all siRNA conditions. Knockdown is expressed as the percentage of endogenous protein remaining compared to a transfection with a nonsense siRNA (siCTRL).

Figure 18: Disruption to Eph-ephrin mediated cell segregation on knockdown of PCP genes

Analysis of the effects of knockdown of different PCP genes on EphB2-ephrinB1 mediated cell segregation. Endpoint analysis of EphB2-GFP/ephrinB1 cell mixtures, with both populations previously transfected with siRNA; siCTRL (A), siDaam1 (B), siDvl2 (C), siDvl3 (D), siDvl23 (E). Disruption to segregation is strongest with siDaam1 (B) and siDvl2 (C). Disruption to segregation is quantified using the perimeter regularity index (PRI) (F). A significant difference in the PRI value is observed for siDaam1, siDvl2 (F, $p<0.001$) and siDvl3 (F, $p<0.05$), but not siDvl23, compared to siCTRL.

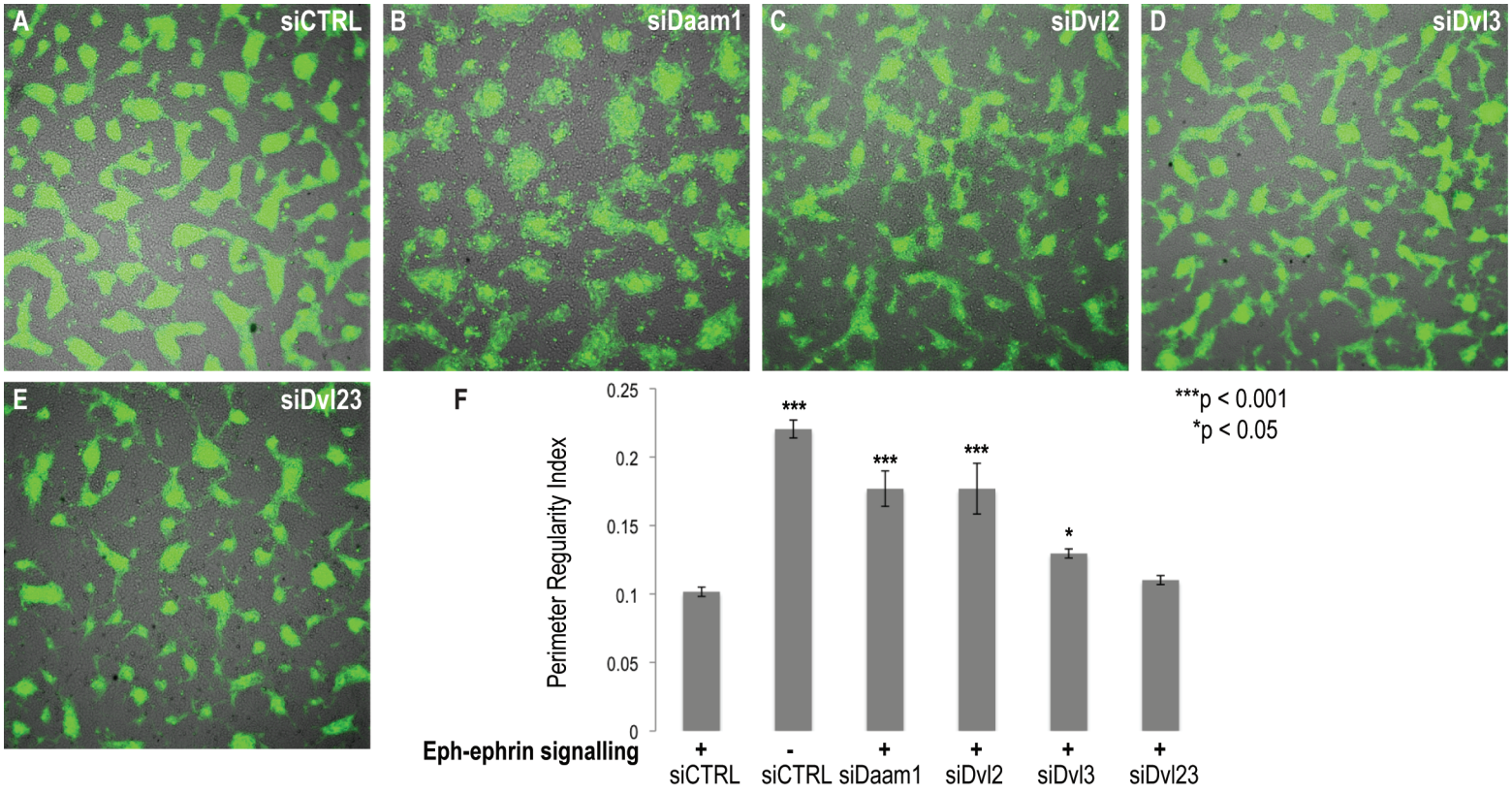
A
siCTRL
B
siDaam1
C
siDvl2
D
siDvl3
E
siDvl23
F
Perimeter Regularity Index
0.25
0.2
0.15
0.1
0.05
0
***
***
***
*
***p < 0.001
*p < 0.05
Eph-ephrin signalling
+
siCTRL
-
siCTRL
+
siDaam1
+
siDvl2
+
siDvl3
+
siDvl23

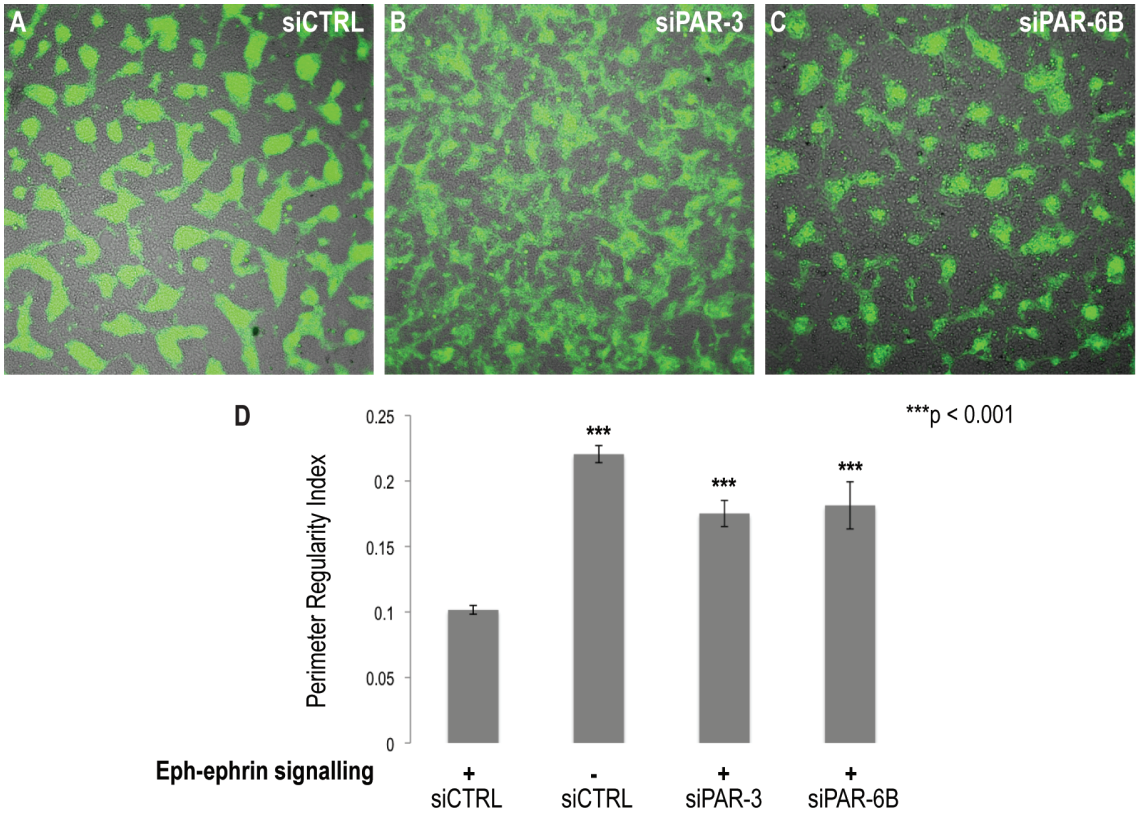

Figure 19: Disruption to Eph-ephrin mediated cell segregation on knockdown of PAR polarity genes

Analysis of the effects of PAR polarity gene knockdown on EphB2-ephrinB1 mediated cell segregation. Endpoint analysis of EphB2-GFP/ephrinB1 cell mixtures, with both populations previously transfected with siRNA; siCTRL (A), siPAR-3 (B), siPAR-6B (C). Disruption to segregation is seen with knockdown of each of PAR-3 and PAR-6B (B, C) relative to the control (A). Disruption to segregation is quantified using the perimeter regularity index (PRI) (D). A significant difference in the PRI value is observed after knockdown of both PAR genes relative to siCTRL (D, $p<0.001$).

4.2.4 Knockdown of PCP and PAR proteins cause disruption to Eph-ephrin mediated boundary sharpening

To further analyse the disruption to EphB2-ephrinB1 mediated boundary sharpness seen on knockdown of PCP or PAR polarity genes, transfected cells were labelled 48 hours after transfection and plated either side of a boundary for the boundary assay. Boundary sharpness was analysed 48 hours after removing the barrier, as previously described. The degree of sharpness is defined by boundary length (pixels).

Analysis of PCP pathway components in the boundary formation assay showed that siRNA knockdown of Daam1 strongly disrupts boundary sharpness compared to controls transfected with siCTRL (Fig. 20 B, F $p<0.001$). Single or double knockdown of Dvl genes revealed that Dvl2 knockdown shows the most significant disruption to boundary length compared to controls (Fig. 20 C, F $p<0.001$). Dvl3 knockdown or double knockdown of both Dvl2 and Dvl3 together (Dvl23) did not cause disruption to boundary length (Fig. 20 D, E, F). This again argues against redundancy between Dvl genes in EphB2-ephrinB1 mediated boundary sharpening and suggests that Dvl2 and Daam1 play a role in EphB2-ephrinB1 mediated boundary sharpening.

Analysis of the effect of PAR polarity knockdown showed both PAR-6B and PAR-3 knockdown to have a similar disruption to boundary sharpness (Fig. 21 B, C), which was significantly different to the control (Fig. 21 D $p<0.001$). This suggests that PAR polarity genes are required for EphB2-ephrinB1 mediated boundary sharpening.

4.2.5 Effect of PCP or PAR polarity and adhesion on Eph-ephrin mediated cell segregation and boundary sharpening

Previous work has shown a role for both repulsion and adhesion downstream of Eph-ephrin signalling (Jorgensen *et al.*, 2009; Poliakov *et al.*, 2008; Zimmer *et al.*), but the contribution of adhesion or repulsion to EphB2-ephrinB1 mediated cell segregation and boundary sharpening is not known. Removing N-cadherin mediated adhesion in the EphB2-ephrinB1 cell segregation and boundary sharpening assays causes disruption to cell segregation (Rosalind Morley, personal communication). The cell sorting that does occur under these conditions we assume to be adhesion-independent and due to the roles of directional migration and repulsion in this system. In order to separate the roles of adhesion and repulsion, the role of polarity was analysed in an adhesion-negative background. Any additional disruption to cell segregation or boundary formation seen, when adhesion is not present in the system, may thus be due only to the role of directional migration and repulsion.

Figure 20: Disruption to Eph-ephrin mediated boundary sharpening on knockdown of PCP genes

Analysis of the effects of knockdown of different PCP genes on EphB2-ephrinB1 mediated boundary sharpening. Endpoint analysis of EphB2-GFP/ephrinB1 cell mixtures, with both populations previously transfected with siRNA; siCTRL (A), siDaam1 (B), siDvl2 (C), siDvl3 (D), siDvl23 (E). Disruption to boundary sharpening is strongest with siDaam1 (B) and siDvl2 (C). Boundary sharpness is quantified by measuring boundary length of 4x magnification images (F). A significant difference in the boundary length is observed for siDaam1 and siDvl2 (F, $p<0.001$), but not siDvl3 or siDvl23 compared to siCTRL. Images taken using 10x lens on Deltavison microscope.

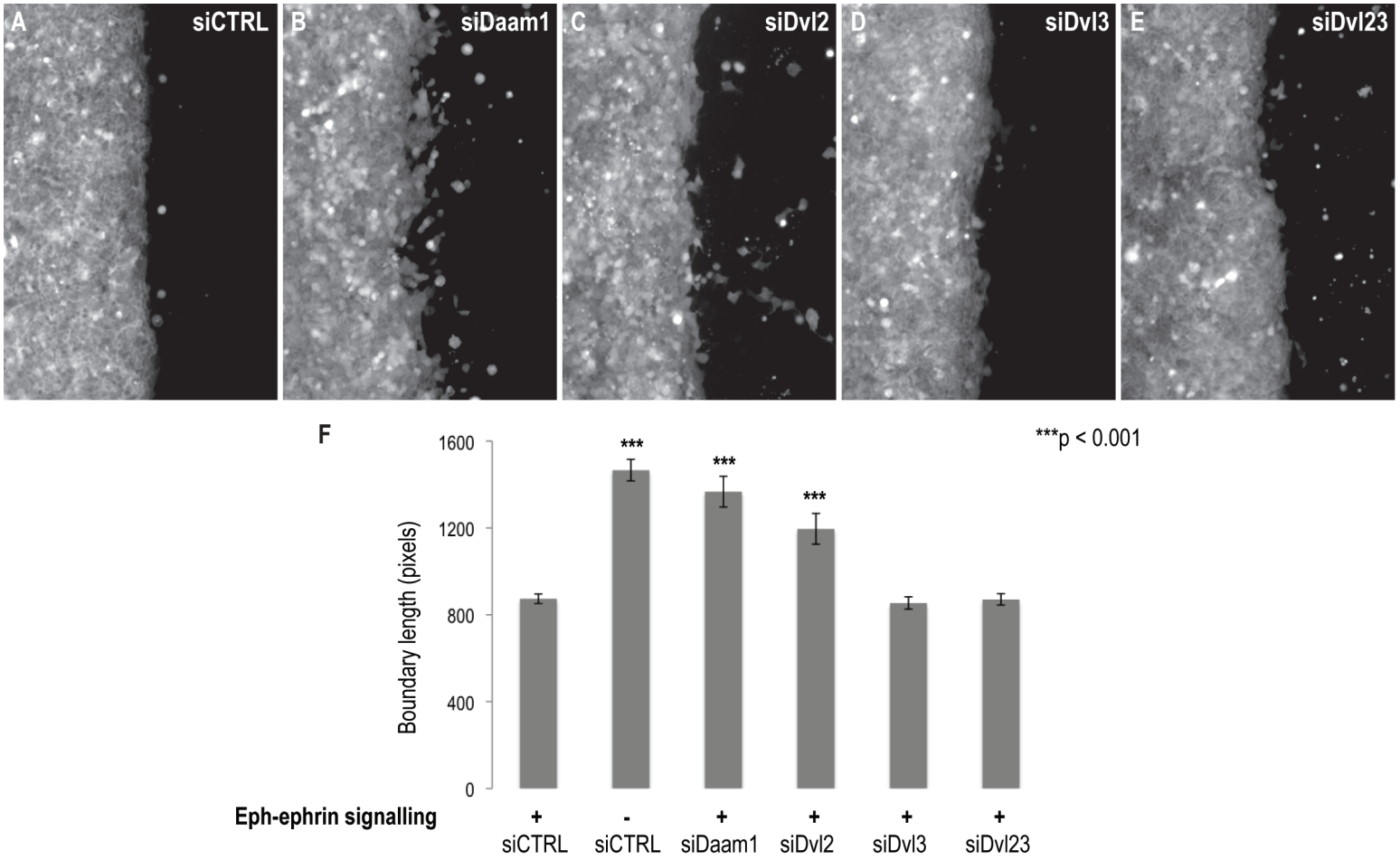
A
siCTRL
B
siDaam1
C
siDvl2
D
siDvl3
E
siDvl23
F
***p < 0.001
Boundary length (pixels)
1600
1200
800
400
0
***
***
***
Eph-ephrin signalling
+
siCTRL
-
siCTRL
+
siDaam1
+
siDvl2
+
siDvl3
+
siDvl23

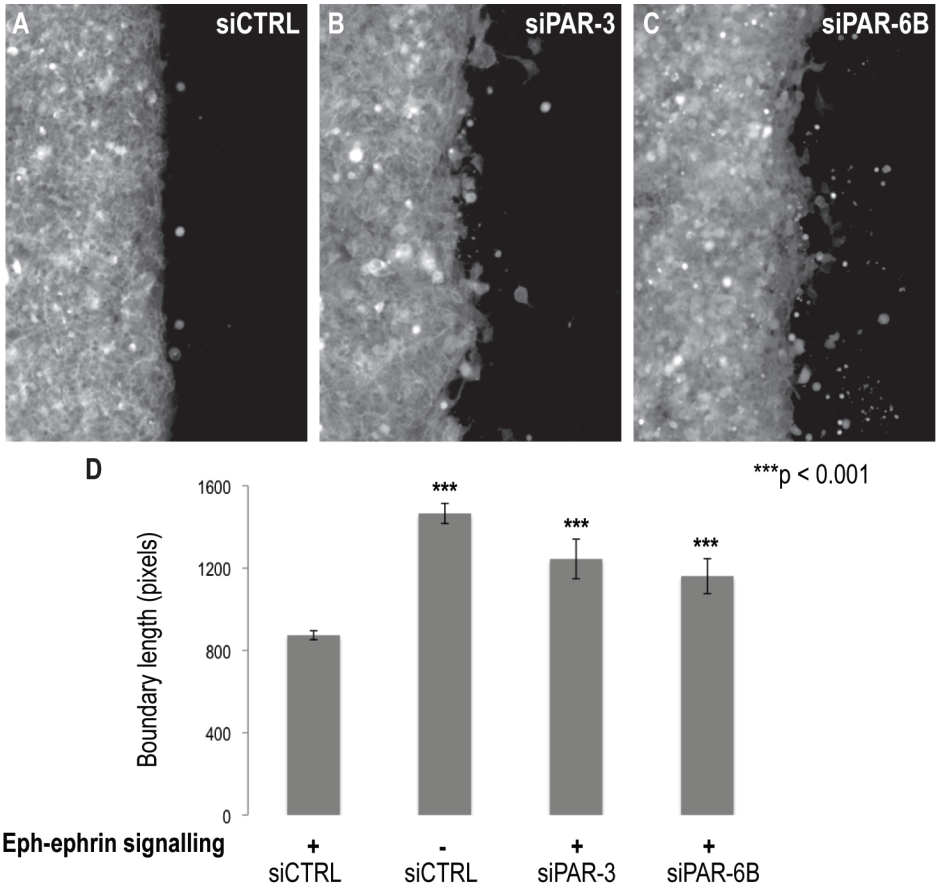

Figure 21: Disruption to Eph-ephrin mediated boundary sharpening on knockdown of PAR polarity genes

Analysis of the effects of PAR polarity gene knockdown on EphB2-ephrinB1 mediated boundary sharpening. Endpoint analysis of EphB2-GFP/ephrinB1 cell mixtures, with both populations previously transfected with siRNA; siCTRL (A), siPAR-3 (B), siPAR-6B (C). Disruption to boundary sharpening is seen with knockdown of each of PAR-3 and PAR6-B (B, C) relative to the control (A). Boundary sharpening is quantified by measuring the boundary length of 4x magnification images (D). A significant difference in the boundary length is observed for both genes compared to siCTRL (D, $p<0.001$). Images taken using 10x lens on Deltavison microscope.

In the HEK293 cell lines used for the cell segregation and boundary assays, N-cadherin is the most highly expressed cell-cell adhesion protein (Rosalind Morley, personal communication). Knockdown of N-cadherin (Cad) using siRNA was used to reduce cell-cell adhesion in combination with the siRNAs to Dvl2 or PAR-6B, as an example each of PCP or PAR polarity pathways. To be consistent with the previously optimised knockdown conditions, the same total amount of siRNA (60pmol) was transfected per condition. For single knockdowns, siCTRL was additionally co-transfected in order to maintain the total levels of siRNA transfected for double knockdowns. When verified, the knockdown achieved for each gene when co-transfected with either siCTRL or siCad was similar, but knockdown for each gene (in particular Dvl2) was less efficient (Fig. 22) than when double the amount of siRNA was used in the previous experiments (Fig. 16 B). It is important to note that even though N-cadherin knockdown reduced the protein level of N-cadherin by 81%, knockdown was not complete (Fig. 22) and residual adhesion could be present in the system.

Comparison of the adhesion, PCP and PAR knockdown conditions showed that only knockdown of Dvl2 leads to a significant disruption to both cell segregation and boundary sharpness (Fig. 23 D, G $p<0.05$, Fig. 24 D, G $p<0.001$), whereas knockdown only of N-cadherin or PAR-6B has a significant disruption only to boundary sharpness (Fig. 23 B, C, G $p<0.001$, Fig. 24 B, C, G $p<0.001$). Interestingly, when Dvl2 or PAR-6B was knocked down in a reduced adhesion background, the disruption to cell segregation and boundary sharpness was dramatically increased (Fig. 23 E-G, $p<0.001$, Fig. 24 E-G, $p<0.001$).

Individual knockdowns of Dvl2 or PAR-6B do not cause disruption to cell segregation or boundary formation to the same extent as previous experiments (Fig. 18, 19, 20, 21). This is to be expected as only half as much siRNA was used in these experiments per gene, and there is subsequently less knockdown. The effect of individual gene knockdown on the disruption to cell segregation differs between the cell segregation and boundary formation assay (Fig. 23, 24), and highlights again that the boundary formation assay is less sensitive to variables that affect the cell segregation assay (see Chapter 3).

Taken together, these data show that there is a disruption to EphB2-ephrinB1 mediated cell segregation and boundary sharpness after knockdown of PCP and PAR polarity genes, and that this disruption also occurs strongly when adhesion is reduced in the system.

4.2.6 Does Eph-ephrin signalling affect cell polarity at boundaries of segregated cells?

4.2.6.1 Polarity in Eph-ephrin boundary formation

Given that knockdown of PCP or PAR genes caused disruption to EphB2-ephrinB1 mediated boundary sharpness and cell segregation, it was important to determine whether general cell polarity was altered

Figure 22: Western blot analysis of endogenous protein expression after knockdown of both adhesion and polarity genes by siRNA

Western blot analysis of polarity proteins showing endogenous expression and the relative knockdown by siRNA in stable HEK293 lines expressing EphB2-GFP. Each knockdown depicted uses a combination of two or three siRNAs to the same gene. 30pmol siRNA was transfected per gene, and a total of 60pmol siRNA was transfected per condition. For example, siCad+Dvl2 includes 30pmol of a combination of siRNAs to N-cadherin and 30pmol of a combination of siRNAs to Dvl2. siDvl2 includes 30pmol of a combination of siRNAs to Dvl2 and 30pmol siCTRL. Knockdown is expressed as the percentage of endogenous protein remaining compared to tubulin control and compared to a transfection with siCTRL.

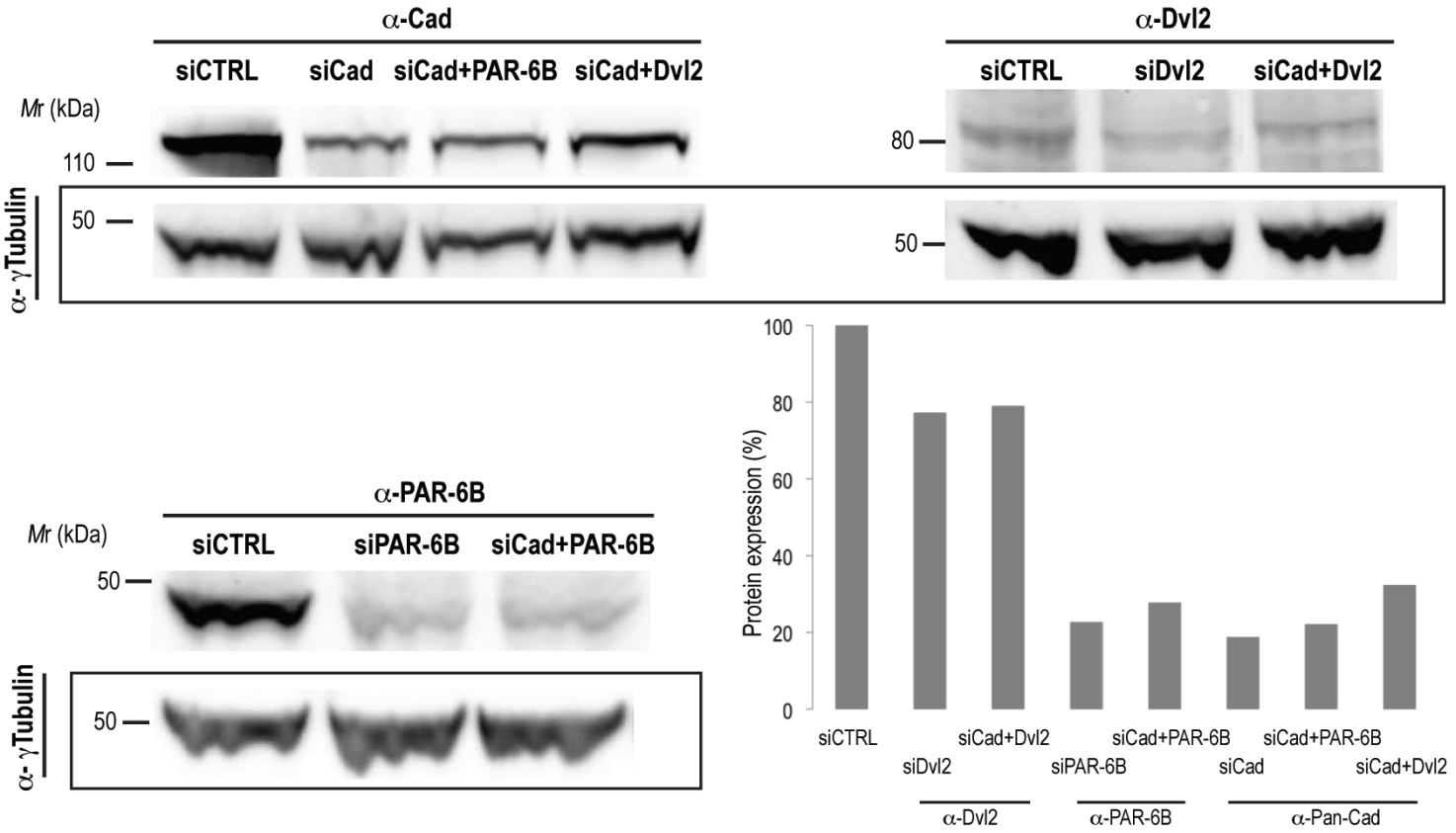
α-Cad
siCTRL
siCad
siCad+PAR-6B
siCad+Dvl2
Mr (kDa)
110
50
α-γTubulin
α-Dvl2
siCTRL
siDvl2
siCad+Dvl2
80
50
α-PAR-6B
siCTRL
siPAR-6B
siCad+PAR-6B
Mr (kDa)
50
50
α-γTubulin
Protein expression (%)
100
80
60
40
20
0
siCTRL
siDvl2
siCad+Dvl2
siPAR-6B
siCad+PAR-6B
siCad
siCad+PAR-6B
siCad+Dvl2
α-Dvl2
α-PAR-6B
α-Pan-Cad

Figure 23: Disruption to Eph-ephrin mediated cell segregation on knockdown of adhesion and polarity genes

Analysis of the effects of adhesion and polarity gene knockdown on EphB2-ephrinB1 mediated cell segregation. Endpoint analysis of EphB2-GFP/ephrinB1 cell mixtures, with both populations previously transfected with siRNA; siCTRL (A), siCad (B), siPAR-6B (C), siDvl2 (D), siCad+PAR-6B (E), siCad+Dvl2 (F). Disruption to segregation is seen in all conditions (B-F) relative to the control (A). Disruption to segregation is quantified using the perimeter regularity index (PRI) (G). A significant difference in the PRI value is observed for conditions transfected with siDvl2 (G, $p<0.05$), siCad+PAR-6B (G, $p<0.001$) and siCad+Dvl2 (G, $p<0.001$) relative to the control.

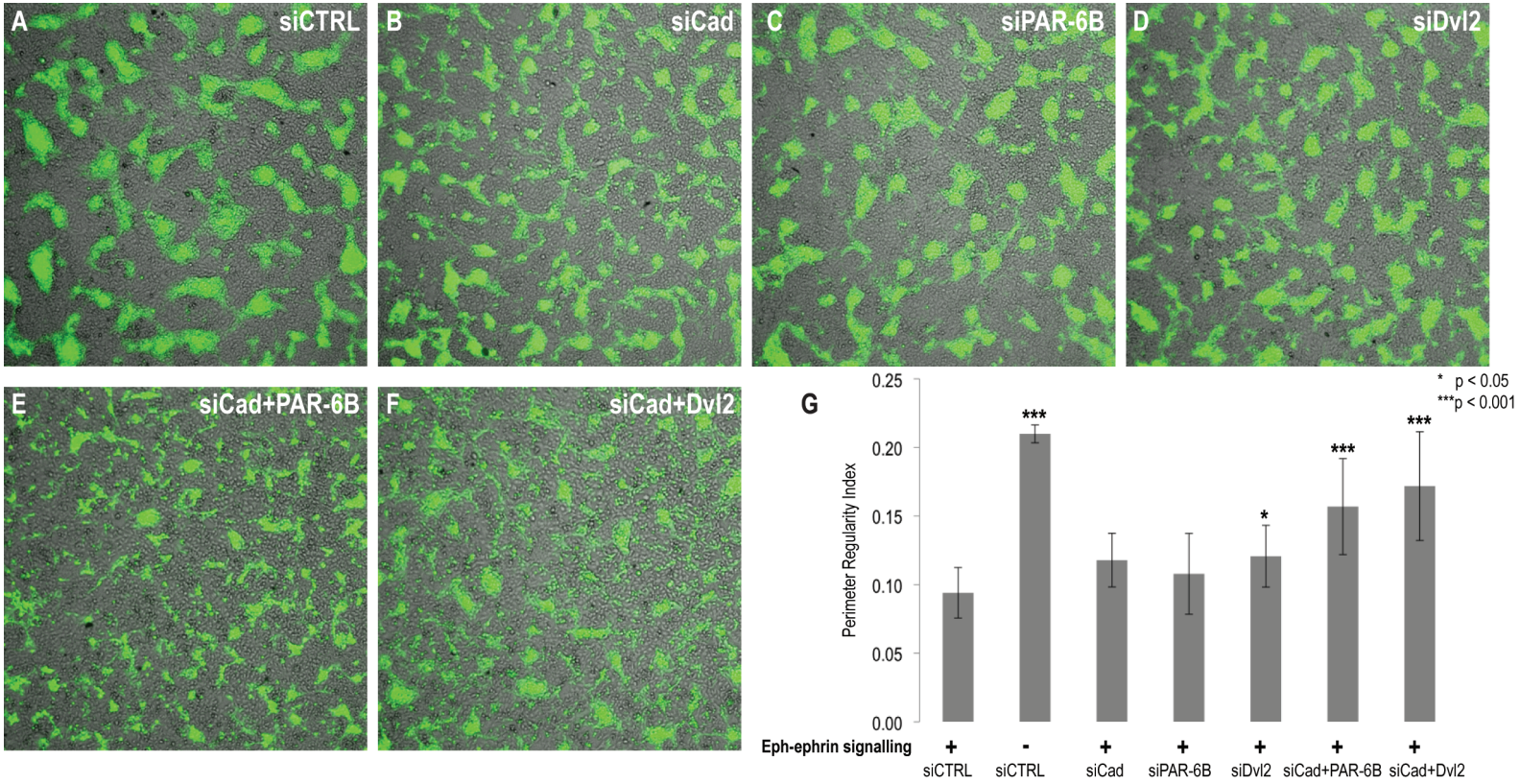
A
siCTRL
B
siCad
C
siPAR-6B
D
siDvl2
E
siCad+PAR-6B
F
siCad+Dvl2
G
* p < 0.05
***p < 0.001
Perimeter Regularity Index
0.25
0.20
0.15
0.10
0.05
0.00
***
***
*
***
***
Eph-ephrin signalling
+
-
+
+
+
+
+
siCTRL
siCTRL
siCad
siPAR-6B
siDvl2
siCad+PAR-6B
siCad+Dvl2

Figure 24: Disruption to Eph-ephrin mediated boundary sharpening on knockdown of both adhesion and polarity genes

Analysis of the effects of adhesion and polarity gene knockdown on EphB2-ephrinB1 mediated boundary sharpening. Endpoint analysis of EphB2-GFP/ephrinB1 cell mixtures, with both populations previously transfected with siRNA; siCTRL (A), siCad (B), siPAR-6B (C), siDvl2 (D), siCad+PAR-6B (E), siCad+Dvl2 (F). Disruption to boundary sharpening is seen in all conditions (B-F) relative to the control (A). Boundary sharpness is quantified by measuring boundary length of 4x magnification images (G). A significant difference in the boundary length is observed for all conditions relative to the control (G, $p<0.001$). Images taken using 10x lens on Deltavison microscope.

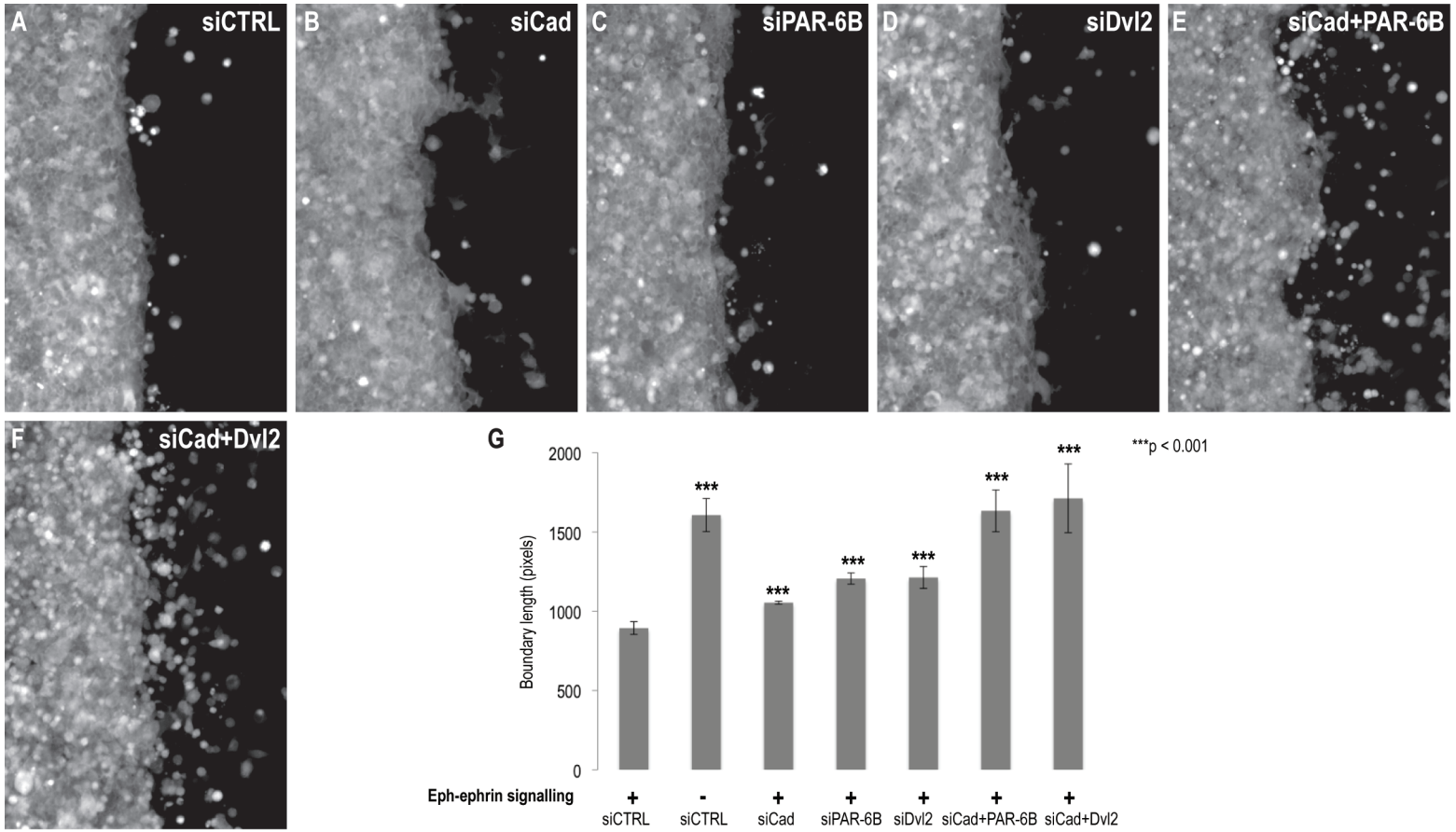
A
siCTRL
B
siCad
C
siPAR-6B
D
siDvl2
E
siCad+PAR-6B
F
siCad+Dvl2
G
***p < 0.001
Boundary length (pixels)
2000
1500
1000
500
0
***
Eph-ephrin signalling
+
-
+
+
+
+
+
siCTRL
siCTRL
siCad
siPAR-6B
siDvl2
siCad+PAR-6B
siCad+Dvl2

due to EphB2-ephrinB1 signalling. A repulsion-based signal from ephrin cells on contact with Eph cells could cause a change in polarity, as demonstrated in contact inhibition of locomotion between EphA and ephrinA cells (Astin *et al.*, 2010), which could underlie EphB2-ephrinB1 mediated boundary sharpness (Fig. 13, 33 Appendix). Golgi position is often used as a read-out of the directionality of movement and is a good indicator of the orientation of the cell polarity axis (de Anda *et al.*, 2005; Kupfer *et al.*, 1982). Cell polarisation was therefore analysed by Golgi position relative to the nucleus at the endpoint of the boundary assay.

Golgi orientation was analysed in each of four cell populations within the boundary assay: EphB2 non-boundary cells (Fig. 25 A1), EphB2 boundary cells (Fig. 25 A2), ephrinB1 non-boundary cells (Fig. 25 A4) and ephrinB1 boundary cells (Fig. 25 A3). For both EphB2 and ephrinB1 populations, cells were defined as a boundary population (with active EphB2-ephrinB1 signalling) if they contacted a different cell type, and as a non-boundary population if they were in the 35% of the population furthest from the boundary. Angles of the nucleus-Golgi vectors relative to the boundary were calculated for each cell type and grouped into 15^{o} intervals.

Non-boundary cells are not polarised, and have an unbiased angle distribution with no difference in distribution between EphB2 and ephrinB1 non-boundary populations (Fig. 25 B1, 4). In contrast, the boundary populations of both EphB2 and ephrinB1 cells were highly polarised, with the angles aligned along the boundary itself and a slight bias of each towards the boundary (Fig. 25 B2, 3). It is important to note that cells at the boundary had a flattened morphology along the boundary, compared to non-boundary populations. These distributions were significantly different when compared to their relevant non-boundary populations ($p<0.01$), but were not different to each other. This suggests that there is no inherent polarity in either EphB2 or ephrinB1 cells, but that cells are polarised along the boundary.

4.2.6.2 Polarity in Eph-ephrin boundary formation when PCP and PAR genes are knocked down

To understand whether cell polarity at EphB2-ephrinB1 boundaries was affected in situations where PCP and PAR components are knocked down, angles of the nucleus-Golgi vectors relative to the boundary were also calculated for each knockdown situation (siDvl2, siDaam1, siPAR-3 and siPAR-6B). The unbiased polarity distribution in the non-boundary populations was unchanged, compared to the non-boundary control, for all genes assessed. Interestingly, each PCP and PAR knockdown led to the boundary population having a more random polarity (Fig. 26), and so showed no significant difference to their respective non-boundary conditions. This was seen similarly for both EphB2 and ephrinB1 populations (data not shown). EphB2 boundary cells showed a less polarised distribution along the boundary axis when each of the PCP and PAR genes were knocked down, compared to the control boundary situation (Fig. 26), which was significantly different for all knockdown conditions apart from

Figure 25: Golgi orientation in Eph-ephrin boundary formation

Analysis of Golgi position relative to the nucleus, and the orientation of cells relative to the boundary. Golgi orientation is measured in EphB2-GFP/ephrinB1 cell mixtures.

(A): Each boundary is split into four populations in which to analyse polarity: EphB2 non-boundary cells (A1), EphB2 boundary cells (A2), ephrinB1 non-boundary cells (A4) and ephrinB1 boundary cells (A3).

(B): Angles of nucleus-Golgi positions relative to the boundary are calculated for each cell type and grouped into 15^{o} intervals. 0^{o} marks the boundary position. Non-boundary cells show a non-polarised distribution (B1, 4) and the boundary cells show a polarised distribution (B2, 3). Boundary distributions are significantly different to their relevant non-boundary populations ($p<0.01$), but not to each other.

(C): Angles are measured of the nucleus-Golgi positions towards or away from the boundary. The nucleus-Golgi positions in cells 1 and 2 have the same orientation towards the boundary and so are counted the same. The nucleus-Golgi position in cell 3 deviates from the boundary by the same amount but is orientated away from the boundary.

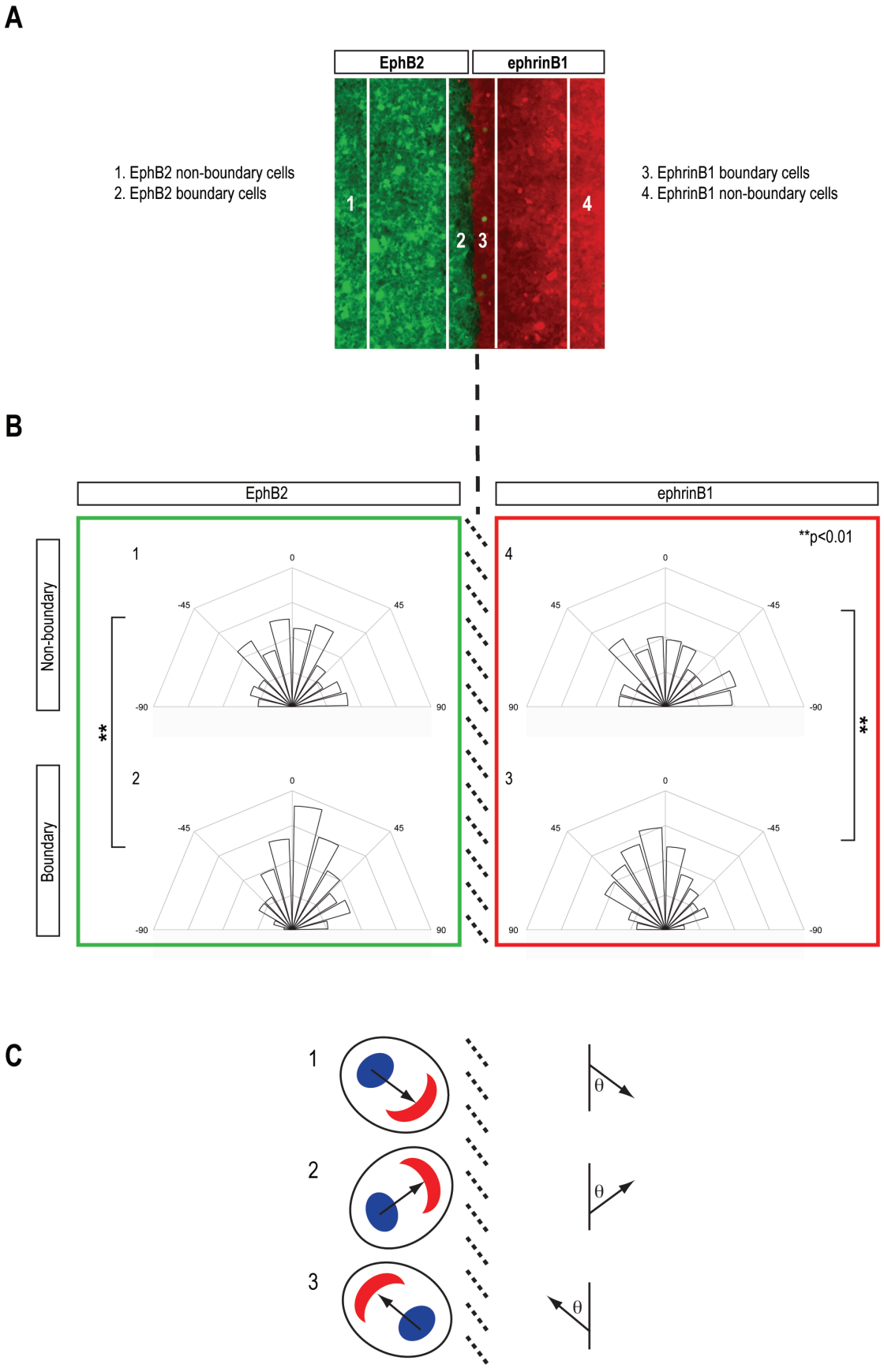
A
EphB2
ephrinB1
1. EphB2 non-boundary cells
2. EphB2 boundary cells
3. EphrinB1 boundary cells
4. EphrinB1 non-boundary cells
1
2
3
4
B
EphB2
ephrinB1
**p<0.01
Non-boundary
Boundary
**
**
0
45
-45
90
-90
C
θ
θ
θ

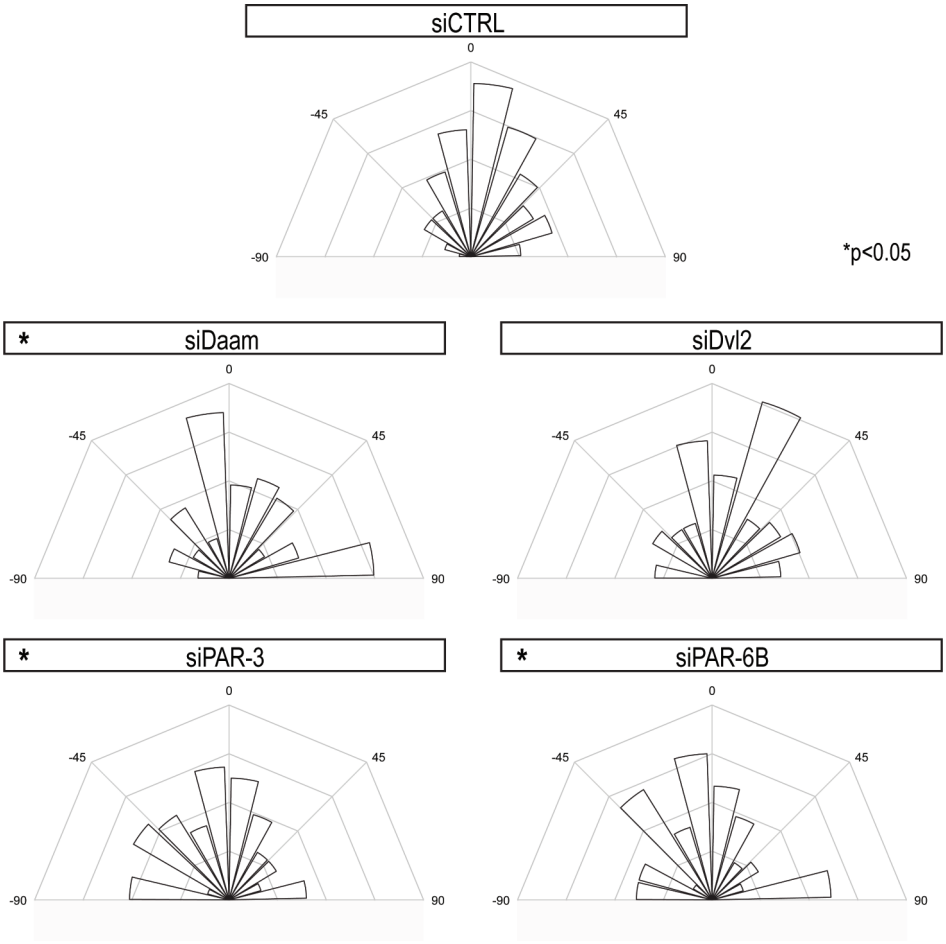

Figure 26: Polarity in Eph-ephrin boundary formation when PCP and PAR polarity genes are knocked down

Analysis of the Golgi position relative to the nucleus, and the orientation relative to the boundary. Golgi orientation is measured in EphB2-GFP/ephrinB1 cell mixtures previously transfected with either siDvl2, siDaam1, siPAR-3 or siPAR-6B. Angles of Golgi-nucleus positions relative to the boundary are calculated for EphB2 boundary cells and grouped into 15^{o} intervals for each condition. 0^{o} marks the boundary position. All siRNA conditions show a less polarised boundary distribution compared to the siCTRL boundary control ($p<0.05$), apart from Dvl2.

Dvl2. This phenotype was more pronounced in the EphB2 cell population compared to the ephrinB1 population (data not shown). This suggests that knockdown of PCP and PAR genes causes Golgi orientation relative to the boundary to become more random in the boundary populations.

4.3 DISCUSSION

Previous work had shown a connection between Eph-ephrin signalling and PCP in cell segregation *in vitro* (Lee *et al.*, 2006; Tanaka *et al.*, 2003), and PCP and cell migration *in vivo* (Carmona-Fontaine *et al.*, 2008; De Calisto *et al.*, 2005). PAR core polarity proteins, together with Rac1, RhoA and Cdc42 GTPases, control the front-rear polarisation of migratory cells by localising and activating Rac1 at the leading edge (Mertens *et al.*, 2006; Pegtel *et al.*, 2007). PAR-6B and PAR-3 were recently identified in a screen for proteins phosphorylated downstream of EphB2-ephrinB1 signalling, and in an siRNA screen of a kinase library in which cell segregation was analysed (Jorgensen *et al.*, 2009). It remains to be established whether EphB2-ephrinB1 signalling regulates cell segregation and boundary sharpening through the PCP or PAR polarity pathway, and whether directional persistence contributes to EphB2-ephrinB1 cell segregation. In order to test these possibilities, the role of key PCP components, Dvl and Daam1, and core polarity components, PAR-6B and PAR-3, were tested in the cell segregation and boundary sharpening assays using siRNA-mediated knockdown of gene expression.

4.3.1 PCP and PAR polarity genes play a role in Eph-ephrin mediated boundary sharpness

siRNA-mediated knockdown of PCP and PAR polarity genes disrupts EphB2-ephrinB1 mediated cell segregation and boundary sharpening, as seen in both the cell segregation and boundary formation assays. Both *in vitro* assays were carried out with EphB2 and ephrinB1 cell populations that were each transfected with the same siRNA mix, as siRNA transfection can potentially cause changes in proliferation and therefore change the ratio of one population to another. Therefore by transfecting both populations, such that there would be an equal or similar effect on both populations, changes in PRI values due to proliferation effects on cluster morphology are minimised (as discussed, Fig. 10). The boundary sharpening assay is potentially less sensitive to variables that affect the cell segregation assay such as changes in proliferation (as discussed in Chapter 3), but knockdown was still carried out in both EphB2 and ephrinB1 populations in order to allow direct comparison of the cell segregation and boundary sharpening assays. Future experiments could address the cell-type specific requirement for PCP or PAR genes in regulating EphB2-ephrinB1 mediated boundary sharpness by transfecting siRNA in either EphB2 or ephrinB1 cells and assessing the disruption to boundary sharpening.

Knockdown of Dvl2, Daam1, PAR-3 and PAR-6B genes show a significant disruption to boundary sharpness in both the cell segregation and boundary formation assays (Fig. 18, 19, 20, 21). As there are

three Dvl genes expressed in HEK293 cells, it is likely that there might be some functional redundancy between them. Analysis of the effect of Dvl2 and Dvl3 on cell segregation and boundary formation was carried out individually and in combination (Fig. 18, 20) in order to assess the contribution of functional redundancy. Disruption to segregation or boundary formation with Dvl3 knockdown or double knockdown of both Dvl2 and Dvl3 together did not cause significant disruption to boundary sharpening (Fig. 18, 20). This argues against a role of redundancy of Dvl genes in EphB2-ephrinB1 mediated boundary sharpening, and suggests Dvl2 plays a role downstream of EphB2-ephrinB1 signalling.

It is not known why Dvl23 knockdown does not disrupt boundary sharpness to the same extent as Dvl2 knockdown. It is possible that the disruption due to Dvl2 knockdown is diluted in the siDvl23 condition as half the amount of Dvl2 siRNA is used in siDvl23 in comparison with siDvl2. It is also possible that Dvl2 and Dvl3 could act in opposition to each other, but there is no supporting evidence for this. The roles of different Dishevelled genes in this process need to be further analysed.

Taken together these results reveal that knockdowns of Dvl2, Daam1, PAR-3 or PAR-6B cause disruption to EphB2-ephrinB1 mediated cell segregation, in agreement with previous studies (Jorgensen *et al.*, 2009; Tanaka *et al.*, 2003). These results also show that knockdowns of Dvl2, Daam1, PAR-3 or PAR-6B cause disruption to EphB2-ephrinB1 mediated boundary sharpness, and therefore that the PCP and PAR polarity pathways may play a role in boundary formation downstream of EphB2-ephrinB1 signalling. As knockdowns of Dvl3 and Dvl23 do not affect EphB2-ephrinB1 mediated boundary sharpness, they were not examined in subsequent experiments.

4.3.1.1 Separating the roles of adhesion and repulsion

Previous work has shown a role for both repulsion and adhesion downstream of Eph-ephrin signalling; both adhesion (Rosalind Morley, personal communication; Cortina *et al.*, 2007; Jorgensen *et al.*, 2009) and polarity proteins (this work; Jorgensen *et al.*, 2009) have been shown to play a role in EphB2-ephrinB1 mediated cell segregation and boundary formation. The idea that differential adhesion can drive cell segregation comes from work by Malcolm Steinberg, who showed that sorting can be driven either by the preferential adhesion of cells expressing the same cadherin, or by differences in the expression level of cadherins between populations (Fig. 2 A) (reviewed (Foty & Steinberg, 2004)). Separating the roles of adhesion and repulsion is difficult; the Steinberg model of differential adhesion could underlie segregation as Eph-ephrin signalling may cause decreased adhesion at an interface between two populations, and/or repulsion could lead to cell migration that underlies segregation.

A number of lines of evidence suggest that Eph-ephrin signalling has a role in the regulation of adhesion. E-cadherin is required for EphA2 receptor localisation at cell-cell contacts in epithelial cells (Orsulic & Kemler, 2000), and EphB signalling has been shown to couple cell contraction with cell-to-cell adhesion by

promoting the recruitment of E-cadherin to the membrane in epithelial tumour cells (Cortina *et al.*, 2007). Sorting between cell lines expressing EphB3 and ephrinB1 was severely impaired when E-cadherin was knocked down, suggesting that cadherin-driven adhesion plays a role in Eph-ephrin mediated cell sorting (Cortina *et al.*, 2007). In addition, EphB2 signalling in Schwann cells induces cell sorting, at least in part by the redistribution of N-cadherin to cell-cell contacts (Parrinello *et al.*, 2010). Mosaic knockdown of EphA4 has been found to lead to cell segregation within rhombomeres of the developing zebrafish hindbrain (Cooke *et al.*, 2005), and has therefore been proposed to sharpen boundaries by modulating cell affinity both at interfaces and within regional domains.

Recent evidence has shown a role for EphB-ephrinB signalling in controlling *Xenopus* embryonic germ layer separation by cycles of transient adhesion and contact-induced cell detachment (Rohani *et al.*, 2011). Adhesion brings Eph receptors and ephrins into contact, inducing a local Rac1- and RhoA-based detachment, which decays after separation, so allowing re-adhesion (Rohani *et al.*, 2011). This suggests a role of dynamic adhesion between Eph- and ephrin-expressing cells in regulating cell segregation. The relative contribution of adhesion/de-adhesion and repulsion to Eph-ephrin mediated cell segregation and boundary formation is not known.

In order to separate the roles of adhesion and repulsion in EphB2-ephrinB1 mediated cell segregation and boundary formation, the role of polarity (Dvl2 and PAR-6B) in a reduced-adhesion background (lower N-cadherin) was analysed. The cell segregation that does occur in reduced adhesion conditions could be due to polarity-driven directional migration and repulsion. However, a complication is that recent evidence has suggested a role for both the PCP and PAR polarity pathways in cell-cell adhesion. Wnt11, a non-canonical Wnt, has been shown to be required for cell adhesion through the dynamic control of E-cadherin subcellular localisation via Rab5c (Ulrich *et al.*, 2005). PAR-6 has been shown to localise at adherens junctions with E-cadherin and play a role in the endocytosis of junctional material and the stability of adherens junctions (Georgiou *et al.*, 2008; Georgiou & Baum, 2010). Since knockdown of N-cadherin is not complete, it could be that the additive effect on disruption to cell segregation and boundary sharpness seen on knockdown of N-cadherin with either Dvl2 or PAR-6B together could be due to further decreasing adhesion in this system. This is unlikely as there is no evidence that the PCP or PAR components are essential for cadherin-mediated adhesion required for segregation, and so we assume that the cell segregation that does occur in reduced adhesion conditions could be due to polarity-driven directional migration and repulsion.

Therefore, if polarity and adhesion function in the same pathway, a knockdown of both adhesion and polarity components is not expected to enhance the disruption to boundary sharpness seen on individual knockdown of these components. Knockdown of N-cadherin and either Dvl2 or PAR-6B together enhance the disruption to cell segregation and boundary sharpness compared to individual knockdowns (Fig. 23, 24). This suggests that cell migration contributes to EphB2-ephrinB1 mediated cell segregation and

boundary formation, and that differential adhesion is not enough. Polarity and adhesion could therefore function in parallel to play a role in EphB2-ephrinB1 mediated cell segregation, and knockdown of both adhesion and polarity components would be expected to enhance the disruption to boundary sharpness seen on individual knockdown of these components, as shown.

Furthermore, computer simulations have suggested that directional persistence can in principle contribute to cell segregation when a basal level of adhesion is present between all cells. Taken together, this suggests that differential adhesion and directional migration may play a synergistic role in regulating cell segregation and boundary sharpening, or that a basal level of adhesion between cells is required for interactions and cell-cell signalling to occur. In the next chapter, I will discuss experiments to test the roles of PCP and PAR components in EphB2-ephrinB1 mediated cell migration.

4.3.2 Cells are polarised in response to Eph-ephrin signalling at the boundary

Given that knockdown of PCP and PAR polarity genes causes disruption to EphB2-ephrinB1 mediated boundary sharpness and cell segregation, it was important to determine whether basal cell polarity was altered during EphB2-ephrinB1 signalling. As described previously, it was thought that ephrin cells could provide a contact inhibition of locomotion-induced repulsion-based signal in Eph cells (Astin *et al.*, 2010), and so a change in polarity. Forward EphA signalling via activation of RhoA due to contact with ephrinA cells is necessary for homotypic CIL in prostate cancer cells (Astin *et al.*, 2010). RhoA activation may cause a loss in forward migration due to membrane withdrawal at the front of the cell and the concurrent inhibition of Rac1. Loss of the leading lamella allows protrusion formation away from the site of contact and cell repolarisation (Astin *et al.*, 2010). My data show that boundaries remain sharp over time (Fig. 14, Fig. 33 Appendix), and it is possible that a repulsion-based signal from ephrin cells on contact with Eph cells could cause a change in polarity, which could underlie EphB2-ephrinB1 mediated boundary sharpening.

Golgi position is often used as a read-out of the directionality of movement and is a good indicator of the orientation of the cell polarity axis (de Anda *et al.*, 2005; Kupfer *et al.*, 1982). Leader migrating cells in a scratch wound assay polarise their Golgi forward of the nucleus in the direction of migration (Kupfer *et al.*, 1982; Nobes & Hall, 1999), but in cells well removed from the wound within the confluent monolayer, the Golgi apparatus and MTOC remained randomly oriented (Kupfer *et al.*, 1982). The positioning of the Golgi apparatus reflects the centrosome position and promotes microtubule formation and directional vesicular transport to the leading edge to facilitate dynamic membrane protrusion formation and cell movement (Ang *et al.*, 2010; Miller *et al.*). Cell repolarisation was therefore analysed by Golgi orientation relative to the nucleus in the endpoint of the boundary assay.

A recent study suggests that when cells migrate collectively, for example in a scratch wound assay, it is the absence of cell-cell contacts that drives cell polarisation of the leader cells towards the contact-free edge (Desai *et al.*, 2009). N-cadherin or E-cadherin at cell contacts controls intracellular organisation, nucleus and centrosome positioning, and cell orientation in various cell types (Desai *et al.*, 2009; Dupin *et al.*, 2009). N-cadherin-dependent cell contacts are also required for collective cell migration and CIL between neural crest cells, and can polarise the cells by inhibiting Rac1 at contacts and increasing Rac1 activity at the free edge; this polarised distribution of Rac1 activity is essential for directional and collective cell migration (Fig. 7 B) (Theveneau *et al.*, 2010).

In the boundary assay there is collective migration of two populations towards each other at early migratory stages, and we would expect that on interaction, the polarisation of the leading migrating cells would be reversed at the boundary if EphB2-ephrinB1 signalling provided a repulsive cue. At the endpoint of the boundary assay, collective migration would not be occurring to the same extent so any polarity in the system should be due to EphB2-ephrinB1 signalling at the boundary. We would thus still expect the Golgi to be oriented away from the boundary if EphB2-ephrinB1 signalling provided a repulsive cue. However, I found that the boundary populations of both EphB2 and ephrinB1 cells were highly polarised parallel to the boundary itself, with only a slight bias towards the boundary (Fig. 25 B2, 3). In contrast, polarity in the non-boundary populations is independent of EphB2-ephrinB1 signalling as expected, with both EphB2 and ephrinB1 populations showing a random distribution of Golgi orientation (Fig. 25 B1, 4).

It is possible that the distribution of Golgi orientation seen is an indirect consequence of the flattened cell morphology observed in boundary cells induced by EphB2-ephrinB1 signalling. Repulsion between EphB2-ephrinB1 cells at the boundary would lead to cytoskeletal collapse and retraction at the interface of the populations. Cells would be unable to move away from the interface due to the dense population of "like" cells behind the boundary. This could cause the flattening of cells along the interface, so indirectly realigning the nucleus-Golgi axis. Another possibility is that interfacial surface tension could play a role in the flattening of cells and repolarisation of the Golgi at the boundary. Interfacial tension depends on the balance between cortical contractile elements and cell-cell adhesive contacts both at the boundary and within a population. Increasing contractility increases mechanical tension, whereas increasing adhesive contacts reduces tension (reviewed in (Lecuit & Lenne, 2007). Therefore de-adhesion or repulsion between EphB2-ephrinB1 cells at the boundary could cause increased interfacial tension along the boundary, and contribute to the flattening and elongation of cells.

Repulsion seems the more likely mechanism to cause the flattening and elongating of cells along the boundary, but a role of tension cannot be ruled out. This change in cell shape would cause the re-localisation of the Golgi and mask any polarity induced by EphB2-ephrinB1 signalling. We can conclude that at the boundary, EphB2-ephrinB1 signalling causes the boundary populations of both EphB2 and ephrinB1 cells to become highly polarised along the boundary itself. However, this phenotype might be

secondary to the actual polarity induced by EphB2-ephrinB1 signalling, and Golgi orientation at the boundary may therefore not be a good read-out of polarity.

4.3.2.1 Eph-ephrin mediated boundary polarity is randomised with PCP or PAR polarity knockdown

The role of polarity components in Golgi or centrosome orientation has been previously described in scratch wound assays. Daam1 and Dishevelled have been shown to play a role in intracellular polarity by regulating centrosome orientation in monolayer scratch assays (Ang *et al.*, 2010; Schlessinger *et al.*, 2007), as has the PAR complex (Etienne-Manneville & Hall, 2001). PAR-3 and PAR-6 can function cooperatively or independently in this process. In scratch wound assays using fibroblasts, disruption of cell-cell contacts at the wound edge leads to the activation of non-canonical Wnt signalling. This couples Dishevelled and Cdc42/PAR-6/aPKC pathways to trigger Golgi and centrosome orientation, and stabilise microtubules towards the leading edge (Schlessinger *et al.*, 2007). This suggests a complex role of the PCP and PAR pathways, independently and cooperatively, in Golgi reorientation on wounding, but their role downstream of EphB2-ephrinB1 signalling is not known.

To order to understand whether general cell polarity was affected in PCP and PAR knockdown situations, angles of nucleus-Golgi positions relative to the boundary were calculated in these conditions. The unbiased polarity in non-boundary populations with each gene knockdown (siDvl2, siDaam1, siPAR-3 and siPAR-6B) was unchanged, as expected (data not shown). In contrast, when for each PAR (PAR-3, PAR-6B) or PCP (Dvl2, Daam1) knockdown the boundary cell population was compared to the siCTRL boundary, cells were less polarised along the boundary axis (Fig. 26). This difference was significantly different for all knockdown conditions apart from Dvl2, and for each gene knockdown, boundary cell distributions were more random with no significant difference to non-boundary cell distributions. As described, polarity observed at the boundary is likely to be due to the flattening of cells caused by EphB2-ephrinB1 induced repulsion. The disruption to polarity in knockdown boundary populations could thus be secondary to more rounded cell morphology at the boundary (data not shown), possibly due to reduced repulsion. This therefore suggests that PCP and PAR polarity pathways could underlie cell repulsion responses induced by EphB2-ephrinB1 signalling at the boundary.

Taken together these data suggest that both PCP and PAR polarity genes lie downstream of EphB2-ephrinB1 mediated cell segregation and boundary sharpening. In order to determine whether EphB2-ephrinB1 mediated directional persistence underlies cell segregation and boundary sharpening, the role of these PCP and PAR genes in EphB2-ephrinB1 mediated directional persistence is analysed in the next Chapter.

5 PCP AND PAR GENES ARE REQUIRED DOWNSTREAM OF EPH-EPHRINS FOR EPH-EPHRIN MEDIATED CHANGE IN DIRECTIONAL MIGRATION

5.1 Introduction to directional persistence

Studies by Alexei Poliakov in the Wilkinson laboratory (unpublished) have shown that interaction with ephrinB1 cells leads to increased directional persistence of EphB2 cells, where directional persistence is defined as the measure of the average time period between "significant" changes in the direction of movement (DiMilla *et al.*, 1993). The signalling pathways underlying Eph-ephrin mediated directional persistence are not known, but it is likely that Eph receptors regulate cell morphology and behaviour by rearranging the cytoskeleton via signalling to Rho GTPases; Cdc42, Rac1 and RhoA (Groeger & Nobes, 2007; Noren & Pasquale, 2004b).

Repulsion responses between cells, due to Eph-ephrin signalling, play a role in axon guidance and inhibit entry into ligand-expressing territory (Flanagan & Vanderhaeghen, 1998; Kullander & Klein, 2002; Poliakov *et al.*, 2004). Repulsion can be characterised by the collapse response of Eph cells in which cell processes collapse and the cells round up (Fig. 5 B, B') (Poliakov *et al.*, 2008). Eph-ephrin mediated activation of RhoA has been shown to lead to growth cone collapse, and is mediated by adaptor proteins such as the Rho GEFs, ephexin and Vav, through Eph receptors (Cowan *et al.*, 2005; Knoll & Drescher, 2004; Pitulescu & Adams, 2010; Sahin *et al.*, 2005; Shamah *et al.*, 2001). Eph-ephrin mediated activation of RhoA could underlie the increased directional migration that is seen after contact between Eph- and ephrin-expressing cells, and so collapse due to repulsion could be the trigger or driving force underlying directional migration.

Similarly, contact inhibition of locomotion (CIL) has been demonstrated to underlie the repulsion and collapse response seen at the site of contact between Eph and ephrin cells (Astin *et al.*, 2010). CIL is "the stopping of the continual locomotion of a cell in the same direction after collision with another cell" (Abercrombie, 1970). In CIL, repulsion mediated by localised RhoA activation and Rac1 inhibition at the site of contact, causes membrane withdrawal and the loss of leading lamella, so inhibiting forward migration (Astin *et al.*, 2010; Miao *et al.*, 2005; Sordella & Van Aelst, 2008). The retraction of protrusions from the site of contact enables the generation of a new protrusion away from the site of contact and cell repolarisation (Mayor & Carmona-Fontaine, 2010). Eph-ephrin induced contact repulsion has been shown to occur upon EphB2-ephrinB1 and EphA-ephrinA interactions in prostate cancer cells (Astin *et al.*, 2010),

EphB4-ephrinB2 interaction in fibroblasts and endothelial cells (Marston *et al.*, 2003), and EphB3-ephrinB1 interaction in epithelial cell migration (Miao *et al.*, 2005).

The stabilisation of leading lamellipodia, which occurs after contact inhibition, is also important in maintaining persistence, as this maintains the orientation of movement (Harms *et al.*, 2005). Therefore, the intracellular signalling pathways active at the leading edge (LE) that regulate actin cytoskeleton remodelling are likely to contribute to directional migration downstream of Eph-ephrin signalling by creating or stabilising local protrusions. Candidate pathways for this, and activating RhoA at the site of contact, include the PCP pathway and core PAR polarity.

PCP has been implicated in the directional migration of some neurons (Bingham *et al.*, 2002; Wada & Okamoto, 2009) and neural crest cells (Carreira-Barbosa *et al.*, 2003; De Calisto *et al.*, 2005; Matthews *et al.*, 2008), and is involved in regulating cytoskeletal changes, cell adhesion and protrusive membrane activity. PCP components, including Dishevelled, have been shown to be required for CIL in neural crest migration (Fig. 7 A) (Carmona-Fontaine *et al.*, 2008). Accumulation of PCP components at the site of cell-cell contact and local RhoA activation causes lamellipodia inhibition, cell repolarisation and initiation of migration away from the site of contact (Carmona-Fontaine *et al.*, 2008; De Calisto *et al.*, 2005; Matthews *et al.*, 2008; Mayor & Carmona-Fontaine, 2010). Cell orientation and migration can be therefore be directed by the PCP pathway acting via RhoA.

As previously described, the PAR complex couples Rho GTPase activity to polarise the nucleus and centrosome along the front-rear axis (Etienne-Manneville & Hall, 2001; Pegtel *et al.*, 2007) and stabilise the formation and orientation of protrusions at the LE (Etienne-Manneville & Hall, 2001; Etienne-Manneville & Hall, 2003), the stability of which correlates with the extent of directional cell movement (Iden & Collard, 2008). As polarity proteins serve as spatial-temporal cues, they are good candidates for the local activation of Rho GTPases and contact-induced directional migration (Ridley *et al.*, 2003).

The PCP and PAR polarity pathways are therefore likely candidates to act downstream of EphB2-ephrinB1 signalling in the directional persistence of migration. Components of these pathways have been shown to contribute to EphB2-ephrinB1 mediated cell segregation and boundary sharpening (Chapter 4). Cell behaviour studies were therefore carried out in order to analyse EphB2-ephrinB1 mediated cell behaviour and test the role of these components in EphB2-ephrinB1 mediated directional persistence. This was also important in order to establish whether directional persistence contributes to cell segregation and boundary formation.

5.2 RESULTS

5.2.1 Eph-ephrin signalling and directional migration

5.2.1.1 Analysis of individual cell-cell interactions

To study the change in behaviour mediated by EphB2-ephrinB1 signalling, Alexei Poliakov in the Wilkinson lab set up cell tracking methods to study individual cell interactions (unpublished data), which I have analysed using a custom designed program. The EphB2-GFP, EphB2 and ephrinB1 stable cell lines (used in previous chapters) were labelled with fluorescent dye and mixed in equal proportion. They were plated at low density to allow cells to freely migrate on glass slides coated with fibronectin. Cells were allowed to settle before time-lapse images were taken at 2 min intervals over a 5 hour time period in order to analyse cell behaviour. XY coordinates of EphB2-GFP cell centroids were used to calculate mean-squared displacement (MSD) curves using a range of overlapping time intervals (DiMilla *et al.*, 1993; Martens *et al.*, 2006) using a single particle tracking algorithm, GMimPro (Mashanov & Molloy, 2007). MSD is proportional to the straight-line distance travelled in a given time interval, and it was assumed that the HEK293 cells move with persistent random walk (DiMilla *et al.*, 1993; Harms *et al.*, 2005) i.e. cells cannot move directly backwards. The MSD of each cell is a function of time, speed and persistence time.

To assess the change in cell behaviour in response to EphB2-ephrinB1 signalling, individual tracks of EphB2-GFP cells were analysed for 1 hour after interaction with either an EphB2- or ephrinB1-expressing cell. Tracks that interact with a further cell in this time are not included in the analysis. The MSD curves showed a clear difference between conditions: EphB2-GFP cells after interaction with ephrinB1 cells (red line) had a greater displacement in a given time than after interaction with other EphB2 cells (blue line), giving a difference in MSD (at 25 min intervals) between the conditions of 197μm^2 (Fig. 27 A). This measurement is taken from a single experiment but is representative of three independent experiments. Analysis of whole EphB2-GFP cell trajectories (green line), where only a small proportion will have recently interacted with an ephrinB1 cell, showed a very similar MSD curve to that of EphB2-GFP cells after interaction with EphB2 cells. This suggests that the increase in MSD seen is due to an EphB2-ephrinB1 mediated change in behaviour after collision.

As MSD is a function of speed and persistence, a change in either of these parameters could cause the increase in MSD seen. To address which of these is most important, the XY coordinates of EphB2-GFP cell positions after an interaction were extracted and the tracks plotted on an axis relative to a central site of interaction at the origin. 50 tracks of 1 hour in length were randomly chosen for each condition. It was found that tracks of EphB2-GFP cells after interaction with ephrinB1 cells (Fig. 27 B) were straighter,

Figure 27: Cell behaviour after Eph-ephrin cell collisions

Analysis of EphB2-ephrinB1 mediated changes in cell behaviour after the point of contact of two cells. Data from Alexei Poliakov; analysis carried out independently.

(A): Tracks of EphB2-GFP cells (of 1 h in length) are analysed after EphB2-GFP/ephrinB1 collisions, EphB2-GFP/EphB2 collisions or the whole trajectory independent of any collision. The mean squared displacement (MSD) is analysed for each situation over changing time intervals (2 min to 25 min). MSD is greater after interaction with ephrinB1 cells than EphB2 cells (n=number of interactions for which MSD was calculated).

(B): The XY coordinates of cell positions after EphB2-GFP/ephrinB1 interactions are plotted relative to a central site of interaction. 50 tracks of 1 h in length were randomly selected and plotted.

(C): The XY coordinates of cell positions after EphB2-GFP/EphB2 interactions are plotted relative to a central site of interaction. 50 tracks of 1 h in length were randomly selected and plotted. Tracks of EphB2-GFP cells after interaction with ephrinB1 cells are straighter (B) than those after interaction with EphB2 cells (C) indicating increased directional persistence.

(D): Analysis of endpoint positions of tracks of 1 h (coloured crosses), and the root mean square displacement of these (solid lines). EphB2-GFP cells after interaction with ephrinB1 cells (red line) move further than those after interaction with EphB2 cells (blue line).

(E): Turning angle analysis (degrees) of trajectories of cell movement. Tracks are analysed in overlapping 4 min intervals on the likelihood of the cell to move in a forward direction. Results are plotted as the probability distribution function (PDF). EphB2-GFP cells after interaction with ephrinB1 cells (red line) are more likely to move within a narrower directional range than those after interaction with EphB2 cells (blue line), that move with a broader range of angles.

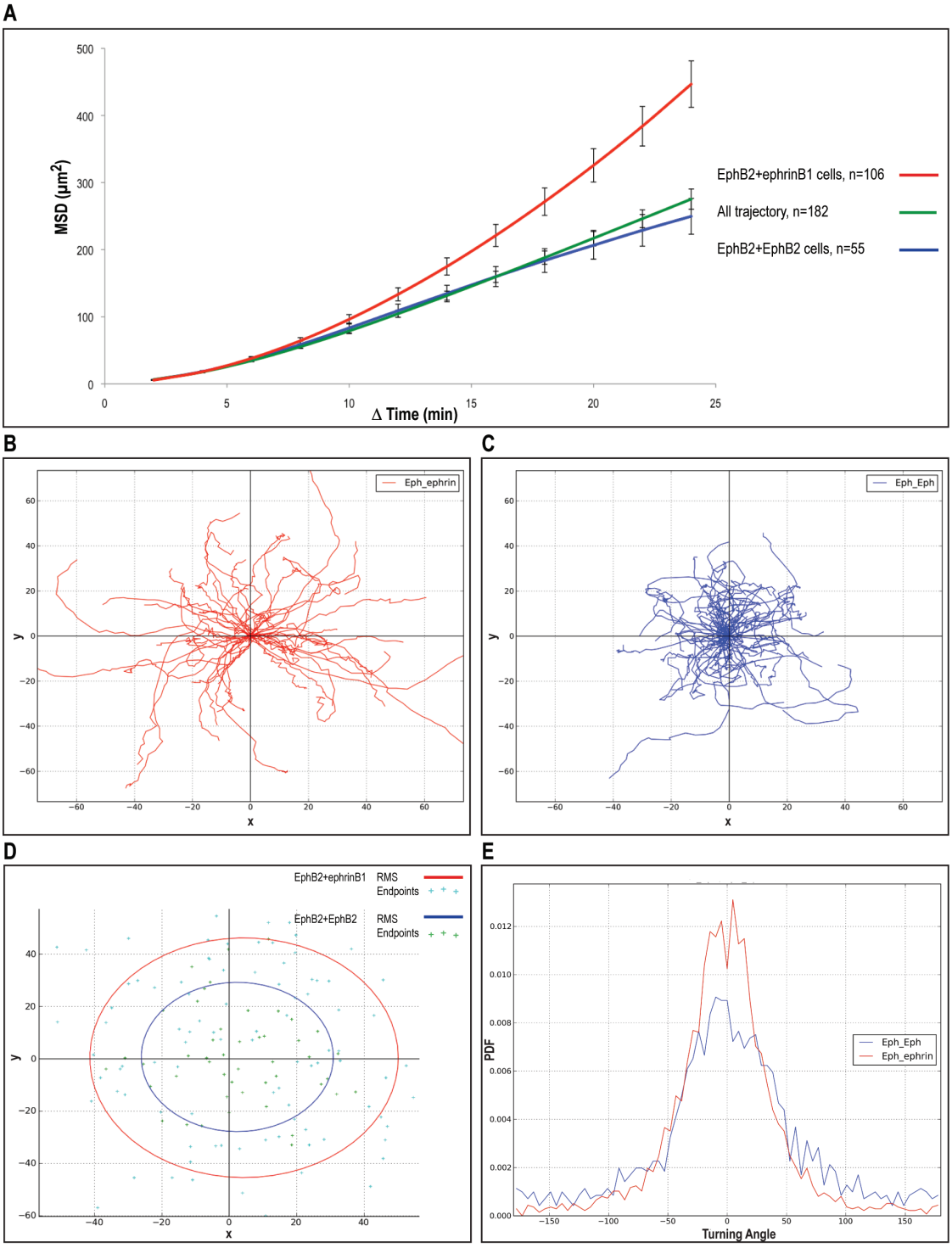
A
MSD (µm²)
Δ Time (min)
EphB2+ephrinB1 cells, n=106
All trajectory, n=182
EphB2+EphB2 cells, n=55
B
Eph_ephrin
C
Eph_Eph
D
EphB2+ephrinB1 RMS
Endpoints
EphB2+EphB2 RMS
Endpoints
E
PDF
Turning Angle
Eph_Eph
Eph_ephrin

suggesting more directional persistence than after interaction with EphB2 cells (Fig. 27 C), and the cells were consequently located further from the point of interaction in a given time interval (Fig. 27 D). The tracks of EphB2-GFP cells after interaction with other EphB2 cells had more frequent changes in direction, so the tracks were more random (Fig. 27 C) and the overall displacement was less (Fig. 27 D).

In principle, a change in speed could also contribute to the changes seen. It is important to measure speed independently of any directional movement to be able to distinguish between speed and persistence. However instantaneous speed has proved difficult to measure accurately, due to difficulties in distinguishing between actual movements of the cells and dye centroid fluctuations (discussed later). As a result, persistence cannot be determined by measuring speed and MSD. To help separate speed and persistence, directionality was analysed by calculating the distribution of turning angles of the EphB2-GFP tracks. This measurement is assumed to be independent of speed (discussed later) and thus representative of directionality only.

Turning angle analysis of cell trajectories gives an indication of the likelihood of the cell to move straight ahead. The angle of deviation of the path of a cell from a predicted straight-line movement from the previous direction is measured using overlapping 4 min intervals. The results for all cells are pooled and plotted as the probability distribution function (PDF) over the turning angle distribution; a narrower PDF curve indicates more directional movement. EphB2-GFP cells are more likely to move in a narrower directional range after interaction with ephrinB1 cells (red line) than after interaction with EphB2 cells (blue line) (Fig. 27 E). Taken together these results suggest EphB2-GFP cells move more persistently, and they have straighter tracks that deviate less from a straight line, after interaction with ephrinB1 cells than with EphB2 cells.

5.2.1.2 A high-throughput approach to analysing Eph-ephrin mediated directional migration

We can conclude from analysis of individual interactions between EphB2-GFP/ephrinB1 and EphB2-GFP/EphB2 cells that EphB2-GFP cells move more directionally after interaction with ephrinB1 cells, and that this is caused by an increase in the persistence of migration (Alexei Poliakov, unpublished data, Fig. 27). In these experiments cells were plated at low density such that there were few interactions in a 5 hour period (approximately 50 per movie), which could be analysed on an individual basis. This method of analysis is accurate but it is time consuming to extract individual tracks using the single particle-tracking algorithm (Mashanov & Molloy, 2007) developed for this purpose. Tracks need to be identified and cropped so that only behaviour just after interaction between two cells is analysed. In addition, there was potential in this approach for bias in choosing tracks in which migration looked directional. In order to analyse the role of downstream components in Eph-ephrin mediated directional persistence, a more high-throughput method was established.

We decided to use a method that analysed tracks of the whole EphB2-GFP population of the dish simultaneously, independently of any interactions (Fig. 28 B). EphB2-GFP cells were labelled green and mixed with either EphB2 or ephrinB1 cells, labelled red (Fig. 28 B). The experimental conditions were carefully optimised, such as the number of cells plated and the length of time tracks were analysed, in order to provide the largest and most reproducible difference in MSD between EphB2-GFP/ephrinB1 and EphB2-GFP/EphB2 conditions. Cell mixtures were plated at higher density to allow more interactions between cells, and imaged for a shorter time period so as not to include many repeat interactions, allowing a difference to be seen in MSD curves on a population level. At the optimised density, half the green EphB2-GFP population interacted with a red cell at over the course of the time-lapse, but rarely more than once (data not shown). Tracking for 2 hours after plating, with 1 min imaging intervals, gave the largest and most reproducible difference in MSD curves between EphB2-GFP/ephrinB1 and EphB2-GFP/EphB2 conditions, and so this was used for further experiments.

These studies revealed an increase in MSD curves in EphB2-GFP/ephrinB1 mixtures (red line) relative to the EphB2-GFP/EphB2 control (blue line) (Fig. 28 A). The increase in MSD observed on EphB2-ephrinB1 signalling at 57 min, 101μm^2, is about half of that observed when analysing individual interactions (197μm^2, Fig. 27 A). These measurements are from a single experiment but are representative of three independent experiments for each condition. The smaller difference in MSD is expected as whole population analysis underestimates the increase in EphB2-ephrinB1 mediated persistence that occurs on cell contact; analysis of tracks occurs independently of the number or timing of interactions, or the type of cell that the interaction occurs with i.e. EphB2-GFP/EphB2 interactions are not discriminated against. Nevertheless, the increase in MSD observed on EphB2-ephrinB1 signalling using whole population analysis is reproducible across experiments, which suggests that this method can be used as a high throughput estimate of MSD.

Analysis of the shape of tracks was applied to whole population analysis, similar to that done with individual interactions. XY coordinates of EphB2-GFP cell positions over the course of full-length tracks (2 hour) were extracted and the tracks plotted relative to a central start site. 100 tracks were randomly chosen for each condition and it was found that tracks of EphB2-GFP cells in EphB2-GFP/ephrinB1 mixtures (Fig. 28 C) were straighter, indicating that the cells moved more directionally than those in EphB2-GFP/EphB2 mixtures (Fig. 28 D); consequently they were found further from the point of interaction in a given time (Fig. 28 E) and had a greater displacement. A larger number of tracks were plotted than for individual interaction analysis so as to more clearly see a trend above the noise caused by the increased number of “like interactions” that occur with whole population analysis. The same trend in directional movement and increase in displacement are observed for EphB2-GFP/ephrinB1 mixtures compared to EphB2-GFP/EphB2 mixtures with whole population analysis as with analysis of individual interactions.

Figure 28: Whole population analysis of Eph-ephrin mediated cell behaviour

Analysis of EphB2-ephrinB1 mediated changes in cell behaviour on a population level and independent of any collisions.

(A): Tracks of EphB2 cells are analysed in EphB2-GFP/ephrinB1 or EphB2-GFP/EphB2 cell mixtures. The mean squared displacement (MSD) is analysed for each situation over changing time intervals (1 min to 57 min). MSD is greater in EphB2-GFP/ephrinB1 than EphB2-GFP/EphB2 cell mixtures.

(B): EphB2-GFP cells are labelled green and plated with either EphB2 or ephrinB1 cells (red). EphB2-GFP cells are tracked independently of any collisions and the whole tracks analysed using a single particle tracking algorithm, GMimPro.

(C): The XY coordinates of EphB2-GFP cell positions of full length (2 h) tracks in EphB2-GFP/ephrinB1 mixtures are plotted relative to a central start site. 100 tracks are plotted.

(D): The XY coordinates of EphB2-GFP cell positions of full length (2 h) tracks in EphB2-GFP/EphB2 mixtures are plotted relative to a central start site. 100 tracks plotted. Tracks of EphB2-GFP cells after interaction with ephrinB1 cells are straighter (C) than those after interaction with EphB2 cells (D).

(E): Analysis of endpoints positions of tracks of 2 h (coloured crosses), and the root mean square displacement of these (solid lines). EphB2-GFP cells after interaction with ephrinB1 cells (red line) move further from the start than those after interaction with EphB2 cells (blue line).

(F): Turning angle analysis (degrees) of trajectories of cell movement. The likelihood of cells to move straight ahead is analysed by the probability distribution function (PDF) of track turning angles over 5 min overlapping intervals. EphB2-GFP cells after interaction with ephrinB1 cells (red line) are more likely to move in a narrower directional range than those after interaction with EphB2 cells (blue line) that move with a broader range.

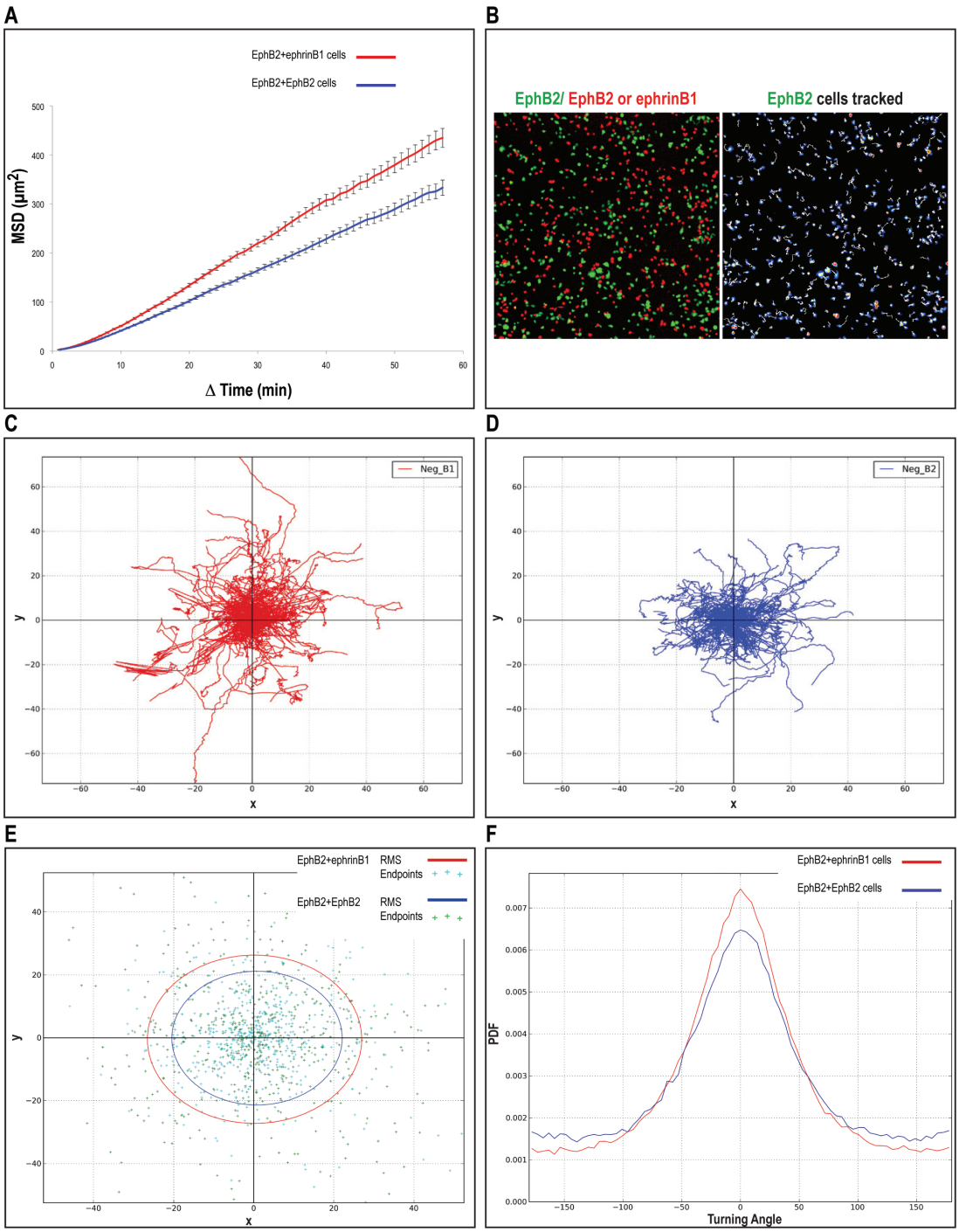
A
EphB2+ephrinB1 cells
EphB2+EphB2 cells
MSD (µm²)
Δ Time (min)
B
EphB2/ EphB2 or ephrinB1
EphB2 cells tracked
C
Neg_B1
D
Neg_B2
E
EphB2+ephrinB1 RMS
Endpoints
EphB2+EphB2 RMS
Endpoints
F
EphB2+ephrinB1 cells
EphB2+EphB2 cells
PDF
Turning Angle

To help separate the effects of speed and persistence, directionality was analysed by calculating the distribution of turning angles of EphB2-GFP tracks. As mentioned previously, turning angle analysis is assumed to be independent of speed. To address this, a range of overlapping time intervals was used to analyse turning angle distributions for full-length (2 hour) tracks of EphB2-GFP cells in both EphB2-GFP/ephrinB1 and EphB2-GFP/EphB2 cell mixtures. Analysis at 1 min intervals suggested that cells are equally likely to move forwards as backwards every minute (Fig. 29). This is likely to be an artifact of the tracking algorithm since cells move with persistent random walk and cannot move directly backwards (DiMilla *et al.*, 1993). However, a trend in turning angle distribution is evident from analysis at 2 min to 10 min intervals (Fig. 29), where a difference is seen between EphB2-GFP/ephrinB1 and EphB2-GFP/EphB2 mixtures. This suggests that these turning angle measurements are independent of noise and speed after 1 min, and as this trend is most distinct at 5 min intervals, this interval was used in future measurements.

EphB2-GFP cells in EphB2-GFP/ephrinB1 mixtures (red line) are more likely to move in a narrower directional range than those in EphB2-GFP/EphB2 mixtures (blue line) (Fig. 28 F). Taken together these results suggest EphB2-GFP cells move more persistently, have straighter tracks and deviate less from a straight line, after interaction with ephrinB1 cells than with EphB2 cells. Since whole population analysis of cell trajectories can provide a more high throughput analysis of the behavioural change seen with EphB2-ephrinB1 signalling, this approach was used to test the role of PCP and PAR polarity components in EphB2-ephrinB1 mediated directional migration.

5.2.2 Knockdown of PCP and PAR proteins cause disruption to Eph-ephrin driven directional migration

In order to understand the role of PCP and PAR polarity in directional migration, whole population analysis of cell behaviour was carried out as previously described. EphB2-GFP cell tracks were analysed simultaneously in EphB2-GFP/ephrinB1 or EphB2-GFP/EphB2 cell mixtures transfected with either siRNA or siCTRL. MSD and turning angle analysis of cell trajectories was carried out in order to help distinguish the role of PCP and PAR polarity in EphB2-ephrinB1 mediated directional persistence.

EphB2-GFP/ephrinB1 or EphB2-GFP/EphB2 cell mixtures transfected with either siRNA or siCTRL were plated and tracked at the same time to provide an internal experimental comparison and minimise any potential variation. Analysis was carried out within an experiment, as there was variation in MSD of different conditions across experimental repeats. However, the trends in any differences in MSD curves between either siCTRL vs. siRNA or EphB2-GFP/ephrinB1 vs. EphB2-GFP/EphB2 cell mixtures across experiments were the same. Differences in MSD were analysed over the largest time intervals analysed i.e. 57 min, and turning angles were calculated from full-length tracks using overlapping 5 min intervals.

Figure 29: Whole population analysis of Eph-ephrin mediated change in turning angle distributions

Analysis of EphB2-ephrinB1 mediated changes in cell behaviour on a population level. Turning angles (degrees) of full-length (2 h) tracks of EphB2-GFP cells are analysed in EphB2-GFP/ephrinB1 or EphB2-GFP/EphB2 cell mixtures. Turning angles are measured using a range of overlapping intervals (1 min to 20 min) and the probability distribution function (PDF) analysed, which represents the likelihood of the cell to continue to move forwards. EphB2-GFP cells after interaction with ephrinB1 cells (blue line) are more likely to move in a narrower directional range than those after interaction with EphB2 cells (green line) that move within a broader range of angles. Analysis at 1 min intervals showed cells to be almost equally likely to move forwards as backwards every minute. The same trend in turning angle distribution is evident from 2 min to 10 min intervals, but becomes less clear from 10 min to 20 min intervals.

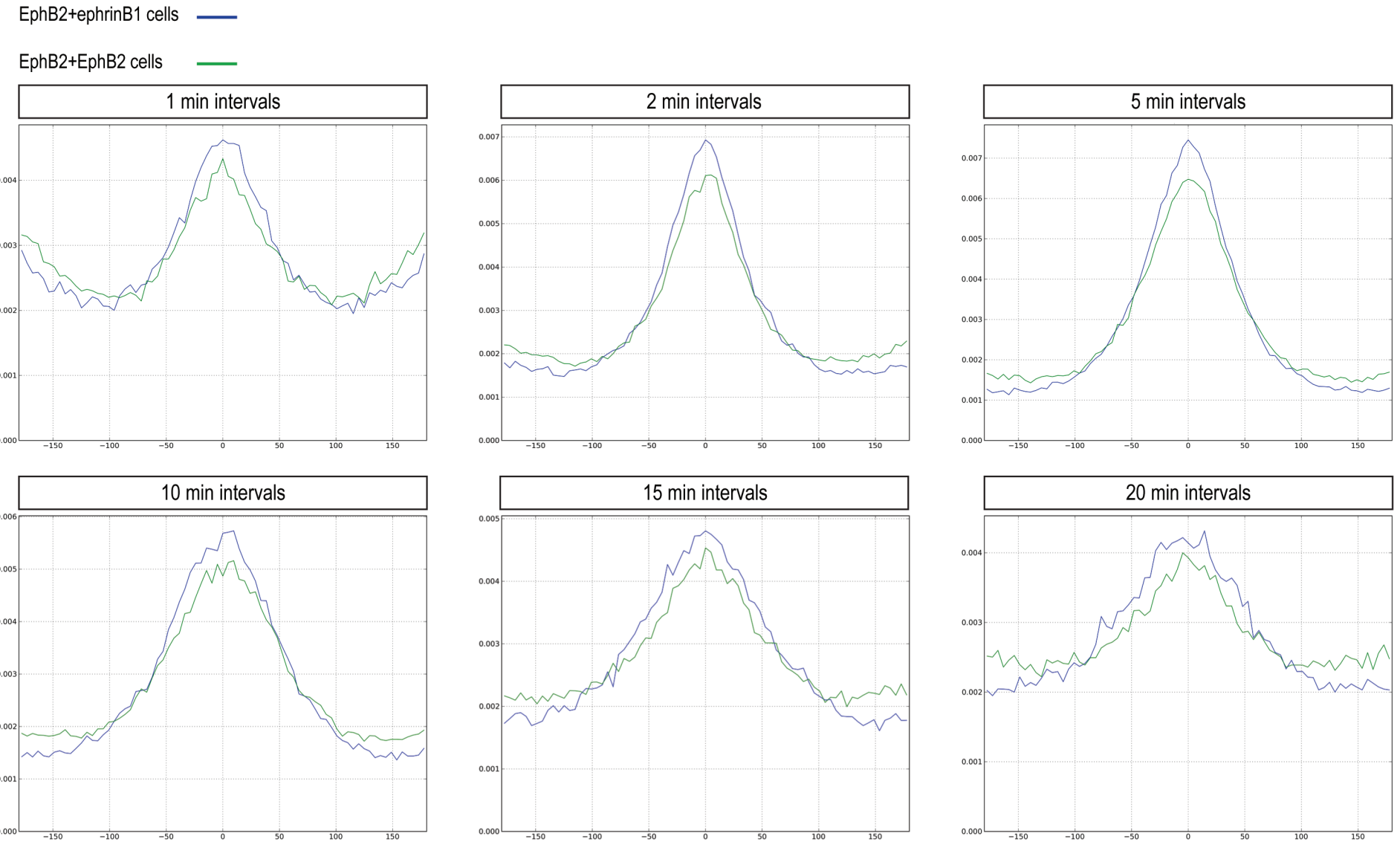
EphB2+ephrinB1 cells
EphB2+EphB2 cells
1 min intervals
2 min intervals
5 min intervals
10 min intervals
15 min intervals
20 min intervals

Results of each siRNA condition are shown of one experiment that is representative of a minimum of three experimental repeats.

If siRNA knockdown affects the ability of EphB2-ephrinB1 signalling to mediate changes in behaviour, then the ratio of EphB2-GFP/ephrinB1 to EphB2-GFP/EphB2 MSD will be reduced for siRNA conditions compared to siCTRL conditions. On the other hand, differences in the siCTRL and siRNA MSD values in EphB2-GFP/EphB2 mixtures would suggest that the basal migratory behaviour of cells is affected in the absence of EphB2-ephrinB1 interactions. The MSD ratio of EphB2-GFP/ephrinB1 to EphB2-GFP/EphB2 was compared for both siCTRL and siRNA conditions, and this relative ratio of endpoints is averaged over a minimum of three experiments. The statistical difference in the relative ratio of endpoints with different siRNA conditions was calculated. Analysis of turning angles and MSD in combination helped distinguish the roles of speed and persistence.

5.2.2.1 Dvl2

Knockdown of Dvl2 reduces the MSD curve for EphB2-GFP/ephrinB1 conditions compared to the siCTRL EphB2-GFP/ephrinB1 condition (Fig. 30 A), but there is no change in the MSD curve for either siCTRL or siDvl2 in the EphB2-GFP/EphB2 condition. This trend is reflected in the endpoint displacements of full length tracks (Fig. 31 A), and there is a reduction in the average MSD ratio of endpoints (at 57 min time intervals) observed when Dvl2 is knocked down compared to the control (Fig. 31 E $p=0.05$). This suggests that knockdown of Dvl2 reduces the displacement induced by EphB2-ephrinB1 signalling, without affecting the general ability of cells to migrate. In addition, the turning angle analysis of trajectories of EphB2-GFP cell movement (Fig. 30 A') reflects the trend seen with MSD curve analysis. On knockdown of Dvl2, a wider distribution of EphB2-GFP turning angles in both EphB2-GFP/ephrinB1 and EphB2-GFP/EphB2 mixtures is seen, similar to EphB2-GFP/EphB2 with siCTRL. This suggests that Dvl2 knockdown can reduce the ability of EphB2-ephrinB1 signalling to induce more directional migration.

5.2.2.2 Daam1

Knockdown of Daam1 does not induce any changes in MSD curves for EphB2-GFP/ephrinB1 or EphB2-GFP/EphB2 conditions, compared to the control (Fig. 30 B), or any differences in the endpoint displacements of full length tracks (Fig. 31 B), so there is no change in the average ratio of MSD endpoints observed (at 57 min time intervals) (Fig. 31 E). In addition, the turning angle analysis of trajectories of cell movement shows no change in the distribution of turning angles of EphB2-GFP/ephrinB1 or EphB2-GFP/EphB2 conditions with siCTRL compared to siDaam1 (Fig. 30 B'). This suggests that Daam1 knockdown does not affect EphB2-ephrinB1 mediated directional migration, or the basal ability of cells to migrate.

Figure 30: Whole population analysis of a change in Eph-ephrin mediated MSD and turning angle distributions on knockdown of PCP and PAR genes

Population level analysis of EphB2-ephrinB1 mediated changes in cell behaviour on a population level with knockdown for different PCP and PAR genes. Tracks of EphB2-GFP cells are analysed simultaneously in both EphB2-GFP/ephrinB1 or EphB2-GFP/EphB2 cell mixtures transfected with either siRNA or siCTRL.

(A-D): The mean squared displacement (MSD) curve is generated for each situation over changing time intervals (1 min to 57 min). MSD plots of a representative experiment for each condition are shown: siDvl2 (A), siDaam (B), siPAR-3 (C), siPAR-6B (D).

(A'-D'): Turning angle analysis of trajectories of cell movement in both EphB2-GFP/ephrinB1 and EphB2-GFP/EphB2 cell mixtures transfected with either siRNA or siCTRL. Turning angles are measured using 5 min time intervals, and probability distribution function (PDF) plots of a representative experiment for each condition are shown.

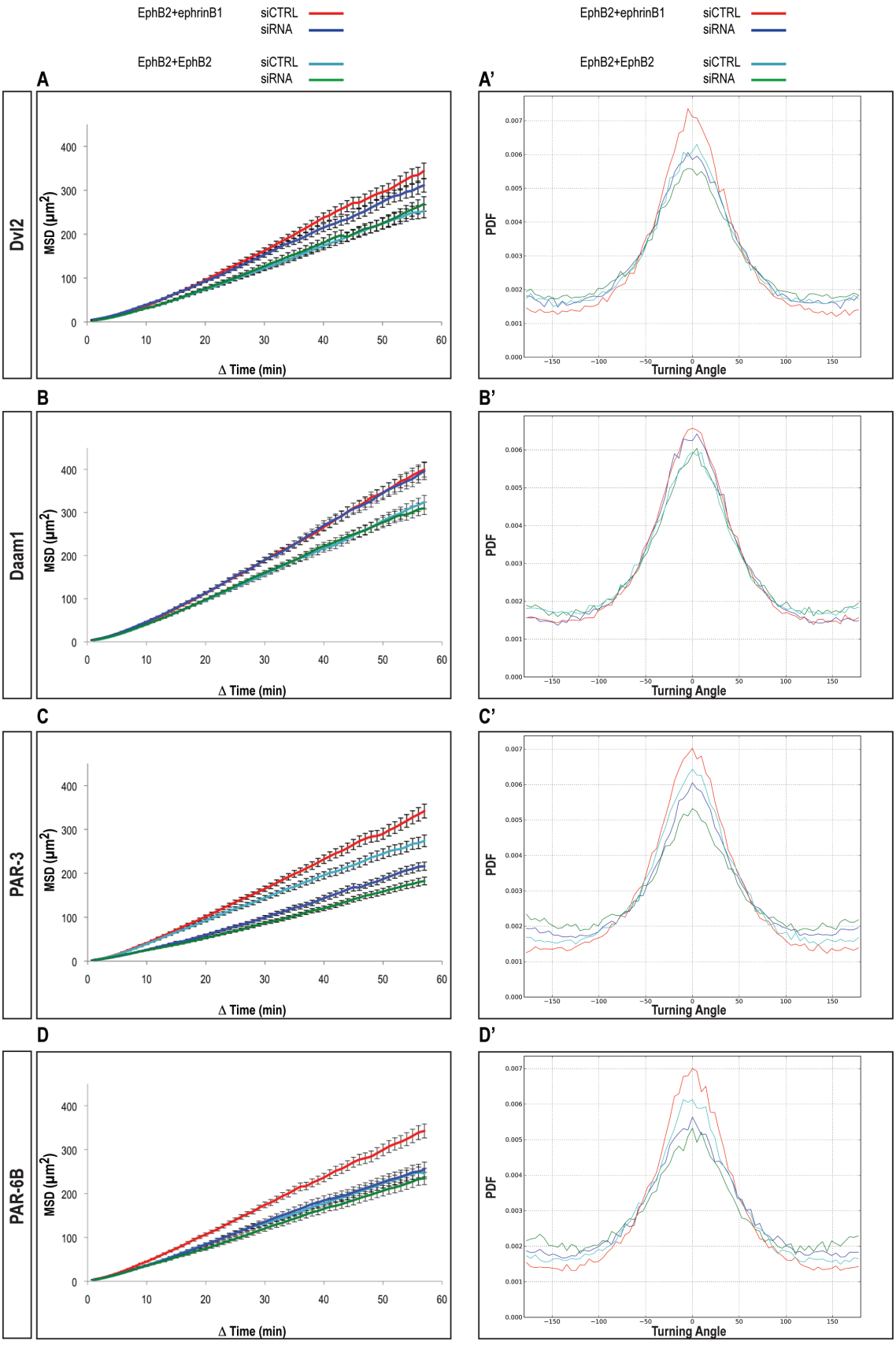
EphB2+ephrinB1
siCTRL
siRNA
EphB2+EphB2
siCTRL
siRNA
A
A'
B
B'
C
C'
D
D'
Dvl2
Daam1
PAR-3
PAR-6B
MSD (µm²)
Δ Time (min)
PDF
Turning Angle

Figure 31: Whole population analysis of a change in Eph-ephrin mediated endpoint displacements on knockdown of PCP and PAR genes

Population level analysis of EphB2-ephrinB1 mediated changes in cell behaviour, with knockdown for different PCP and PAR genes. Tracks of EphB2-GFP cells are analysed simultaneously in both EphB2-GFP/ephrinB1 and EphB2-GFP/EphB2 cell mixtures, transfected with either siRNA or siCTRL.

(A-D): The endpoint coordinates of full length tracks (2 h) are plotted as individual points around a central origin with the root mean square displacement of these as a solid line around the origin. Endpoint plots of a representative experiment for each condition are shown: siDvl2 (A), siDaam (B), siPAR-3 (C), siPAR-6B (D).

(E): Analysis of the relative ratio of MSD measured at 57 min intervals averaged over a minimum of three experiments. The MSD ratio of EphB2-GFP cells in EphB2-GFP/ephrinB1 versus EphB2-GFP/EphB2 mixtures is compared for both siCTRL and siRNA conditions. There is a significant difference between the ratios of siCTRL and siDvl2 ($p=0.05$) and siCTRL and siPAR-6B ($p<0.05$).

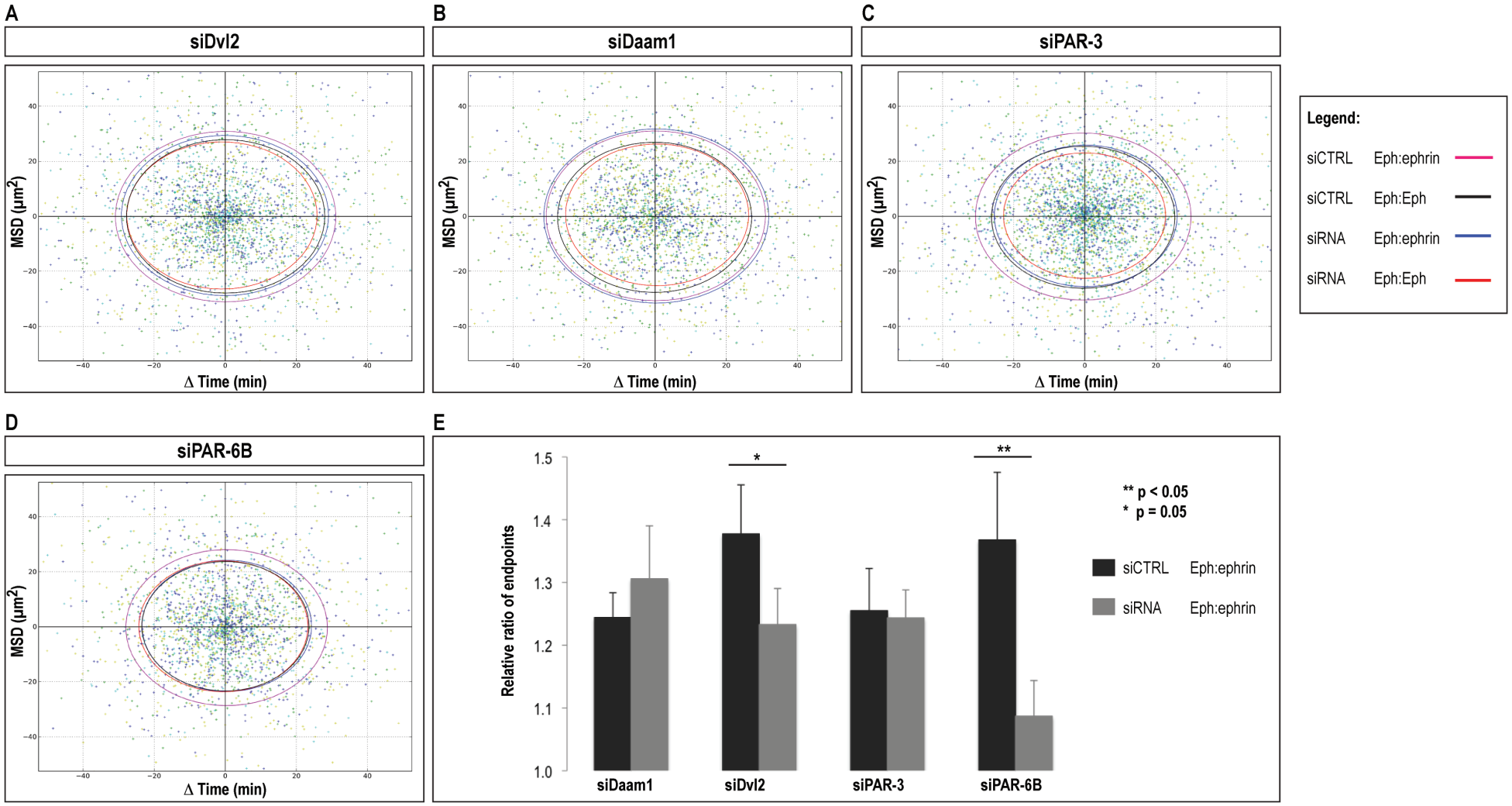
A
siDvl2
B
siDaam1
C
siPAR-3
D
siPAR-6B
E
MSD (µm²)
Δ Time (min)
Legend:
siCTRL Eph:ephrin
siCTRL Eph:Eph
siRNA Eph:ephrin
siRNA Eph:Eph
Relative ratio of endpoints
1.5
1.4
1.3
1.2
1.1
1.0
*
**
** p < 0.05
* p = 0.05
siCTRL Eph:ephrin
siRNA Eph:ephrin
siDaam1
siDvl2
siPAR-3
siPAR-6B

5.2.2.3 PAR-3

Knockdown of PAR-3 induces a decrease in MSD curves for both EphB2-GFP/ephrinB1 and EphB2-GFP/EphB2 mixtures. MSD is much lower than that seen for siCTRL EphB2-GFP/ephrinB1 and EphB2-GFP/EphB2 conditions (Fig. 30 C), suggesting that the basal motility of the EphB2-GFP cells might be affected by the knockdown. This is reflected in the endpoint displacements of full length tracks where the same trend of smaller displacements is seen (Fig. 31 C). There is no change in the average MSD ratio of endpoints observed (at 57 min time intervals) (Fig. 31 E), which suggests that PAR-3 acts independently of EphB2-ephrinB1 signalling to affect migratory behaviour. In addition, the turning angle analysis of trajectories of cell movement reflects the trend seen with MSD curve analysis (Fig. 30 C'), suggesting that PAR-3 knockdown reduces the ability of cells to migrate directionally and this might underlie the decrease in MSD curves seen, but that this mechanism is independent of EphB2-ephrinB1 signalling.

5.2.2.4 PAR-6B

Knockdown of PAR-6B reduces the MSD curve for the EphB2-GFP/ephrinB1 condition compared to the siCTRL EphB2-GFP/ephrinB1 condition (Fig. 30 D), but the MSD curve for the EphB2-GFP/EphB2 condition is unaltered. This trend is reflected in the endpoint displacements of full length tracks (Fig. 31 D), where the average MSD ratio of endpoints (at 57 min time intervals) is reduced on knockdown of PAR-6B compared to the control (Fig. 31 E $p<0.05$). Taken together this suggests PAR-6B knockdown might reduce the displacement induced by EphB2-ephrinB1 signalling, independently of the basal ability of cells to migrate. The turning angle analysis of trajectories of EphB2-GFP cell movement reflects the trend seen with MSD curve analysis (Fig. 30 D'). On knockdown of PAR-6B, a wider distribution of EphB2-GFP turning angles is seen in both EphB2-GFP/ephrinB1 and EphB2-GFP/EphB2 mixtures, similar to EphB2-GFP/EphB2 mixtures with siCTRL. This suggests that that PAR-6B knockdown can reduce the ability of EphB2-ephrinB1 signalling to induce more directional migration.

5.3 DISCUSSION

Analysis of individual interactions between EphB2/ephrinB1 and EphB2/EphB2 cells show that EphB2 cells move more directionally after interaction with ephrinB1 cells, and that this is caused by an increase in the persistence of migration (Alexei Poliakov, unpublished data, Fig. 27). The PCP and PAR polarity pathways are likely candidates to act downstream of EphB2-ephrinB1 signalling in the directional persistence of migration, as components of these pathways have been linked to EphB2-ephrinB1 mediated cell segregation and boundary formation (Chapter 4). A high-throughput method of analysing cell behaviour was established in order to analyse EphB2-ephrinB1 mediated cell behaviour and test the role of these components in EphB2-ephrinB1 mediated directional persistence.

5.3.1 Whole population analysis of cell trajectories provides a high throughput method of analysis of cell behaviour

5.3.1.1 Eph-ephrin signalling causes an increase in directional persistence of migration

Whole population analysis of cell mixtures has shown EphB2-GFP cells to move more directionally and have a higher displacement in EphB2-GFP/ephrinB1 than EphB2-GFP/EphB2 cell mixtures (Fig. 28). MSD curve analysis has shown an overall increase in endpoint displacement, which is also reflected in the analysis of endpoint coordinates, and a narrower turning angle distribution induced on EphB2-ephrinB1 signalling. This suggests that EphB2-ephrinB1 signalling causes an increase in the displacement of cells, which is due to a more directional migration seen even over short time intervals during turning angle analysis (Fig. 29). This directional movement is maintained over time, as seen by the coordinates of individual tracks, which are straighter for EphB2-GFP/ephrinB1 mixtures (Fig. 28 C) than EphB2-GFP/EphB2 (Fig. 28 D). This suggests that EphB2-ephrinB1 signalling induces directional migration, and the maintenance or persistence of this is responsible for the greater increase in displacement seen. We suggest that these changes in cell behaviour might underlie the segregation and boundary sharpening responses observed in the other assays.

5.3.1.2 Experimental limitations

It was difficult to compare MSD datasets of the same condition across experimental repeats in order to determine the significance of any change in behaviour seen. The MSD measurements obtained varied slightly from day to day and this could be due to a number of factors: temperature of the imaging chamber, age of cells, variation in siRNA transfection, density of cells plated, and the time that cells were allowed to settle before imaging. These conditions were standardised and control conditions were always imaged in parallel with siRNA conditions to provide an internal experimental comparison.

Previous analysis of cell behaviour in our cell lines has shown substantial variability in the cell responses between EphB2 cells and ephrinB1 cells (Poliakov *et al.*, 2008). This is thought to be due, at least in part, to the number of contacts EphB2 cells have made with ephrinB1 cells as repeated activation and endocytosis of receptor (Marston *et al.*, 2003; Zimmer *et al.*, 2003) decreases the steady-state level of cell surface EphB2 (Alexei Poliakov, unpublished data). At the optimised cell density used for whole population analysis, half the green EphB2-GFP population interacted with a red cell at least once over the course of the time-lapse with few repeat interactions (data not shown), but variation in the number of interactions could cause variation in the MSD across experiments.

In addition, variation was introduced due to the whole population approach of analysis used. The trajectories of all tracks were analysed independently of the number of, or time of, interaction with another cell i.e. tracks were not analysed immediately after interaction, as in the individual cell behaviour analysis. For example, in EphB2-GFP/ephrinB1 mixtures, all tracks of green EphB2 cells were analysed; analysis included interactions with ephrinB1 cells or with other EphB2-GFP cells, as well as tracks of cells not moving or not adhered to the dish. Whole population analysis is therefore an underestimate of the increase in EphB2-ephrinB1 mediated persistence and comparisons were therefore always made to EphB2-GFP/EphB2 mixtures in order to assess any relative change seen. However, the trends observed in MSD curves, turning angle distributions and endpoints using whole population analyses, were consistent across experimental repeats. Comparisons were made between experimental conditions by comparing trends in data defined by a minimum of three experimental repeats.

5.3.1.3 Separating the roles of speed and persistence in MSD

MSD is proportional to the displacement of cells, defined by the straight-line distance between the start and endpoint coordinates in a specified time interval (DiMilla *et al.*, 1993; Harms *et al.*, 2005). As discussed previously, a change in displacement could be caused by an increase in either speed or persistence or both. This has been shown by migration studies in different contexts in which removal of different cell polarity components causes a decrease in the persistence of cell migration either independently of speed (Pegtel *et al.*, 2007), or with an increase in speed (LaMonica *et al.*, 2009). Previous studies have demonstrated the advantages of fitting MSD curves to the persistent random walk function in order to identify values for speed and persistence (Martens *et al.*, 2006). This was not possible for the MSD values obtained from whole population analysis. Because there was so much variability within the population of cells we were analysing, the MSD plots were more similar to a straight line than the curve normally seen for persistent random walk, and the fitting was therefore inaccurate.

As MSD is a function of speed and persistence, measuring instantaneous speed would allow the contribution of persistence in MSD to be determined. It is important to measure speed independently of any directional movement, but instantaneous speed has proved difficult to measure accurately. Instantaneous speed is estimated from the displacements of the smallest time intervals that accurately measure the actual distance a cell travels in the given time. We calculated it using 1 min and 5 min intervals in our system. Speed measured over too small an interval will also be inaccurate as it is likely to measure internal movements of the cell centroid or fluctuations in the levels of tracker dye, instead of actual migration. Speed measured over too large a time interval will be inaccurate, as it will be based on displacement rather than the actual distance that the cell has travelled. In this case, speed measured over 5 min intervals could be an overestimate, but this is unlikely due to the resolution of the system; 1 min measurements give an average displacement of one third of a pixel and so speed measurements using this interval are likely to be inaccurate, whereas 5 min displacements are 1 pixel and are likely to be a real

estimate of speed. A ratio increase in speed of 1.06 for 1 min and 1.07 for 5 min intervals of EphB2-GFP/ephrinB1 to EphB2-GFP/EphB2 mixtures (averaged over three experimental repeats) was measured, and even though these measurements do not differ greatly, the 5 min interval measurement is likely to be more accurate. It is important to note that the speed does not seem to change significantly between EphB2-GFP/ephrinB1 and Eph-B2-GFP/EphB2 mixtures.

To help separate further the effects of speed and persistence, directionality was analysed by calculating the distribution of turning angles over a range of time intervals. Analysis at 1 min intervals showed cells to be equally likely to move forwards as backwards (Fig. 29), which suggests these measurements contain an element of noise since as cells move with persistent random walk they cannot move directly backwards (DiMilla *et al.*, 1993). Recent studies have also recognised fluctuations in the directionality of migrating cells when tracking using short time intervals (Uetrecht & Bear, 2009). This is likely to reflect the fact that cells are moving slowly, and slight inaccuracies in tracking could result in significant fluctuations in the calculated current direction of movement. However, a trend in differences in turning angle distributions between EphB2-GFP/ephrinB1 to EphB2-GFP/EphB2 mixtures is evident from 2 min to 10 min intervals (Fig. 29). The trend is most distinct at 5 min intervals and so we assume that turning angle distributions at 5 min intervals represent a measurement of directionality independent of noise and speed. It is important to note that we assume persistence and speed can be measured independently, but this may not be the case.

Taken together this evidence argues that displacement or turning angles at 5 min intervals are representative of actual cell movements. However, it is not known whether the 1.07 fold increase in speed seen between EphB2-GFP/ephrinB1 and Eph-B2-GFP/EphB2 mixtures is significant i.e. whether EphB2-GFP cells move faster after interaction with ephrinB1 cells than EphB2 cells. This trend is consistent between experiments and so raises the question of whether the 1.07 fold difference in speed between EphB2-GFP/ephrinB1 and Eph-B2-GFP/EphB2 mixtures in 5 min intervals can account for the overall 1.3 fold increase in MSD seen over 57 min intervals (Fig. 28 A). Using the formula that defines MSD (DiMilla *et al.*, 1993; Martens *et al.*, 2006), we determined that a 1.07 fold increase in speed at 5 min intervals can only account for a 1.15 fold increase in MSD at 57 min intervals. This suggests that even if there is a slight difference in speed after EphB2-GFP/ephrinB1 collisions compared to Eph-B2-GFP/EphB2 collisions, this does not account for the overall increase in displacement seen over longer time intervals (1.3 fold increase), and further suggests a role for directional persistence in increasing the displacement seen after EphB2-ephrinB1 signalling.

We suggest that whole population analysis of cell trajectories can provide a more high throughput analysis of the behavioural change seen on EphB2-ephrinB1 signalling, and has strengths in identifying changes in either MSD or persistence on a population level. However this method has limitations in further dissecting the role of various mechanisms underlying changes in cell behaviour, due to some inaccuracy in precisely

measuring parameters such as speed and persistence. An improved method of analysis would involve higher resolution whole population analysis or analysis of cell behaviour after individual cell-cell interactions.

5.3.2 Predicting trends in MSD and turning angle distributions when varying speed and persistence

Even though EphB2-ephrinB1 signalling induces an increase in MSD curves due to an increase in directional persistence independently of speed, knockdown of PCP or PAR polarity components could affect MSD curves due to changes in speed or persistence, or both. Given the assumption that 5 min interval analysis of turning angles represents a measurement of directionality independent of noise and speed, we can predict how varying speed and persistence in our system would affect trends in endpoint displacement and turning angle distributions. The analysis of these scenarios helps to understand changes seen in knockdown situations.

1. Same speed, different persistence.

If speed is the same between two conditions and persistence is changed, then over short time intervals the displacement will be unchanged. Endpoint displacements would vary however, and cells with a higher persistence will have a higher displacement. We would expect the cells that have a greater persistence to have a greater MSD and narrower turning angle distribution.

2. Same persistence, different speed.

If persistence is the same between two conditions and speed is changed, then over short time intervals faster cells will have a greater displacement, as they will travel a further distance in a given time. Endpoint displacements would also vary and cells with a greater speed will have a higher displacement. We would expect no difference in turning angle distributions between conditions, but faster cells would have a greater MSD.

3. High persistence with low speed, low persistence with high speed.

Cells with high persistence and low speed will have a smaller displacement over short time intervals than cells with low persistence and high speed, as only speed affects displacement over short time intervals. Over longer time intervals, the endpoint displacements could be similar as high speed could compensate for low persistence and vice versa. We would expect a difference in turning angle distributions between conditions due to a difference in persistence between the two situations, but MSD curves could be similar.

Analysis of these situations demonstrates the importance of using analysis of MSD in combination with turning angle distributions, as analysis of only MSD does not reveal changes in the underlying cell

behaviour. A change in turning angle distribution would suggest an underlying change in persistence, whereas a change in MSD could be due to a change in speed or persistence. Analysis of both turning angles and MSD together helps distinguish the changes in speed or persistence.

5.3.3 The role of PCP and PAR polarity in Eph-ephrin induced directional persistence of migration

Combined analysis of MSD and turning angle distributions allowed the roles of PCP and PAR polarity components in EphB2-ephrinB1 induced directional migration to be determined. A specific effect of an siRNA knockdown on EphB2-ephrinB1 mediated changes in behaviour is seen by a reduction in the MSD ratio of EphB2-GFP/ephrinB1 to EphB2-GFP/EphB2 conditions compared to siCTRL conditions. However, it is important that the MSD of the siRNA EphB2-GFP/EphB2 condition is no different to the siCTRL EphB2-GFP/EphB2 condition. A change in the MSD curve of EphB2 cells in the absence of ephrinB1 signalling would suggest that the general ability of the cells to migrate is affected and that the siRNA-mediated change in MSD is not EphB2-ephrinB1 specific. Affecting general migration may mask any EphB2-ephrinB1 mediated changes in behaviour, so the results need to be interpreted carefully.

Knockdown of either Dvl2 or PAR-6B reduces the ability of cells to migrate directionally since turning angle distributions are wider and MSD over long time intervals is reduced (Fig. 30 A-A', D-D'). Both changes are specific to EphB2-GFP/ephrinB1 cell mixtures and there is no change induced by knockdown in the EphB2-GFP/EphB2 mixtures compared to the siCTRL. In addition, there is a reduction in the average MSD ratio of endpoints when Dvl2 or PAR-6B is knocked down compared to the control (Fig. 31 E $p=0.05$, $p<0.05$ respectively). Taken together this suggests that both Dvl2 and PAR-6B knockdown can reduce the ability of cells to migrate with EphB2-ephrinB1 mediated directional persistence. The possible mechanisms by which Dvl2 and PAR-6B might mediate EphB2-ephrinB1 induced directional persistence will be discussed further in Chapter 6.

Knockdown of Daam1 has no effect on MSD in either EphB2-GFP/ephrinB1 or EphB2-GFP/EphB2 mixtures (Fig. 30 B), or the average MSD ratio of endpoints observed compared to the control (Fig. 31 E). Previous work has shown knockdown of Daam1 to increase both the randomness and speed of migration with Daam1 knockdown cells showing multiple protrusions (LaMonica *et al.*, 2009). It is therefore possible that if persistence is reduced, an increase in speed could account for the same difference in MSD seen. This is not the case, as Daam1 knockdown has no effect on turning angle distributions in either EphB2-GFP/ephrinB1 or EphB2-GFP/EphB2 mixtures (Fig. 30 B'). This suggests that Daam1 knockdown does not affect EphB2-ephrinB1 mediated directional migration, and is a surprising result given that Daam1 knockdown has a strong effect on EphB2-ephrinB1 mediated cell segregation and boundary sharpening (Fig. 18 B, 20 B). Daam1 must therefore mediate these effects through a mechanism independent of

EphB2-ephrinB1 mediated directional migration and speed. It is known that there are two branches to the PCP pathway downstream of Dishevelled that lead to activation of RhoA via Daam1, or Rac1 independently of Daam1 (reviewed in (Gao & Chen, 2010)). Differing roles of the different branches of the PCP pathway in either EphB2-ephrinB1 mediated behaviour or general cell motility could explain the differences seen on knockdown of Dvl2 compared to Daam1. However, this fails to explain why a weaker phenotype is seen for Dvl2 than Daam1 in the segregation and boundary assays if Dvl2 is acting in multiple pathways. This will be discussed further in Chapter 6.

PAR-3 knockdown affects the general motility of cells as the MSD is reduced for both EphB2-GFP/ephrinB1 and EphB2-GFP/EphB2 mixtures compared to the siCTRL conditions (Fig. 30 C). The same trend is seen for the turning angle analysis, which shows distributions that are broader for the knockdown situation compared to the siCTRL conditions for both EphB2-GFP/ephrinB1 and EphB2-GFP/EphB2 mixtures (Fig. 30 C'), and suggests that PAR-3 knockdown cells migrate more randomly. PAR-3 can function with aPKC/Tiam1 at the LE of migrating keratinocytes, to stabilise front–rear polarisation via the microtubule system and activation of Rac1 at the LE (Pegtel *et al.*, 2007). This suggests that knockdown of PAR-3 could affect the basal migratory behaviour of cells in an EphB2-ephrinB1 independent manner, as there is no change in the MSD ratio of endpoints observed (Fig. 31 E). There is evidence that PAR-3 and PAR-6 can act independently and be functionally and spatially separate in the formation and maintenance of front-rear polarity (Goldstein & Macara, 2007), which could explain the differences in MSD seen on knockdown of PAR-3 and PAR-6B; for example PAR-3/TIAM1/aPKC mediates stable front–rear polarisation in keratinocytes (Pegtel *et al.*, 2007) and PAR-6/aPKC is active at the LE of astrocytes (Etienne-Manneville & Hall, 2001; Etienne-Manneville & Hall, 2003). We suggest that PAR-6B knockdown can reduce the ability of cells to migrate with EphB2-ephrinB1 mediated directional persistence, but PAR-3 might function in the general ability of cells to migrate with persistent random walk, independently of EphB2-ephrinB1 signalling.

Taken together these results suggest that the increase in MSD seen on EphB2-ephrinB1 signalling is due to an increase in the persistence of migration, which is likely to be mediated through Dvl2 and PAR-6B. There is evidence that the PCP pathway can cooperate with the PAR complex to promote directional migration (Schlessinger *et al.*, 2007; Zhang *et al.*, 2007), and this will be discussed in Chapter 6, but further work needs to be done to identify the roles of these polarity components downstream of EphB2-ephrinB1 signalling and establish whether they act in the same pathway or synergistically. In addition, the possible roles of other PCP and PAR components, Daam1 and PAR-3, independent of EphB2-ephrinB1 mediated directional migration, need to be further addressed.

6 CONCLUDING PERSPECTIVES

6.1 The role of PCP and PAR polarity in EphB2-ephrinB1 induced directional persistence of migration and boundary sharpening

Studies by Alexei Poliakov in the Wilkinson laboratory (unpublished) have shown that interaction with ephrinB1 cells leads to increased directional persistence of EphB2 cells. Furthermore, computer simulations have suggested that directional persistence can in principle contribute to cell segregation. This raised the question of which pathways downstream of EphB2 activation underlie cell segregation and boundary sharpening, as some of these were therefore likely to contribute to directional persistence. Previous work suggested a role of PCP and PAR polarity components in EphB2-ephrinB1 mediated cell segregation (Jorgensen *et al.*, 2009; Tanaka *et al.*, 2003). Quantitative analysis of EphB2-ephrinB1 mediated cell behaviour in a number of *in vitro* assays, developed for this purpose, showed Dvl2, Daam1, PAR-3 and PAR-6B to be required for EphB2-ephrinB1 mediated cell segregation and boundary sharpening.

In order to determine whether EphB2-ephrinB1 mediated directional persistence underlies cell segregation and boundary sharpening, the role of these PCP and PAR genes in EphB2-ephrinB1 mediated directional persistence was analysed. Both Dvl2 and PAR-6B knockdown reduces the ability of cells to migrate with EphB2-ephrinB1 mediated directional persistence, which suggests that Dvl2 and PAR-6B act downstream of EphB2-ephrinB1 signalling in a specific manner and independently of basal cell motility. It is therefore likely that Dvl2 and PAR-6B mediate cell segregation and boundary sharpening through EphB2-ephrinB1 mediated directional persistence. Daam1 knockdown has no effect, which suggests that Daam1 does not mediate directional persistence, and PAR-3 knockdown affects the basal motility of cells independently of EphB2-ephrinB1 mediated directional migration. The potential roles and interactions of these polarity components are further discussed below.

6.2 EphB2-ephrinB1 signalling mediates a collapse and repulsion response that could underlie directional persistence of migration

Directional persistence is increased on contact of EphB2 cells with ephrinB1 cells (Fig. 27, 28), and it is likely that polarity underlies this directional migration. We suggest that this is initiated at the site of interaction, causing repolarisation of the cell with subsequent stabilisation of this polarity that leads to persistence of migration. Previous evidence to support a contact-based repolarisation model comes from

work that identified a repulsion response to EphB2-ephrinB1 signalling, in which cell processes collapse and the cells round up (Fig. 5) (Poliakov *et al.*, 2008).

Additional evidence has suggested that Eph-ephrin induced contact inhibition of locomotion (CIL) underlies the repulsion and collapse response seen at the site of contact between EphA-ephrinA or EphB2-ephrinB1 prostate cancer cells (Astin *et al.*, 2010). Localised RhoA activation and Rac1 inhibition at the leading edge (LE) of two interacting cells has been shown to cause membrane withdrawal and collapse at the front with the loss of leading lamella, so inhibiting forward migration (Astin *et al.*, 2010; Miao *et al.*, 2005; Nakayama *et al.*, 2008). This allows the generation of a new protrusion away from the site of contact and cell repolarisation (Mayor & Carmona-Fontaine, 2010). The repolarisation of the cell and the stabilisation of leading lamellipodia, that maintain the orientation of movement, are important in maintaining persistence (Harms *et al.*, 2005).

The level and localisation of Rac1 activity are important for the formation and orientation of lamellipodia (Pankov *et al.*, 2005). High levels of cellular Rac1 promote the formation of peripheral lamellae during random migration, while lower but localised levels of active Rac1 suppress peripheral lamellae and favour the formation of lamellae only at the LE, so contributing to the polarisation of migrating cells (Pankov *et al.*, 2005). Persistence usually depends on the orientation of cell protrusions, and once Rac1 is active numerous feedback loops help to maintain directional protrusions (Ridley *et al.*, 2003). Rho GTPases can regulate each others activity; Rac1 and RhoA can mutually antagonise each other (Iden & Collard, 2008; Nakayama *et al.*, 2008; Nobes & Hall, 1995), so the temporal and spatial balance of these activities helps maintain the front-rear polarity required for cell migration, with Rac1 activated at the LE and RhoA activated at the trailing edge (TE) (Ridley *et al.*, 2003).

It is likely that EphB2-ephrinB1 induced directional persistence is mediated by recruitment of PCP or PAR proteins to the site of contact between EphB2- and ephrinB1-expressing cells, causing the transient and localised activation of RhoA or inhibition of Rac1. How these pathways cause cell repolarisation and the stabilisation of lamellipodia is not known. The question remains as to how EphB2-ephrinB1 activation leads to an increase in directional persistence.

6.3 Distinct roles of PAR-6B and PAR-3

The PAR complex couples with Rho GTPase activity to polarise the nucleus, centrosome and LE along the front-rear axis (Etienne-Manneville & Hall, 2001), the stability of which correlates with the extent of directional cell movement (Iden & Collard, 2008). The asymmetric localisation of the PAR proteins and Rho GTPases to the LE plays a crucial role in this; for example, PAR-3/Tiam1 associates with the PAR-6/aPKC complex (Nishimura *et al.*, 2005; Shi *et al.*, 2003), triggering localised Rac1 activation, lamellipodia formation and actin reorganisation (Mertens *et al.*, 2006; Pegtel *et al.*, 2007).

As PAR polarity proteins serve as spatial and temporal cues in initiating polarity, it is likely that they function in mediating EphB2-ephrinB1 induced repolarisation relative to the site of contact between two cells. Both PAR-3 and PAR-6B are required for EphB2-ephrinB1 mediated cell segregation and boundary sharpening (Fig. 19, 21), but their roles in EphB2-ephrinB1 mediated directional persistence differ. PAR-6B knockdown reduces the ability of cells to migrate with EphB2-ephrinB1 mediated directional persistence, independently of general motility, whereas PAR-3 knockdown affects the general ability of cells to migrate, independently of EphB2-ephrinB1 signalling (Fig. 30). This suggests that PAR-3 is not required for directional persistence and could have a different role downstream of EphB2-ephrinB1 signalling. We therefore suggest that PAR-3 and PAR-6B have distinct functions.

6.3.1 A suggested role for PAR-6B in EphB2-ephrinB1 mediated directional persistence

There is evidence that PAR-6 can act independently from PAR-3 in the formation and maintenance of front-rear polarity (Goldstein & Macara, 2007), for example PAR-3/Tiam1/aPKC mediates stable front–rear polarisation in keratinocytes (Pegtel *et al.*, 2007) and PAR-6/aPKC is active at the LE of astrocytes (Etienne-Manneville & Hall, 2001; Etienne-Manneville & Hall, 2003). It is likely that PAR-6B acts independently of PAR-3 in our assay and plays a specific role in EphB2-ephrinB1 mediated directional persistence, and we propose that the PAR-6B/aPKC complex is localised at the LE of migrating EphB2 cells, to activate Rac1 and stabilise lamellipodia protrusions.

Recent evidence has identified that PAR-6B is de-phosphorylated in EphB2 cells on interaction with ephrinB1 cells (Jorgensen *et al.*, 2009). It is thought that phosphorylation of PAR-6B is required for its activation (Ogawa *et al.*, 2009) and so de-phosphorylation by EphB2-ephrinB1 signalling would inactivate PAR-6B. We therefore propose a role for EphB2-ephrinB1 signalling in the inactivation of the PAR complex at the site of contact between an EphB2- and ephrinB1-expressing cell. This would cause the LE of both of these cells to be inhibited, as removal of the mechanism of Rac1 activation causes de-repression of RhoA activation and collapse of protrusions. This would allow a new LE to form away from the point of contact. This model suggests that the role of PAR-6B in EphB2-ephrinB1 mediated directional persistence could also underlie the disruption to cell segregation and boundary formation seen on knockdown of PAR-6B (Fig. 19, 21).

6.3.2 A suggested role for PAR-3 in general cell motility

PAR-3 knockdown affects the general motility of cells as the MSD is reduced for both EphB2-GFP/ephrinB1 and EphB2-GFP/EphB2 mixtures (Fig. 30 C). The turning angle analysis shows distributions that are broader for PAR-3 knockdown (Fig. 30 C') and so we suggest that the differences in

MSD are due to defects in the ability of cells to move with the basal directionality required for persistent random walk. This is independent of EphB2-ephrinB1 induced directional migration as there is no change in the MSD ratio of endpoints observed (Fig. 31 E), suggesting that PAR-3 knockdown cells have a directional persistence response to EphB2 activation.

PAR-3 has been shown to localise at cell-cell contacts instead of the LE in wound-induced migrating cells (Etienne-Manneville & Hall, 2001; Schmoranzer *et al.*, 2009). However, knockdown of PAR-3 did not affect the localisation of junctional markers, such as N-cadherin and ß-catenin, suggesting no role in adhesion between cells (Schmoranzer *et al.*, 2009), although PAR-3 and Tiam1 have been shown to localise with E-cadherin at cell contacts (Georgiou & Baum, 2010; Malliri *et al.*, 2004). Instead, a possible role of PAR-3 is to tether microtubules at sites of cell contacts, as PAR-3 associates with dynein, to maintain a central position of the centrosome at the cell centre (Schmoranzer *et al.*, 2009). The tension created could position the centrosome or allow microtubules to resist forces that might otherwise displace the centrosome from the cell centre. Contacts therefore act as spatial markers to orientate the centrosome/nucleus axis towards the LE, similar to the orientation caused by the presence of N-cadherin at cell contacts in collective migration (Dupin *et al.*, 2009; Theveneau *et al.*, 2010). The loss of PAR-3 causes a loss of directionality of migration at the wound edge (Schmoranzer *et al.*, 2009). PAR-3 and dynein mediate their effects at cell-cell contacts independently of PAR-6/aPKC, due to the fact that both PAR-6 and dynein interact with the PDZ1 domain of PAR-3, so the interaction of PAR-3 with dynein and PAR-6 is mutually exclusive (Schmoranzer *et al.*, 2009).

In the cell segregation and boundary formation assays, PAR-3 is required for EphB2-ephrinB1 mediated cell segregation and boundary sharpening (Fig 19, 21). In these high-density cultures, we suggest that the role of PAR-3 could be to coordinate polarity cues from cell-cell contacts to the microtubules and polarise the intracellular axis. On knockdown of PAR-3, the ability of cells to migrate relative to each other is reduced and this could cause a disruption to the segregation of EphB2- and ephrinB1-expressing cells, independently of EphB2-ephrinB1 signalling.

Cells at a wound edge polarise the Golgi to face the direction of migration, yet some freely migrating cells do not. Recent evidence has shown that the Golgi position relative to the nucleus remains fairly constant over time but is independent of the direction of migration, suggesting cells have the ability to maintain internal organisation independent of peripheral structures, such as the LE (Uetrecht & Bear, 2009). Freely migrating cells lack junctional input, which could result in the uncoupling of Golgi-nucleus positioning from peripheral events (Uetrecht & Bear, 2009). In radially migrating zebrafish neurons, the centrosome does not persistently lead the nucleus in the direction of migration. The centrosome passes the nucleus during the preparatory phase of nuclear movement, but with each forward migratory step the nucleus passes the centrosome (Distel *et al.*, 2010). Our tracking studies have a low cell density and so internal cell

organisation is uncoupled from peripheral events, but PAR-3 must play a role in maintaining this organisation to allow migration, as on knockdown the ability of cells to migrate is clearly reduced.

PAR-3 is known to play a role in the front-rear stabilisation of freely migrating cells by stabilising microtubules towards the LE (Pegtel *et al.*, 2007). Knockdown of PAR-3, normally localised with aPKC to the LE of freely migrating keratinocytes, decreases the activity of Rac1 and decreases the persistence of cell migration independently of speed (Pegtel *et al.*, 2007). Our data also shows that knockdown of PAR-3 leads to a decrease in the persistence of EphB2 cells (Fig. 30 C'). The recruitment of PAR-3/aPKC to the LE may therefore play a crucial role in the general ability of cells to migrate in our system by activating Rac1 and stabilising microtubules, and the localisation of PAR-3 may be due to extracellular cues, such as the adhesion signal from integrins and Cdc42 (Nakayama *et al.*, 2008), instead of EphB2-ephrinB1 signalling.

Recent evidence has identified that PAR-3 is phosphorylated in EphB2 cells on interaction with ephrin cells (Jorgensen *et al.*, 2009). It is known that at the TE of migrating cells, the Rho effector ROCK can phosphorylate PAR-3 (in its aPKC-binding region), which disrupts the association of PAR-3/aPKC/PAR-6 complex and prevents Rac1 activation at the TE (Nakayama *et al.*, 2008). We propose that phosphorylation of PAR-3 by EphB2-ephrinB1 signalling could lead to its inactivation, but as our data suggests PAR-3 is not required for directional persistence downstream of EphB2-ephrinB1 signalling (Fig. 30), this phosphorylation is likely to play a role in another process downstream of EphB2-ephrinB1 signalling.

Taken together, these results suggest a role for PAR-3 in maintaining the internal polarity of cells caused by the presence of contacts at high cell density, and in maintaining the intrinsic internal polarity of cells important for cell migration. In addition it is likely that at lower cell density and when PAR-3 is not present at cell-cell contacts, PAR-3 might function instead at the LE of migrating cells in specifying directionality. We suggest that these roles are independent of EphB2-ephrinB1 signalling, but that on contact between an EphB2- and ephrinB1-expressing cell, EphB2-ephrinB1 signalling could cause the disruption of the PAR-3/aPKC/Tiam1 complex and reduction in Rac1 activation, to facilitate more efficient repolarisation. More work is required to understand the role of EphB2-ephrinB1 mediated phosphorylation of PAR-3 in directional cell migration.

6.4 Distinct roles of Daam1 and Dvl2

PCP components, including Dishevelled, have been shown to be required for Eph-ephrin independent (basal) CIL in neural crest migration (Fig. 7 A) (Carmona-Fontaine *et al.*, 2008). Accumulation of PCP components and local RhoA activation at the site of cell-cell contact causes lamellipodia inhibition, cell repolarisation and initiation of migration away from sites of cell-cell contact (Carmona-Fontaine *et al.*,

2008; De Calisto *et al.*, 2005; Matthews *et al.*, 2008; Mayor & Carmona-Fontaine, 2010). It is therefore likely that PCP components play a role in EphB2-ephrinB1 mediated directional persistence by activating RhoA at the site of contact and initiating a repulsion response.

Both Dvl2 and Daam1 are required for EphB2-ephrinB1 mediated cell segregation and boundary sharpening (Fig 18, 20), but whereas Dvl2 knockdown specifically reduces the ability of cells to migrate with EphB2-ephrinB1 mediated directional persistence, Daam1 knockdown has no effect (Fig. 30). This suggests that Daam1 functions independently of EphB2-ephrinB1 mediated directional persistence but plays a role in EphB2-ephrinB1 mediated cell segregation and boundary sharpening, and that Dvl2 functions independently of Daam1 in EphB2-ephrinB1 mediated directional persistence.

Dishevelled is known to play key roles in both the canonical and non-canonical Wnt pathway, whereas the role of Daam1 is specific to the non-canonical Wnt pathway (Boutros & Mlodzik, 1999; Gao & Chen, 2010; Poliakov *et al.*, 2004). It is possible that a role for the canonical Wnt pathway in EphB2-ephrinB1 signalling could distinguish the functions of Dvl2 and Daam1 in EphB2-ephrinB1 mediated directional persistence. The role for the canonical Wnt pathway has not been tested experimentally and remains an important question, but there is no evidence that this pathway functions in directional migration.

Instead, there is evidence for a link between non-canonical Wnt signalling and processes that involve cell migration, such as convergent extension (Tada & Smith, 2000; Wallingford *et al.*, 2000), by causing directional lamellipodia protrusions that favour movement in one direction (Carreira-Barbosa *et al.*, 2003; Wallingford *et al.*, 2000). In addition, a connection between PCP and ephrinB1 has been shown in cell migration: Dishevelled is required downstream of ephrinB1 for cell migration to the *Xenopus* eye field, whereas Eph forward signalling and the canonical Wnt pathway are not required (Lee *et al.*, 2006). The DEP domain of Dishevelled is required for PCP signalling (Boutros & Mlodzik, 1999; Poliakov *et al.*, 2004) and interacts with the C-terminal region of ephrinB1 leading to localisation of Dishevelled at the cell membrane (Lee *et al.*, 2006), a hallmark of PCP signalling (Fig. 6 A) (Axelrod *et al.*, 1998; Boutros & Mlodzik, 1999). This suggests that the activation of the PCP pathway by ephrinB1 is important for migration of cells to the eye field. Taken together, this suggests that the role of the canonical Wnt pathway in EphB2-ephrinB1 signalling is unlikely to explain the differences in the apparent roles of Dvl2 and Daam1 in EphB2-ephrinB1 mediated directional persistence.

6.4.1 A suggested role for Dvl2 in EphB2-ephrinB1 mediated directional persistence

There are two branches of the PCP pathway downstream of Dishevelled that lead to activation of RhoA via Daam1, or Rac1 independently of Daam1 (reviewed in (Gao & Chen, 2010)). Dishevelled can activate

Rac1, which stimulates its downstream effector JNK to regulate cell polarity and movements during Xenopus gastrulation, in a RhoA/Daam1-independent manner (Habas *et al.*, 2003). As Rac1 directs lamellipodia formation and focal complex formation via JNK at the LE of cells (Ridley *et al.*, 2003), this suggests one mechanism by which PCP regulates cell migration. In addition, both JNK and RhoA are required downstream of ephrinB1 for cell migration in the *Xenopus* eye field (Lee *et al.*, 2006), and Dishevelled is required for the segregation of EphB2- and ephrinB1-expressing cells in an *in vitro* cell aggregation assay, via RhoA activation (Tanaka *et al.*, 2003).

As Dvl2 knockdown specifically reduces the ability of cells to migrate with EphB2-ephrinB1 mediated directional persistence but Daam1 does not (Fig. 30), we suggest that the Dishevelled-Daam1 independent branch of the PCP pathway acts in EphB2-ephrinB1 mediated directional persistence. We suggest that Dvl2 activates Rac1 during cell migration, but at the site of contact between an EphB2- and ephrinB1-expressing cell, EphB2-ephrinB1 signalling initiates down-regulation of Rac1 activation via phosphorylation of Dvl2, allowing RhoA activation and cell repulsion. This role of Dvl2 is specific to EphB2-ephrinB1 mediated directional persistence and is independent of general motility, as knockdown of Dvl2 has no effect on the MSD of EphB2-GFP/EphB2 cell mixtures (Fig. 30). An effect on directional persistence could underlie the disruption to cell segregation and boundary formation seen on knockdown of Dvl2 (Fig. 18, 20).

An alternative possibility is that Dishevelled is recruited to the site of contact between an EphB2- and ephrinB1 expressing cell and activates RhoA, so initiating an EphB2-ephrinB1 specific repulsion response that underlies directional persistence, similar to that seen in the basal CIL between neural crest cells (Carmona-Fontaine *et al.*, 2008; De Calisto *et al.*, 2005; Matthews *et al.*, 2008; Mayor & Carmona-Fontaine, 2010). This is a possibility, but Daam1 knockdown has no effect on EphB2-ephrinB1 directional persistence in our experiments (Fig. 30), and as the evidence so far has not identified a role for Daam1 in this process in neural crest cells, this would suggest a role for Dvl2 in activating RhoA independently of Daam1. Differing roles of the different branches of the PCP pathway in EphB2-ephrinB1 mediated cell behaviour and general cell motility could explain the differences seen on knockdown of Dvl2 vs. Daam1, and will be discussed in more detail.

6.4.2 A suggested role for Daam1 in basal contact inhibition of locomotion

As previously discussed, the role of PCP and Dishevelled in the basal CIL of neural crest cells has been studied in *Xenopus*. Cell-cell contacts lead to the localised activation of PCP through recruitment of Dishevelled, which is required for the activation of RhoA, the localised collapse of cell protrusions and a change in cell migration (Carmona-Fontaine *et al.*, 2008). PCP signalling through Daam1 has also been shown to coordinate cell growth and migration in endothelial cells, predominantly through microtubule assembly and stabilisation (Ju *et al.*, 2010). As Daam1 knockdown does not affect the EphB2-ephrinB1

mediated change in MSD, unlike Dvl2 knockdown (Fig. 30), the Dishevelled-Daam1 branch of the PCP pathway is unlikely to function in increasing directional persistence on contact between EphB2- and ephrinB1- expressing cells. The Daam1-dependent PCP pathway is more likely to function in a general cell polarity mechanism independently of EphB2-ephrinB1 signalling, for example in basal CIL where interactions between cells cause an activation of RhoA and a change in direction to prevent migration over each other. This pathway is unlikely to lead to sustained directional persistence after cell contacts, unlike EphB2-ephrinB1 induced directional persistence.

Results from the cell tracking assay suggest that EphB2-ephrinB1 induced directional persistence is different from basal CIL, as directional persistence is increased when EphB2-ephrinB1 signalling is present from the basal level seen in EphB2/EphB2 mixtures. Since there is no change in directional persistence on knockdown of Daam1 in EphB2/ephrinB1 mixtures, EphB2-ephrinB1 mediated cell repulsion is still present. We propose that the effect of Daam1 knockdown is that cells would not be able to undergo basal CIL. It is unlikely that an inability to respond to basal CIL would be detected as an overall change in speed or persistence on a population level when the number of collisions is small, as the cells are at low confluence. We would predict that no difference in MSD or turning angle distribution would be seen, and this fits the MSD data of knockdown of Daam1 in EphB2/EphB2 mixtures, where there is no change in directional persistence (Fig. 30). This could be analysed more effectively by analysis of MSD and turning angle distributions for individual cell-cell interactions, or by higher magnification imaging and analysis of behaviour only after interactions. In addition, the same analysis at higher density could help to determine the role of Daam1 in basal CIL, as if there were more contacts being analysed on a population level, it is likely that disruption to basal CIL could affect overall MSD.

We suggest an explanation in which PCP via Daam1 is required for basal CIL between all cells and Dvl2 has an additional specific role downstream of EphB2-ephrinB1 signalling. In a confluent situation, such as the boundary or cell segregation assays, basal CIL is more prevalent, but it is not known whether CIL could contribute to cell segregation. Whether the defects seen in EphB2-ephrinB1 mediated cell segregation and boundary sharpening (Fig. 18, 20) on Daam1 knockdown are due to a disruption in basal CIL requires further investigation. The role of Dvl2 in the JNK/Rac1 branch of the PCP pathway has not been investigated downstream of EphB2-ephrinB1 signalling. These two possibilities provide a likely explanation for differences in the results seen between Daam1 and Dvl2 in behavioural studies, but fail to explain why a weaker disruption to boundary sharpness is seen for Dvl2 than for Daam1 in the segregation and boundary assays, as Dvl2 would be acting in multiple pathways. In order to fully dissect the role of the PCP pathways in EphB2-ephrinB1 directional migration and segregation, the functions of the other Dishevelled (1 and 3) and Daam (2) genes need to be analysed in these assays, as one possibility is that a different Dishevelled gene could function with Daam1 and independently of Dvl2.

6.5 Cooperative roles of Dvl2 and PAR-6B downstream of EphB2-ephrinB1 signalling?

6.5.1 Intrinsic signalling potential of Eph receptors and ephrins

Interestingly, recent evidence has identified that ephrins have an intrinsic signalling potential independent of phosphorylation by Eph receptors and this cell autonomous function can activate Rac1 for neuronal outgrowth. Eph-ephrin activation can cause a switch in response causing RhoA activation and collapse/repulsion. Similarly for Eph receptors, in the absence of ephrins, Eph-bound ephexin activates Rac1, RhoA and Cdc42 in the growth cone stimulating outgrowth. EphrinA stimulation of EphA induces tyrosine phosphorylation of ephexin, which enhances specificity towards RhoA so promoting growth cone collapse (Knoll & Drescher, 2004). In addition, Vav2 can bind to EphA4/B2 and is phosphorylated in response to ephrin binding. This promotes local Rac1-dependent endocytosis of the ephrin-Eph complex (Cowan *et al.*, 2005), so converting the initial adhesive interaction to repulsion and mediating growth cone collapse.

Cell autonomous ephrin function is also required for directional migration. For example, loss of ephrinB2 causes random migration, unstable lamellipodial protrusions and cell detachment at the TE is compromised (Foo *et al.*, 2006). Analysis of freely migrating ephrinB2- and ephrinB1-expressing cells has shown an increase in migration speed and a decrease in the persistence of directional migration compared to non-expressing cells (Bochenek *et al.*, 2010), although this response is cell type specific. Interestingly it has been observed that the MSD of EphB2-GFP cells is increased compared to wild-type HEK293 cells, although whether this is due to persistence or speed has not been analysed (Rosalind Morley, personal communication). This implies an intrinsic signalling potential of EphB2 receptors independent of phosphorylation by ephrinB1 (excluding auto-activation of EphB2 receptors (Tanaka *et al.*, 2003)), although some low level EphB2-ephrinB1 signalling may be occurring due to the endogenous ephrinB1 ligands expressed in HEK293 cells.

Knockdown of Dvl2 and PAR-6B cause very similar patterns of disruption to EphB2-ephrinB1 mediated directional persistence, cell segregation and boundary formation. Importantly, knockdown of Dvl2 and PAR-6B cause a decrease in MSD in EphB2-GFP/ephrinB1 but not in EphB2-GFP/EphB2 cell mixtures, and analysis of turning angle distributions suggests this is due to a decrease in persistence (Fig. 30). Taken together, this suggests that both Dvl2 and PAR-6B knockdown can reduce the ability of cells to migrate with EphB2-ephrinB1 mediated directional persistence, which disrupts cell segregation and boundary formation. The similarities between the phenotypes in each of the assays suggest that these two proteins might function cooperatively or play similar roles downstream of EphB2-ephrinB1 signalling.

6.5.2 Roles of Dvl2 and PAR-6B with ephrinB1

There is potential for signalling pathways downstream of Eph receptors to function in promoting motility, which may be disrupted on contact between Eph- and ephrin-expressing cells. Dishevelled recruitment, via the adaptor protein Grb4, to ephrinB1-stimulated EphB2 and EphB2-stimulated ephrinB1, leads to its phosphorylation and the activation of RhoA during the segregation of ephrinB1- from EphB2-expressing cells in an *in vitro* aggregation assay (Tanaka *et al.*, 2003). Dishevelled is also constitutively recruited directly to unphosphorylated ephrinB1, but this interaction does not activate RhoA (Fig. 6 A) (Tanaka *et al.*, 2003). In X*enopus*, Dishevelled association with ephrinB1 mediates cell migration independently of activation by EphB2, and requires both JNK and RhoA (Lee *et al.*, 2006). Tyrosine phosphorylation of ephrinB1 by the cognate Eph receptor blocks the interaction between ephrinB1 and Dishevelled and inhibits cell migration (Lee *et al.*, 2009).

The PAR-6/aPKC/Cdc42-GTP complex localises to apical cell junctions to regulate tight junction formation, and associates with the actin cytoskeleton for the reorganisation, formation and maintenance of cell–cell contacts. EphrinB1 can disrupt tight junction formation by binding PAR-6 via its C-terminus and competing with Cdc42 for association with PAR-6 (Lee *et al.*, 2008); this competition causes inactivation of the PAR complex, resulting in the loss of tight junctions. The ephrinB1/PAR-6 interaction is disrupted by tyrosine phosphorylation of the intracellular domain of ephrinB1 by binding the cognate EphB receptor, which results in the proper establishment of tight junctions (Lee *et al.*, 2008).

In both of these examples, ephrinB1 binding to either PAR-6 or Dishevelled is constitutive. The complex is disrupted on phosphorylation due to Eph-ephrin signalling. As intrinsic signalling potential of EphB2 receptor has also been suggested to occur in EphB2 cells (Rosalind Morley, personal communication), Dishevelled and PAR-6 may play a role in EphB2-mediated cell migration which is disrupted on EphB2-ephrinB1 signalling.

In addition, there is evidence for a physical association between Dvl2 and PAR-6 complex that is involved in a number of processes. A constitutive interaction between PAR-6 and Dvl2 has been demonstrated in cell lines (Narimatsu *et al.*, 2009) consistent with previous observations in neurons, where the interaction of the DEP domain of Dishevelled with aPKC is required for guidance in isolated hippocampal neurons (Zhang *et al.*, 2007). In scratch wound assays of fibroblasts, disruption of cell-cell contacts at the wound edge leads to the activation of non-canonical Wnt signalling and the binding of Dvl2 to aPKC independent of its activation. This couples Dvl2 and Cdc42/PAR-6/aPKC pathways to trigger Golgi and centrosome orientation, and stabilise microtubules towards the LE (Schlessinger *et al.*, 2007). Taken together this evidence suggests that Dvl2 and PAR-6 could function together in a complex to mediate EphB2-ephrinB1 induced directional persistence.

6.5.2.1 Model of Dvl2 and PAR-6B in EphB2-ephrinB1 mediated directional persistence

We suggest a model whereby Dvl2 and PAR-6B function together at the LE of migrating EphB2 cells to allow cells to migrate with a basal level of directionality that is higher than in cells lacking EphB2. There is evidence that Dishevelled and PAR-6 can function independently to locally activate Rac1 and regulate the formation and stabilisation of protrusions (Etienne-Manneville & Hall, 2001; Etienne-Manneville & Hall, 2003; Habas *et al.*, 2003; Ridley *et al.*, 2003), so the LE is defined by localisation of Dvl2/PAR-6/aPKC complex. Basal directionality could be maintained due to interaction of this complex with the unphosphorylated C-terminus of the un-clustered EphB2 (Fig. 32 A), which in cells not stimulated by their cognate ligand/receptor are localised around the plasma membrane (Alexei Poliakov, unpublished observation). Dishevelled is known to bind phosphorylated EphB2 via Grb4 (Tanaka *et al.*, 2003), but there is no evidence for an interaction between either Dishevelled or PAR-6 and unphosphorylated Eph receptor, although there is evidence for constitutive interaction with Dishevelled or PAR-6 and ephrinB1 (Tanaka *et al.*, 2003).

EphB2-ephrinB1 signalling de-phosphorylates PAR-6B (Jorgensen *et al.*, 2009) causing its inactivation, and can phosphorylate Dishevelled (Tanaka *et al.*, 2003), although it is not known how phosphorylation of Dishevelled affects its function (Gao & Chen, 2010). The Dvl2/PAR-6B complex could constitutively interact with the EphB2 receptor, so phosphorylation and clustering of the EphB2 receptor on interaction with an ephrinB1-expressing cell could cause dissociation of the complex, as Dvl2 cannot directly bind phosphorylated EphB2 receptor (Fig. 32 B). Phosphorylated Dvl2 could then bind the activated EphB2 receptor independently of PAR-6B and via an adaptor protein and lead to activation of RhoA. If interaction of the complex with the EphB2 receptor is not constitutive, phosphorylation of the EphB2 receptor by ephrinB1-expressing cells could cause the recruitment of Dvl2 (and PAR-6B) to the EphB2 receptor, which is dependent on adaptor proteins (Tanaka *et al.*, 2003), and the de-phosphorylation of PAR-6B and phosphorylation of Dvl2. Both scenarios would result in a decrease in the activation of Rac1 and de-repression of RhoA.

Inactivation of the PAR complex would remove the mechanism of localised Rac1 activation and subsequently cause RhoA activation due to the inhibitory crosstalk between Rho GTPases (Iden & Collard, 2008; Nakayama *et al.*, 2008; Nobes & Hall, 1995), leading to collapse of protrusions. In addition, inactivation of PAR-6B could cause the direct de-repression of RhoA, as a role of PAR-6/aPKC is to inactivate RhoA via either the recruitment of the ubiquitin ligase, Smurf1, which binds RhoA to promote RhoA ubiquitination and degradation (Wang *et al.*, 2003), or via interaction with the negative regulator of RhoA, p190ARhoGAP (Zhang & Macara, 2008b). This could rapidly cause the activation of RhoA at the site of contact (Fig. 32 B), collapse of protrusions, and repulsion (Carmona-Fontaine *et al.*, 2008; Iden & Collard, 2008; Nakayama *et al.*, 2008). Activated Rac1 would therefore be able to accumulate away from the point of contact, which would allow a new LE to be specified (Mayor & Carmona-Fontaine, 2010), as

Figure 32: A possible role of Dvl2 and PAR-6B in EphB2-ephrinB1 mediated directional persistence

(A): The possible localisation of the Dvl2/PAR-6B/aPKC complex to the leading edge of a migrating EphB2 cell could cause activation of Rac1. The complex could interact with the C-terminal of unphosphorylated EphB2. Activated PAR-6B represses the activity of RhoA via the recruitment of the ubiquitin ligase, Smurf1, or by interaction with the negative regulator of RhoA, p190ARhoAGAP. This would allow Rac1 activation and the formation of protrusions at the leading edge in the direction of migration.
(B): On interaction with an ephrinB1-expressing cell, EphB2 becomes clustered and phosphorylated at the site of interaction. This could lead to de-phosphorylation and inactivation of PAR-6B and the phosphorylation of Dvl2, which would cause the dissociation of Dvl2/PAR-6B from the EphB2 receptor. The combined activities of inactivation of this complex, which would remove localised Rac1 activation, and inactivation of PAR-6B, which would cause the direct de-repression of RhoA, could rapidly cause the activation of RhoA at the site of contact, collapse of protrusions and repulsion. Activated Rac1 would therefore be able to accumulate away from the point of contact, so specifying the site of contact as the new trailing edge.

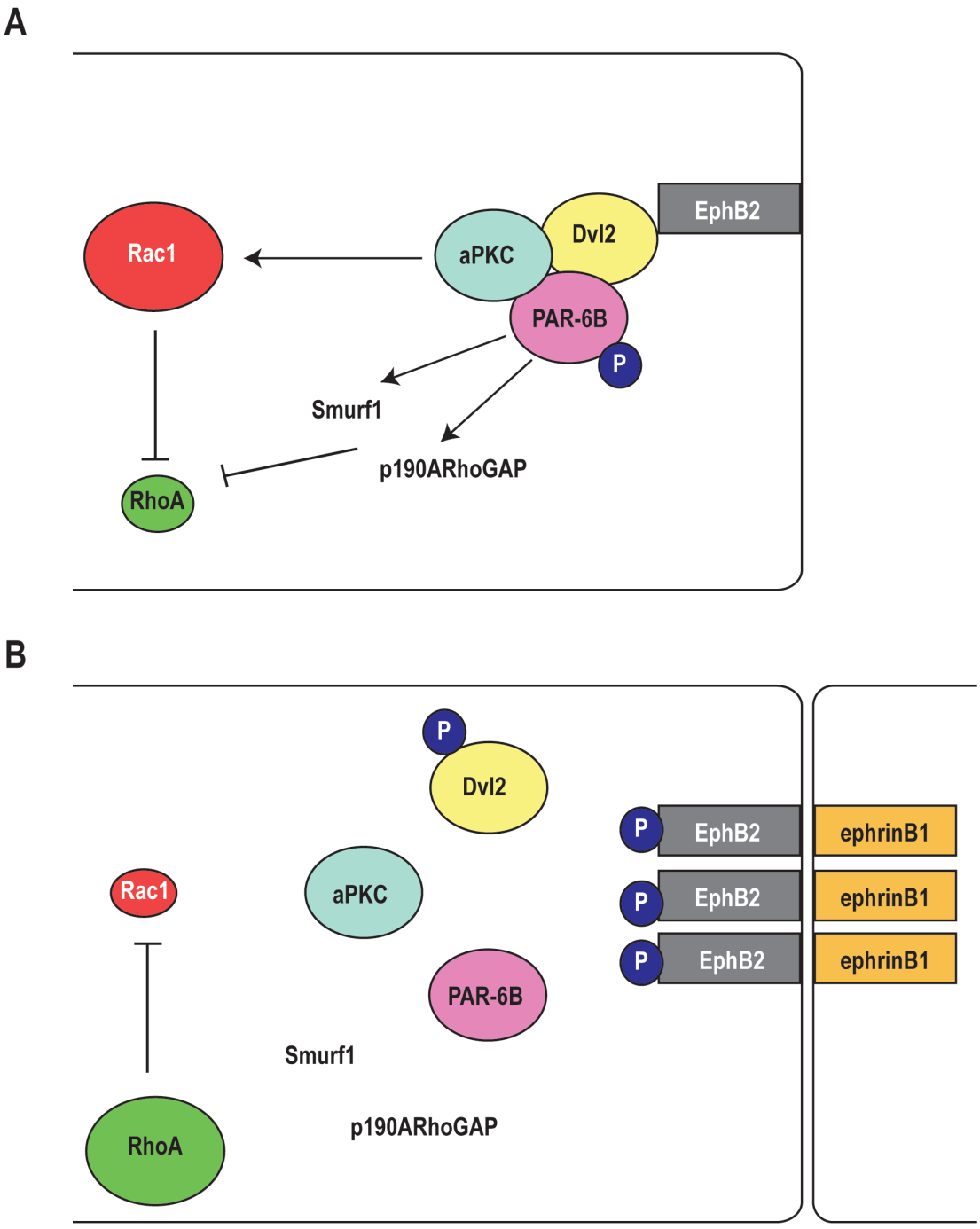
A
Rac1
aPKC
Dvl2
EphB2
PAR-6B
P
Smurf1
p190ARhoGAP
RhoA
B
P
Dvl2
P
EphB2
ephrinB1
Rac1
aPKC
P
EphB2
ephrinB1
P
EphB2
ephrinB1
PAR-6B
Smurf1
p190ARhoGAP
RhoA

Rac1 has been shown to activate the PAR complex through PAR-6 (Lin *et al.*, 2000) and stabilise the complex at the new LE.

Asymmetric localisation of PAR-6/aPKC at the cell cortex is important in maintaining the directionality of migrating cells; PAR-6/aPKC is required independently of, or together with, Dvl2 for centrosome and Golgi localisation and stabilisation of microtubules towards the LE in scratch-induced migrating fibroblasts (Cau & Hall, 2005; Schlessinger *et al.*, 2007). The stabilisation of this polarity could play a crucial role in the maintenance of EphB2-ephrinB1 directional persistence.

A rapid collapse response has been observed in EphB2 cells on stimulation with ephrinB1 cells (Poliakov *et al.*, 2008) (Fig. 5), which suggests an active increase in RhoA due to EphB2-ephrinB1 signalling. This model suggests that the activation of RhoA is indirect and occurs by removal of Rac1 or de-repression of RhoA. As previously described, it is likely that basal CIL occurs between all cells in an EphB2-ephrinB1 independent manner. However, activation of RhoA on contact between an EphB2- and ephrinB1-expressing cell due to basal CIL could act in parallel to the removal of Rac1 activation or de-repression of RhoA due to Eph-ephrin signalling, which could accelerate the switch in Rac1 to RhoA activation at the site of contact.

In addition, PCP-induced phosphorylation of Dishevelled, bound to PAR-6B, is known to lead to the recruitment of Smurfs and degradation of Prickle, causing the asymmetric localisation of PCP components (Narimatsu *et al.*, 2009). It is possible that Dvl2/PAR-6B recruitment of Smurf1 could be mediated by activated EphB2 receptor so causing degradation of a molecule involved in establishing polarity. This could also accelerate the switch from Rac1 to RhoA activation. However this fails to explain why a larger disruption to boundary sharpness and cell segregation in not seen on Dvl2 knockdown compared to Daam1 knockdown, if Dvl2 has roles in multiple pathways. One possible explanation is that there is redundancy between different Dishevelled genes.

6.5.3 The role of adhesion in directional migration

Adhesion molecules have also been shown to regulate cell polarity and play a role in basal CIL. Recent evidence has reported activation of RhoA as a result of cell-cell adhesion in a number of cell types (Mayor & Carmona-Fontaine, 2010). In addition, N-cadherin-dependent cell contacts are required for collective cell migration and basal CIL between neural crest cells, and can polarise the cells by inhibiting Rac1 at the site of cell contact and increasing Rac1 activity at the free edge; this polarised distribution of Rac1 activity is essential for the neural crest cells to respond to a chemoattractant and for directional and collective cell migration (Fig. 7 B) (Theveneau *et al.*, 2010). Association of N-cadherin with p120-cadherin has been shown to lead to RhoA activation in myogenesis, but it is not known whether a similar mechanism occurs in migratory cells (Mayor & Carmona-Fontaine, 2010). N-cadherin and E-cadherin at cell-cell contacts are

also required for centrosome orientation, nucleus positioning, and cell orientation in various cell types (Desai *et al.*, 2009; Dupin *et al.*, 2009), suggesting that adhesion plays a role in directional migration by regulating the intracellular polarity required for polarisation.

Mutually exclusive areas of Rac1 and RhoA activity can therefore be controlled by basal CIL driven by PCP or N-cadherin. EphB signalling has been shown to promote the recruitment of E-cadherin to the membrane in epithelial tumour cells (Cortina *et al.*, 2007), and EphB2 signalling causes the redistribution of N-cadherin to cell-cell contacts in Schwann cells (Parrinello *et al.*, 2010). It is possible that adhesion and PCP could act cooperatively downstream of EphB2-ephrinB1 signalling to mediate contact-mediated repolarisation, which underlies persistent migration.

6.5.3.1 A cooperative role of adhesion and polarity?

A link between the non-canonical Wnt pathway and cell-cell adhesion has been suggested: non-canonical Wnt signalling via Wnt11 controls cell cohesion of prechordal plate progenitors by modulating the subcellular localisation of E-cadherin in these cells via Rab5c-dependent endocytosis (Ulrich *et al.*, 2005), and Wnt11/Fz7/Dsh accumulation promotes the local perdurance of cell contacts and adhesion to control coherent cell migration (Ulrich *et al.*, 2005; Witzel *et al.*, 2006). These mechanisms serve to globally regulate the dynamics of cell cohesion. It is possible that the PCP pathway plays a role in modulating cell adhesion downstream of EphB2-ephrinB1 signalling to play a role in cell polarisation, but it is more likely that adhesion and polarity cooperate to modulate processes required for general migration.

A double knockdown of N-cadherin and Dvl2 has suggested a synergistic role in cell segregation and boundary formation mediated by EphB2-ephrinB1 signalling (discussed in Chapter 4), as the disruption to boundary sharpness is enhanced compared to that seen with individual knockdown (Fig. 23, 24). N-cadherin knockdown affects boundary sharpening and we previously suggested that a level of adhesion between cells is required for interactions and cell-cell signalling to occur. However, it is also likely that the disruption to boundary sharpening and cell segregation seen on knockdown of N-cadherin could be due to a role of N-cadherin in a general migratory process, such as basal CIL. Dvl2 acts downstream of EphB2-ephrinB1 mediated directional persistence and so it is unsurprising that an enhanced disruption to boundary sharpness is seen on knockdown of N-cadherin in combination with Dvl2. However, PCP and adhesion could play a role in migratory processes, such as basal CIL, via other Dishevelled genes or Daam1. To test this, knockdown of N-cadherin with Daam1 or Dvl2/3 could be carried out to see whether disruption to EphB2-ephrinB1 mediated cell segregation and boundary sharpening is enhanced or remains the same. If boundary sharpening is not further disrupted, this would suggest that N-cadherin and PCP are involved in the same process required for general migration, and likely independent of EphB2-ephrinB1 mediated directional migration.

6.5.3.2 Endocytosis

The role of endocytosis has not been studied in our system and provides a future direction of research, as Rac1-dependent endocytosis is known to play a role in separation of EphB4 and ephrinB2 cells (Marston *et al.*, 2003). In addition, non-canonical Wnt signalling induces the formation of a complex of phosphorylated EphB, Dvl2 and Daam1, which is incorporated into endocytic vesicles in a dynamin-dependent manner. This results in the removal of EphB from the cell surface and cell repulsion, followed by the initiation of convergent extension cell movements in the zebrafish notochord (Kida *et al.*, 2007). This could play a role in cell repolarisation on EphB2-ephrinB1 cell contact, and as signalling persists after endocytosis (Marston *et al.*, 2003), this process could play a role in prolonging the persistence response seen after EpB2-ephrinB1 signalling.

Work by Alexei Poliakov has suggested that the repeated activation and endocytosis of receptor (Marston *et al.*, 2003; Zimmer *et al.*, 2003) decreases the steady-state level of cell surface EphB2 (Alexei Poliakov, unpublished data), but it is possible that this may be an artifact of the over-expression model used. If this is the case, EphB2-ephrinB1 signalling will be attenuated at the cell surface over time and direct downstream events such as the collapse response could not maintain sharp boundaries. However, recent evidence has shown a role for EphB-ephrinB signalling in controlling *Xenopus* embryonic germ layer separation by cycles of transient adhesion and contact-induced cell detachment (Rohani *et al.*, 2011). Adhesion brings ephrins and Eph receptors into contact, inducing a local Rac1- and RhoA-based repulsion, which decays after segregation and allows re-adhesion (Rohani *et al.*, 2011). This suggests that cycles of adhesion and repulsion mediated by Eph-ephrin signalling are important for maintaining boundaries.

6.6 Further analysis

In order to analyse further the role of components of the PCP and PAR polarity pathways and to test our model, it is crucial to be able to analyse the intracellular relocalisation and dynamics of components in real time. Transient transfection of fluorescently-tagged polarity proteins in our cell lines would allow analysis of the localisation of proteins in freely migrating cells, and any relocalisation at the point of contact between an EphB2- and ephrinB1-expressing cell. This can also be analysed in the *in vitro* boundary assay in order to assess the effect of longer term signalling on polarity component localisation. In addition, it is important to be able to analyse the effect of these signalling pathways on Rac1 and RhoA activation. FRET analysis is currently the most effective measurement of this, and would help to further understand the roles of Dvl2 and PAR-6B downstream of EphB2-ephrinB1 signalling.

The PAR-6/aPKC complex is required for the maintenance of apical-basal polarity in the hindbrain neuroepithelium and for correct facial branchiomotor neuron migration (Grant & Moens, 2010). This complicates the study of PAR-6 in Eph-ephrin migration, but it would be interesting to determine the expression pattern of PAR-6 and Dvl2 (and other PAR and PCP components) at boundaries in the zebrafish hindbrain in order to understand their roles in Eph-ephrin mediated boundary formation *in vivo*.

The role of tension has not been studied downstream of Eph-ephrin signalling, but is known to contribute to the segregation of two populations of cells due to the generation of actomyosin-dependent interfacial tension (Krieg *et al.*, 2008; Major & Irvine, 2005). It is possible that Eph-ephrin signalling generates tension between two populations. To assess this in more detail, analysis of cell shape and actin-myosin elements at zebrafish hindbrain boundaries would be informative.

6.7 Conclusions

In conclusion, we have developed *in vitro* assays to analyse EphB2-ephrinB1 mediated cell behaviour, which show that EphB2-ephrinB1 signalling mediates cell segregation, boundary sharpening and directional persistence. This work has tested the roles of PCP and PAR polarity genes in these processes, which suggests a novel role for Dvl2 and PAR-6B in EphB2-ephrinB1 mediated boundary sharpening and cell segregation, and suggests that segregation underlies the process of boundary sharpening. In addition, this work suggests a novel and specific role for Dvl2 and PAR-6B in mediating directional persistence downstream of EphB2-ephrinB1 signalling. As computer simulations have suggested that directional persistence can in principle contribute to cell segregation, we propose that Dvl2 and PAR-6B play a role in this process. The data suggests that Daam1 mediates cell segregation via a mechanism independent of directional migration, and we propose a role of Daam1 in the process of basal CIL. In addition, PAR-3 acts independently of PAR-6B in the regulation of general cell motility, and we propose that this is independent of EphB2-ephrinB1 signalling.

Taken together, this evidence suggest that EphB2-ephrinB1 mediated directional persistence can underlie the process of cell segregation and boundary sharpening. The roles of Dvl2 and PAR-6B need to be further analysed in this process. The plethora of signalling pathways downstream of Eph-ephrin signalling that differ in their cellular contexts, highlights how dynamic Eph-ephrin signalling is. It is likely that Dvl2-PAR-6B mediated de-repression of RhoA is just one of the mechanisms that acts downstream of EphB2-ephrinB1 signalling. Further work needs to address how Eph-ephrin signalling is modulated in different contexts.

7 DOES PCP MEDIATE THE ROLE OF EPH-EPHRIN SIGNALLING IN CELL SORTING AND BOUNDARY FORMATION *IN VIVO?*

7.1 Introduction

One of the best examples of cell segregation during vertebrate development is found in the hindbrain (Fraser *et al.*, 1990), where sharp boundaries form at the interface of segments called rhombomeres (Lumsden & Krumlauf, 1996; Pasini & Wilkinson, 2002) (Fig. 1 A). Rhombomere boundaries correspond to segmental, periodic domains of gene expression of members of the Eph receptor and ephrin gene family (Fig. 1 B); Eph receptors are expressed in odd-numbered rhombomeres and ephrins in even-numbered rhombomeres (Becker *et al.*, 1994; Flanagan & Vanderhaeghen, 1998; Gale *et al.*, 1996).

Eph-ephrin signalling plays a key role in the restriction of intermingling across hindbrain boundaries (Mellitzer *et al.*, 1999; Xu *et al.*, 1999) and the formation of sharp boundaries between rhombomeres (Fig. 2 C, C') (Cooke *et al.*, 2005), and is the primary mechanism for lineage restriction and boundary formation at the interface of segments. Eph-ephrin interactions contribute to the sharpening of segments by regulating both repulsion at interfaces and cell segregation properties that differ between rhombomeres (Cooke *et al.*, 2005; Pasini & Wilkinson, 2002). Taken together with evidence from embryo explant experiments, this suggests Eph-ephrin signalling is sufficient to drive segregation of the populations with the formation of smooth boundaries (Fig. 2 B, B') (Mellitzer *et al.*, 1999; Tanaka *et al.*, 2003 2005), although the mechanisms that underlie cell segregation and boundary formation are not known.

A candidate pathway to mediate Eph-ephrin cell segregation and boundary formation is the planar cell polarity pathway (PCP), a key component of which is Dishevelled, as has been described in the previous chapters. Dishevelled has been shown to be required for the segregation of EphB2 and ephrinB1 cells (Tanaka *et al.*, 2003), and the migration of cells to the *Xenopus* eye field (Lee *et al.*, 2006). Crucially the DEP domain of Dishevelled was required and this suggests a role for the PCP pathway downstream of Eph-ephrin signalling in mediating cell segregation and migration (Lee *et al.*, 2006; Tada *et al.*, 2002; Tanaka *et al.*, 2003).

The PCP pathway branches at the level of Dishevelled to activate Rac1 via JNK and RhoA via Daam1. Both branches have been shown to play a role in the morphogenetic process of convergent extension, which is the process of medio-lateral narrowing (convergence) and anterior-posterior elongation (extension) of vertebrate embryos during gastrulation (Habas *et al.*, 2001; Habas *et al.*, 2003; Wallingford *et al.*, 2002a), by causing a directional activity of the lamellipodia that favours movement in one direction

(Carreira-Barbosa *et al.*, 2003; Wallingford *et al.*, 2000). Mutation of core PCP proteins, such as Dishevelled, disrupts embryonic axis formation without affecting cell fate in zebrafish and *Xenopus* embryos (Tada & Smith, 2000; Wallingford *et al.*, 2000). Dishevelled has also been shown to play a role in the morphogenesis of the *Xenopus* hindbrain, as expressing dominant-negative Dishevelled (specific to the PCP pathway) causes irregular shaped and distorted rhombomeres 3 and 5 (r3/r5). This disruption to hindbrain segmentation is thought to be independent of convergent extension (Tanaka *et al.*, 2003).

This raised the possibility that EphB2 and ephrinB1 act through the PCP pathway to control cell migration and segregation during development. In order to analyse whether the PCP pathway mediates Eph-ephrin signalling in cell segregation and boundary formation *in vivo,* approaches were initially taken to understand the role of PCP in the boundary sharpening process that occurs between rhombomeres of the developing zebrafish hindbrain. The approaches used had various technical limitations, which made analysis difficult. As a result, studies subsequently focussed on the relationship between PCP and Eph-ephrin signalling *in vitro*, as described in Chapters 3-6. The efforts initially taken to analyse the *in vivo* role of PCP in Eph-ephrin mediated boundary sharpening are discussed in this Chapter.

7.2 RESULTS

7.2.1 The effect of EphA4 knockdown on cell sorting and boundary formation

Sharpening of the boundaries of r3/r5 occurs partly due to *krox20* upregulating EphA4 expression, thus leading to segregation (Theil *et al.*, 1998). Disruption to Eph-ephrin signalling has a strong effect on hindbrain boundary sharpening, since knockdown of EphA4, using injection of antisense morpholino oligonucleotides (MOs) in the zebrafish hindbrain, was shown to be efficient and led to fuzzy interfaces of *krox20* expression between r3/r5 and adjacent segments (Fig. 2 C, C') (Cooke *et al.*, 2005). Although this study analysed *krox20* expression at a number of developmental stages (1-10 somite stage (ss)), expression during the boundary sharpening period (10-16ss) and the effect of EphA4 knockdown was not analysed. Therefore I analysed the expression of *krox20* during the period of boundary sharpening in hindbrain development, and the effect of EphA4MO on its expression pattern.

RNA *in situ* hybridisations were performed to analyse *krox20* expression in the hindbrain of wild-type zebrafish embryos. *Krox20* mRNA was detected at high levels in r3/r5 between the 10ss and 24 hours-post-fertilisation (hpf) stages of development that were analysed (Fig. 33 A-E). Boundaries in controlMO-injected embryos were sharp from 10ss stage (Fig. 33 A) but the phenotype between sibling embryos was most consistent at 16ss and 18ss stage (Fig. 33 C, D). In contrast, embryos injected with EphA4MO showed fuzzy boundaries until 18ss, before sharpening by 24hpf (Fig. 33 A'-E'). The most distinctive and reproducible phenotype was at 16ss (Fig. 33 C'), when disruption to sorting at boundaries in the EphA4

Figure 33: Timecourse of krox20 expression in the hindbrain of developing zebrafish embryos

RNA *in situ* hybridisation analysis showing the expression of *krox20* in the hindbrain of wild-type zebrafish embryos injected with *Control+p53* MO (A-E) or *EphA4+p53* MO (A'-F'). Embryos were injected at 1-2 cell stage and the expression of *krox20* analysed by *in situ* hybridisation from 10ss to 24hpf. Images show the hindbrain from the dorsal view with anterior to the top.

(A-F): Boundaries of rhombomeres 3 and 5 (r3/r5) have sharpened by 10ss in control embryos, but are at their most sharp at 16ss.

(A'-F'): r3/r5 boundaries remain fuzzy until 18ss in EphA4 morphants, but are sharp by 24hpf.

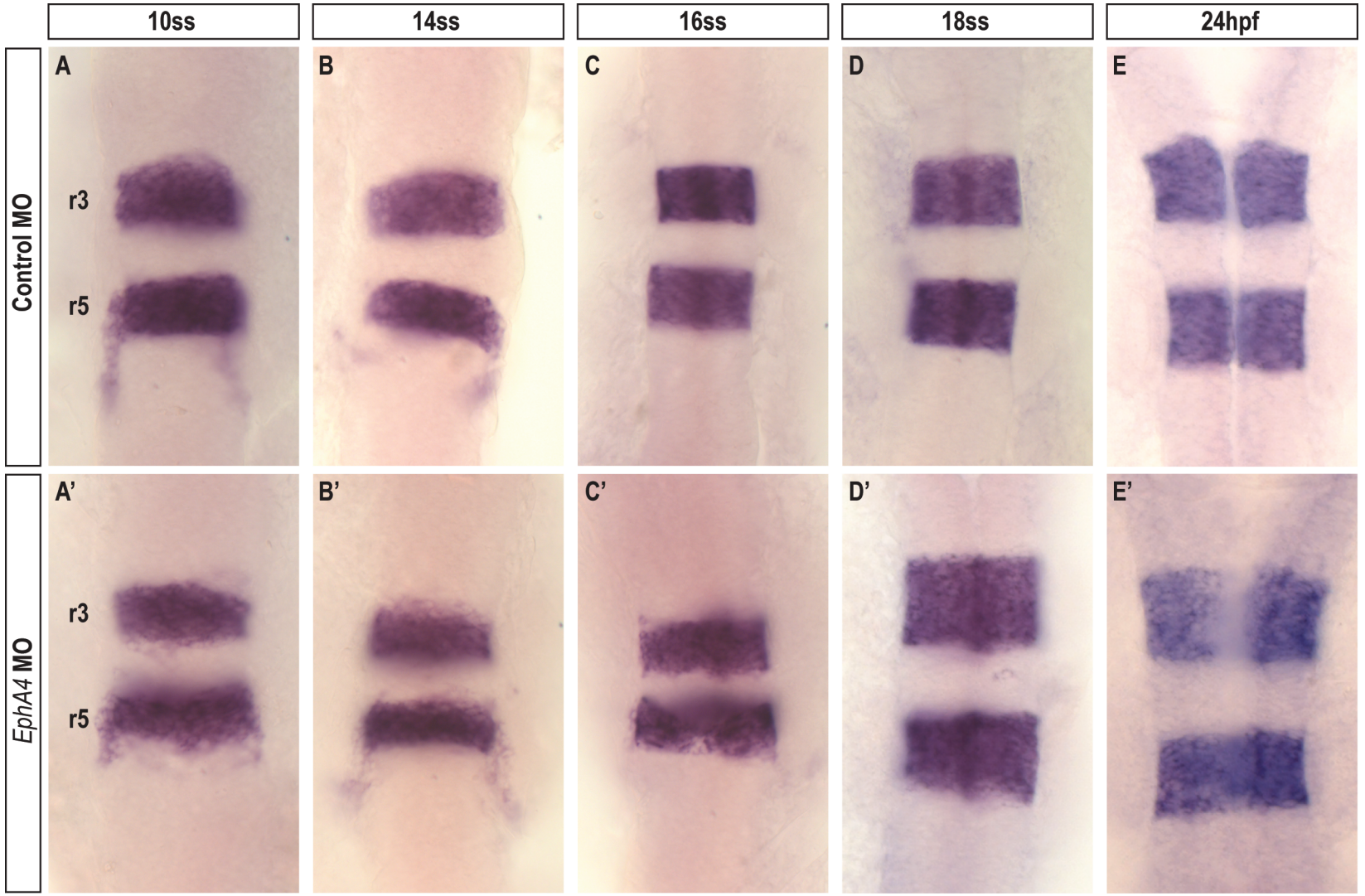
10ss
14ss
16ss
18ss
24hpf
Control MO
EphA4 MO
A
B
C
D
E
A'
B'
C'
D'
E'
r3
r5
r3
r5

morphant was the most different from the control situation (Fig. 33 C). This is different from published work where the 18ss stage was shown to have the most penetrant phenotype (Cooke *et al.*, 2005). It was concluded that further work analysing the disruption to Eph-ephrin mediated sorting at boundaries would be investigated at 16-18ss embryonic stages.

7.2.2 Preliminary expression and functional studies of Dishevelled

Since many core PCP genes are widely expressed and involved in early morphogenetic movements, such as convergent extension, it was predicted that PCP gene knockdowns could be difficult to interpret independently of large scale cell movements. I therefore took the approach of blocking Dishevelled (Dsh) by transgenic expression of dominant-negative (DN) proteins.

DN-Dsh constructs were obtained (gift of Masa Tada), which are deletion constructs for each of the DIX, and PDZ domains of *Xenopus* Dsh (Fig. 34), and block the canonical and/or PCP Wnt pathway both in *Xenopus* and zebrafish (Carmona-Fontaine *et al.*, 2008; Tada & Smith, 2000). The DEP domain is known to be essential for recruitment of Dsh to Frizzled at the membrane (Axelrod *et al.*, 1998; Boutros & Mlodzik, 1999), and interaction with the C-terminal region of ephrinB1 leads to localisation at the membrane (Lee *et al.*, 2006). The Dsh-DEP+ construct has been shown to specifically inhibit the PCP pathway (Rothbacher *et al.*, 2000; Sokol, 1996; Tada & Smith, 2000; Wallingford *et al.*, 2000), and Dsh-ΔPDZ (Xdd1) has been widely used as a dominant-negative for the PCP pathway, but is known to also interfere with the canonical pathway in some contexts (Rothbacher *et al.*, 2000; Sokol, 1996; Tanaka *et al.*, 2003; Wallingford *et al.*, 2000). Experiments were carried out with both of these constructs and Dsh-WT, a full length Dsh construct (wild-type). The DN-Dsh proteins were Myc-tagged, which allowed their expression to be visualised by Myc immunostaining. If the PCP pathway is involved in mediating Eph-ephrin signalling, it is predicted that mosaic knockdown will lead to disruption of boundary sharpening, and that widespread knockdown could lead to disruption of morphogenetic movements, such as convergent extension. A number of different approaches were attempted to achieve expression to test roles in boundary sharpening in the hindbrain of the zebrafish embryo.

7.2.2.1 Spatial control of transgene expression

The initial approach aimed to target specific expression of the dominant-negative constructs spatially to r3/r5 in order to test roles in Eph-ephrin mediated cell segregation independently of convergent extension. The DN-Dsh constructs were inserted into a custom miniTol2 site-flanked, dual UAS vector, expressing H2B-citrine from one 5xUAS sequence, and DN-Dsh from the second 5xUAS (Gerety & Wilkinson, 2011). These constructs, pminiTol2-UAS-H2Bcitrine-UAS-DN-Dsh, were injected into embryos of the Tg*(krox20-Gal4::UAS-RFP)* fish line. This would allow early expression of the constructs in r3/r5 via the Gal4-UAS

Figure 34: Dishevelled dominant-negative and deletion constructs

Xenopus Dishevelled and deletion constructs obtained from Masa Tada (adapted from (Tada & Smith, 2000)). The effect of the constructs on the canonical Wnt and planar cell polarity (PCP) pathways is shown, as reviewed from the literature. Annotation is as follows: ++ strongly active, - weakly inhibitory, -- strongly inhibitory, X no effect.

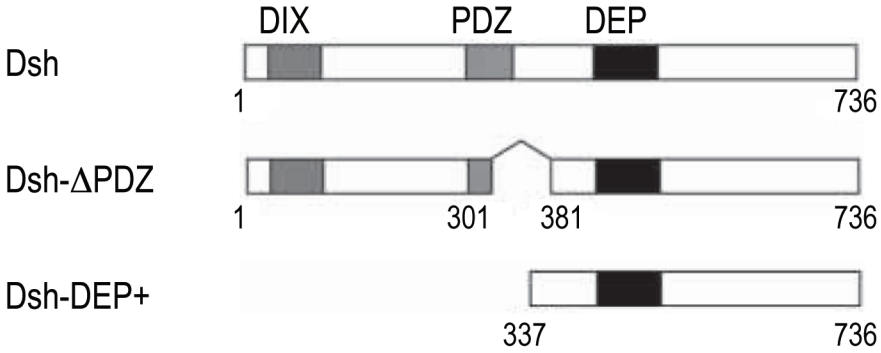

	Canonical pathway	Planar cell polarity pathway
Dsh	+ +	- -
Dsh-ΔPDZ	-	- -
Dsh-DEP+	X	- -

system, driven by the *krox20* regulatory element. RFP acts as a reporter for Gal4 expression and citrine acts as a reporter for the construct. Disruption to cell segregation at hindbrain boundaries is easiest to distinguish between 16-18ss in *EphA4* morphants (Fig. 33), but the stability of the RFP protein also enables this phenotype to be visualised at later stages by RFP expression. This allows stronger expression of the UAS construct both in the levels of expression and number of cells expressing the construct, so initially embryos were analysed at 25hpf.

Expression of all of the dominant-negative constructs in r3/r5 are mosaic, as would be expected, but seemingly do not cause cell segregation and the rhombomere boundaries remain sharp (Fig. 35). It is possible that this negative result is because the timing was not correct and/or amount of expression was not sufficient. Similarly, at earlier time points the levels of expression and number of cells expressing the dominant-negative construct per rhombomere were less and no disruption to sorting was seen (data not shown). In addition, the markers for the two UAS cassettes in the constructs (Myc and citrine) were not always co-localised in the same cell (Fig. 35). This suggests a potential problem with the expression of the dominant-negative constructs, and it was later discovered that the UAS construct vectors used were missing the E1B transcriptional start site that marks the first methionine for transcriptional initiation. This is likely to affect the levels of expression seen and could explain the poor co-expression between Myc, which acts as a marker for the DN-Dsh, and citrine, which acts as a marker for the vector itself. It was also possible that the dominant-negative constructs are not functional. Further experiments were carried out to test that the dominant-negative reagents worked when expressed at an earlier developmental stage and/or at higher levels.

7.2.2.2 Ubiquitous transgene expression at earlier stages

7.2.2.2.1 Injection of DN-Dsh constructs with Gal4 mRNA

In order to address whether the timing and/or amount of expression accounts for the lack of effect of DN-Dsh on boundary sharpness, the constructs were co-injected with Gal4 mRNA (10pg and 5pg) in wild-type embryos and disruption to boundary sharpness analysed at 16ss by *krox20 in situ* hybridisation. This was to provide earlier Gal4 expression, at higher levels and without spatial restriction, whilst maintaining mosaicism to avoid the potential problems of ubiquitous Dsh expression.

Injection of DN-Dsh with 10pg Gal4 mRNA was found to give the highest number of cells and levels of expression, but many of these embryos had either disruption to convergent extension or defects in both convergent extension and boundary sharpening (Fig. 36). Disruption to convergent extension only was seen in 25% Dsh-ΔPDZ injected embryos and 0% Dsh-WT injected embryos (Dsh-DEP+ injected

Figure 35: Expression of Dsh deletion constructs in Tg(krox20-Gal4::UAS-RFP) zebrafish embryos

Expression of Dsh deletion constructs in *Tg(krox20-Gal4::UAS-RFP)* zebrafish embryos; (A): pminiTol2-UAS-H2Bcitrine-UAS-Myc-Dsh-WT, (B): pminiTol2-UAS-H2Bcitrine-UAS-Myc-Dsh-ΔPDZ, (C): pminiTol2-UAS-H2Bcitrine-UAS-Myc-Dsh-DEP+. Embryos were co-injected with *Tol2* mRNA (25pg) at the 1-2 cell stage and fixed at 25hpf for immunostaining. Immunostaining labels the Dsh construct (α-Myc, blue, X), first UAS cassette (α-citrine, green, X') and *krox20* (α-RFP, red, X''), reported by Gal4 expression. Labelling is merged (X'''). Images show confocal Z-stack projections of the hindbrain from the dorsal view with anterior to the top. Mosaic expression of the constructs is observed and the rhombomere boundaries remain sharp.

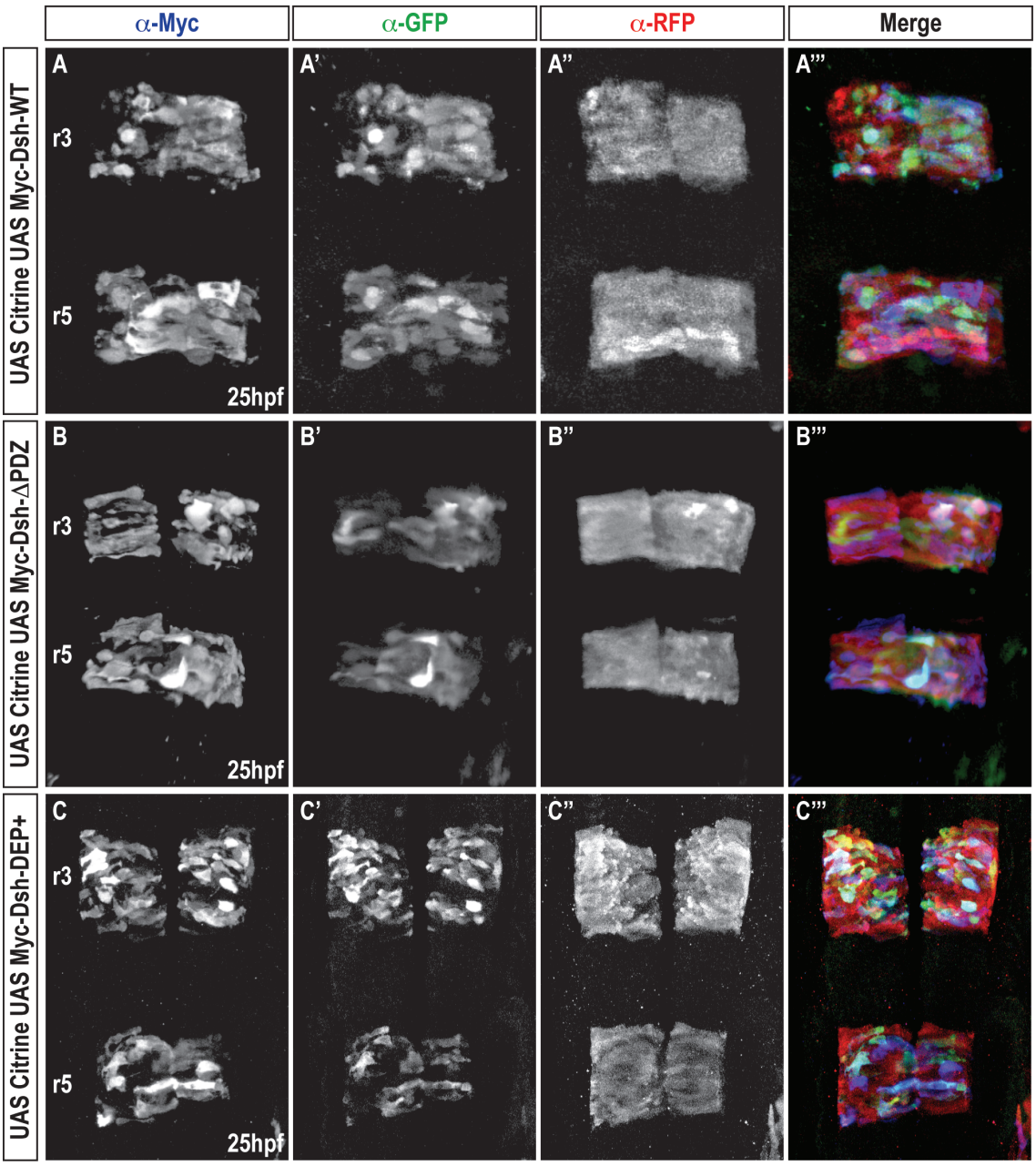
α-Myc
α-GFP
α-RFP
Merge
UAS Citrine UAS Myc-Dsh-WT
UAS Citrine UAS Myc-Dsh-ΔPDZ
UAS Citrine UAS Myc-Dsh-DEP+
A
A'
A''
A'''
B
B'
B''
B'''
C
C'
C''
C'''
r3
r5
25hpf

Figure 36: Ubiquitous expression of Dsh deletion constructs in zebrafish embryos

(A): *In situ* hybridisations showing expression of *krox20* (fast red), immunostained for the expression of Dsh deletion constructs in wild-type zebrafish embryos (α-Myc); (Aa-b): pminiTol2-UAS-H2Bcitrine-UAS-Myc-Dsh-WT, (Ac-f): pminiTol2-UAS-H2Bcitrine-UAS-Myc-Dsh-ΔPDZ, (Ag-j): pminiTol2-UAS-H2Bcitrine-UAS-Myc-Dsh-DEP+. Embryos were injected at the 1-2 cell stage with Dsh construct DNA, *Tol2* mRNA (25pg) and Gal4 mRNA (10pg) and fixed at 16ss. Images show confocal merge Z-stack projections of the zebrafish hindbrain from the dorsal view with anterior to the top. Image Aj is an example of a disruption to convergent extension. Image Ad is an example of a convergent extension phenotype and disruption to cell sorting.

(B): Table depicting quantification of embryos that have a disruption to convergent extension (CE) or convergent extension and boundary sharpness. X = not quantified.

A

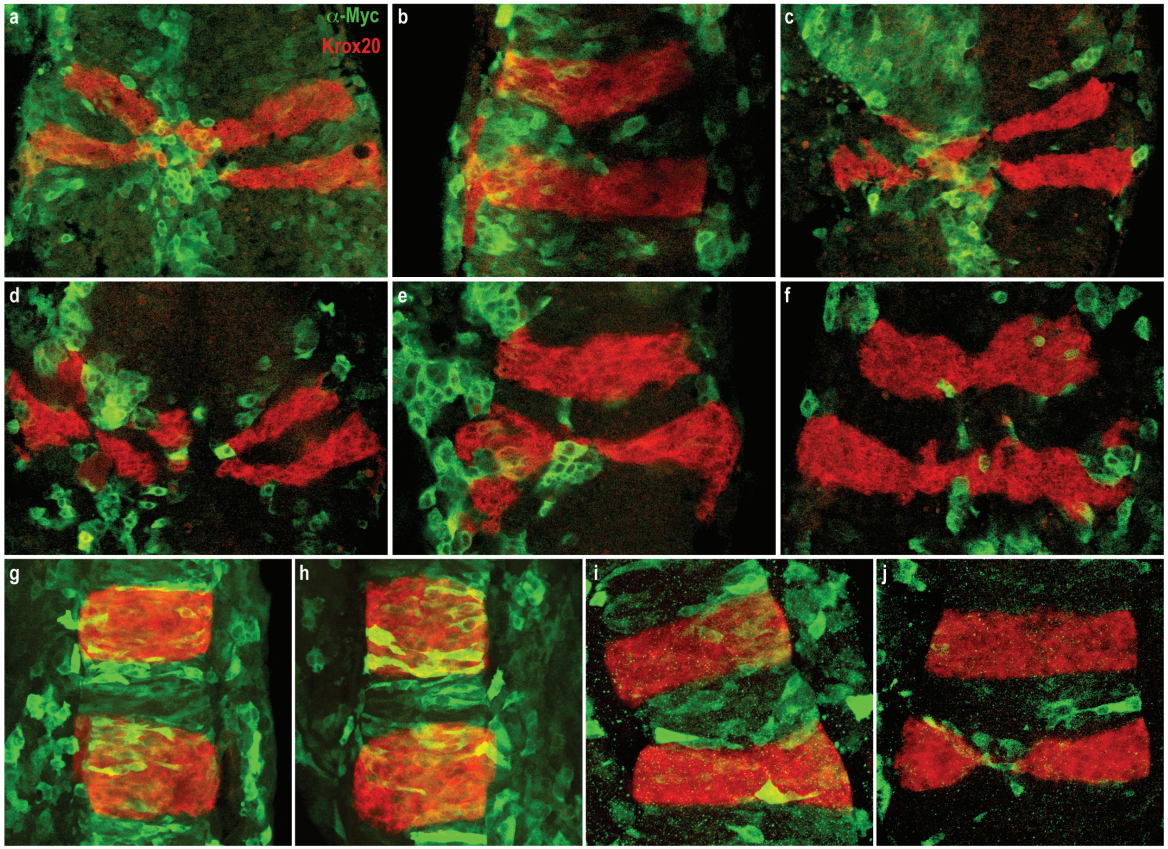

B

	Percentage of embryos injected that showed disruption	
	CE only	CE and boundary sharpness
Dsh-WT	0	50
Dsh-ΔPDZ	25	65
Dsh-DEP+	x	0

embryos not quantified). Disruption to both convergent extension and boundary sharpness was seen in 65% Dsh-ΔPDZ injected embryos (Fig. 36 A c-f), 50% Dsh-WT injected embryos (Fig. 36 A a-b) and 0% Dsh-DEP+ injected embryos (Fig. 36 A g-j) (displayed in Fig. 36 B). Interestingly, fewer boundary defects were seen in embryos injected with the dominant-negative reagent specific only to the PCP pathway (Dsh-DEP+), and when all DN-Dsh constructs were injected with smaller amounts of Gal4 (5pg, data not shown).

This suggests that Dsh-WT, Dsh-DEP+ and Dsh-ΔPDZ cause disruption to convergent extension but only Dsh-ΔPDZ and Dsh-WT may also be causing a disruption to cell sorting at rhombomere boundaries. However the results of these experiments were very variable, potentially due to variability in expression levels that could be caused by constructs lacking the E1B site. As a result, a different approach was used to try to address the same problems of timing and levels of expression of Dsh, and to test whether the DN-Dsh reagents are functional.

7.2.2.2.2 Injection of Dsh-WT or DN-Dsh mRNA

It was expected that injection of Dsh-WT or DN-Dsh mRNA (200pg) into wild-type embryos would give similar results to co-injection of UAS-DN-Dsh DNA constructs with Gal4 mRNA, due to early and ubiquitous expression provided by both methods. However, injection of DN-Dsh mRNA overcomes potential problems of expression from the DNA constructs, and so provides a better test of functionality. Hindbrain boundaries were visualised by *krox20 in situ* hybridisation, and embryos were analysed at 16ss. In both Dsh-DEP+ and Dsh-ΔPDZ mRNA-injected embryos, strong convergent extension defects, disruption to boundaries and duplicate axes were observed (Fig. 37 I-L and E-H respectively). Only convergent extension defects were observed for Dsh-WT mRNA-injected embryos (Fig. 37 A-D).

These results suggest that injection of DN-Dsh mRNA causes some disruption to sharpening of rhombomere boundaries, but these phenotypes are not consistent. This experiment confirms the results from co-injection of Dsh-ΔPDZ DNA with Gal4 mRNA in which both disruption to convergent extension and boundary sharpness were observed (Fig. 36 Ac-f), but is in contrast to experiments where Dsh-DEP+ DNA with Gal4 mRNA were co-injected in which no disruption to boundary sharpness was observed (Fig. 36 Ag-j). These results suggest a role for Dishevelled in boundary sharpening. It is not possible to distinguish the roles of the canonical Wnt or PCP pathway as both Dsh-DEP+ and Dsh-ΔPDZ mRNA-injected embryos show disruption to boundary sharpening. Analysis of all the embryos from these experiments suggests that any disruption seen is always more dorsal, affects r5 more than r3 and Dsh-ΔPDZ-expressing cells are often excluded from r5 (Fig. 36, 37). However these observations have not been quantified and the significance is not known.

Figure 37: Ubiquitous expression of Dsh deletion mRNA in zebrafish embryos

In situ hybridisations showing expression of *krox20* (fast red), immunostained for the expression of Dsh deletion mRNA in wild-type zebrafish embryos (α-Myc); (A-D): Myc-Dsh-WT, (E-H): Myc-Dsh-ΔPDZ, (I-L): Myc-Dsh-DEP+. Embryos were injected at the 1-2 cell stage with 200pg Dsh construct mRNA and fixed at 16ss. Images show confocal merge Z-stack projections of the zebrafish hindbrain from the dorsal view with anterior to the top. Embryos injected with Myc-Dsh-WT mRNA (A-D) show no phenotype or a mild disruption to convergent extension compared to embryos injected Myc-Dsh-ΔPDZ (E-H) and Dsh-DEP+ (I-L) which show a stronger disruption to convergent extension and some double axis embryos (H, K, L).

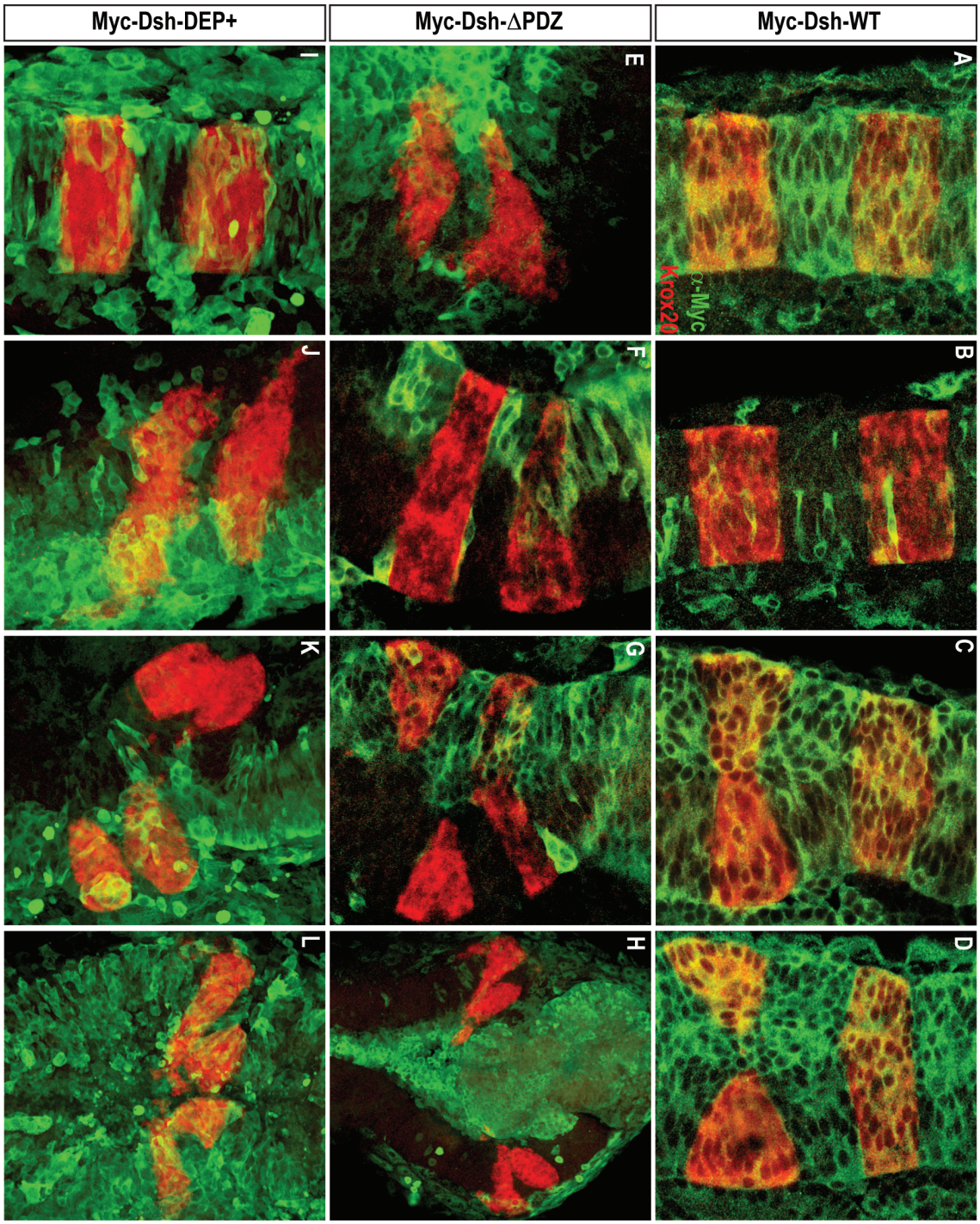
Myc-Dsh-DEP+
Myc-Dsh-ΔPDZ
Myc-Dsh-WT
I
E
A
α-Myc
Krox20
J
F
B
K
G
C
L
H
D

Dsh-WT or DN-Dsh mRNA injection is not a suitable approach for determining the role of PCP in the hindbrain, as it leads to early expression that disrupts convergent extension. As a further approach, DN-Dsh reagents were generated in a heat shock vector to enable controlled temporal expression to address this issue and bypass the role Dsh plays in early development.

7.2.2.3 Controlled temporal transgene expression

DN-Dsh cDNA was cloned into pminiTol2-HSP-MCS-Myc heat shock vectors to enable controlled temporal expression. Initially only the pminiTol2-HSP-Dsh-DEP+Myc construct was injected into embryos and the embryos were heat-shocked at 6ss (38^{o}C for 1 hour) to obtain protein expression at 8ss. The aim was to cause disruption to cell segregation at hindbrain boundaries, with stronger expression of DN-Dsh reagents, without affecting convergent extension. High levels of Myc-epitope expression were seen 2.5 hours after heat-shock for both control vector and Dsh-DEP+ expressing embryos, but no disruption to hindbrain sharpening was seen by *krox20 in situ* hybridisation in Dsh-DEP+ expressing embryos fixed at 16-18ss (Fig. 38 C-F).

7.3 DISCUSSION

7.3.1 Levels and timing of DN-Dsh expression create difficulties in analysing the role of PCP in Eph-ephrin mediated boundary formation

A number of different approaches were attempted to achieve either spatial or temporal control of high levels of expression of Dsh-WT and DN-Dsh, in order to analyse the potential role of the PCP pathway in Eph-ephrin mediated boundary sharpening in the hindbrain of the zebrafish embryo. The results from the different approaches have proved difficult to interpret, potentially due to both the levels and timing of expression of the DN-Dsh constructs, which gave extremely variable results.

7.3.1.1 Establishing functionality

A series of experiments were carried out to over-express the DN-Dsh proteins to test that the reagents were functional: co-expression of DN-Dsh DNA with Gal4 mRNA, DN-Dsh mRNA injection and controlled temporal expression using a heat-shock approach. Each of these experiments changes the timing or strength of promoter-driven expression. The combined results from all of these experiments showed that embryos expressing DN-Dsh had a disruption to convergent extension and some effect on cell sorting and

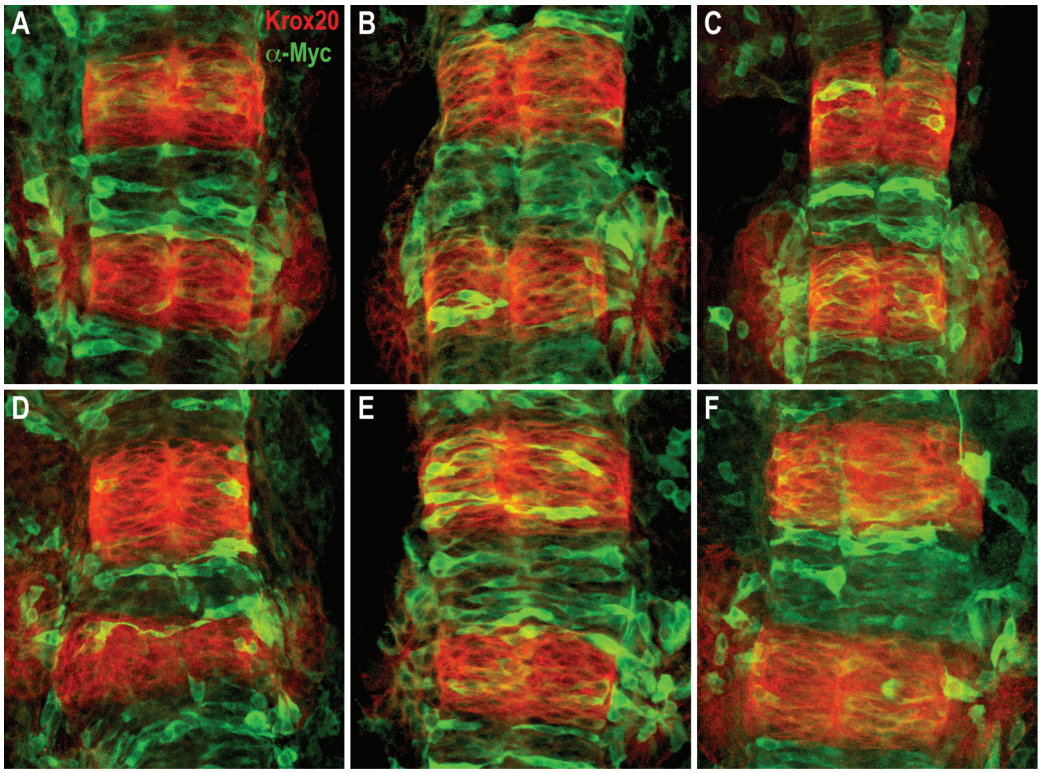

Figure 38: Temporal control of expression of Dsh-DEP+ in zebrafish embryos

Expression of Dsh-DEP+ under the control of the heat shock promoter in wild-type zebrafish embryos; (A-B): pminiTol2-HSP-MCS-Myc, (C-F): pminiTol2-HSP-Myc-Dsh-DEP+. Embryos were co-injected with *Tol2* mRNA (25pg) at the 1-2 cell stage, heat-shocked at 6ss at 38^{o}C for 1 h and fixed 2.5 h after heat-shock at 16-18ss. *In situ* hybridisation shows expression of *krox20* (fast red) and immunostaining shows the expression of construct DNA (α-Myc). Images show confocal merge Z-stack projections of the zebrafish hindbrain from the dorsal view with anterior to the top.

boundary sharpness (Fig. 36, 37). This suggests that DN-Dsh does indeed cause a disruption to convergent extension (Tada & Smith, 2000; Wallingford *et al.*, 2000) and that the DN-Dsh reagents are functional. The effect on boundary sharpness, however, was highly variable which could be due to the variability in both the numbers of cells expressing the reagents and the levels of expression.

As discussed previously, the results from mRNA injection or heat-shock expression of DN-Dsh are more likely to be reliable than UAS-construct expression, as these approaches overcome the likely problems of UAS-construct expression that lacks an E1B site: this problem was only uncovered in the late phase of the studies. Embryos expressing Dsh-ΔPDZ mRNA, which is able to inhibit the canonical Wnt pathway as well as the PCP pathway, or Dsh-DEP+ mRNA, which specifically inhibits the PCP pathway, show a similar disruption to convergent extension and boundary sharpness (Fig. 37). However, when Dsh-DEP+ is expressed at a later stage using heat-shock, there was no disruption to either boundary sharpness or convergent extension. The discrepancies between these results seen on inhibiting the PCP pathway could be due to the timing of expression; the active period of cell sorting is 1-10ss (Cooke *et al.*, 2005), and so heat-shock at 6ss might be too late to see a clear effect on disruption to boundaries. It will be important to test this at earlier stages of heat-shock. It is clear that disrupting the function of Dishevelled can disrupt convergent extension and boundary sharpness, but whether this is due to interference with the canonical Wnt or PCP pathway needs to be determined. This can be done by comparing disruption to convergent extension and boundary sharpness with that seen on injection with DN-Dsh proteins specific to the canonical pathway (Dsh-ΔDIX) or other proteins specific to the PCP pathway (DN-Daam).

Expression of Dsh-ΔPDZ in *Xenopus* has previously been shown to cause irregular shaped and distorted rhombomeres (r3/r5) (Tanaka *et al.*, 2003), but the expression of Dsh-WT did not. This disruption to hindbrain segmentation is thought to be independent of convergent extension (Tanaka *et al.*, 2003). Our results showed that all embryos expressing DN-Dsh that had a disruption to boundary sharpness also had a disruption to convergent extension, and overexpression of Dsh-WT also causes defects in both convergent extension and boundary sharpness. However, convergent extension and cell segregation that leads to boundary sharpening are two different processes. Therefore, we assume that the processes of convergent extension and boundary sharpening are independent, but an effect of disrupted convergent extension on boundary sharpening cannot be ruled out.

Taken together, this suggests that ubiquitous expression of DN-Dsh is not an ideal approach for determining roles in the hindbrain, as it leads to early expression that disrupts convergent extension and potentially other processes. It remains a problem that the early period of convergent extension that occurs in embryonic development overlaps with the period of active cell sorting at rhombomere boundaries (1-10ss) (Cooke *et al.*, 2005). We can however conclude that the reagents are functional when expressed at high levels or early in development and that disrupting the function of Dsh does cause defects in both convergent extension and boundary sharpening.

7.3.1.2 The problems of spatial rhombomeric expression

The approach I took to analyse a role of the PCP pathway in Eph-ephrin mediated boundary formation independently of convergent extension was to target expression of DN-Dsh to r3/r5. However, mosaic expression had no effect on the sharpening of the r3/r5 boundaries of 25hpf embryos (Fig. 35). This could be because the timing of analysis was too late to see a disruption to boundary sharpness, but at earlier time points the levels of expression and number of cells expressing the dominant-negative construct per rhombomere were much less, and no disruption to boundary sharpening was seen (data not shown). A possible factor is the timing of expression; Gal4 mRNA is not produced until the 3ss stage (Tomomi Watanabe, unpublished observations), so construct expression might occur too late (6ss) or at too low a level to have an effect on cell sorting, for which the active period is between 1ss and 10ss (Cooke *et al.*, 2005). A likely problem when targeting the expression of DN-Dsh to r3/r5 is insufficient expression of the protein due to the constructs missing the E1B site for transcriptional initiation. Both the number of cells that express the reagent and levels of expression in the hindbrain are critical for this assay in order to visualise disruption to boundary sharpening. This is highlighted by the functionality tests of the constructs, where ubiquitous expression of these reagents often caused defects in boundary sharpening. It would be possible to add more UAS sequences to the constructs in order to increase the levels of expression of the dominant-negative reagents, but the DN-Dsh reagents should also be re-cloned into the UAS constructs containing the corrected E1B site, and the previous experiments repeated with these constructs.

In addition, the numbers of cells expressing the DN-Dsh reagents in r3/r5 are low when ubiquitous expression approaches are used, compared to the surrounding even-numbered rhombomeres, and it cannot be ruled out that overexpression of DN-Dsh causes cell-specific apoptosis. As a consequence, in experiments where expression of DN-Dsh is targeted to r3/r5, fewer DN-Dsh expressing cells would remain or those that survive would express lower levels. This could potentially contribute to the mosaicism seen. The effect of expressing DN-Dsh on the induction of apoptosis could be tested using immunostaining to caspases.

7.3.1.3 Cell identity switching

Disruption to boundary sharpening could not be easily distinguished across the range of techniques attempted, and was variable within experiments. Single or small groups of cells are known to be able to switch identity when transplanted between hindbrain segments (Schilling *et al.*, 2001; Trainor & Krumlauf, 2000), and this plasticity is likely to contribute to the maintenance of sharp borders. Therefore a possible limiting factor is that detection of *krox20* expression is not a sensitive enough read-out of increased cell intermingling due to the phenomenon of cell identity switching. However, this is unlikely as knockdown of EphA4 shows a disruption to the boundaries of *krox20* expression (Cooke *et al.*, 2005), and in addition the

perdurance of RFP in our experiments potentially allows visualisation of disruption to boundaries at later stages when *krox20* staining is normally sharp.

7.3.2 Further work

It remains important to have a positive control to test the reliability of the assay, for example that disrupting EphA4 function by the same transgenic approach used to disrupt PCP does cause disruption to hindbrain boundary sharpening. This could be addressed by the transgenic expression of DN-EphA4 in wild-type zebrafish embryos and analysing the disruption to boundary sharpening by *krox20* expression.

If a disruption to boundary sharpening is seen from expression of DN-Dsh proteins it would be interesting to test whether downstream PCP components also mediate a cell segregation response. Analysis of Dvl1a, 1b, 2a, 2b, 3, 3l, Daam1, 2 and 1l expression may be informative as there is some evidence for a more restricted expression pattern of specific PCP genes in other species: for example mouse Daam2 expression is restricted to r3/r5 at 17ss (Nakaya *et al.*, 2004). If a spatially restricted expression pattern is seen, morpholinos could be used to target expression to endogenous expression domains to analyse the role of the PCP pathway in boundary sharpening. In addition, transplants of PCP morpholino-injected cells into wild-type embryos would allow the analysis of knockdown of PCP in a mosaic manner.

Recruitment of Dsh to the cell membrane is a hallmark of PCP signalling and is important for the function of this pathway (Axelrod *et al.*, 1998; Boutros & Mlodzik, 1999; Poliakov *et al.*, 2004). In another approach, analysis of the localisation of PCP components and polarisation of cells at hindbrain boundaries would clarify whether these are consistent with a role of this pathway in the hindbrain. In addition it would be interesting to study whether cell polarity is altered in embryos in which PCP signalling has been disrupted i.e. Golgi orientation (to analyse cell orientation) or subcellular localisation of other PCP components, in embryos expressing DN-Dsh constructs or in wild-type embryos with transplanted cells from a DshMO or DaamMO injected donor embryo.

We can conclude from these studies that ubiquitous expression of dominant-negative Dishevelled (for both the PCP and canonical Wnt pathway) causes disruption to convergent extension and r3/r5 boundary sharpening *in vivo*. The approaches used had various technical limitations, which made analysis difficult. As a result, studies subsequently focussed on the relationship between PCP and Eph-ephrin signalling *in vitro.*

BIBLIOGRAPHY

Abercrombie, M. (1970). Contact inhibition in tissue culture. *In Vitro* **6**, 128-142.

Alexander, T., Nolte, C. & Krumlauf, R. (2009). Hox genes and segmentation of the hindbrain and axial skeleton. *Annual review of cell and developmental biology* **25**, 431-456.

Ang, S. F., Zhao, Z. S., Lim, L. & Manser, E. (2010). DAAM1 is a formin required for centrosome re-orientation during cell migration. *PLoS One* **5**.

Astin, J. W., Batson, J., Kadir, S., Charlet, J., Persad, R. A., Gillatt, D., Oxley, J. D. & Nobes, C. D. (2010). Competition amongst Eph receptors regulates contact inhibition of locomotion and invasiveness in prostate cancer cells. *Nature cell biology* **12**, 1194-1204.

Axelrod, J. D., Miller, J. R., Shulman, J. M., Moon, R. T. & Perrimon, N. (1998). Differential recruitment of Dishevelled provides signaling specificity in the planar cell polarity and Wingless signaling pathways. *Genes & development* **12**, 2610-2622.

Bass, M. D., Roach, K. A., Morgan, M. R. & other authors (2007). Syndecan-4-dependent Rac1 regulation determines directional migration in response to the extracellular matrix. *The Journal of cell biology* **177**, 527-538.

Batlle, E., Henderson, J. T., Beghtel, H. & other authors (2002). Beta-catenin and TCF mediate cell positioning in the intestinal epithelium by controlling the expression of EphB/ephrinB. *Cell* **111**, 251-263.

Becker, N., Seitanidou, T., Murphy, P., Mattei, M. G., Topilko, P., Nieto, M. A., Wilkinson, D. G., Charnay, P. & Gilardi-Hebenstreit, P. (1994). Several receptor tyrosine kinase genes of the Eph family are segmentally expressed in the developing hindbrain. *Mechanisms of development* **47**, 3-17.

Bell, E., Wingate, R. J. & Lumsden, A. (1999). Homeotic transformation of rhombomere identity after localized Hoxb1 misexpression. *Science (New York, NY* **284**, 2168-2171.

Bingham, S., Higashijima, S., Okamoto, H. & Chandrasekhar, A. (2002). The Zebrafish trilobite gene is essential for tangential migration of branchiomotor neurons. *Developmental biology* **242**, 149-160.

Birgbauer, E. & Fraser, S. E. (1994). Violation of cell lineage restriction compartments in the chick hindbrain. *Development (Cambridge, England)* **120**, 1347-1356.

Bochenek, M. L., Dickinson, S., Astin, J. W., Adams, R. H. & Nobes, C. D. (2010). Ephrin-B2 regulates endothelial cell morphology and motility independently of Eph-receptor binding. *J Cell Sci* **123**, 1235-1246.

Boutros, M., Paricio, N., Strutt, D. I. & Mlodzik, M. (1998). Dishevelled activates JNK and discriminates between JNK pathways in planar polarity and wingless signaling. *Cell* **94**, 109-118.

Boutros, M. & Mlodzik, M. (1999). Dishevelled: at the crossroads of divergent intracellular signaling pathways. *Mechanisms of development* **83**, 27-37.

Carmona-Fontaine, C., Matthews, H. K., Kuriyama, S., Moreno, M., Dunn, G. A., Parsons, M., Stern, C. D. & Mayor, R. (2008). Contact inhibition of locomotion in vivo controls neural crest directional migration. *Nature* **456**, 957-961.

Carreira-Barbosa, F., Concha, M. L., Takeuchi, M., Ueno, N., Wilson, S. W. & Tada, M. (2003). Prickle 1 regulates cell movements during gastrulation and neuronal migration in zebrafish. *Development (Cambridge, England)* **130**, 4037-4046.

Carvalho, R. F., Beutler, M., Marler, K. J., Knoll, B., Becker-Barroso, E., Heintzmann, R., Ng, T. & Drescher, U. (2006). Silencing of EphA3 through a cis interaction with ephrinA5. *Nat Neurosci* **9**, 322-330.

Cau, J. & Hall, A. (2005). Cdc42 controls the polarity of the actin and microtubule cytoskeletons through two distinct signal transduction pathways. *J Cell Sci* **118**, 2579-2587.

Cheng, Y. C., Amoyel, M., Qiu, X., Jiang, Y. J., Xu, Q. & Wilkinson, D. G. (2004). Notch activation regulates the segregation and differentiation of rhombomere boundary cells in the zebrafish hindbrain. *Developmental cell* **6**, 539-550.

Christensen, J. H., Soerensen, M. B., Linghui, Z., Chen, S. & Jensen, M. O. (2010). Pre-diagnostic digital imaging prediction model to discriminate between malignant melanoma and benign pigmented skin lesion. *Skin Res Technol* **16**, 98-108.

Clarke, J. D. & Lumsden, A. (1993). Segmental repetition of neuronal phenotype sets in the chick embryo hindbrain. *Development (Cambridge, England)* **118**, 151-162.

Cooke, J. E., Kemp, H. A. & Moens, C. B. (2005). EphA4 Is Required for Cell Adhesion and Rhombomere-Boundary Formation in the Zebrafish. *Current Biology* **15**, 536-542.

Cortina, C., Palomo-Ponce, S., Iglesias, M. & other authors (2007). EphB-ephrin-B interactions suppress colorectal cancer progression by compartmentalizing tumor cells. *Nat Genet*.

Cowan, C. A. & Henkemeyer, M. (2001). The SH2/SH3 adaptor Grb4 transduces B-ephrin reverse signals. *Nature* **413**, 174-179.

Cowan, C. W., Shao, Y. R., Sahin, M. & other authors (2005). Vav family GEFs link activated Ephs to endocytosis and axon guidance. *Neuron* **46**, 205-217.

Dahmann, C., Oates, A. C. & Brand, M. (2011). Boundary formation and maintenance in tissue development. *Nat Rev Genet* **12**, 43-55.

Davis, S., Gale, N. W., Aldrich, T. H., Maisonpierre, P. C., Lhotak, V., Pawson, T., Goldfarb, M. & Yancopoulos, G. D. (1994). Ligands for EPH-related receptor tyrosine kinases that require membrane attachment or clustering for activity. *Science (New York, NY* **266**, 816-819.

de Anda, F. C., Pollarolo, G., Da Silva, J. S., Camoletto, P. G., Feiguin, F. & Dotti, C. G. (2005). Centrosome localization determines neuronal polarity. *Nature* **436**, 704-708.

De Calisto, J., Araya, C., Marchant, L., Riaz, C. F. & Mayor, R. (2005). Essential role of non-canonical Wnt signalling in neural crest migration. *Development (Cambridge, England)* **132**, 2587-2597.

Depaepe, V., Suarez-Gonzalez, N., Dufour, A., Passante, L., Gorski, J. A., Jones, K. R., Ledent, C. & Vanderhaeghen, P. (2005). Ephrin signalling controls brain size by regulating apoptosis of neural progenitors. *Nature* **435**, 1244-1250.

Desai, R. A., Gao, L., Raghavan, S., Liu, W. F. & Chen, C. S. (2009). Cell polarity triggered by cell-cell adhesion via E-cadherin. *J Cell Sci* **122**, 905-911.

DiMilla, P. A., Stone, J. A., Quinn, J. A., Albelda, S. M. & Lauffenburger, D. A. (1993). Maximal migration of human smooth muscle cells on fibronectin and type IV collagen occurs at an intermediate attachment strength. *The Journal of cell biology* **122**, 729-737.

Distel, M., Wullimann, M. F. & Koster, R. W. (2009). Optimized Gal4 genetics for permanent gene expression mapping in zebrafish. *Proceedings of the National Academy of Sciences of the United States of America* **106**, 13365-13370.

Distel, M., Hocking, J. C., Volkmann, K. & Koster, R. W. (2010). The centrosome neither persistently leads migration nor determines the site of axonogenesis in migrating neurons in vivo. *The Journal of cell biology* **191**, 875-890.

Duguay, D., Foty, R. A. & Steinberg, M. S. (2003). Cadherin-mediated cell adhesion and tissue segregation: qualitative and quantitative determinants. *Developmental biology* **253**, 309-323.

Dupin, I., Camand, E. & Etienne-Manneville, S. (2009). Classical cadherins control nucleus and centrosome position and cell polarity. *The Journal of cell biology* **185**, 779-786.

Eaton, S., Wepf, R. & Simons, K. (1996). Roles for Rac1 and Cdc42 in planar polarization and hair outgrowth in the wing of Drosophila. *The Journal of cell biology* **135**, 1277-1289.

Egea, J. & Klein, R. (2007). Bidirectional Eph-ephrin signaling during axon guidance. *Trends Cell Biol* **17**, 230-238.

EphNomenclatureCommittee (1997). Unified Nomenclature for Eph Family Receptors and Their Ligands, the Ephrins. *Cell* **90**, 403-404.

Etienne-Manneville, S. & Hall, A. (2001). Integrin-mediated activation of Cdc42 controls cell polarity in migrating astrocytes through PKCzeta. *Cell* **106**, 489-498.

Etienne-Manneville, S. & Hall, A. (2003). Cdc42 regulates GSK-3beta and adenomatous polyposis coli to control cell polarity. *Nature* **421**, 753-756.

Fijnvandraat, A. C., van Ginneken, A. C., de Boer, P. A., Ruijter, J. M., Christoffels, V. M., Moorman, A. F. & Lekanne Deprez, R. H. (2003). Cardiomyocytes derived from embryonic stem cells resemble cardiomyocytes of the embryonic heart tube. *Cardiovasc Res* **58**, 399-409.

Flanagan, J. G. & Vanderhaeghen, P. (1998). The Ephrins and EPH Receptors in Neural Development. *Annual Review of Neuroscience* **21**, 309-346.

Flenniken, A. M., Gale, N. W., Yancopoulos, G. D. & Wilkinson, D. G. (1996). Distinct and overlapping expression patterns of ligands for Eph-related receptor tyrosine kinases during mouse embryogenesis. *Developmental biology* **179**, 382-401.

Foo, S. S., Turner, C. J., Adams, S. & other authors (2006). Ephrin-B2 controls cell motility and adhesion during blood-vessel-wall assembly. *Cell* **124**, 161-173.

Foty, R. A. & Steinberg, M. S. (2004). Cadherin-mediated cell-cell adhesion and tissue segregation in relation to malignancy. *Int J Dev Biol* **48**, 397-409.

Foty, R. A. & Steinberg, M. S. (2005). The differential adhesion hypothesis: a direct evaluation. *Developmental biology* **278**, 255-263.

Fraser, S., Keynes, R. & Lumsden, A. (1990). Segmentation in the chick embryo hindbrain is defined by cell lineage restrictions. *Nature* **344**, 431-435.

Gale, N. W., Holland, S. J., Valenzuela, D. M. & other authors (1996). Eph receptors and ligands comprise two major specificity subclasses and are reciprocally compartmentalized during embryogenesis. *Neuron* **17**, 9-19.

Gao, C. & Chen, Y. G. (2010). Dishevelled: The hub of Wnt signaling. *Cell Signal* **22**, 717-727.

Garcia-Bellido, A. & Santamaria, P. (1972). Developmental analysis of the wing disc in the mutant engrailed of Drosophila melanogaster. *Genetics* **72**, 87-104.

Garcia-Bellido, A., Ripoll, P. & Morata, G. (1973). Developmental compartmentalisation of the wing disk of Drosophila. *Nat New Biol* **245**, 251-253.

Garcia-Bellido, A. (1975). Genetic control of wing disc development in Drosophila. *Ciba Found Symp* **0**, 161-182.

Gavalas, A., Studer, M., Lumsden, A., Rijli, F. M., Krumlauf, R. & Chambon, P. (1998). Hoxa1 and Hoxb1 synergize in patterning the hindbrain, cranial nerves and second pharyngeal arch. *Development (Cambridge, England)* **125**, 1123-1136.

Gavalas, A., Ruhrberg, C., Livet, J., Henderson, C. E. & Krumlauf, R. (2003). Neuronal defects in the hindbrain of Hoxa1, Hoxb1 and Hoxb2 mutants reflect regulatory interactions among these Hox genes. *Development (Cambridge, England)* **130**, 5663-5679.

Georgiou, M., Marinari, E., Burden, J. & Baum, B. (2008). Cdc42, Par6, and aPKC regulate Arp2/3-mediated endocytosis to control local adherens junction stability. *Curr Biol* **18**, 1631-1638.

Georgiou, M. & Baum, B. (2010). Polarity proteins and Rho GTPases cooperate to spatially organise epithelial actin-based protrusions. *J Cell Sci* **123**, 1089-1098.

Gerety, S. S. & Wilkinson, D. G. (2011). Morpholino artifacts provide pitfalls and reveal a novel role for pro-apoptotic genes in hindbrain boundary development. *Developmental biology* **350**, 279-289.

Giudicelli, F., Taillebourg, E., Charnay, P. & Gilardi-Hebenstreit, P. (2001). Krox-20 patterns the hindbrain through both cell-autonomous and non cell-autonomous mechanisms. *Genes & development* **15**, 567-580.

Goldstein, B. & Macara, I. G. (2007). The PAR proteins: fundamental players in animal cell polarization. *Developmental cell* **13**, 609-622.

Gomes, E. R., Jani, S. & Gundersen, G. G. (2005). Nuclear movement regulated by Cdc42, MRCK, myosin, and actin flow establishes MTOC polarization in migrating cells. *Cell* **121**, 451-463.

Gong, Y., Mo, C. & Fraser, S. E. (2004). Planar cell polarity signalling controls cell division orientation during zebrafish gastrulation. *Nature* **430**, 689-693.

Graham, A., Papalopulu, N. & Krumlauf, R. (1989). The murine and Drosophila homeobox gene complexes have common features of organization and expression. *Cell* **57**, 367-378.

Grant, P. K. & Moens, C. B. (2010). The neuroepithelial basement membrane serves as a boundary and a substrate for neuron migration in the zebrafish hindbrain. *Neural Dev* **5**, 9.

Greer, J. M., Puetz, J., Thomas, K. R. & Capecchi, M. R. (2000). Maintenance of functional equivalence during paralogous Hox gene evolution. *Nature* **403**, 661-665.

Groeger, G. & Nobes, C. D. (2007). Co-operative Cdc42 and Rho signalling mediates ephrinB-triggered endothelial cell retraction. *Biochem J* **404**, 23-29.

Gros, J., Serralbo, O. & Marcelle, C. (2009). WNT11 acts as a directional cue to organize the elongation of early muscle fibres. *Nature* **457**, 589-593.

Guthrie, S. & Lumsden, A. (1991). Formation and regeneration of rhombomere boundaries in the developing chick hindbrain. *Development (Cambridge, England)* **112**, 221-229.

Guthrie, S., Prince, V. & Lumsden, A. (1993). Selective dispersal of avian rhombomere cells in orthotopic and heterotopic grafts. *Development (Cambridge, England)* **118**, 527-538.

Habas, R., Kato, Y. & He, X. (2001). Wnt/Frizzled activation of Rho regulates vertebrate gastrulation and requires a novel Formin homology protein Daam1. *Cell* **107**, 843-854.

Habas, R., Dawid, I. B. & He, X. (2003). Coactivation of Rac and Rho by Wnt/Frizzled signaling is required for vertebrate gastrulation. *Genes & development* **17**, 295-309.

Hansen, M. J., Dallal, G. E. & Flanagan, J. G. (2004). Retinal axon response to ephrin-as shows a graded, concentration-dependent transition from growth promotion to inhibition. *Neuron* **42**, 717-730.

Harms, B. D., Bassi, G. M., Horwitz, A. R. & Lauffenburger, D. A. (2005). Directional persistence of EGF-induced cell migration is associated with stabilization of lamellipodial protrusions. *Biophys J* **88**, 1479-1488.

Hattori, M., Osterfield, M. & Flanagan, J. G. (2000). Regulated cleavage of a contact-mediated axon repellent. *Science (New York, NY* **289**, 1360-1365.

Heyman, I., Kent, A. & Lumsden, A. (1993). Cellular morphology and extracellular space at rhombomere boundaries in the chick embryo hindbrain. *Dev Dyn* **198**, 241-253.

Heyman, I., Faissner, A. & Lumsden, A. (1995). Cell and matrix specialisations of rhombomere boundaries. *Dev Dyn* **204**, 301-315.

Holley, R. W. & Kiernan, J. A. (1968). "Contact inhibition" of cell division in 3T3 cells. *Proceedings of the National Academy of Sciences of the United States of America* **60**, 300-304.

Holmberg, J., Genander, M., Halford, M. M., Anneren, C., Sondell, M., Chumley, M. J., Silvany, R. E., Henkemeyer, M. & Frisen, J. (2006). EphB receptors coordinate migration and proliferation in the intestinal stem cell niche. *Cell* **125**, 1151-1163.

Hueck, I. S., Hollweg, H. G., Schmid-Schonbein, G. W. & Artmann, G. M. (2000). Chlorpromazine modulates the morphological macro- and microstructure of endothelial cells. *Am J Physiol Cell Physiol* **278**, C873-878.

Huelsken, J. & Birchmeier, W. (2001). New aspects of Wnt signaling pathways in higher vertebrates. *Current opinion in genetics & development* **11**, 547-553.

Huynh-Do, U., Stein, E., Lane, A. A., Liu, H., Cerretti, D. P. & Daniel, T. O. (1999). Surface densities of ephrin-B1 determine EphB1-coupled activation of cell attachment through alphavbeta3 and alpha5beta1 integrins. *The EMBO journal* **18**, 2165-2173.

Iden, S. & Collard, J. G. (2008). Crosstalk between small GTPases and polarity proteins in cell polarization. *Nat Rev Mol Cell Biol* **9**, 846-859.

Inoue, T., Tanaka, T., Takeichi, M., Chisaka, O., Nakamura, S. & Osumi, N. (2001). Role of cadherins in maintaining the compartment boundary between the cortex and striatum during development. *Development (Cambridge, England)* **128**, 561-569.

Irvine, K. D. & Rauskolb, C. (2001). Boundaries in development: formation and function. *Annual review of cell and developmental biology* **17**, 189-214.

Irving, C., Flenniken, A., Alldus, G. & Wilkinson, D. G. (1996). Cell-cell interactions and segmentation in the developing vertebrate hindbrain. *Biochem Soc Symp* **62**, 85-95.

Jaffe, A. B. & Hall, A. (2005). Rho GTPases: biochemistry and biology. *Annual review of cell and developmental biology* **21**, 247-269.

Janes, P. W., Saha, N., Barton, W. A. & other authors (2005). Adam meets Eph: an ADAM substrate recognition module acts as a molecular switch for ephrin cleavage in trans. *Cell* **123**, 291-304.

Joberty, G., Petersen, C., Gao, L. & Macara, I. G. (2000). The cell-polarity protein Par6 links Par3 and atypical protein kinase C to Cdc42. *Nature cell biology* **2**, 531-539.

Jorgensen, C., Sherman, A., Chen, G. I. & other authors (2009). Cell-specific information processing in segregating populations of Eph receptor ephrin-expressing cells. *Science (New York, NY* **326**, 1502-1509.

Ju, R., Cirone, P., Lin, S., Griesbach, H., Slusarski, D. C. & Crews, C. M. (2010). Activation of the planar cell polarity formin DAAM1 leads to inhibition of endothelial cell proliferation, migration, and angiogenesis. *Proceedings of the National Academy of Sciences of the United States of America* **107**, 6906-6911.

Kardash, E., Reichman-Fried, M., Maitre, J. L., Boldajipour, B., Papusheva, E., Messerschmidt, E. M., Heisenberg, C. P. & Raz, E. (2009). A role for Rho GTPases and cell-cell adhesion in single-cell motility in vivo. *Nature cell biology* **12**, 47-53; sup pp 41-11.

Kawakami, K., Shima, A. & Kawakami, N. (2000). Identification of a functional transposase of the Tol2 element, an Ac-like element from the Japanese medaka fish, and its transposition in the zebrafish germ lineage. *Proceedings of the National Academy of Sciences of the United States of America* **97**, 11403-11408.

Kemp, H. A., Cooke, J. E. & Moens, C. B. (2009). EphA4 and EfnB2a maintain rhombomere coherence by independently regulating intercalation of progenitor cells in the zebrafish neural keel. *Developmental biology* **327**, 313-326.

Kida, Y. S., Sato, T., Miyasaka, K. Y., Suto, A. & Ogura, T. (2007). Daam1 regulates the endocytosis of EphB during the convergent extension of the zebrafish notochord. *Proceedings of the National Academy of Sciences of the United States of America* **104**, 6708-6713.

Kiecker, C. & Lumsden, A. (2005). Compartments and their boundaries in vertebrate brain development. *Nature reviews* **6**, 553-564.

Kimmel, C. B., Ballard, W. W., Kimmel, S. R., Ullmann, B. & Schilling, T. F. (1995). Stages of embryonic development of the zebrafish. *Dev Dyn* **203**, 253-310.

Klein, R. (2004). Eph/ephrin signaling in morphogenesis, neural development and plasticity. *Curr Opin Cell Biol* **16**, 580-589.

Klein, R. (2009). Bidirectional modulation of synaptic functions by Eph/ephrin signaling. *Nat Neurosci* **12**, 15-20.

Knoll, B. & Drescher, U. (2004). Src family kinases are involved in EphA receptor-mediated retinal axon guidance. *J Neurosci* **24**, 6248-6257.

Koshida, S., Kishimoto, Y., Ustumi, H., Shimizu, T., Furutani-Seiki, M., Kondoh, H. & Takada, S. (2005). Integrinalpha5-dependent fibronectin accumulation for maintenance of somite boundaries in zebrafish embryos. *Developmental cell* **8**, 587-598.

Krieg, M., Arboleda-Estudillo, Y., Puech, P. H., Kafer, J., Graner, F., Muller, D. J. & Heisenberg, C. P. (2008). Tensile forces govern germ-layer organization in zebrafish. *Nature cell biology* **10**, 429-436.

Kullander, K. & Klein, R. (2002). Mechanisms and functions of Eph and ephrin signalling. *Nat Rev Mol Cell Biol* **3**, 475-486.

Kupfer, A., Louvard, D. & Singer, S. J. (1982). Polarization of the Golgi apparatus and the microtubule-organizing center in cultured fibroblasts at the edge of an experimental wound. *Proceedings of the National Academy of Sciences of the United States of America* **79**, 2603-2607.

LaMonica, K., Bass, M. & Grabel, L. (2009). The planar cell polarity pathway directs parietal endoderm migration. *Developmental biology* **330**, 44-53.

Landsberg, K. P., Farhadifar, R., Ranft, J., Umetsu, D., Widmann, T. J., Bittig, T., Said, A., Julicher, F. & Dahmann, C. (2009). Increased cell bond tension governs cell sorting at the Drosophila anteroposterior compartment boundary. *Curr Biol* **19**, 1950-1955.

Langheinrich, U., Hennen, E., Stott, G. & Vacun, G. (2002). Zebrafish as a model organism for the identification and characterization of drugs and genes affecting p53 signaling. *Curr Biol* **12**, 2023-2028.

Lawrence, P. A. (1973). A clonal analysis of segment development in Oncopeltus (Hemiptera). *J Embryol Exp Morphol* **30**, 681-699.

Lecuit, T. & Lenne, P. F. (2007). Cell surface mechanics and the control of cell shape, tissue patterns and morphogenesis. *Nat Rev Mol Cell Biol* **8**, 633-644.

Lee, H. S., Bong, Y. S., Moore, K. B., Soria, K., Moody, S. A. & Daar, I. O. (2006). Dishevelled mediates ephrinB1 signalling in the eye field through the planar cell polarity pathway. *Nature cell biology* **8**, 55-63.

Lee, H. S., Nishanian, T. G., Mood, K., Bong, Y. S. & Daar, I. O. (2008). EphrinB1 controls cell-cell junctions through the Par polarity complex. *Nature cell biology* **10**, 979-986.

Lee, H. S., Mood, K., Battu, G., Ji, Y. J., Singh, A. & Daar, I. O. (2009). Fibroblast growth factor receptor-induced phosphorylation of ephrinB1 modulates its interaction with Dishevelled. *Mol Biol Cell* **20**, 124-133.

Lekanne Deprez, R. H., Fijnvandraat, A. C., Ruijter, J. M. & Moorman, A. F. (2002). Sensitivity and accuracy of quantitative real-time polymerase chain reaction using SYBR green I depends on cDNA synthesis conditions. *Anal Biochem* **307**, 63-69.

Lewis, E. B. (1978). A gene complex controlling segmentation in Drosophila. *Nature* **276**, 565-570.

Lin, D., Edwards, A. S., Fawcett, J. P., Mbamalu, G., Scott, J. D. & Pawson, T. (2000). A mammalian PAR-3-PAR-6 complex implicated in Cdc42/Rac1 and aPKC signalling and cell polarity. *Nature cell biology* **2**, 540-547.

Lumsden, A. & Keynes, R. (1989). Segmental patterns of neuronal development in the chick hindbrain. *Nature* **337**, 424-428.

Lumsden, A. & Krumlauf, R. (1996). Patterning the vertebrate neuraxis. *Science (New York, NY* **274**, 1109-1115.

Maconochie, M., Nonchev, S., Morrison, A. & Krumlauf, R. (1996). Paralogous Hox genes: function and regulation. *Annu Rev Genet* **30**, 529-556.

Mahmood, R., Kiefer, P., Guthrie, S., Dickson, C. & Mason, I. (1995). Multiple roles for FGF-3 during cranial neural development in the chicken. *Development (Cambridge, England)* **121**, 1399-1410.

Major, R. J. & Irvine, K. D. (2005). Influence of Notch on dorsoventral compartmentalization and actin organization in the Drosophila wing. *Development (Cambridge, England)* **132**, 3823-3833.

Major, R. J. & Irvine, K. D. (2006). Localization and requirement for Myosin II at the dorsal-ventral compartment boundary of the Drosophila wing. *Dev Dyn* **235**, 3051-3058.

Malliri, A., van Es, S., Huveneers, S. & Collard, J. G. (2004). The Rac exchange factor Tiam1 is required for the establishment and maintenance of cadherin-based adhesions. *J Biol Chem* **279**, 30092-30098.

Margolis, S. S., Salogiannis, J., Lipton, D. M. & other authors (2010). EphB-mediated degradation of the RhoA GEF Ephexin5 relieves a developmental brake on excitatory synapse formation. *Cell* **143**, 442-455.

Marquardt, T., Shirasaki, R., Ghosh, S., Andrews, S. E., Carter, N., Hunter, T. & Pfaff, S. L. (2005). Coexpressed EphA receptors and ephrin-A ligands mediate opposing actions on growth cone navigation from distinct membrane domains. *Cell* **121**, 127-139.

Marston, D. J., Dickinson, S. & Nobes, C. D. (2003). Rac-dependent trans-endocytosis of ephrinBs regulates Eph-ephrin contact repulsion. *Nature cell biology* **5**, 879-888.

Martens, L., Monsieur, G., Ampe, C., Gevaert, K. & Vandekerckhove, J. (2006). Cell_motility: a cross-platform, open source application for the study of cell motion paths. *BMC Bioinformatics* **7**, 289.

Martinez, S., Geijo, E., Sanchez-Vives, M. V., Puelles, L. & Gallego, R. (1992). Reduced junctional permeability at interrhombomeric boundaries. *Development (Cambridge, England)* **116**, 1069-1076.

Mashanov, G. I. & Molloy, J. E. (2007). Automatic detection of single fluorophores in live cells. *Biophys J* **92**, 2199-2211.

Matthews, H. K., Marchant, L., Carmona-Fontaine, C., Kuriyama, S., Larrain, J., Holt, M. R., Parsons, M. & Mayor, R. (2008). Directional migration of neural crest cells in vivo is regulated by Syndecan-4/Rac1 and non-canonical Wnt signaling/RhoA. *Development (Cambridge, England)*.

Mayor, R. & Carmona-Fontaine, C. (2010). Keeping in touch with contact inhibition of locomotion. *Trends Cell Biol* **20**, 319-328.

Mellitzer, G., Xu, Q. & Wilkinson, D. G. (1999). Eph receptors and ephrins restrict cell intermingling and communication. *Nature* **400**, 77-81.

Mertens, A. E., Rygiel, T. P., Olivo, C., van der Kammen, R. & Collard, J. G. (2005). The Rac activator Tiam1 controls tight junction biogenesis in keratinocytes through binding to and activation of the Par polarity complex. *The Journal of cell biology* **170**, 1029-1037.

Mertens, A. E., Pegtel, D. M. & Collard, J. G. (2006). Tiam1 takes PARt in cell polarity. *Trends Cell Biol* **16**, 308-316.

Miao, H., Strebhardt, K., Pasquale, E. B., Shen, T. L., Guan, J. L. & Wang, B. (2005). Inhibition of integrin-mediated cell adhesion but not directional cell migration requires catalytic activity of EphB3 receptor tyrosine kinase. Role of Rho family small GTPases. *J Biol Chem* **280**, 923-932.

Miller, P. M., Folkmann, A. W., Maia, A. R., Efimova, N., Efimov, A. & Kaverina, I. (2009). Golgi-derived CLASP-dependent microtubules control Golgi organization and polarized trafficking in motile cells. *Nature cell biology* **11**, 1069-1080.

Miura, K., Nam, J. M., Kojima, C., Mochizuki, N. & Sabe, H. (2009). EphA2 engages Git1 to suppress Arf6 activity modulating epithelial cell-cell contacts. *Mol Biol Cell* **20**, 1949-1959.

Mochizuki, A., Wada, N., Ide, H. & Iwasa, Y. (1998). Cell-cell adhesion in limb-formation, estimated from photographs of cell sorting experiments based on a spatial stochastic model. *Dev Dyn* **211**, 204-214.

Moens, C. B., Yan, Y. L., Appel, B., Force, A. G. & Kimmel, C. B. (1996). valentino: a zebrafish gene required for normal hindbrain segmentation. *Development (Cambridge, England)* **122**, 3981-3990.

Moens, C. B. & Prince, V. E. (2002). Constructing the hindbrain: insights from the zebrafish. *Dev Dyn* **224**, 1-17.

Monier, B., Pelissier-Monier, A., Brand, A. H. & Sanson, B. (2010). An actomyosin-based barrier inhibits cell mixing at compartmental boundaries in Drosophila embryos. *Nature cell biology* **12**, 60-65; sup pp 61-69.

Nakaya, M. A., Habas, R., Biris, K., Dunty, W. C., Jr., Kato, Y., He, X. & Yamaguchi, T. P. (2004). Identification and comparative expression analyses of Daam genes in mouse and Xenopus. *Gene Expr Patterns* **5**, 97-105.

Nakayama, M., Goto, T. M., Sugimoto, M., Nishimura, T., Shinagawa, T., Ohno, S., Amano, M. & Kaibuchi, K. (2008). Rho-kinase phosphorylates PAR-3 and disrupts PAR complex formation. *Developmental cell* **14**, 205-215.

Nance, J. & Zallen, J. A. (2011). Elaborating polarity: PAR proteins and the cytoskeleton. *Development (Cambridge, England)* **138**, 799-809.

Narimatsu, M., Bose, R., Pye, M. & other authors (2009). Regulation of planar cell polarity by Smurf ubiquitin ligases. *Cell* **137**, 295-307.

Niessen, C. M. & Gumbiner, B. M. (2002). Cadherin-mediated cell sorting not determined by binding or adhesion specificity. *The Journal of cell biology* **156**, 389-399.

Nieto, M. A., Gilardi-Hebenstreit, P., Charnay, P. & Wilkinson, D. G. (1992). A receptor protein tyrosine kinase implicated in the segmental patterning of the hindbrain and mesoderm. *Development (Cambridge, England)* **116**, 1137-1150.

Nishimura, T., Yamaguchi, T., Kato, K., Yoshizawa, M., Nabeshima, Y., Ohno, S., Hoshino, M. & Kaibuchi, K. (2005). PAR-6-PAR-3 mediates Cdc42-induced Rac activation through the Rac GEFs STEF/Tiam1. *Nature cell biology* **7**, 270-277.

Nittenberg, R., Patel, K., Joshi, Y., Krumlauf, R., Wilkinson, D. G., Brickell, P. M., Tickle, C. & Clarke, J. D. (1997). Cell movements, neuronal organisation and gene expression in hindbrains lacking morphological boundaries. *Development (Cambridge, England)* **124**, 2297-2306.

Nobes, C. D. & Hall, A. (1995). Rho, rac, and cdc42 GTPases regulate the assembly of multimolecular focal complexes associated with actin stress fibers, lamellipodia, and filopodia. *Cell* **81**, 53-62.

Nobes, C. D. & Hall, A. (1999). Rho GTPases control polarity, protrusion, and adhesion during cell movement. *The Journal of cell biology* **144**, 1235-1244.

Nonchev, S., Vesque, C., Maconochie, M. & other authors (1996). Segmental expression of Hoxa-2 in the hindbrain is directly regulated by Krox-20. *Development (Cambridge, England)* **122**, 543-554.

Noren, N. K., Lu, M., Freeman, A. L., Koolpe, M. & Pasquale, E. B. (2004a). Interplay between EphB4 on tumor cells and vascular ephrin-B2 regulates tumor growth. *Proceedings of the National Academy of Sciences of the United States of America* **101**, 5583-5588.

Noren, N. K. & Pasquale, E. B. (2004b). Eph receptor-ephrin bidirectional signals that target Ras and Rho proteins. *Cell Signal* **16**, 655-666.

Nose, A., Nagafuchi, A. & Takeichi, M. (1988). Expressed recombinant cadherins mediate cell sorting in model systems. *Cell* **54**, 993-1001.

Ogawa, H., Ohta, N., Moon, W. & Matsuzaki, F. (2009). Protein phosphatase 2A negatively regulates aPKC signaling by modulating phosphorylation of Par-6 in Drosophila neuroblast asymmetric divisions. *J Cell Sci* **122**, 3242-3249.

Orsulic, S. & Kemler, R. (2000). Expression of Eph receptors and ephrins is differentially regulated by E-cadherin. *J Cell Sci* **113 (Pt 10)**, 1793-1802.

Oxtoby, E. & Jowett, T. (1993). Cloning of the zebrafish krox-20 gene (krx-20) and its expression during hindbrain development. *Nucleic acids research* **21**, 1087-1095.

Palazzo, A. F., Joseph, H. L., Chen, Y. J., Dujardin, D. L., Alberts, A. S., Pfister, K. K., Vallee, R. B. & Gundersen, G. G. (2001). Cdc42, dynein, and dynactin regulate MTOC reorientation independent of Rho-regulated microtubule stabilization. *Curr Biol* **11**, 1536-1541.

Pankov, R., Endo, Y., Even-Ram, S., Araki, M., Clark, K., Cukierman, E., Matsumoto, K. & Yamada, K. M. (2005). A Rac switch regulates random versus directionally persistent cell migration. *The Journal of cell biology* **170**, 793-802.

Parker, M., Roberts, R., Enriquez, M., Zhao, X., Takahashi, T., Pat Cerretti, D., Daniel, T. & Chen, J. (2004). Reverse endocytosis of transmembrane ephrin-B ligands via a clathrin-mediated pathway. *Biochem Biophys Res Commun* **323**, 17-23.

Parrinello, S., Napoli, I., Ribeiro, S. & other authors (2010). EphB signaling directs peripheral nerve regeneration through Sox2-dependent Schwann cell sorting. *Cell* **143**, 145-155.

Pasini, A. & Wilkinson, D. G. (2002). Stabilizing the regionalisation of the developing vertebrate central nervous system. *Bioessays* **24**, 427-438.

Pasquale, E. B. (2005). Eph receptor signalling casts a wide net on cell behaviour. *Nat Rev Mol Cell Biol* **6**, 462-475.

Pasquale, E. B. (2010). Eph receptors and ephrins in cancer: bidirectional signalling and beyond. *Nat Rev Cancer* **10**, 165-180.

Pegtel, D. M., Ellenbroek, S. I., Mertens, A. E., van der Kammen, R. A., de Rooij, J. & Collard, J. G. (2007). The Par-Tiam1 complex controls persistent migration by stabilizing microtubule-dependent front-rear polarity. *Curr Biol* **17**, 1623-1634.

Petrie, R. J., Doyle, A. D. & Yamada, K. M. (2009). Random versus directionally persistent cell migration. *Nat Rev Mol Cell Biol* **10**, 538-549.

Pitulescu, M. E. & Adams, R. H. (2010). Eph/ephrin molecules--a hub for signaling and endocytosis. *Genes & development* **24**, 2480-2492.

Poliakov, A., Cotrina, M. & Wilkinson, D. G. (2004). Diverse Roles of Eph Receptors and Ephrins in the Regulation of Cell Migration and Tissue Assembly. *Developmental cell* **7**, 465-480.

Poliakov, A. & Wilkinson, D. G. (2006). Ephrins make eyes with planar cell polarity. *Nature cell biology* **8**, 7-8.

Poliakov, A., Cotrina, M. L., Pasini, A. & Wilkinson, D. G. (2008). Regulation of EphB2 activation and cell repulsion by feedback control of the MAPK pathway. *The Journal of cell biology* **183**, 933-947.

Pourquie, O. (2001). Vertebrate somitogenesis. *Annual review of cell and developmental biology* **17**, 311-350.

Rauzi, M., Verant, P., Lecuit, T. & Lenne, P. F. (2008). Nature and anisotropy of cortical forces orienting Drosophila tissue morphogenesis. *Nature cell biology* **10**, 1401-1410.

Redies, C. & Takeichi, M. (1996). Cadherins in the developing central nervous system: an adhesive code for segmental and functional subdivisions. *Developmental biology* **180**, 413-423.

Ridley, A. J., Schwartz, M. A., Burridge, K., Firtel, R. A., Ginsberg, M. H., Borisy, G., Parsons, J. T. & Horwitz, A. R. (2003). Cell migration: integrating signals from front to back. *Science (New York, NY* **302**, 1704-1709.

Riley, B. B., Chiang, M. Y., Storch, E. M., Heck, R., Buckles, G. R. & Lekven, A. C. (2004). Rhombomere boundaries are Wnt signaling centers that regulate metameric patterning in the zebrafish hindbrain. *Dev Dyn* **231**, 278-291.

Rohani, N., Canty, L., Luu, O., Fagotto, F. & Winklbauer, R. (2011). EphrinB/EphB Signaling Controls Embryonic Germ Layer Separation by Contact-Induced Cell Detachment. *PLoS Biol* **9**, e1000597.

Rothbacher, U., Laurent, M. N., Deardorff, M. A., Klein, P. S., Cho, K. W. & Fraser, S. E. (2000). Dishevelled phosphorylation, subcellular localization and multimerization regulate its role in early embryogenesis. *The EMBO journal* **19**, 1010-1022.

Sahin, M., Greer, P. L., Lin, M. Z. & other authors (2005). Eph-dependent tyrosine phosphorylation of ephexin1 modulates growth cone collapse. *Neuron* **46**, 191-204.

Santiago, A. & Erickson, C. A. (2002). Ephrin-B ligands play a dual role in the control of neural crest cell migration. *Development (Cambridge, England)* **129**, 3621-3632.

Sawamiphak, S., Seidel, S., Essmann, C. L., Wilkinson, G. A., Pitulescu, M. E., Acker, T. & Acker-Palmer, A. (2010). Ephrin-B2 regulates VEGFR2 function in developmental and tumour angiogenesis. *Nature* **465**, 487-491.

Schilling, T. F., Prince, V. & Ingham, P. W. (2001). Plasticity in zebrafish hox expression in the hindbrain and cranial neural crest. *Developmental biology* **231**, 201-216.

Schlessinger, K., McManus, E. J. & Hall, A. (2007). Cdc42 and noncanonical Wnt signal transduction pathways cooperate to promote cell polarity. *The Journal of cell biology* **178**, 355-361.

Schmoranzer, J., Fawcett, J. P., Segura, M., Tan, S., Vallee, R. B., Pawson, T. & Gundersen, G. G. (2009). Par3 and dynein associate to regulate local microtubule dynamics and centrosome orientation during migration. *Curr Biol* **19**, 1065-1074.

Schneider-Maunoury, S., Seitanidou, T., Charnay, P. & Lumsden, A. (1997). Segmental and neuronal architecture of the hindbrain of Krox-20 mouse mutants. *Development (Cambridge, England)* **124**, 1215-1226.

Shamah, S. M., Lin, M. Z., Goldberg, J. L. & other authors (2001). EphA receptors regulate growth cone dynamics through the novel guanine nucleotide exchange factor ephexin. *Cell* **105**, 233-244.

Shi, S. H., Jan, L. Y. & Jan, Y. N. (2003). Hippocampal neuronal polarity specified by spatially localized mPar3/mPar6 and PI 3-kinase activity. *Cell* **112**, 63-75.

Sokol, S. Y., Klingensmith, J., Perrimon, N. & Itoh, K. (1995). Dorsalizing and neuralizing properties of Xdsh, a maternally expressed Xenopus homolog of dishevelled. *Development (Cambridge, England)* **121**, 1637-1647.

Sokol, S. Y. (1996). Analysis of Dishevelled signalling pathways during Xenopus development. *Curr Biol* **6**, 1456-1467.

Sordella, R. & Van Aelst, L. (2008). Dialogue between RhoA/ROCK and members of the Par complex in cell polarity. *Developmental cell* **14**, 150-152.

Stein, E., Lane, A. A., Cerretti, D. P., Schoecklmann, H. O., Schroff, A. D., Van Etten, R. L. & Daniel, T. O. (1998). Eph receptors discriminate specific ligand oligomers to determine alternative signaling complexes, attachment, and assembly responses. *Genes & development* **12**, 667-678.

Steinberg, M. S. (1962). On the mechanism of tissue reconstruction by dissociated cells. I. Population kinetics, differential adhesiveness. and the absence of directed migration. *Proceedings of the National Academy of Sciences of the United States of America* **48**, 1577-1582.

Steinberg, M. S. (1963). Reconstruction of tissues by dissociated cells. Some morphogenetic tissue movements and the sorting out of embryonic cells may have a common explanation. *Science (New York, NY* **141**, 401-408.

Steinberg, M. S. (1970). Does differential adhesion govern self-assembly processes in histogenesis? Equilibrium configurations and the emergence of a hierarchy among populations of embryonic cells. *J Exp Zool* **173**, 395-433.

Studer, M., Lumsden, A., Ariza-McNaughton, L., Bradley, A. & Krumlauf, R. (1996). Altered segmental identity and abnormal migration of motor neurons in mice lacking Hoxb-1. *Nature* **384**, 630-634.

Sun, T. Q., Lu, B., Feng, J. J., Reinhard, C., Jan, Y. N., Fantl, W. J. & Williams, L. T. (2001). PAR-1 is a Dishevelled-associated kinase and a positive regulator of Wnt signalling. *Nature cell biology* **3**, 628-636.

Tada, M. & Smith, J. C. (2000). Xwnt11 is a target of Xenopus Brachyury: regulation of gastrulation movements via Dishevelled, but not through the canonical Wnt pathway. *Development (Cambridge, England)* **127**, 2227-2238.

Tada, M., Concha, M. L. & Heisenberg, C. P. (2002). Non-canonical Wnt signalling and regulation of gastrulation movements. *Seminars in cell & developmental biology* **13**, 251-260.

Tanaka, M., Kamo, T., Ota, S. & Sugimura, H. (2003). Association of Dishevelled with Eph tyrosine kinase receptor and ephrin mediates cell repulsion. *The EMBO journal* **22**, 847-858.

Tanegashima, K., Zhao, H. & Dawid, I. B. (2008). WGEF activates Rho in the Wnt-PCP pathway and controls convergent extension in Xenopus gastrulation. *The EMBO journal* **27**, 606-617.

Theil, T., Frain, M., Gilardi-Hebenstreit, P., Flenniken, A., Charnay, P. & Wilkinson, D. G. (1998). Segmental expression of the EphA4 (Sek-1) receptor tyrosine kinase in the hindbrain is under direct transcriptional control of Krox-20. *Development (Cambridge, England)* **125**, 443-452.

Theveneau, E., Marchant, L., Kuriyama, S., Gull, M., Moepps, B., Parsons, M. & Mayor, R. (2010). Collective chemotaxis requires contact-dependent cell polarity. *Developmental cell* **19**, 39-53.

Trainor, P. & Krumlauf, R. (2000). Plasticity in mouse neural crest cells reveals a new patterning role for cranial mesoderm. *Nature cell biology* **2**, 96-102.

Uetrecht, A. C. & Bear, J. E. (2009). Golgi polarity does not correlate with speed or persistence of freely migrating fibroblasts. *Eur J Cell Biol* **88**, 711-717.

Ulrich, F., Krieg, M., Schotz, E. M. & other authors (2005). Wnt11 functions in gastrulation by controlling cell cohesion through Rab5c and E-cadherin. *Developmental cell* **9**, 555-564.

Vincent, J. P. (1998). Compartment boundaries: where, why and how? *Int J Dev Biol* **42**, 311-315.

Vladar, E. K., Antic, D. & Axelrod, J. D. (2009). Planar cell polarity signaling: the developing cell's compass. *Cold Spring Harb Perspect Biol* **1**, a002964.

Wada, H. & Okamoto, H. (2009). Roles of noncanonical Wnt/PCP pathway genes in neuronal migration and neurulation in zebrafish. *Zebrafish* **6**, 3-8.

Wallingford, J. B., Rowning, B. A., Vogeli, K. M., Rothbacher, U., Fraser, S. E. & Harland, R. M. (2000). Dishevelled controls cell polarity during Xenopus gastrulation. *Nature* **405**, 81-85.

Wallingford, J. B., Fraser, S. E. & Harland, R. M. (2002a). Convergent extension: the molecular control of polarized cell movement during embryonic development. *Developmental cell* **2**, 695-706.

Wang, H. R., Zhang, Y., Ozdamar, B., Ogunjimi, A. A., Alexandrova, E., Thomsen, G. H. & Wrana, J. L. (2003). Regulation of cell polarity and protrusion formation by targeting RhoA for degradation. *Science (New York, NY* **302**, 1775-1779.

Wang, Y. & Nathans, J. (2007). Tissue/planar cell polarity in vertebrates: new insights and new questions. *Development (Cambridge, England)* **134**, 647-658.

Wang, Y., Nakayama, M., Pitulescu, M. E. & other authors (2010). Ephrin-B2 controls VEGF-induced angiogenesis and lymphangiogenesis. *Nature* **465**, 483-486.

Waskiewicz, A. J., Rikhof, H. A. & Moens, C. B. (2002). Eliminating zebrafish pbx proteins reveals a hindbrain ground state. *Developmental cell* **3**, 723-733.

Wei, S., Xu, G., Bridges, L. C., Williams, P., White, J. M. & DeSimone, D. W. (2010). ADAM13 induces cranial neural crest by cleaving class B Ephrins and regulating Wnt signaling. *Developmental cell* **19**, 345-352.

Wei, S. Y., Escudero, L. M., Yu, F. & other authors (2005). Echinoid is a component of adherens junctions that cooperates with DE-Cadherin to mediate cell adhesion. *Developmental cell* **8**, 493-504.

Wilkinson, D. G., Bhatt, S., Chavrier, P., Bravo, R. & Charnay, P. (1989a). Segment-specific expression of a zinc-finger gene in the developing nervous system of the mouse. *Nature* **337**, 461-464.

Wilkinson, D. G., Bhatt, S., Cook, M., Boncinelli, E. & Krumlauf, R. (1989b). Segmental expression of Hox-2 homoeobox-containing genes in the developing mouse hindbrain. *Nature* **341**, 405-409.

Wilkinson, D. G. (2001). Multiple roles of EPH receptors and ephrins in neural development. *Nature reviews* **2**, 155-164.

Wimmer-Kleikamp, S. H., Janes, P. W., Squire, A., Bastiaens, P. I. & Lackmann, M. (2004). Recruitment of Eph receptors into signaling clusters does not require ephrin contact. *The Journal of cell biology* **164**, 661-666.

Witzel, S., Zimyanin, V., Carreira-Barbosa, F., Tada, M. & Heisenberg, C. P. (2006). Wnt11 controls cell contact persistence by local accumulation of Frizzled 7 at the plasma membrane. *The Journal of cell biology* **175**, 791-802.

Xu, Q., Holder, N., Patient, R. & Wilson, S. W. (1994). Spatially regulated expression of three receptor tyrosine kinase genes during gastrulation in the zebrafish. *Development (Cambridge, England)* **120**, 287-299.

Xu, Q., Alldus, G., Holder, N. & Wilkinson, D. G. (1995). Expression of truncated Sek-1 receptor tyrosine kinase disrupts the segmental restriction of gene expression in the Xenopus and zebrafish hindbrain. *Development (Cambridge, England)* **121**, 4005-4016.

Xu, Q., Mellitzer, G., Robinson, V. & Wilkinson, D. G. (1999). In vivo cell sorting in complementary segmental domains mediated by Eph receptors and ephrins. *Nature* **399**, 267-271.

Zallen, J. A. (2007). Planar Polarity and Tissue Morphogenesis. *Cell* **129**, 1051-1063.

Zhang, G., Fenyo, D. & Neubert, T. A. (2008a). Screening for EphB signaling effectors using SILAC with a linear ion trap-orbitrap mass spectrometer. *J Proteome Res* **7**, 4715-4726.

Zhang, H. & Macara, I. G. (2006). The polarity protein PAR-3 and TIAM1 cooperate in dendritic spine morphogenesis. *Nature cell biology* **8**, 227-237.

Zhang, H. & Macara, I. G. (2008b). The PAR-6 polarity protein regulates dendritic spine morphogenesis through p190 RhoGAP and the Rho GTPase. *Developmental cell* **14**, 216-226.

Zhang, X., Zhu, J., Yang, G. Y. & other authors (2007). Dishevelled promotes axon differentiation by regulating atypical protein kinase C. *Nature cell biology* **9**, 743-754.

Zhu, S., Liu, L., Korzh, V., Gong, Z. & Low, B. C. (2006). RhoA acts downstream of Wnt5 and Wnt11 to regulate convergence and extension movements by involving effectors Rho kinase and Diaphanous: use of zebrafish as an in vivo model for GTPase signaling. *Cell Signal* **18**, 359-372.

Zimmer, M., Palmer, A., Kohler, J. & Klein, R. (2003). EphB-ephrinB bi-directional endocytosis terminates adhesion allowing contact mediated repulsion. *Nature cell biology* **5**, 869-878.